UNIVERSIDADE FEDERAL DE GOIÁS (UFG)
INSTITUTO DE INFORMÁTICA (INF)
PROGRAMA DE PÓS–GRADUAÇÃO EM CIÊNCIA DA COMPUTAÇÃO

GABRIEL DA SILVA VIEIRA

Methods for Analyzing Leaf Damage and Recognizing Agricultural Pests Using Computer Techniques

GOIÂNIA
2024

UNIVERSIDADE FEDERAL DE GOIÁS
INSTITUTO DE INFORMÁTICA

TERMO DE CIÊNCIA E DE AUTORIZAÇÃO (TECA) PARA DISPONIBILIZAR VERSÕES ELETRÔNICAS DE TESES

E DISSERTAÇÕES NA BIBLIOTECA DIGITAL DA UFG

Na qualidade de titular dos direitos de autor, autorizo a Universidade Federal de Goiás (UFG) a disponibilizar, gratuitamente, por meio da Biblioteca Digital de Teses e Dissertações (BDTD/UFG), regulamentada pela Resolução CEPEC nº 832/2007, sem ressarcimento dos direitos autorais, de acordo com a Lei 9.610/98, o documento conforme permissões assinaladas abaixo, para fins de leitura, impressão e/ou download, a título de divulgação da produção científica brasileira, a partir desta data.

O conteúdo das Teses e Dissertações disponibilizado na BDTD/UFG é de responsabilidade exclusiva do autor. Ao encaminhar o produto final, o autor(a) e o(a) orientador(a) firmam o compromisso de que o trabalho não contém nenhuma violação de quaisquer direitos autorais ou outro direito de terceiros.

1. Identificação do material bibliográfico

[ ] Dissertação   [X] Tese   [ ] Outro*:_____

*No caso de mestrado/doutorado profissional, indique o formato do Trabalho de Conclusão de Curso, permitido no documento de área, correspondente ao programa de pós-graduação, orientado pela legislação vigente da CAPES.

Exemplos: Estudo de caso ou Revisão sistemática ou outros formatos.

2. Nome completo do autor

Gabriel da Silva Vieira

3. Título do trabalho

Methods for Analyzing Leaf Damage and Recognizing Agricultural Pests Using Computer Techniques

4. Informações de acesso ao documento (este campo deve ser preenchido pelo orientador)

Concorda com a liberação total do documento [X] SIM   [ ] NÃO[1]

[1] Neste caso o documento será embargado por até um ano a partir da data de defesa. Após esse período, a possível disponibilização ocorrerá apenas mediante:
a) consulta ao(à) autor(a) e ao(à) orientador(a);
b) novo Termo de Ciência e de Autorização (TECA) assinado e inserido no arquivo da tese ou dissertação.
O documento não será disponibilizado durante o período de embargo.
Casos de embargo:
- Solicitação de registro de patente;
- Submissão de artigo em revista científica;
- Publicação como capítulo de livro;
- Publicação da dissertação/tese em livro.

Obs. Este termo deverá ser assinado no SEI pelo orientador e pelo autor.

Documento assinado eletronicamente por **Fabrizzio Alphonsus Alves De Melo Nunes Soares**, **Coordenador de Pós-Graduação**, em 29/10/2024, às 16:12, conforme horário oficial de Brasília, com fundamento no § 3º do art. 4º do Decreto nº 10.543, de 13 de novembro de 2020.

Documento assinado eletronicamente por **Gabriel Da Silva Vieira**, **Discente**, em 29/10/2024, às 17:56, conforme horário oficial de Brasília, com fundamento no § 3º do art. 4º do Decreto nº 10.543, de 13 de novembro de 2020.

A autenticidade deste documento pode ser conferida no site https://sei.ufg.br/sei/controlador_externo.php?acao=documento_conferir&id_orgao_acesso_externo=0, informando o código verificador **4929767** e o código CRC **0F2883F5**.

Referência: Processo nº 23070.025989/2024-11   SEI nº 4929767

GABRIEL DA SILVA VIEIRA

Métodos para Análise de Dano Foliar e Reconhecimento de Pragas na Agricultura

Usando Técnicas Computacionais

Tese apresentada ao Programa de Pós–Graduação em Ciência da Computação, do Instituto de Informática (INF), da Universidade Federal de Goiás (UFG), como requisito para obtenção do título de Doutor em Ciência da Computação.
Área de Concentração: Ciência da Computação.
Linha de Pesquisa: Sistemas Inteligentes e Aplicações.

Orientador: Prof. Dr. Fabrizzio Alphonsus Alves de Melo Nunes Soares

GOIÂNIA
2024

UNIVERSIDADE FEDERAL DE GOIÁS

INSTITUTO DE INFORMÁTICA

ATA DE DEFESA DE TESE

Ata Nº **19/2024** da sessão de Defesa de Tese de **Gabriel da Silva Vieira** que confere o título de Doutor em **Ciência da Computação**, na área de concentração em **Ciência da Computação.**

Aos dois dias do mês de agosto de dois mil e vinte e quatro, a partir das nove horas, na sala 151 do Instituto de Informática, realizou-se a sessão pública de Defesa de Tese intitulada "**Methods for Recognizing Multiple Insect Species and Analyzing Leaf Damage Using Computational Techniques**". Os trabalhos foram instalados pelo Orientador, Professor Doutor Fabrizzio Alphonsus Alves de Melo Nunes Soares (INF/UFG) com a participação dos demais membros da Banca Examinadora: Professor Doutor Helio Pedrini (IC/UNICAMP), membro titular externo; Professor Doutor Christian Dias Cabacinha (ICA/UFMG), membro titular externo; cujas participações ocorreram através de videoconferência; Professor Doutor Ronaldo Martins da Costa (INF/UFG), membro titular interno; Professor Doutor Gustavo Teodoro Laureano (INF/UFG), membro titular interno. Durante a arguição os membros da banca fizeram sugestão de alteração do título do trabalho, conforme descrito abaixo. A Banca Examinadora reuniu-se em sessão secreta a fim de concluir o julgamento da Tese tendo sido o candidato **aprovado** pelos seus membros. Proclamados os resultados pelo Professor Doutor Fabrizzio Alphonsus Alves de Melo Nunes Soares, Presidente da Banca Examinadora, foram encerrados os trabalhos e, para constar, lavrou-se a presente ata que é assinada pelos Membros da Banca Examinadora, aos dois dias do mês de agosto de dois mil e vinte e quatro.

TÍTULO SUGERIDO PELA BANCA

Methods for Analyzing Leaf Damage and Recognizing Agricultural Pests Using Computer Techniques

Referência: Processo nº 23070.025989/2024-11   SEI nº 4715922

Gabriel da Silva Vieira

received his bachelor's degree in Software Engineering from the Institute of Informatics, Federal University of Goiás, Brazil 2012. He is one of the first 13 Software Engineers with a degree from Brazil. In 2018, he obtained his Master's Degree in Computer Science. He is currently a professor at the Federal Institute of Education, Science, and Technology of Goiano, Urutaí, where he is a member of the Computer Vision Laboratory.

To my family for helping me slow down in a very fast-paced world.

Acknowledgement

It could be a day like any other. A week of hard work followed by a long trip home. I had already driven for two hours and still had almost two hours to get home. That day, something bothered me. My chest was tight from losing valuable people and friends before and during the global pandemic. As I continued my journey, bad feelings accompanied me, along with intense pain in my arm caused by exhausting days of hard work. Then something unexpected happened. After being deeply depressed, I looked to the right side, and, surprisingly, in the middle of nowhere, there was a billboard saying, "Jesus Loves You." All that could be seen around were just pasture fields and a few trees. Why would someone spend time and money preparing that structure without referencing his/her name or business? Why right there? Why was my attention drawn to those words? These questions no longer mattered and my heart was filled with grace and hope.

This thesis is the result of five years well lived. There were many adversities, but the sun shone once again. My daughter gained a little brother, and my family rejoiced even more. During this period, I strengthened my friendships and had the satisfaction of creating new bonds. I remember talking to my friend Bruno Rocha while cradling my baby in my arms many nights. I remember talking with my friend Afonso Fonseca countless times about work progress and casual matters. I remember having good conversations and reliving good memories with my friend Naiane Maria. I remember organizing work presentations with my friend Thamer Nascimento and writing some articles with my friend Juliana Félix. I remember learning a lot from the high-level presentations of my friends Cristiane Ferreira, Jaline Mombach, and Emília Nogueira. I remember the weekly meetings at the Pixellab research group and the brilliant minds that are or have been there, like Deborah Fernandes, Wellington Galvão, Priscila Kai, and Allan Kardec. Most importantly, I remember having significant meetings with my advisor, Fabrizzio Soares, who helped me define the direction of the research and achieve the intended results. If anyone doubts the existence of professors committed to science in Brazil, look for Prof. Fabrizzio, and you will find the best human being with high standards of integrity and goodness. For these reasons, I thank all the people who allowed me to follow some of their work, helped me in this search for constant improvement, and allowed me to share moments of great joy and inspiration.

Agradecimentos

Poderia ser um dia como qualquer outro. Uma semana de muito trabalho seguido de uma viagem longa para casa. Eu já dirigia por duas horas, e ainda faltava quase duas horas para eu chegar em casa. Naquele dia, algo me incomodava. Meu peito estava apertado por ter perdido pessoas valiosas e amigos antes e durante a pandemia. Na medida em que seguia minha viagem, sentimentos ruins me acompanhavam junto com dores intensas no braço provocadas por jornadas exaustivas de muito trabalho. Então, algo inesperado aconteceu. Depois de estar profundamente depressivo olhei para o lado direito, e, surpreendentemente, no meio do nada havia um outdoor escrito "Jesus te Ama." Ao redor tudo que se podia ver eram apenas campos de pastagem e poucas árvores. Por que alguém gastaria tempo e dinheiro para preparar aquela estrutura sem fazer nenhuma referência para seu nome ou de seu negócio? Por que justamente ali? Por que minha atenção se voltou àquelas palavras? Aos poucos essas perguntas não importavam mais e meu coração se encheu de graça e esperança.

Essa tese é resultado de cinco anos bem vividos. Houve muitas adversidades, mas o sol brilhou mais uma vez. Minha filha ganhou um irmãozinho e minha família se alegrou ainda mais. Nesse período, fortaleci minhas amizades e tive a satisfação de criar novos laços. Lembro de em muitas noites conversar com meu amigo Bruno Rocha enquanto ninava meu bebê nos braços. Eu lembro de conversar inúmeras vezes com o meu amigo Afonso Fonseca sobre o andamento dos trabalhos e assuntos casuais. Lembro de ter boas conversas e reviver boas lembranças com minha amiga Naiane Maria. Lembro de organizar apresentação de trabalhos com meu amigo Thamer Nascimento e de escrever alguns artigos junto com a minha amiga Juliana Félix. Lembro de aprender muito com as apresentações de alto nível das minhas amigas Cristiane Ferreira, Jaline Mombach, e Emília Nogueira. Lembro dos encontros semanais no grupo de pesquisa Pixellab e das mentes brilhantes que estão ou passaram por ali como Deborah Fernandes, Wellington Galvão, Priscila Kai, e Allan Kardec. E, principalmente, lembro de ter ótimas reuniões com meu orientador Fabrizzio Soares que me ajudaram a definir o rumo das pesquisas e alcançar os resultados pretendidos. Se alguém tem dúvida da existência de professores comprometidos com a ciência em nosso país, basta procurar pelo prof. Fabrizzio e encontrará o que há de melhor, um ser humano de alta valia e padrões

elevados de hombridade e respeito. Por essas razões, agradeço a todas as pessoas que me permitiram acompanhar um pouco de seus trabalhos, que me ajudaram nesta busca por aperfeiçoamento constante, e que me deram a honra de compartilhar momentos de muita alegria e inspiração.

Uma jornada desse tamanho não seria possível sem o apoio das pessoas que residem há muito em meu coração. Agradeço à minha esposa Dayara por estar ao meu lado e por me dar os dois melhores presentes que já ganhei e que me trazem muito orgulho, nossos filhos Luísa e William. Com eles, o que era difícil se tornou fácil. Um olhar, um carinho, e tudo mudava para melhor. Minha família é meu porto seguro, meu jardim de flores. Saber que eles estão comigo me traz paz. Eu me aconchego em um abraço, em um beijo, e renovo minhas forças para mais um dia. Meus pais, Cristina e Sinomar, igualmente merecem meus sentimentos de gratidão. Os vejo quase todos os dias e sei que estão lá para os bons momentos e também para os não tão bons. Como poderia ser o que sou sem a orientação deles em priorizar o certo ao invés do oportunismo de ocasião? Meu irmão Josué também aprendeu a virtude da honestidade e me ajudou a lidar com vários problemas me possibilitando tempo para escrever essa tese. Por isso, fica o registro de minha profunda gratidão à minha amada família.

Agradeço ao corpo docente e técnicos administrativos do Instituto de Informática da Universidade Federal de Goiás pelo empenho em manter um programa de pós-graduação da mais elevada qualidade em estudos avançados. Em especial dedico meu agradecimento as secretárias Mariana Santana e Mirian Amorim pela proficiência em atender qualquer solicitação e dar sempre provimento as melhores soluções. Agradeço também aos professores Gustavo Laureano e Ronaldo Costa por participarem da minha banca de qualificação e apresentarem valiosas contribuições a nossa pesquisa. Igualmente, estendo meus agradecimentos a todos do Instituto de Informática que contribuíram direta ou indiretamente para minha formação.

Agradeço aos meus colegas de trabalho que sempre foram bastante atenciosos com minhas solicitações e prestativos com minhas necessidades. Dedico um agradecimento especial à Vivian Cirino por ter sido a primeira a acreditar em meu trabalho e à Monica Sakuray pelo carinho e palavras amigas de todos os dias. Agradeço à Rachel Carcute, Jorcivan Ramos, Wenio Vieira, e Cristiane Cardoso pelas conversas para além do trabalho. Igualmente, agradeço ao Paulo Mansur e Junio Lima pelas parcerias de muitos momentos. Registro ainda meus mais sinceros agradecimentos ao Júlio Ferreira pela amizade e coração imenso que me acolheu em momentos muito conturbados.

Com muita satisfação também deixo meus agradecimento aos professores avaliadores, Prof. Dr. Christian Cabacinha, Prof. Dr. Hélio Pedrini, Prof. Dr. Gustavo Laureano, e Prof. Dr. Ronaldo Martins, pelo esforço em sincronizar suas agendas e viabilizar a banca de defesa. Além disso, agradeço aos professores avaliadores pelas excelentes con-

tribuições que muito agregaram para o enriquecimento e qualidade desta tese.

Finalmente, agradeço à pessoa anônima que preparou àquele outdoor posto em meu caminho e à Dra. Dilma Rebehy, minha fisioterapeuta, por me presentear com uma bíblia sagrada de onde aprendi lições inspiradoras e selecionei algumas passagens para colocar como epígrafes dos capítulos desta tese.

"I wake up early to live more."

Omar Aziz

Resumo

Vieira, Gabriel da Silva. **Métodos para Análise de Dano Foliar e Reconhecimento de Pragas na Agricultura Usando Técnicas Computacionais**. Goiânia, 2024. 211p. Tese de Doutorado. Instituto de Informática (INF), Universidade Federal de Goiás (UFG).

Técnicas computacionais aplicadas à agricultura têm aprimorado atividades rurais e contribuído com o monitoramento de lavouras, proteção de plantas e melhor rendimento geral. Nesta tese, destacamos a análise foliar como ferramenta para inspeção e melhora contínua de plantações, bem como para subsidiar tomada de decisões e intervenções no manejo agrícola. Alterações foliares podem significar perdas irreparáveis de produtividade, entrega de produtos de baixa qualidade, e prejuízos econômicos significativos. Para mitigar prejuízos de produção, é necessário um monitoramento eficiente que aponte se a presença de pragas pode levar ao comprometimento da produtividade. Contudo, danos na silhueta foliar comprometem métodos automatizados de análise e a diversidade no formato de folhas e composição de danos dificultam o delineamento das regiões de borda comprometidas. Nesse sentido, apresentamos métodos originais baseados em computador, capazes de lidar com danos nas extremidades de folha, que viabilizam a estimativa de desfolha, detecção de dano, reconstrução de superfície foliar, e classificação de pragas. Dentre as novidades desse estudo estão o reconhecimento de padrões por meio de correspondência de templates e classificação de pragas usando apenas vestígios de danos foliares. O delineamento metodológico do estudo compreende revisão de literatura, investigação de técnicas de processamento digital de imagens, visão computacional e aprendizado de máquina, construção de software, e formulação de teste experimentais. Os resultados apontam para uma alta assertividade na estimativa de perda de área foliar com correlação linear de 0.98, detecção de dano e classificação de pragas com assertividade acima de 90%, e recomposição visual de regiões foliares afetadas por herbivoria com pontuações SSIM entre 0.68 e 0.94.

Palavras–chave

Análise Foliar, Herbivoria por Insetos, Estimativa de Desfolha, Detecção de Objeto, Reconstrução de Imagem, Classificação de Insetos.

Abstract

Vieira, Gabriel da Silva. **Methods for Analyzing Leaf Damage and Recognizing Agricultural Pests Using Computer Techniques**. Goiânia, 2024. 211p. PhD. Thesis. Instituto de Informática (INF), Universidade Federal de Goiás (UFG).

The application of computer techniques in agriculture has significantly improved rural activities, particularly crop monitoring, plant protection, and overall yield. This thesis emphasizes leaf analysis as a valuable tool for inspecting and continually improving plantations, as well as supporting decision-making and agricultural management interventions. Changes in leaves can lead to irreparable losses in productivity, the delivery of low-quality products, and significant economic impacts. To prevent production failures, it is crucial to efficiently monitor and identify whether pests are affecting productivity or remaining within acceptable levels. However, damage to the leaf silhouette can limit automated analysis, and the diversity in leaf shape and damage levels makes it challenging to delineate the compromised edge regions. This study introduces original computer-based methods for defoliation estimate, damage detection, leaf surface reconstruction, and pest classification that are prepared to address damage to the leaf boundaries. Notable aspects of this study include template matching for pattern recognition and pest classification using only traces of leaf damage. The methodological design of the study consists of a literature review, investigation of digital image processing techniques, computer vision and machine learning, software development, and formulation of experimental tests. The results indicate high accuracy in estimating leaf area loss with a linear correlation of 0.98, damage detection and pest classification with assertiveness above 90%, and visual restoration of regions affected by herbivory with SSIM scores between 0.68 and 0.94.

Keywords

Leaf Analysis, Herbivory by Insects, Defoliation Estimation, Object Detection, Image Reconstruction, Insect Classification.

Contents

List of Figures

List of Tables

List of Abbreviations

ACC Accuracy

AUC Area Under the Curve

CO2 atmospheric carbon dioxide

CNN Convolutional Neural Network

EMD Earth Mover's Distance

FN False Negative

FNR False Negative Rate

FP False Positive

FPR False Positive Rate

GB Gigabytes

GDP Gross Domestic Product

GHz Gigahertz

GPU Graphics Processing Unit

Grad-CAM Gradient-weighted Class Activation Mapping

HOG Histogram of Oriented Gradients

IMPRS-IS International Max Planck Research School for Intelligent Systems

IoA Intersection over Area

IoT Internet of Thing

IoU Intersection over Union

LBP Local Binary Pattern

MAE Mean Absolute Error

MB Megabytes

MKL Multiple Kernel Learning

Mmt million metric tons

RAM Random Access Memory

R-CNN Faster R-Convolutional Neural Networks

RGB Red, Green, Blue

RMSE Root Mean Square Error

ROC Receiver Operating Characteristic

ROI region of interest

SIFT Scale-Invariant Feature Transform

SSIM Structural Similarity Index

SVM Support Vector Machine

TN True Negative

TNR True Negative Rate

TP True Positive

TPR True Positive Rate

Introduction

You are the light of the world.

This thesis presents some computational techniques applied to constructing leaf analysis models with attention to defoliation estimation, foliar damage detection, leaf surface reconstruction, and pest classification. As a starting point, we worked on identifying compromised leaf regions caused by defoliation to propose solutions with accurate responses to agriculture. Defoliation is the process of consuming leaf area caused by some harmful agent that affects plants' physiology, primary production, and photosynthetic capacity. The defoliation process generates visual effects, and inspection guides the delineation of compromised leaf areas. With damage detection and loss estimation, leaf regions consumed by pests can be artificially restored to a supposed stage preceding defoliation. Likewise, the discriminating characteristics between the bite patterns of different defoliators can be used to categorize the agents causing defoliation.

We explore different approaches to building solutions for leaf analysis and present detailed processes that involve preparing template models, evaluating the similarity between images, computing defoliation, and highlighting attention areas. Thus, we group processing steps for detecting and estimating leaf loss, image restoration, and pest classification based on bite signatures. We analyzed the results obtained by assessing different evaluation metrics and conducted comparative studies that considered similar works. Hence, our methods automatically detect the regions where defoliation occurs, estimate defoliation, underline compromised leaf areas, and prepare image restoration.

Our leaf analysis models follow software architecture guidelines in which program components are modularized; the processes are sequenced into input, transformation, and output stages; data is processed by independent functionalities; and the results are measured and recorded for later analysis. This strategy is consistent with the construction of complex systems, as it facilitates the development of maintainable solutions, simplifies code debugging, and reduces the impact of coupling and uncoupling software components in situations of experimental evaluation of different algorithm designs. Simi-

larly, we presented lightweight processes that could be used on devices with low computational power and models that could be integrated into smart farming ecosystems through the composition of services.

Another innovation of our work is the models' ability to deal with leaf damage inside the leaves and leaf losses in edge regions. Damage to the ends of the leaves makes it difficult to estimate defoliation, as the curvature that connects the margin segments is compromised. Estimating leaf loss involves recovering the shape of damaged leaves and requires strategies that make it possible to trace the margin contours and connect the points at the ends. We use the leaf shape as a reference to build image templates and the constructed templates to recover the compromised leaf regions.

We also show that our leaf analysis models can be applied to different plant species such as apple, blueberry, cherry, corn, grape, peach, pepper, potato, raspberry, soybean, strawberry, and tomato. Regardless of the leaf structures observed, the models can present satisfactory results even with variations in leaf shapes, sample positioning, and image shading. Therefore, the models are effective as they present defoliation estimation, damage detection, leaf reconstruction, and indirect pest classification. Likewise, the models are efficient, suggesting their use on equipment with low computational power.

Divided into eight chapters, we introduce the work in Chapter 1 and present a computational model for leaf reconstruction of areas consumed by herbivory in Chapter 2. We improved the model previously presented and discussed the segmentation of bite marks from chewing insects in Chapter 3. In Chapter 4, we present a model for estimating leaf loss. We keep working with the counting of injured leaf areas and present a new version of the program to assess damage caused by insects in Chapter 5. In Chapter 6, we present details of the software developed by the authors for leaf analysis, and in Chapter 7, we evaluate deep neural network models for classifying insects and mollusks based on bite patterns. Finally, we present conclusions of the work in chapter 8. Besides, Appendix A presents a list of contributions made by the authors during the research, such as original papers, software, and new datasets.

1.1   Motivation and Significance

Technological advances in recent years have triggered a series of innovations in various sectors of the economy, including agriculture. With an expanding world population, the demand for agricultural products has been growing in proportion to human subsistence needs. From 8.2 billion in 2024, population growth is estimated to reach 9.7 billion in 2050 and 10.3 billion in 2080 (UN-DESA, 2022; UN-DESA, 2024; LIU; RAFTERY, 2024). Therefore, meeting the food demand and ensuring the agricultural sector's sustainable development is critical (PRESTI *et al.*, 2023). Fortunately, the food

supply follows population growth, and the capacity to increase global productivity is based on some aspects, all of them with a technological basis.

Cutting-edge technologies have contributed to intensifying production systems, and new computer-assisted approaches have increased success in rural activities. Agricultural management supported by technological devices helps monitor and continuously improve the quality of soil and crops so that they are compatible with high productivity. Genetic materials are investigated in situations of adaptation to local climatic conditions and resistance to pests, and technical harvesting and storage protocols are constantly reviewed to avoid loss and preserve the quality of products (JÚNIOR; LOPES, 2023).

The insertion of technological innovations in typically rural activities launches daily micro-revolutions in agriculture. Due to the number of solutions available for agriculture, rural activities that use innovative instruments for measurement, monitoring, analysis, management, control, and projections are conventionally called precision agriculture. Precision agriculture is a conceptual term that marks a new stage in agricultural production. Essentially marked by the introduction of technological advances in agriculture, it is characterized by the presentation of detailed information for decision-making, improvement of rural management based on reliable data, and maintenance of production within global consumption expectations (KARUNATHILAKE *et al.*, 2023; SARANYA *et al.*, 2023).

Since countless innovations have entered rural activities, it was also necessary to investigate and discuss the integration of these solutions. Datasets from different instances could be processed to create even more sophisticated attention processes, such as soil and plant conservation, pest control, and future harvest projections. As a result, we can observe the combination of different solutions in communication protocols with standardized input and output for integrated computing processes. As integration has become critical, advanced technologies were integrated into agriculture systems, transforming precision agriculture to Agriculture 4.0, or smart farming (KARUNATHILAKE *et al.*, 2023; JAVAID *et al.*, 2022).

In smart farming, many parameters, such as environmental conditions, soil status, production and plant management, and pest and damage estimates, are observed to reduce the costs of agricultural process inputs (PRAKASH *et al.*, 2023; NUKALA *et al.*, 2016). In this context, data processing devices are mainly used to automate manual processes, control and coordinate equipment remotely, measure and estimate production and loss, detect production failures such as in planting lines, mechanize pest control, expand the monitoring space, scan using unmanned aerial and ground vehicles, and inspect the quality of grains, flowers, and fruits.

Among the research possibilities in precision agriculture, leaf analysis is a crucial tool for classifying and judging agricultural management options. Leaves are elemen-

tary plant organs with interconnected functional elements directed toward strategies for improving productivity with limited resources and are considered the leading site for photosynthesis and plant carbon acquisition (ROTH-NEBELSICK; KRAUSE, 2023; LAWSON; MILLIKEN, 2023). Changes in leaf structures can compromise plant development by reducing its energy capacity, affecting its physiology and primary production, consequently reducing the size, weight, and overall quality of fruits, grains, flowers, and seeds. For large-scale production, foliar changes can mean an irreparable loss in productivity, delivery of low-quality products, and significant economic impact (PRESTI *et al.*, 2023; FERNANDES *et al.*, 2022).

Leaf damage and loss can occur naturally, with rain and winds breaking the leaf surface or promoting premature leaf fall. When the cause is natural and sporadic, the loss can be repaired by strengthening the plants. However, abiotic and biotic stresses can influence plant morphological traits and physiological processes (PANDEY *et al.*, 2015). The first refers to environmental conditions such as temperature, irradiance, water availability, salinity, and atmospheric carbon dioxide (CO_2). The second refers to the damage caused by pests and pathogens such as insects, bacteria, fungi, viruses, and nematodes that progressively consume the leaves as they grow and multiply in the crop (PRESTI *et al.*, 2023; ESGARIO *et al.*, 2022).

In the case of insects, their presence in farming is inevitable. Plants and insects are in a co-evolution process that started millions of years ago, ensuring the survival of both in the terrestrial ecosystem (SANTOS, 2011). Many of them bring benefits by helping to pollinate flowers and decompose organic matter (WIETZKE *et al.*, 2018; VERMA *et al.*, 2023). Others, such as chewing and sucking insects, can lead to productive loss when their reproduction is rapid, and the abundance of insects leads to unrestrained consumption of crops and forests (ERGASHEVA; MAKHMUDOVA, 2023; RAFFA *et al.*, 2023). To mitigate situations of this type, efficient crop monitoring is necessary, in which pest detection and leaf loss are used to check whether the presence of insects is within expected levels (QIN *et al.*, 2024; MACHADO *et al.*, 2016). When the estimate points to a relevant loss, the degree of infestation guides pest management strategies and the adoption of insect-pest control strategies (BERECIARTUA-PÉREZ *et al.*, 2023; SILVA *et al.*, 2019).

The estimation of leaf loss has been the subject of interdisciplinary study between areas of interest in agriculture and computing. This has led to structuring semi-automatic (MALOOF *et al.*, 2013; EASLON; BLOOM, 2014) or fully automated systems based on knowledge from conventional manual approaches (SILVA *et al.*, 2021; VIEIRA *et al.*, 2021a). Process automation has been investigated to deal with some limitations of traditional methods due to erroneous estimates, excessive human work, and dependence on specialized knowledge (BERECIARTUA-PÉREZ *et al.*, 2023; VIEIRA *et al.*, 2023).

Although equipment is available for estimating leaf area, they fail for leaves with edge damage, are expensive, and require maintenance (VIEIRA *et al.*, 2024). For these reasons, computing-based solutions have been good alternatives, as they present low cost and very assertive results.

In the same way, detecting leaf surface regions attacked by pests is essential for directing actions to combat infestations (VIEIRA *et al.*, 2022; ZHU *et al.*, 2024). With computer-assisted leaf analysis, it is possible to restrict compromised leaf regions and outline pest identification strategies. In a plantation, the computer can point out the areas with the highest incidence of damage and establish an alert point for directing insect collection, pest control, and damage counting. Therefore, detecting leaf damage and estimating defoliation are potent tools for discriminating healthy plants from injured plants and are valid for feeding selective spraying systems, reducing production costs, and contingency chemical applications in plantations. It is worth mentioning that approximately 90% of agricultural lands are affected by environmental stresses, and it is estimated that insects consume about 14% of the total global crop yields (PRESTI *et al.*, 2023; NABITY *et al.*, 2009). Consequently, foliar analysis can help increase crop productivity by assisting agricultural producers in providing food for a growing global population.

1.2   Problems

The initial research problem involves analyzing damaged leaves to identify and quantify areas compromised by herbivorous defoliators. The goal is to measure the percentage of leaf loss by calculating the pixel count corresponding to damaged regions in digital images. The computational model must accurately detect and quantify these compromised areas to estimate the extent of the damage. Figure 1.1 illustrates a damaged leaf with different types of damage.

(a) *damaged leaf*   (b) *internal damage (trivial)*   (c) *edge damage (complex)*
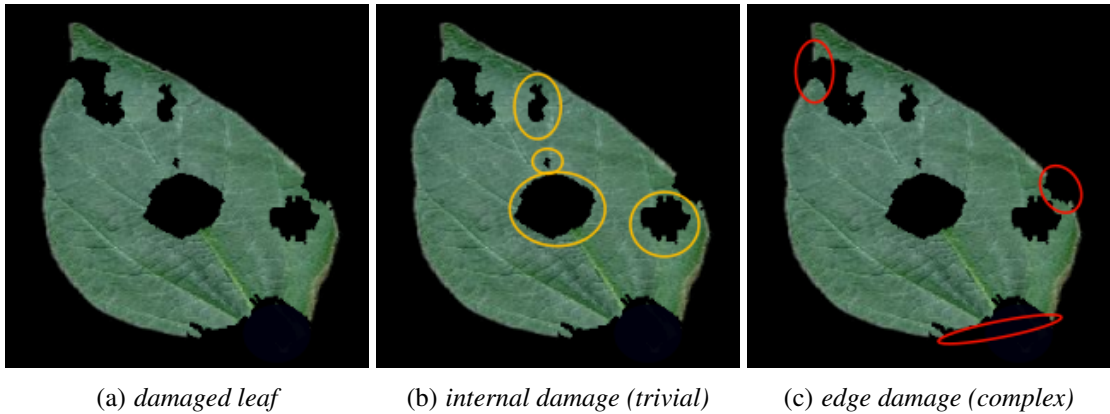
Figure 1.1: *Trivial and complex challenges in automatic leaf analysis.*

| (a) *straight line* | (b) *curved line* | (c) *ideal line* |
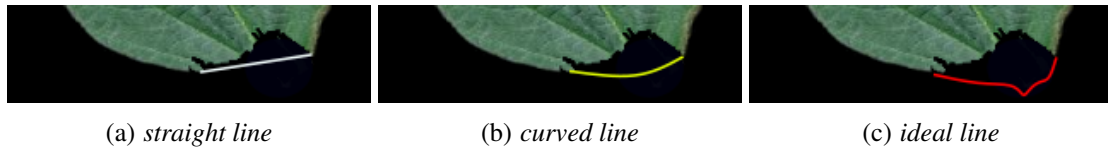
Figure 1.2: *Connecting compromised leaves endpoints using different line patterns to determine the leaf silhouette.*

Thus, this research problem was divided into two categories. The first concerns damage inside the leaf, while the second considers damage at the edges. The first category can be solved with logical and morphological operations because the leaf silhouette is not compromised. Therefore, it is a trivial problem. On the other hand, in the second category, the compromised leaf edges need to be estimated, which is difficult given the diversity of leaf shapes. Thus, this is a complex problem.

To provide a clear view of the complexity of estimating the leaf contour, Figure 1.2 shows two alternatives for connecting compromised leaf endpoints. The first used a straight line, and the second a curved line. As can be seen, neither strategy was sufficient to approximate the actual shape of the compromised leaf silhouette, which is characterized by a unique layout that is difficult to predict.

The second research problem is related to the indirect classification of pests, i.e., the association between leaf damage and the species that caused the observed deterioration. When a plant is healthy, it becomes attractive to many insects and other pests. Some chewing insects, for example, use leaves as a primary food source or use them to build nests or cultivate other organisms on which they feed (IMENES; IDE, 2002). In any case, traces are left on the leaf surface that can be visually perceived. Although each species has its mandibular characteristic, the traces of damage caused by them are difficult to distinguish due to the size of each bite, whose magnitude is millimetric. In addition, observed damage may result from consecutive biting actions that overlap the injury and generate damage compositions of different sizes and shapes on the leaf surface. Figure 1.3 shows simulated leaf damage caused by different species of chewing insects and mollusks. In a purely visual assessment, it is difficult to relate the damage to the right defoliator without having the labels or annotations at hand.

The third problem involves building low-cost computational models with lightweight processes for systems with limited processing power and memory. Although there are trends to modernize equipment, access is very limited or expensive, making the application of high-cost solutions unfeasible for many agricultural producers. Modeling effective and low-cost solutions is essential to ensure access to the most modern tools for monitoring and decision-making in farming businesses. However, computationally ef-

---

[1]The insect leaf predation dataset is publicly available. See Appendix A.

(a) *Anticarsia gemmatalis (Insecta: Lepidoptera: Noctuidae) (Caterpillar)*

(b) *Phylum of Mollusca (slugs and snails) (Gastropods)*

(c) *Rhammatocerus schistocercoides (Orthoptera: Acrididae: Gomphocerinae) (Grasshopper)*

(d) *Diabrotica speciosa (Coleoptera: Chrysomelidae) (Green cow)*
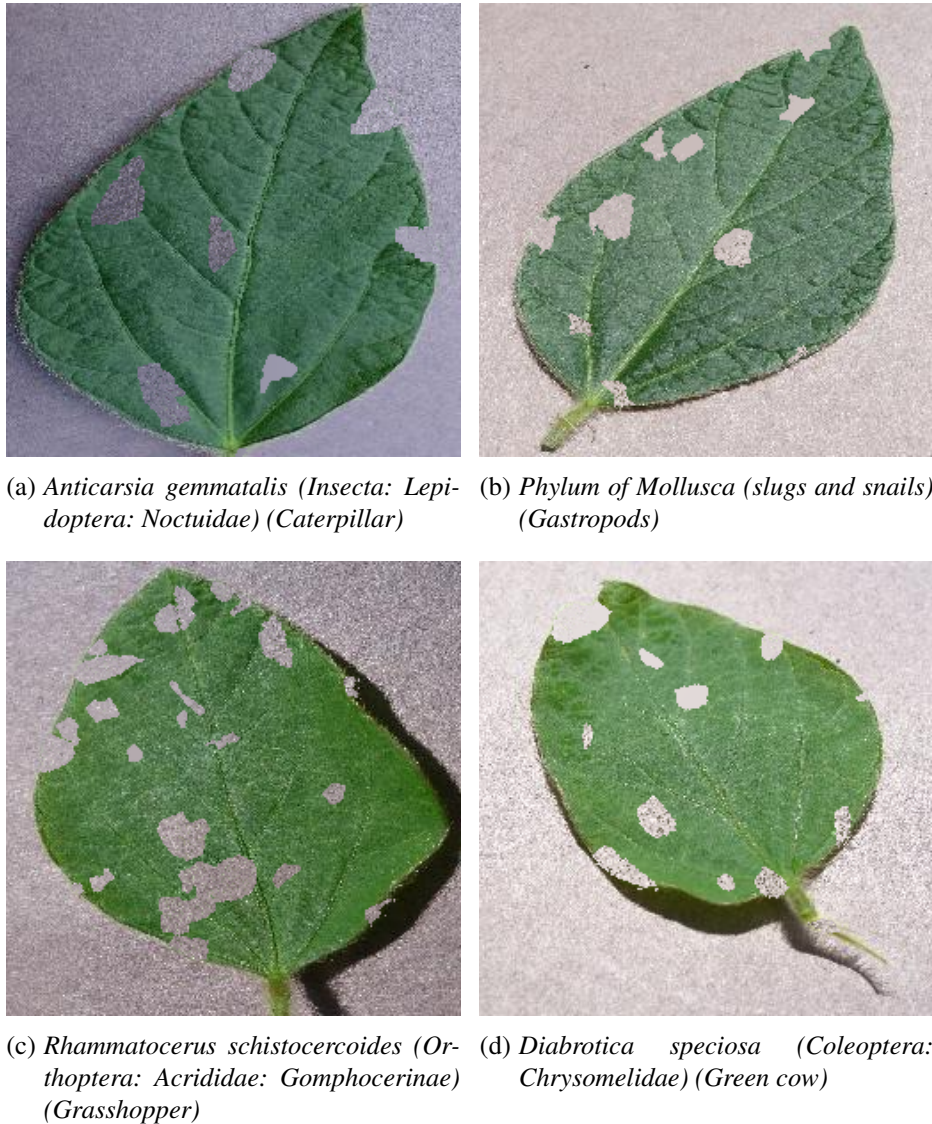
Figure 1.3: *Simulated leaf damage caused by different pests on soybean leaves*[1].

ficient methods requiring little computational power must present results as assertive as those produced using cutting-edge techniques. Therefore, low-cost models must be efficient considering computational limitations and perform comparably to modern tools.

The fourth problem is the limitation of image datasets with samples of damaged leaves caused by herbivory. Image databases are necessary because computational models encode the most relevant features of target objects so that the recognized patterns are used in categorization or prediction tasks. An appropriate set of exemplars is required to identify common properties between objects, and observing selected patterns makes it possible to build representative models. Therefore, to build computational models, it is necessary to have databases with significant samples of the objects of interest, which can be a major challenge in modeling systems for agriculture. For example, a plant species may have different leaf shapes depending on its level of maturity. Genetic modifications in

plants lead to changes in leaf shape, and various leaf damage can make pattern recognition difficult. Furthermore, it is quite complex to build databases with foliar damage caused by insects and other pests as they can vary in stages of development, species, and severity of the damage caused. To overcome these challenges, researchers have presented leaf reconstruction approaches based on artificial filling and applying synthetic alterations that simulate foliar predation.

1.3 Questions

The research problems can be summarized into four questions:

1. How can we trace the contour of the leaf surface when the foliar silhouette is compromised?
2. Is it possible to find out which defoliator caused the leaf damage considering only the bite traces?
3. What computer techniques are suitable for preparing efficient and low-cost algorithms for leaf analysis?
4. How can we simulate defoliation and prepare image datasets with leaf samples of damaged leaves?

1.4 Hypothesis

To answer the research questions, we formulated four hypotheses as follows.

1. The leaves have a certain "standardization" in shape, which can be used to find foliar patterns.
2. Each pest produces its own "marks" when feeding so that traces left on the leaf surface indicate the pest that caused the damage.
3. Template matching is a qualified technique to perform efficient and low-cost solutions for leaf analysis.
4. A reasonable way to simulate the diversity of damage caused by defoliation processes is by using actual samples of pest bites.

1.5 Aims

In this thesis, we investigate the development of leaf analysis models for estimating leaf loss, detecting damaged areas, reconstructing leaf surfaces, and classifying

pests according to their bite traces. In this sense, we aim to prepare computer-based solutions for precision agriculture with attention to lightweight computing processes with high assertiveness and algorithms capable of generalizing to different crop species.

More precisely, we investigate the following research topics related to the agricultural area:

1. Measurements of foliar damage caused by herbivory.
2. Estimate of leaf damage for planning agricultural management actions.
3. Demarcation of compromised leaf areas, including edge regions.
4. Preparation of visual inspections of injured leaf areas in addition to numerical evaluations.
5. Classification of pests in farming.

Also, we investigate the following research topics related to the computing area:

1. Digital image techniques for image analysis.
2. Pattern recognition based on template matching.
3. Similarity evaluation between pairs of images.
4. Image segmentation, object detection, and image restoration.
5. Image classification with machine learning algorithms.
6. Performance of experimental tests considering assertiveness and execution time.

1.6   Methodology

The research methodology used during this work consisted of the following steps:

- Literature review with research on leaf analysis, precision agriculture, and modeling of computer-based solutions for agriculture.
- Investigation of digital image processing techniques in leaf analysis studies and outcomes provided by computer vision approaches.
- Researching public databases to identify useful data for leaf analysis research.
- Construction of algorithm projects with attention to implementing lightweight processes and high-performance programs for leaf analysis.
- Development of software architectural models with code modularization and self-contained functionalities.
- Planning and implementing algorithms capable of simulating leaf damage caused by crop defoliators.
- Formulating experimental tests to evaluate the computational models presented in this research study.

- Preparation of comparative essays with related works considering quantitative and qualitative aspects.
- Organization and presentation of research results as scientific papers for publication in journals and international conferences.

1.7   Contributions

This thesis results from investigative research on constructing computational models for precision agriculture, whose central focus is the automation of leaf analysis through computing processes. This study examines four main aspects of foliar analysis: measurement of leaf loss caused by herbivory, detection of predation on plants, foliar reconstruction of injured leaves, and pest classification. Each of the examined points led to the development of algorithms suitable for executing automated tasks in which results are obtained without human intervention or expert dependence.

The presence of experts is significant for decision-making in agricultural management. Greater levels of specialization result in greater prosperity. However, specialized professionals can be challenging to find. As farming is generally far from large urban centers, hiring committed employees to conduct fieldwork can be difficult. For this reason, computational tools for leaf analysis are essential to reduce human labor and operational costs with tedious manual operations and increase accuracy with subjectivity-free processes (MACHADO *et al.*, 2016; ZHANG *et al.*, 2022a; YANG *et al.*, 2023).

Subjectivity in leaf analysis tasks can be risky, leading to inaccurate information and mistaken judgments (SILVA *et al.*, 2019). Depending on the crop size, the number of leaf samples can be ample to represent a significant population group. As the work increases and the pressure to deliver results is accentuated, the quality of the information can be notably compromised. Process automation assists in tasks requiring significant data sets and supports assessments by experts, indicating points of attention for more in-depth analysis. This work presents solutions based on image processing techniques, computer vision, and machine learning to automate leaf analysis processes.

The desired automation faced some challenges inherent to operating with digital images. Image acquisition can lead to variations in image scale, positioning of target objects at different viewing angles, and sensitivity to noise and lighting (ROCHA *et al.*, 2022; TANG *et al.*, 2022). To address these issues, we model the programs to work independently of the scale, rotation, or noise applied to leaf images. Additionally, we explored solutions for analyzing leaves with damage in the edge region. Some existing solutions from related work present poor performance for leaf edge damage or were not designed for this task (MALOOF *et al.*, 2013; EASLON; BLOOM, 2014). In this thesis, we present leaf analysis models in which image acquisition can be performed

without restricted control, and good performance can be achieved even in leaf samples with damage in the edge region. Also, we developed algorithms for generating synthetic damage on leaves with actual damage characteristics.

Another highlight of this work is the concern with building computational models with cohesive software components and lightweight processes suitable for smart farming. Low-cost models are crucial for agricultural environments with limited computing resources and processing power (INTARAVANNE; SUMRIDDETCHKAJORN, 2015; PIVOTO *et al.*, 2018; ROCHA *et al.*, 2022; LIN *et al.*, 2022). In this sense, we measure the results in terms of the effectiveness and efficiency of the proposed methods for automatic leaf analysis. The experiments present highly assertive results and involve the timely execution of models. Furthermore, we explored the models in different plant species, verifying that our work can be extended to various crops while maintaining similar execution time and accuracy. The models' ability to generalize is a crucial characteristic that enables their use in different planting scenarios, from large to small cultivation areas and different plant species.

While similar works focus only on numerical information (SILVA *et al.*, 2019; SILVA *et al.*, 2021), our work presents visual results that enable insights from the presentation of compromised leaf regions. Our programs identify attacked leaf areas, segment bite traces, restore injured leaves, and classify pests. Among the new features, we highlight the visual representation of the lost leaf area, the delineation by bounding boxes of leaf damage, tracking of herbivory lines, and restoration of leaves consumed by defoliators to representations before predation. Furthermore, we highlight the classification of pests based on bite traces. To the best of our knowledge, we started the discussion on categorizing pests through records of mandibular damage on plants by applying machine learning models in the prediction when we published the paper "Automatic Detection of Insect Predation Through the Segmentation of Damaged Leaves" (VIEIRA *et al.*, 2022).

Research involving the classification of pests seeks characteristics that uniquely identify each of the pest categories (DENG *et al.*, 2018; CHENG *et al.*, 2017; SHEN *et al.*, 2018). Databases with insect images are used, and computational learning models are used to recognize insects in crops. In practice, these models are challenging because they require the preliminary capture of insects in which traps must be prepared and strategically positioned. These traps use attractive pheromones that work for some but not all insect species. Therefore, choosing the appropriate bait is also a relevant task. For camera monitoring systems, classification using images of pests is also complex because they can move fast, be camouflaged or grouped in clusters, be hidden in holes, or be so small that they are unnoticeable. For this reason, we work from another perspective. We use leaf damage caused by defoliators to classify pests whose bite signatures are used to train learning models. This way, we do not need to capture herbivorous pests and deal

with the complexity of planning traps and collecting specimens.

Another contribution of this thesis is the scientific paper published with partial results of this investigative study. For each of the results achieved, we describe the motivating context, model the proposals, specify the algorithms, prepare experimental tests, perform data analysis, discuss the observed results, and suggest future work. This way, we organized and presented papers, publicized our algorithms, prepared databases with leaf damage, and implemented original software.

In summary, the main contributions of this thesis are:

- Estimate leaf damage caused by herbivory.
- Detecting predation on leaves.
- Segmentation of bite traces.
- Pest classification based on bite signatures.
- Modularized computer programs for leaf analysis.
- Leaf analysis methods based on image processing, computer vision, and machine learning.
- Algorithms for leaf analysis with implementation of synthetic leaf damage and assessment metrics.
- Computer models with high performance and assertiveness.
- Scientific production with research results.
- Publication of computer codes and image database with leaf damage.
- Original software publication.

1.8   Organization of the Thesis

This thesis is divided into eight chapters, where the first and last one deal with the introduction and conclusion of the research work. Also, the thesis contains an appendix that presents original papers, software, and datasets developed by the authors. To present an overview of each of the internal chapters (2–7) and the appendix, we present some topics of interest and their content below.

In Chapter 2, we present a method for leaf reconstruction based on artificial filling. An initial task is to determine the compromised leaf regions, demarcate them, and apply image restoration algorithms. The injured leaf region is estimated by comparing the damaged leaf with image templates constructed with images of healthy leaves. The best template is used to draw the missing leaf area. From delineating the compromised leaf area, we investigated two filling techniques: image blending and image inpainting. The results are compared and presented visually and numerically. The motivation for this chapter is to enable experts to compare leaf loss with image representations that precede

defoliation. Another motivation is the increase in databases with images of reconstructed leaves as opposed to the discarding of injured leaves from leaf image databases.

In Chapter 3, we present a new version of the method explained previously, but this time for detecting leaf predation and segmenting insect bite traces. In the previous version, we used different variations of healthy leaves to build the image templates. The main problem with that approach was memory consumption, which considerably limited the size of image templates. In this updated version, we removed the variations to healthy leaves to free up memory space and reduce execution time when checking correspondence between image pairs (injured leaf versus template images). Even so, the method consistently detected and segmented leaf predation regions. Also, we explore the model with variations in image scale, image rotation, noise addition, and different percentages of leaf damage. Despite this, the method achieves significant results in other scenarios, such as the variations experienced.

In Chapter 4, we expand the method for estimating leaf loss. With the distinction of leaf areas consumed by defoliators, we counted the existing leaf area and compared it with the compromised leaf regions to calculate the percentage of defoliation. The experiments indicate a strong linear correlation between the estimated and actual values of leaf loss (ground truth). They also show the ability of the method to estimate foliar damage at low or high defoliation percentages. Unlike previous versions of our programs that used images in Red, Green, Blue (RGB) format to represent image templates, we started using image templates as binary images. We then reduced the execution time in the similarity-checking operations between images and the amount of memory to store the templates. In this version, we also achieve results comparable to related works and maintain high accuracy in calculating the percentage of leaf damage.

In Chapter 5, we keep improving the method for estimating leaf damage. We noticed that image segmentation between background and region of interest (foreground) led to misinterpretations when spurious elements appeared as target objects (leaf area). With this observation, we stopped using Otsu segmentation and started using a segmentation model based on deep learning. Furthermore, we made changes to the model by adopting the area of the intersection divided by the union as a measure of similarity between image templates and injured leaves – Intersection over Union (IoU). Previously, we used distance metrics such as Earth Mover's Distance (EMD) or subtraction of intersection areas. Another new feature applied to the model is processing template images and damaged leaves with the convex hull operator. In this step, points from a binary image are used to find the smallest polygon whose perimeter encloses all leaf points in an image. We added this step to standardize the images so that the shape of injured leaves would be even closer to the leaf templates. We carried out experiments and noticed the improvement of the method in terms of assertiveness in calculating the percentage of leaf damage.

In Chapter 6, we present our leaf analysis software capable of estimating the percentage of defoliation, detecting compromised leaf areas, and reconstructing leaf surfaces. Although these features are the three main requirements, we also describe our algorithm for leaf damage simulation and provide different evaluation metrics that can be used to measure the program's accuracy and compare related studies. Throughout scientific research, we developed several algorithms and organized, documented, and made them public to the entire community. In this way, we present the software architecture, demonstrate its functionalities, describe the solution's impact, indicate the program code repositories, and show details about the license, version, and implementation language. This chapter combines the three functionalities described in previous chapters into a single solution. All functionalities were integrated, maintaining cohesion and low coupling, and new comparative studies were carried out considering the most current version of the method.

In Chapter 7, we compare deep learning models for classifying pests based on leaf damage. Initially, we identify insects and mollusks causing economic loss in the cultivation area and collect samples of damaged leaves caused by these pests. Then, we prepare leaf damage templates and apply them to images of healthy leaves to simulate defoliation processes. These steps were used to build a database with injured leaves for each selected pest. We use this database to train convolutional neural network classifiers and verify the learning models' ability to classify image samples of bite traces correctly. The promising results reveal the feasibility of identifying pests in farming using only the bite marks found on injured leaves. We explore this idea, show the models' aptitude to generalize to unseen data, and point out the potential of this strategy for agricultural production environments. The experimental tests show high assertiveness and motivate the continuation of this investigative study in other plant species and pest categories. Additionally, we publish the database used in the experiments and indicate intentions for future work.

Except for Chapter 7, whose manuscript is being prepared for submission to a journal, the other chapters were published in conferences and journals, as presented below.

- **Chapter 2**

    Vieira, Gabriel Da Silva, Naiane Maria de Sousa, Bruno Rocha, Afonso U. Fonseca, and Fabrizzio Soares. "A method for the detection and reconstruction of foliar damage caused by predatory insects." In 2021 IEEE 45th Annual Computers, Software, and Applications Conference (COMPSAC), pp. 1502-1507. IEEE, 2021. (VIEIRA *et al.*, 2021)

- **Chapter 3**

    da Silva Vieira, Gabriel, Bruno Moraes Rocha, Afonso Ueslei Fonseca, Naiane Maria de Sousa, Julio Cesar Ferreira, Christian Dias Cabacinha,

and Fabrizzio Soares. "Automatic detection of insect predation through the segmentation of damaged leaves." Smart Agricultural Technology 2 (2022): 100056. (VIEIRA *et al.*, 2022)

- **Chapter 4**

  Vieira, Gabriel S., Afonso U. Fonseca, Bruno M. Rocha, Naiane M. Sousa, Julio C. Ferreira, Juliana P. Felix, Junio C. Lima, and Fabrizzio Soares. "Insect predation estimate using binary leaf models and image-matching shapes." Agronomy 12, no. 11 (2022): 2769. (VIEIRA *et al.*, 2022)

- **Chapter 5**

  Vieira, Gabriel S., Afonso U. Fonseca, Naiane Maria de Sousa, Julio C. Ferreira, Juliana Paula Felix, Christian Dias Cabacinha, and Fabrizzio Soares. "An automatic method for estimating insect defoliation with visual highlights of consumed leaf tissue regions." Information Processing in Agriculture (2024). (VIEIRA *et al.*, 2024)

- **Chapter 6**

  Vieira, Gabriel S., Afonso U. Fonseca, Julio C. Ferreira, and Fabrizzio Soares. "ProtectLeaf: An insect predation analyzer for agricultural crop monitoring." SoftwareX 24 (2023): 101537. (VIEIRA *et al.*, 2023)(VIEIRA *et al.*, 2022)

- **Chapter 7**

  Vieira, Gabriel S., et al. Soybean Pests Classification and Foliar Predation Recognition Using Bite Traces. The manuscript is being prepared for submission to a journal.

Appendix A presents a list of original papers, software, and image datasets prepared by the authors, and Appendix B shows authorizations for reusing the published papers presented in this thesis.

During the research period, we investigated other agricultural research lines and relevant topics in retrieval information and disparity from stereo images. We were also involved with a research team that investigated computer applications in classifying human diseases, interaction using smartwatches, super-resolution images for crop line imagery, sugarcane classification, detection of plantation lines, skew angle correction in text images, and saliency methods and volume estimation of trees. A list of the research results can be found in Appendix A. Besides that, some original software is presented with descriptions and links to the repositories. The computer programs were designed to support crop monitoring activities, retrieve images from large-scale data sets, compute disparity from image pairs, and detect and segment tree crowns. Furthermore, new image

datasets for estimating defoliation, classifying pests, computing disparity in rural and semi-rural environments, and segmenting trees are presented in that section.

In summary, Appendix A presents a list of 6 scientific papers directly related to this thesis, 12 papers prepared by the Ph.D. candidate on other research topics, and 30 papers in contributions with research partners. In addition, 5 original software programs prepared by the authors and 4 new datasets developed during this research are made available to the scientific community.

1.9   Behind the Scenes

Every story starts somewhere, and this one begins with a visit. I was teaching when a co-worker knocked on my classroom door and called me. I excused myself from the students and stood at the door. The professor who called me started talking about his work on estimating leaf loss and the importance of this topic for agriculture. I was pretty excited because the subject was unknown to me, and the motivation immediately seemed very relevant. After he spoke, I asked him to give me a few days to put into practice some ideas that were emerging in me while he was speaking. I went back to my class, but my thoughts stayed there.

After a few days of implementing some algorithms, I had something to show. I called that colleague and showed him what we could do using image processing and computer vision for the problem he was investigating. Then, that was his turn to get excited. We kept going in a good conversation, and I told him we would need a database with images to continue the work. He said it would not be a problem as he always took pictures of leaves in agriculture and showed me some of them.

After a few days, we met again. Suddenly, everything that was going very well then fell apart. He told me he talked to one of his agronomist colleagues. His colleague said that what we were doing was very simple and that he could do it. Given his other colleague's interest in carrying out the research, the partnership we had started a few weeks before was broken. That was frustrating, and worst of all, the promised image database never came, so we had to look for alternatives.

At that time, I was working on other projects and had put aside the research proposal for leaf analysis. We were researching the construction of disparity maps with stereo images of trees and were getting our first results. My friend Bruno Rocha invited me to work on his planting row detection project, and I immediately made myself available. In a short time, we achieved good results by preparing automatic methods for analyzing aerial images obtained by unmanned aerial vehicles. My friend Naiane Maria was researching saliency in images and invited me to work with her on applying saliency

methods to segment images of rural environments. We worked together, and we obtained exciting results.

Some study possibilities also emerged through study exchange programs. We applied to the International Max Planck Research School for Intelligent Systems (IMPRS-IS) with a project to develop autonomous drone flight algorithms and to the Fulbright educational exchange program with a project to detect and classify lung diseases. We also applied for the Google Awards with a proposal to detect tree trunks using supervised methods. Unfortunately, we were unsuccessful in any of them, but they were unique experiences in seeing all the processes being carried out and how rigorous they are. As there is a reason for everything, I realized the best thing was to stay in Brazil since shortly after, we were faced with a global pandemic, and the borders were closed. Home is the best and safest place to stay in any circumstances.

Due to the proposal submitted to Fulbright, I began working more closely with my friend Afonso Fonseca to develop computer-assisted methods for analyzing medical images. This was a very productive partnership, and we achieved really cool results. Likewise, I began to delve deeper into the work of my friend Juliana Félix, and we wrote some papers on the automatic classification of amyotrophic lateral sclerosis. Also, I started following the tree diameter estimation research developed by Wellington Galvão, the work on improving aerial images of plantations by Emília Nogueira, and the work on gesture recognition on smartwatches by Thamer Nascimento. Those were very productive moments, only possible thanks to the leadership of Professor Fabrizzio Soares.

During that time, I prepared for the qualification test. At this stage of the studies, I needed to present my research intentions, expected results, and an execution schedule to an evaluation panel. After the presentation, it was not what I expected. Many points should be improved to make the study proposal viable within my deadline. Professors Gustavo Laureano and Ronaldo Costa, with my advisor, Fabrizzio Soares, gave me crucial directions, but I still had a long way to go. Suddenly, two days later, I received an email about a subject I still did not know about. I read an article about content-based image retrieval systems, and it was what I needed to direct my research on the right path. Shortly afterward, we achieved good results and published some articles on this subject.

We were pretty excited and decided to return to the problems related to leaf analysis and wrote a paper with the results we already had. At that time, I was under the positive influence of the Computer Science Seminar course taught by Professor Rogerio Salvini. We talked a lot about delivering complete results for publication and avoiding fragmentation of work. Then, we sent our manuscript to a journal, and in the first round, we received the message that the article was too long, so it was rejected. What could have been a problem for other people, my advisor and I saw a great opportunity. Thus, there was no way we divided the work, published partial results, and compiled the outcomes

that gave rise to this doctoral thesis.

Reconstruction of Foliar Damage Caused by Predatory Insects

> Get up, take up your bed, and go to your house.
>
> *Matthew 9:6*

Management of agricultural production and rural activities have been supported by recognizing machine learning patterns and algorithms, as in the automation of leaf analysis. However, leaf border damage compromises leaf structures, making it difficult to estimate the lost contours. Effects caused by predatory insects are difficult to monitor by inspection processes, and the harmful results caused by them can deteriorate the performance of machine learning models. In this sense, plant leaves that are not fresh or intact are avoided. Consequently, the number of samples for use in training steps is reduced, leading to problems with data balancing and limited generalization models. This chapter presents an automatic method for reconstructing an injured leaf at a probable stage before defoliation. Also, the proposed method provides visual results that allow the agronomic analyst to verify the regions of leaf damage and the components of the basic leaf structure affected by predatory insects. Based on the experimental results, we conclude that the proposed method can accurately delimit the injured leaf silhouette and restore the leaf regions affected by herbivory attacks. This chapter was published at the International Conference on Computers, Software, and Applications (COMPSAC) (VIEIRA *et al.*, 2021a).

2.1 Introduction

Agriculture businesses move billions of dollars every year in many countries. In Brazil, agricultural activities were responsible for 21.4% of the Gross Domestic Product (GDP) in 2019 (BRASIL, 2020). In 2020, Brazil surpassed the largest soybean producer in the world, the United States, with a production of 126 million tons with an average price

of $409 per ton (USDA, 2020e; INDEX MUNDI, 2020). In the same year, led by China and the United States, corn reached a record price of $362 per ton, something that has not been seen since 2015 (USDA, 2020c). The production of fresh deciduous fruits, such as apples, grapes, and pears, increased compared to previous years and the production of stone fruits exceeded expectations in Turkey and the European Union (USDA, 2020a; USDA, 2020b).

Despite the promising results, world consumption of agricultural products is expected to increase significantly in 2021. In this sense, leaf analysis is one of the tasks that has generated helpful information for agricultural production and, consequently, to meet global demand. As the leaf area is responsible for the photosynthesis process, the growth of the plants and the filling of the grains can be monitored through visual inspections of the state of the leaves, which enables more precise crop management, such as the application of insecticide.

However, the effects caused by predatory insects are difficult to be monitored by inspection processes. Leaf damage in border regions compromises leaf structures, making it difficult to estimate the lost contours. There are approaches for this task based on computer-based solutions, but with some limitations. (MACHADO *et al.*, 2016) developed a mobile application for the quantification of leaf herbivory that depends on the user's ability to interact with it, and (SILVA *et al.*, 2019) developed a deep neural network model to estimate the level of defoliation but that requires several artificial simulations of leaf damage and a large number of images for the training stage.

Furthermore, computer identification of plant species generally ignores samples with marginal and severe damage to prioritize fresh and intact plant leaves (BARRÉ *et al.*, 2017; WÄLDCHEN; MÄDER, 2018). As the performance of machine learning classifiers can change due to samples with variations in leaf shape, color, and texture caused by damage, leaf images are selected considering their original shape and appearance (CARRANZA-ROJAS; MATA-MONTERO, 2016). On the other hand, these classifiers require samples in sufficient quantity for each class in the data set, and the exclusion of samples can generate imbalanced data, also deteriorating the overall performance of the machine learning models (HUSSEIN *et al.*, 2020). Consequently, leaf reconstruction could significantly contribute to expanding the number of samples. In classifying injured leaves, they could be reconstructed before the identification process, increasing the chances of an assertive classification (HUSSEIN *et al.*, 2021).

To deal with the limitations of related works and contribute to this field of study, we developed a computational method to reconstruct the contours of the leaf edge and restore the foliar canopy. The proposed method does not depend on the user's expertise to obtain the desired results and uses a few leaf samples to construct an image model. Besides, the proposed method provides visible results that allow the agronomic analyst

(a) *injured leaf*   (b) *boundaries*   (c) *reconstructed leaf*
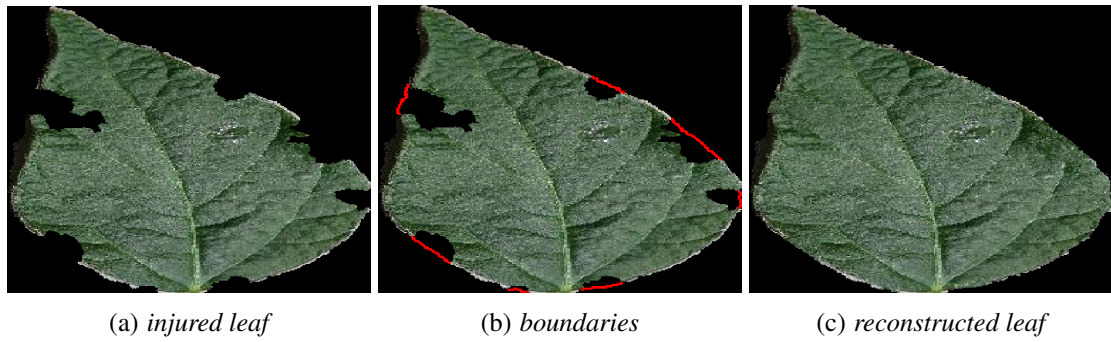
Figure 2.1: *An overview of the proposed method. For an injured leaf (a), the boundaries of the damaged area are automatically traced (b), and the leaf shape is recovered (c).*

to verify the regions of occurrence of leaf damage and the components of the primary leaf structure affected by predatory insects. Figure 2.1 illustrates the edge of a leaf being traced and the result of the reconstruction process for an initially damaged leaf.

This study presents an automatic method for reconstructing an injured leaf at a probable stage before defoliation. We focus on leaf edge restoration by structuring a method capable of determining the damaged area and reconstructing the damaged leaves in a format similar to the original one. The novelty of our method is that it uses computational vision and digital image processing techniques combined with geometric leaf properties and statistical measurements to present a simple, inexpensive, and robust solution that can effectively contribute to decision-making in cultivars.

Our main contributions are as follows:

- automatic detection of damaged leaves caused by insect herbivory;
- visual reconstruction of the damaged regions through artificial filling;
- a versatile approach that works properly in a variety of cultivars;
- a useful application to support agricultural management decisions based on foliar analysis.

The remaining organizational structure of this chapter is as follows: Section 2.2 summarizes the related work. Section 2.3 presents the method provided in detail. Section 2.4 describes the experiment setup as the database used, input parameters, and evaluation metrics. Section 2.5 provides experimental results and analysis. Finally, in Section 2.6, we draw our conclusions and suggest ideas for future work in this field.

2.2   Related Work

Computer-based techniques are often applied to fill missing or damaged regions in digital images. Restoration processes are used to recover images affected by natural

degradation or when artifacts need to be removed with visual preservation of the original images. There are several useful image restoration applications (KHAN *et al.*, 2018), especially in precision agriculture, where they play a significant role in improving the quality of pictures obtained from unmanned aircraft, poor quality videotape, and blurred satellite images (CHICKERUR *et al.*, 2010).

The detection of pest attacks on plants makes it possible to identify regions of damaged leaf areas, which is beneficial in the quantification of damage caused by insects and subsequent management and treatment of possible infestations (MACHADO *et al.*, 2016; SILVA *et al.*, 2019). In leaf damage detection approaches, the compromised area is estimated so that the total leaf area can be recognized and the missing parts can be noted and analyzed.

In this sense, Zhao *et al.* (2012) developed an algorithm for the recognition of damage in oilseed rape leaves. Bradshaw *et al.* (2007) used digital scanners and image manipulation software to estimate the leaf surface area that was damaged by insect herbivory. Liang *et al.* (2018) identified methodologies for estimating leaf border and defoliation percentage in soybean plantations. Machado *et al.* (2016) developed a mobile application to quantify leaf damage using digital image processing techniques. Besides that, Silva *et al.* (2019) used convolutional neural networks to estimate missing areas on injured leaves.

The proposal prepared by Hussein *et al.* (2021) stands out among the works related to our study. The authors investigated leaf reconstruction so that damaged leaves could be recovered to increase the sample number in constructing learning models. Although the results are promising, in this approach, the regions of foliar damage need to be indicated in the form of training masks. Therefore, leaves with damage on leaf edges may require the manual preparation of these masks, which is very laborious and tedious.

Unlike related works, our proposal was designed to work regardless of the cultivar type. We show through experimental results that our method works on various crop species important for global trade, such as soybean, corn, and fresh deciduous fruits. Furthermore, the proposed method is fully automatic and requires only a few leaf samples to build an evaluation model. The method does not require specialized equipment and uses only digital images acquired by conventional RGB cameras. Our approach also uses digital image processing techniques as performed in the related works. In addition, we deal with restoring the leaf boundary and shape through manipulation and artificial filling of the compromised leaf area.

2.3 Method

Our pipeline for the reconstruction of damaged leaves consists of six cohesive steps that can be seen in Figure 2.2, whose descriptions are presented in the following sections.

```
┌─────────────────────────┐
│   Leaf Segmentation     │
└─────────────────────────┘
             │
             ▼
┌─────────────────────────┐
│  Leaf Feature Detection │
└─────────────────────────┘
             │
             ▼
┌─────────────────────────┐
│    Leaf Adjustment      │
│  & Model Construction   │
└─────────────────────────┘
             │
             ▼
┌─────────────────────────┐
│ Leaf Sample Preparation │
└─────────────────────────┘
             │
             ▼
┌─────────────────────────┐
│  Similarity Evaluation  │
└─────────────────────────┘
             │
             ▼
┌─────────────────────────┐
│ Leaf Canopy Reconstruction │
└─────────────────────────┘
```
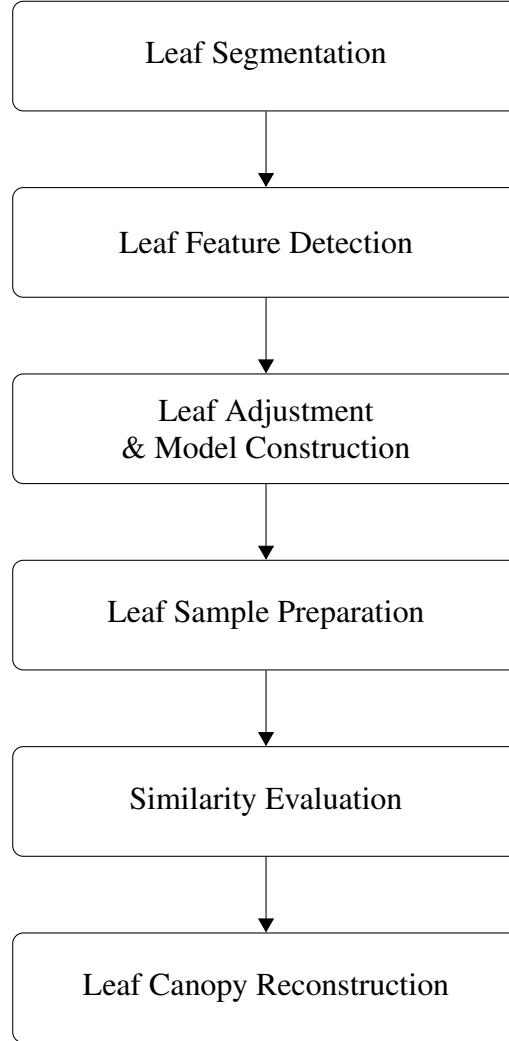
Figure 2.2: *Architecture components of the proposed method.*

2.3.1 Leaf Segmentation

In this step, we segment the leaf region from the image's background. Initially, we use an image filter in the original image through the median and average convolution processes, both with a kernel size equal to 5×5. Then, the Green channel of the RGB image is exceeded using an arithmetic operation in which the pixel values of the Green channel are doubled and subtracted from the Red and Blue channels ($\mathbf{G}' = 2\mathbf{G} - \mathbf{R} - \mathbf{B}$). Then, the Otsu threshold method (OTSU, 1979) is applied, and the binary image obtained is used to exclude the non-leaf regions from the original image (Figure 2.3(b)).

2.3.2 Leaf Feature Detection

We identified leaf features from their geometric shape and morphological structure in this step. Here, two approaches are employed. In the first, the interior pixels of the leaf are removed from the leaf area so that only the leaf outline, or border pixels, remain. Then, the distance between these edge pixels is calculated using the Mahalanobis distance (DODGE, 2008). In this way, we find the two pixels most distant from each other, which allows us to draw a straight line that possibly indicates the central leaf vein (Figure 2.3(c)). In the second approach, Sobel's edge detector (KANOPOULOS *et al.*, 1988) is applied over the Green channel of the original image, and a binary image is obtained. Then, this binary image is used to detect rectilinear shapes using the Hough transform (GONZA-LEZ; WOODS, 2008), which allows us to identify the other leaf veins, such as the lateral veins. Figure 2.3(d) presents some lines superimposed on a segmented leaf after applying the Hough transform.

(a) *input image*

(b) *segmented leaf*
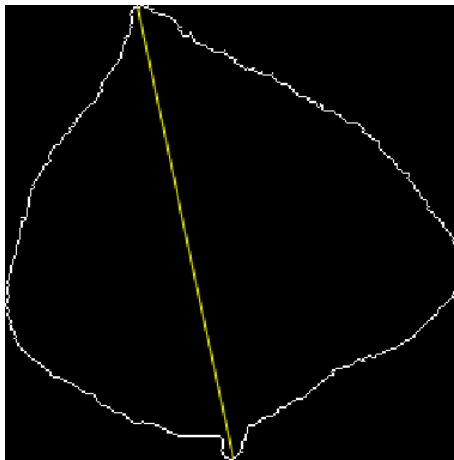
(c) *leaf margin (white) and reference line (yellow)*
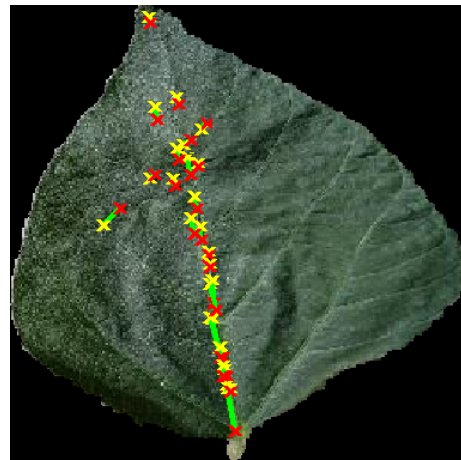
(d) *detected features after Hough transform.*

Figure 2.3: *Leaf segmentation and feature extraction by Hough transform.*

2.3.3 Leaf Adjustment and Model Construction

The leaf images are rotated to a position where the leaf tip possibly points up or down. We used the image features obtained in the previous step (straight lines) to check the inclination of the leaves and rotate them. After the rotation, the leaf area is identified and surrounded by a bounding box. Then, the image is cropped, and the area outside the bounding box is deleted. Finally, the resulting image is resized to the original size of the initial image. This procedure creates leaf models equal to the number of image features. Figure 2.4 presents the visual results of the adjustment steps applied to an input image.

(a)

(b)

(c)

(d)
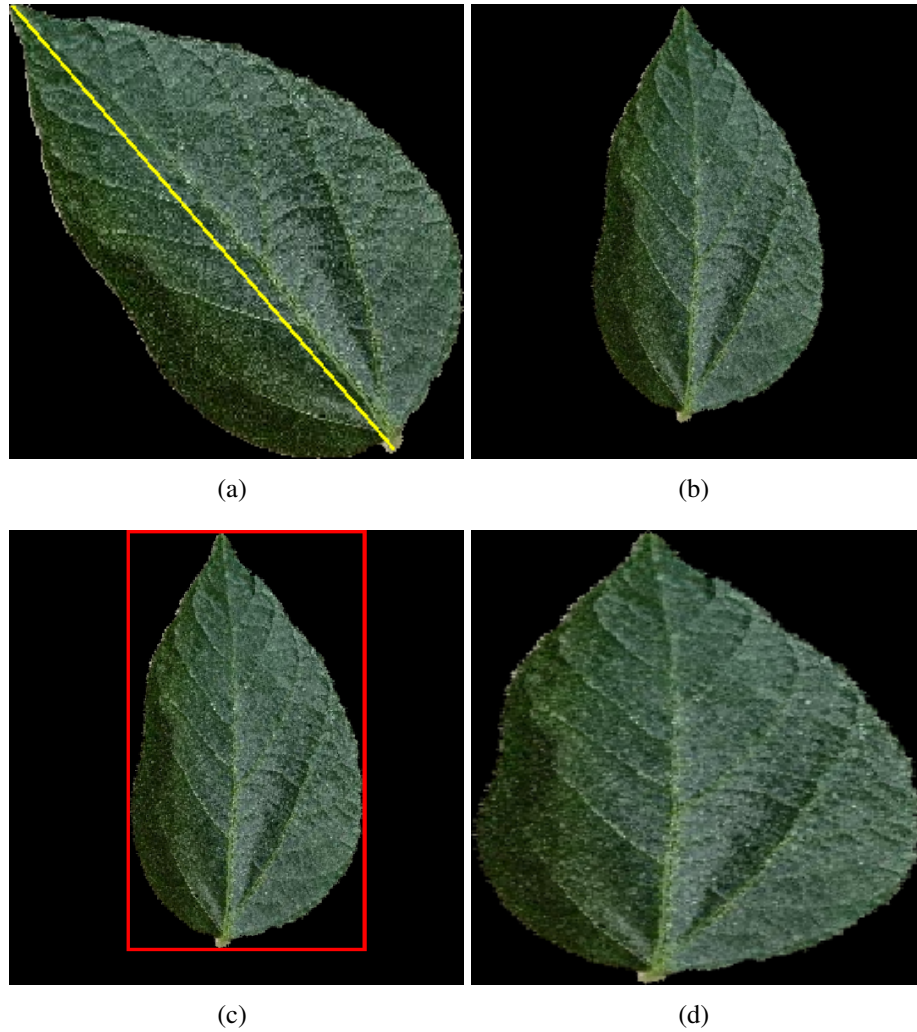
Figure 2.4: *Leaf model construction process: (a) segmented image with its reference line, (b) image after rotation transformation, (c) leaf surrounded by a bounding box, and (d) image after being cropped and resized.*

2.3.4   Leaf Sample Preparation

After positioning the input image into new positions and creating the collection of leaf models, some image templates are applied to each leaf model to simulate leaf area loss. Six templates are used to crop the leaf models' left, right, top, and bottom areas, where the reference line (Section 2.3.2) is used to guide the positioning of the templates into the images.

One of the templates removes 50% of the leaf area to the left of the reference line. Three other templates remove 50% right, 50% above, and 50% below, respectively. The remaining templates remove 25% on both the left and right sides of the leaf, while the other removes 25% on both the upper and lower sides. After this process, the leaf area is detected to select the region of interest and guide the cropping and resizing of the foliar area. Thus, six damaged leaf samples are associated with each leaf model $\mathbf{w}_r \in \mathbf{W}$.

Figure 2.5 shows some results from the leaf sample preparation process in which six defoliation samples are produced. These samples are then cropped and scaled according to leaf area detection.
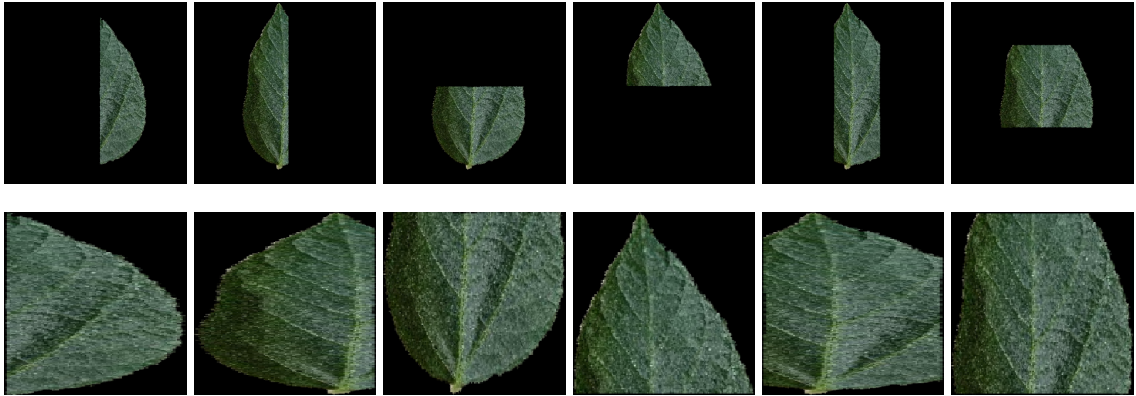
Figure 2.5: *Results of the leaf sample preparation process. The first and second lines show the results of this process before and after image cropping and resizing, respectively.*

2.3.5   Similarity Evaluation

The previous four steps are repeated for all images in a given healthy leaf image database, and the first three steps are also applied to the damaged input leaf. Each image generated from the damaged input leaf is compared to the leaf models and their damaged samples. Then, the estimated costs are associated with the comparisons made.

This comparison is performed by measuring the similarity between the distributions of the damaged leaf area with the prepared models and samples. The Earth Mover's

Distance[1] (EMD) (RUBNER *et al.*, 2000) is used, and the similarities between them quantify the proximity between the damaged leaf and the image models. To perform this evaluation and in addition to the EMD[2], we propose a cost function that evaluates the correspondence between image pairs (of size $n \times m$) using their similarities and the non-overlapping areas between them.

The three terms of Eq. 2-1 describe the proposed cost function:

$$Cost = \omega_1 + \omega_2 + \omega_3, \tag{2-1}$$

where

$$\omega_1 = EMD(\mathbf{I}_a, \mathbf{I}_b)$$
$$\omega_2 = \psi + \zeta + \phi$$
$$\omega_3 = \nu + \tau$$

and

$$F(\mathbf{I}_a, \mathbf{I}_b) = \frac{1}{nm} \sum_{i=1}^{n} \sum_{j=1}^{m} (p_{ij} \wedge q_{ij})$$

$$F_A(\mathbf{I}_a, \mathbf{I}_b) = \frac{1}{nm} \sum_{i=1}^{n} \sum_{j=1}^{m} (p_{ij} \vee q_{ij}) \wedge \neg(p_{ij} \wedge q_{ij})$$

$$\psi = F_A(\mathbf{I}_a, \mathbf{I}_b)$$

$$\zeta = F(\mathbf{I}_a, \neg\mathbf{I}_b)$$

$$\phi = F(\neg\mathbf{I}_a, \mathbf{I}_b)$$

$$\nu = F(\neg\mathbf{I}_b, \mathbf{w}_r)$$

$$\tau = F(\mathbf{I}_b, \neg\mathbf{w}_r)$$

where ψ is a function that calculates the area that is outside of the intersection between a damaged leaf model ($\mathbf{I}_a$) and the damaged input leaf ($\mathbf{I}_b$); ζ calculates the area that is in the damaged leaf model but not in the input leaf; ϕ calculates the area that is in the input leaf but not in the damaged leaf model; ν calculates the area that is in the healthy leaf model ($\mathbf{w_r}$), corresponding to the damaged leaf model $\mathbf{I}_a$, but not in the input leaf ($\mathbf{I}_b$); τ returns the area that is in the input leaf but not in the healthy leaf model.

---

[1]It is also referred to as the Wasserstein distance and the Monge-Kantorovich problem.
[2]We use the code provided by Liu *et al.* (2018) to calculate the Earth Mover's Distance.

Then, with the cost resulting from the comparison performed, the leaf model with the most minor error is the chosen one, Eq. 2-2.

$$e = \arg\min\left(Cost\right), \tag{2-2}$$

where e is the minimum error resulting from the cost function between the damaged leaf and all leaf models.

Figure 2.6 presents an example of the similarity evaluation between a damaged leaf and the template images. From the three leaf models, six defoliation samples are prepared for each one of them. The damaged leaf is compared with all templates, and the best match is used to identify the compromised area.

Leaf Models →

Defoliaiton Samples
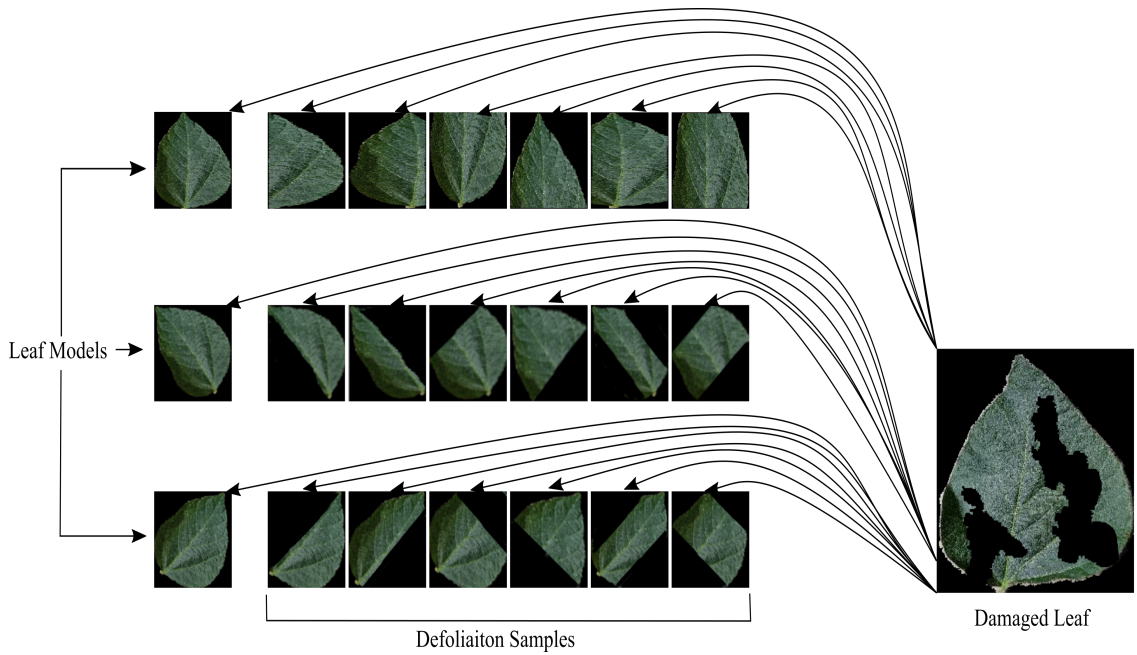
Damaged Leaf

Figure 2.6: *Comparing a damaged leaf to template images.*

2.3.6 Leaf surface reconstruction

This step converts the retrieved image model and the damaged input leaf to a binary image. In Eq. 2-3, logical conjunction is applied to the binary image **A** (damaged input leaf) and **B** (retrieved image model), resulting in **L**, a logical image with the missing areas.

$$\mathbf{L} = \neg\mathbf{A} \wedge \mathbf{B} \tag{2-3}$$

A multiresolution pyramid approach, referred to as image blending, is applied to reconstruct the damaged leaf. This technique aims to improve spatial and color consistencies between a source (retrieved model) and a target image (damaged leaf) by

using the resolution band independently, resulting in a multiresolution mixing that focuses on generating a realistic image given the composite ones (WANG *et al.*, 2017). Also, we look at image reconstruction through interpolation strategies in which an injured leaf is restored based on the values in undamaged areas. Image inpainting techniques are representative examples of this approach and belong to the area of digital image processing. This study uses the technique proposed by Bornemann and März (2007).

2.4   Materials

2.4.1   Database

We consider some crop species available in the public database prepared by Hughes and Salathé (2015) to evaluate the proposal. It is a diverse data set of leaf images obtained in various lighting conditions, including healthy and disease-affected leaves. From this database, we evaluate the proposed method considering 12 types of cultivars: Apple, Blueberry, Cherry, Corn, Grape, Peach, Bell Pepper, Potato, Raspberry, Soybean, Strawberry, and Tomato. The size of the images is 256×256.

2.4.2   Experiment setup

In the evaluation, we consider only images of healthy leaves that are transformed by an automatic synthetic defoliation method elaborated by the authors. Our defoliation approach involves extracting bite signatures in real herbivory cases and preparing foliar damage templates to promote different leaf defoliation levels. It receives a healthy leaf as input and returns a damaged leaf and its level of defoliation. It uses four random variables to determine (1) the number of insect bites to use, (2) select one or more samples from the bite models, (3) apply a rotation transformation to the selected bite samples, (4) and resize the bite samples to a random size. Besides, the defoliation level is an input parameter, and the desired defoliation level can be set from 1 to 99%.

Each crop species of the database is divided into two groups: (i) data modeling and (ii) test data, selected randomly from the number of images in the database. The first is used to construct the leaf models, and the second is used to validate the proposal. The synthetic defoliation is applied only to the test data group to sample damaged leaves at different levels from 1 to 30% defoliation. Also, 42 images are used in the data modeling group, and 30 images in the test data group for each 12 crop species under investigation.

2.4.3 Evaluation Metrics

The Structural Similarity Index (SSIM) (WANG *et al.*, 2004) is used in the tests to quantify the image quality and measure the similarity between the reconstructed leaves and their corresponding ground truth images. SSIM is standardized because the results are presented on a scale ranging from only -1 to 1, where a score closer to 1 means that the two images are very similar.

The SSIM quality assessment index is a multiplicative combination of luminance, contrast, and structural terms. The overall index (Eq. 2-4) is a multiplicative combination of measures of location, dispersion, and regularization constants.

$$\text{SSIM}(\mathbf{T},\mathbf{Y}) = \frac{(2\mu_t\mu_y + C_1)(2\sigma_{ty} + C_2)}{(\mu_t^2 + \mu_y^2 + C_1)(\sigma_t^2 + \sigma_y^2 + C_2)}, \tag{2-4}$$

where μ_t, μ_y, σ_t, σ_y, σ_{ty} are the local means, standard deviations, and cross-covariance for images $\mathbf{T}$ (ground truth) and $\mathbf{Y}$ (reconstructed leaf). C_1 and C_2 are regularization constants that avoid instability for image regions where the local mean or standard deviation is near zero. Furthermore, the average SSIM value for the test data set is:

$$\overline{\text{SSIM}} = \frac{1}{n}\sum_{i=1}^{n}\text{SSIM}(\mathbf{T}_i, \mathbf{Y}_i) \tag{2-5}$$

where n is the number of samples in the test data set.

Entropy is used to assess the texture of the reconstructed leaves concerning ground truth images. It is a statistical measure of randomness, which is defined as (ROMÁN *et al.*, 2019):

$$E(\mathbf{I}) = -\sum_{k=0}^{L-1} p(k)\log_2(p(k)), \tag{2-6}$$

where $\mathbf{I}$ is the original image, $p(k)$ is the probability of occurrence of the value k in the image $\mathbf{I}$, and $L = 2^q$ indicates the number of different intensity levels in a digital image, in our case $q = 8$.

From Eq. 2-6, the Root Mean Square Error (RMSE) is used to evaluate the difference between the entropy values of the ground truth images and the reconstructed leaf using blending and inpainting techniques (Eq. 2-7).

$$\text{RMSE}(eT, eY) = \sqrt{\frac{\sum_{i=1}^{n}(eT_i - eY_i)^2}{n}}, \tag{2-7}$$

where $\{E(\mathbf{T_1}), \cdots, E(\mathbf{T_n})\} \subset eT$ and $\{E(\mathbf{Y_1}), \cdots, E(\mathbf{Y_n})\} \subset eY$, and n is the number of images in the test data group ($n = 30$). Compared to SSIM, lower RMSE values indicate

a better fit (SOARES *et al.*, 2011).

We use the Jaccard or Intersection-Over-Union (IoU) index to measure the accuracy of the leaf canopy reconstruction. Commonly applied in the evaluation of segmentation processes, this index allows us to verify the area of overlap between predicted segmentation and the ground truth. It is a straightforward metric that ranges from 0 to 1 ($0 - 100\%$) with 0 signifying no overlap and 1 signifying perfectly overlapping segmentation. The IoU similarity coefficient of two sets A and B is expressed according to Eq. 2-8:

$$\text{IoU(A,B)} = \frac{|A \cap B|}{|A \cup B|} \tag{2-8}$$

where A corresponds to the leaf area of the reference image (ground truth) and B the leaf area of the damaged leaf after reconstruction.

Likewise, we use the Dice index, or F1 score, to verify the similarity between the reconstructed images in relation to the ground truth. In this metric, as in IoU, the coefficient will be equal to 1 if the sets are equal and 0 if they are disjoint. Eq. 2-9 describes this evaluation metric.

$$\text{Dice(A,B)} = \frac{2|A \cap B|}{|A| + |B|} \tag{2-9}$$

where $|A|$ and $|B|$ represent the cardinal of set A and B, respectively.

2.5   Results and Discussion

In our proposal, leaf reconstruction is a process that approximates an image with leaf damage to a healthy leaf. Harmonizing these images, in terms of image blending or image inpainting, allows us to create a visual representation in which an injured leaf is recovered at a stage before defoliation.

In evaluating leaf reconstruction, we compared the reference images (ground truth) with the two digital image processing techniques selected for this study: image blending and image inpainting. The results indicated a slight improvement in the reconstruction process through the interpolation of images; however, it was not far from the other model under analysis. The image blending obtained $\overline{SSIM}$ values from 0.24 to 0.63 and the image inpainting from 0.24 to 0.64. It also shows that image inpainting improved over image blending, which indicates that other image inpainting techniques can be investigated in future work.

Table 2.1 presents the average SSIM obtained by each of the 12 cultivars observed in this study. The proposed method obtained the best results with corn leaves, reaching an SSIM value of 0.64. Cherry and grape also showed promising results with

Table 2.1: *Leaf reconstruction evaluation: Average and Standard Deviation of the SSIM scores.*

	Image Blending	Image Inpainting
Apple	0.242 ± 0.070	0.242 ± 0.073
Blueberry	0.379 ± 0.064	0.376 ± 0.065
Cherry	0.520 ± 0.099	0.525 ± 0.100
Corn	0.637 ± 0.120	0.642 ± 0.125
Grape	0.513 ± 0.067	0.518 ± 0.068
Peach	0.368 ± 0.119	0.368 ± 0.119
Pepper	0.401 ± 0.050	0.402 ± 0.052
Potato	0.403 ± 0.086	0.406 ± 0.088
Raspberry	0.434 ± 0.074	0.440 ± 0.070
Soybean	0.327 ± 0.044	0.330 ± 0.046
Strawberry	0.464 ± 0.054	0.464 ± 0.056
Tomato	0.310 ± 0.086	0.312 ± 0.089

values of 0.52 and 0.51, respectively. Despite the diversity of samples and diversified lighting, the other cultivars achieved results above 0.24. Also, the extent of leaf damage can explain the high standard deviation of cherry, corn, and peach. As the damage becomes more severe, the image reconstruction quality tends to be reduced.

Table 2.2 shows the rates of assertiveness in the reconstruction of missing leaf areas. The IoU values were higher for corn and potato, which reveals that the proposed method estimate reached 98% and 89% accuracy, respectively. Soybean and strawberry also achieved important results in which leaf canopy could be restored in 87% and 89%. According to the Dice index, the similarity measured between the reconstructed leaf and the ground truth was also high for pepper and grape, whose values were above 86%. Moreover, IoU and Dice indexes show that assertiveness was lower in apples and tomatoes, with percentages close to 80%. On the other hand, peach presented the lowest result, which can be explained by the shading effect in the database, which greatly limited the segmentation process. The shadow treatment may be applied in future works to obtain

Table 2.2: *Leaf area reconstruction: IoU and Dice scores.*

	IoU (%)	Dice (%)
Apple	81.7	89.7
Blueberry	86.5	92.7
Cherry	82.9	90.3
Corn	98.5	99.2
Grape	87.0	93.0
Peach	66.0	78.2
Pepper	86.0	92.3
Potato	89.5	94.3
Raspberry	85.9	92.2
Soybean	87.9	93.5
Strawberry	88.9	94.0
Tomato	80.1	88.7

better results.

Figure 2.7 shows the average *Entropy* scores for each crop species in which the values listed correspond to the statistical properties of the reference images ($\mathbf{T}$) and the reconstructed images ($\mathbf{Y}$). The results show that the entropy of the reference images is very similar to those obtained with the leaf reconstruction process. Besides, it shows no significant difference between the techniques employed since the entropy values for the image blending and image inpainting are close and above 90%. Nonetheless, according to Figure 2.8, the image inpainting achieved the lowest error, which indicates that other image inpainting techniques can be investigated in future work.

Upon visual inspection, we observed that the proposed method accurately delimits the injured leaf silhouette. The damage in border regions is recovered, which makes it possible to identify the areas where insect predation occurred. Comparing the image reconstruction techniques, we observed that the image blending better preserved the leaf vein structures. In contrast, the image inpainting smoothed the reconstructed regions, making the perception of the leaf veins unfeasible.
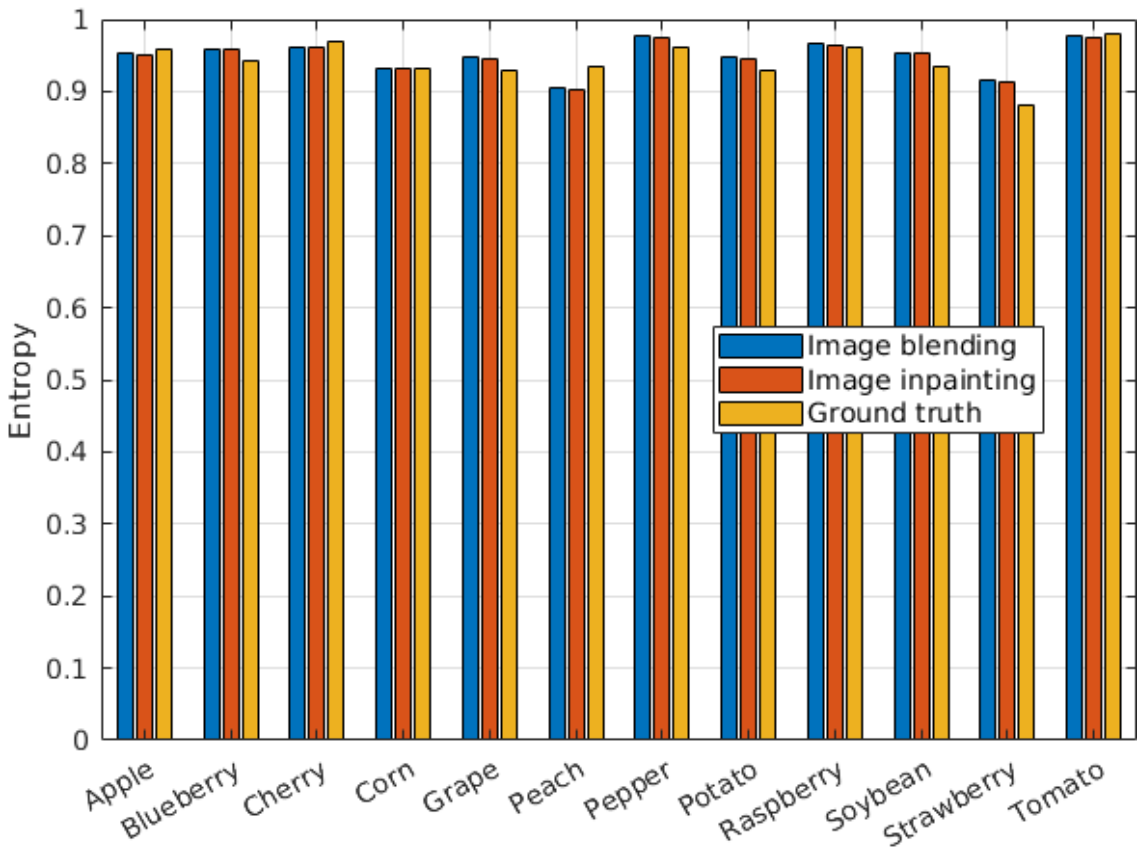
Figure 2.7: *Leaf reconstruction evaluation: Entropy scores.*
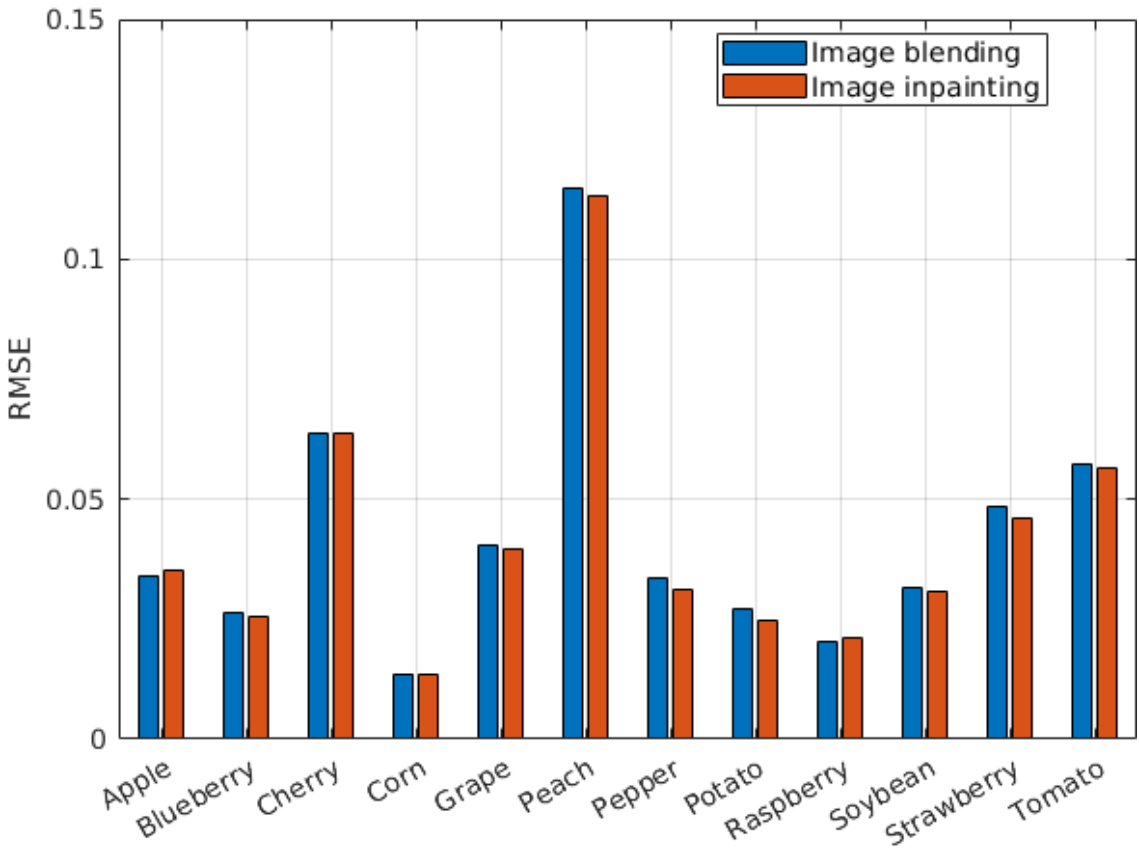
Figure 2.8: *Leaf reconstruction evaluation: RMSE scores.*

Figure 2.9 presents an example of a damaged leaf, the image model that best matches it, and the reconstructed leaves after image blending and inpainting techniques. Figure 2.10 shows a sample of each crop species with visual results achieved after applying our leaf reconstruction method using image blending and inpainting. It is important to note that even for low SSIM values, the image reconstruction process correctly fills the regions of leaf damage. The results are so promising that the reconstructed leaf images visually resemble the undamaged leaves in an almost undetectable manner.

(a) *Damaged leaf.*   (b) *SSIM = 0.59*

(c) *SSIM = 0.65*   (d) *SSIM = 0.68*
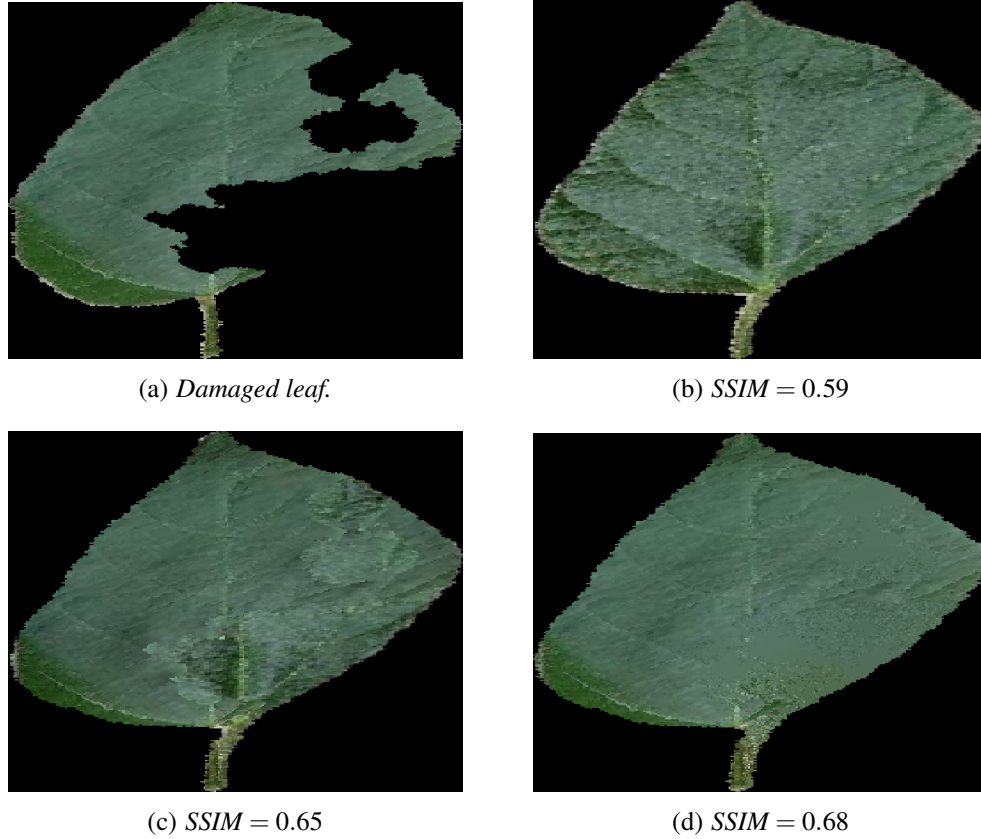
Figure 2.9: *Leaf reconstruction examples: (a) Damaged leaf, (b) the best matching model, (c) reconstruction with image blending (WANG et al., 2017), (d) reconstruction with image inpainting (BORNEMANN; MÄRZ, 2007).*

We can assert that our proposal can effectively estimate missing leaf regions based on the results. Our strategy to build the leaf model proved adequate to represent a set of leaves from a crop. Likewise, the preparation of leaf samples at six levels of defoliation expanded the model to make it robust for the similarity assessment step. The adopted procedures made the proposed method capable of dealing with digital image problems such as scale, rotation, and noise. In this way, the database used in the evaluation showed that our approach achieved significant results even in the diversity of leaf design, crop species, and positioning and lighting of the image samples. However, we observed that we could obtain better results if leaf samples were more homogeneous, avoiding
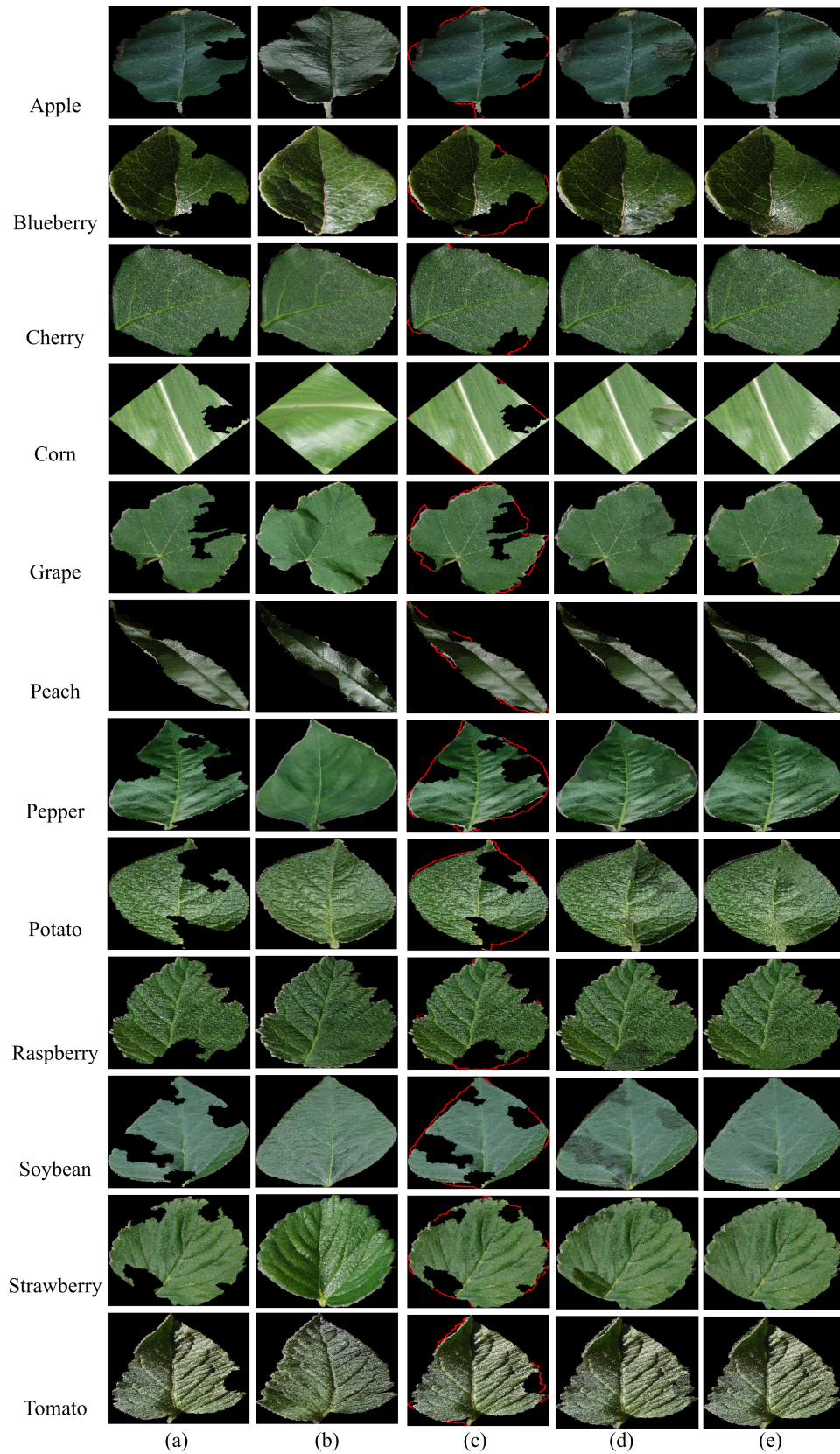
Figure 2.10: *Edge restoration and leaf reconstruction using image blending and inpainting. (a) injured leaf by predatory herbivores, (b) retrieved image model, (c) leaf border reconstruction, (d) blending, (e) inpainting.*

overestimating and underestimating damaged areas. On the other hand, actual situations of foliar analysis consider some pattern, such as selecting samples in a determined plant position or samples extracted from the same genetic group. This procedure can bring greater homogeneity to the leaf analysis, increasing the assertiveness of the proposed method. Finally, we point out that the segmentation strategy may not be appropriate for leaf samples with a complex background. Therefore, this is a step that needs to be improved in future work.

2.6   Conclusion

This chapter presented an automatic method for reconstructing an injured leaf at a probable stage before defoliation. We focused on the problem of leaf edge restoration by structuring a method capable of reconstructing damaged leaves to a format similar to their original shape. The results indicate a satisfactory reconstruction in which the damaged leaf edge can be effectively recovered. In addition, the injured leaf area can be filled, allowing visual analysis of the regions affected by herbivory. In evaluating leaf reconstruction, the method achieved results above 40% for most cultivar understudy types and an SSIM value equal to 64% for corn leaves. In this sense, the proposed method can contribute to monitoring crops to avoid losses due to excessive damage caused by predatory insects, as well as maximize the usefulness of images by increasing the number of individual leaf samples.

Automatic Detection of Insect Predation Through the Segmentation of Damaged Leaves

I am the vine, you are the branches.

John 15:5

Leveraged by the production of grains, oilseeds, and fresh deciduous fruits, food production has reached new heights, exceeding the amount produced in previous years and with an estimate of new records for the coming years. In this sense, technological advances are essential to reduce costs and increase quality and productivity. This chapter presents a novel method to detect insect predation on plant leaves that uses geometric leaf properties and digital image processing techniques to construct image models. Unlike other approaches, our method detects and highlights the regions of leaves attacked by insects and segments the contours of insect bites. We evaluated our proposal considering 12 crucial crops for the world market, and it demonstrated to be effective, even in the presence of noise, image scale, and rotation. Besides, it identifies insect predation areas regardless of the plant species with precision above 90% in blueberry, corn, potato, and soybean leaves. Thus, this chapter introduces a new approach to automatic leaf analysis and contributes to reducing human effort in identifying the occurrence of pests. This chapter was published in the Journal of Smart Agricultural Technology (VIEIRA *et al.*, 2022).

3.1   Introduction

The activities performed in agricultural fields respond to high value-added businesses, which are economically important in producing grains, oilseeds, ornamental and medicinal plants, and green vegetables. World soybean production reached 336.59 million metric tons (Mmt) in 2019/2020, moving 31.2 billion U.S. dollars, with only the United States production of 96.67 Mmt (USDA, 2020e). Although lower than the production of 2018/2019, Corn production reached $1,116.2$ Mmt, with an average price of around

$362 per ton, the highest since August 2015 (USDA, 2020c). Centrifugal sugar production reached 166.17 Mmt, in which Brazil has been leading the world production in the last five years with production above 29.92 Mmt (USDA, 2020d).

In the same way, fresh deciduous fruits and stone fruits play an important role in global food production. In 2020, China was the largest producer of apples, grapes, and pears, launching more than 62 million tons of these fruits in the domestic consumer market (USDA, 2020a). Furthermore, that same year, the European Union and Chile exported the most significant number of peaches and cherries, totaling 395 metric tons (USDA, 2020b).

The improvement of technologies for automation contributes significantly to agricultural production, making it more effective and sustainable through intelligent support for decision-making, operation, and farming management (PIVOTO *et al.*, 2018). Methods for detecting leaf damage and monitoring insects in farming are examples of computer vision and machine learning techniques to address real problems that can cause significant losses in the production process. Therefore, if an attack of insects is detected in advance, the management of solutions can be more accurate, saving resources, safeguarding cultivation, potentially increasing yield, and protecting crops.

Detecting insects allows the analyst to verify occurrences of losses above expectations and carry out mitigation and control actions. This verification is necessary to distinguish between situations of normality in which the ecosystem is in balance and when the population growth of certain species becomes a risk factor for agricultural development. Because of this, some proposals focus on insect detection and classification through computer learning systems where several samples of insects are collected to build classification models using machine learning algorithms (KASINATHAN *et al.*, 2020; LU *et al.*, 2019; THENMOZHI; Srinivasulu Reddy, 2019).

Although detection systems make it possible to identify the presence of insects in plantations, it is difficult to infer from them the line that crosses population normality and the outbreak of a given species. Among the factors that limit these solutions, the mobility of insects between plants stands out because as they move, there may be different records for the exact specimen in various plants, and vision systems may not be able to record their presence when they move fast or are camouflaged, hidden and in clusters. On the other hand, damage caused by insects is limited to the location of the injured plants, which can be used to direct foliar analyses and verify the crops' local and global health, even in the absence of the insect that induced the losses. From there, inferences about the ecological balance can be made.

In this sense, we propose a novel approach to identifying insect predation marks and point out the places where leaf damage occurs. Therefore, we do not detect insects; we only detect the damage they cause. It is a way of treating the same problem innovatively to identify the occurrence of insects in the plantation, even with their absence. Thus, it makes

our method more versatile as it can detect damage of different proportions, including damage to leaf border regions and pest incidence to varying stages of development.

Quantifying the number of damaged leaves is a potential use of the proposed method that can answer questions related to insect population growth, the ability of plants to develop in the face of predators, and whether there is a potential risk to crop yields. In these cases, the previous analysis would justify interventions to reduce losses and re-balance the ecosystem in the crops. Furthermore, the bite trace segments presented as an output of the proposed method enable the analyst/specialist through visual inspection to determine the category of insects, for example, differentiating leaf-chewing insects (e.g., caterpillars) from leaf-cutting insects (ants, leafcutter bees, grasshopper, and others).

Our method uses geometric leaf properties and digital image processing techniques to construct image models. Initially, healthy leaves are used as input in the model construction process. Then, with the constructed models, an injured leaf is processed, and the image model that best fits it is selected and used to detect the damaged leaf areas and segment the insect bites. The strategies used in this proposal demonstrated effectiveness in the presence of noise and geometric distortions caused by image acquisition processes, in detecting insect predation in different foliar structures and morphologies, and in segmenting insect bites in low or severe defoliation.

We evaluated our proposal considering 12 critical crops for the world market, including soybean, sugarcane, corn, apple, grape, peach, and cherry. We explore different levels of defoliation in a vast and diverse set of leaf images and investigate the behavior of our method in computer vision challenges, such as image rotation, scale variation, and noise. Due to the assertiveness of the proposed method, the results are promising to assist experts, agronomists, ecophysiologists, and farmers in making better decisions in cultivars, including insecticide evaluations and proper crop management.

The main contributions of the proposed method are:

- A novel method for recognition of insect attack on plant leaves.
- A systematic approach to highlighting insect-damaged leaf regions.
- A synthetic defoliation strategy using real insect attack cases.
- A methodology for evaluating line segmentation approaches (insect bite traces).

The remainder of the chapter is organized as follows. Section 3.2 summarizes existing studies of insect predation in farming. Section 3.3 introduces our proposed method in detail. Section 3.4 describes vital information about the experimental design, such as the database used and evaluation metrics. Section 3.5 provides the experimental results and analysis. Section 3.5.6 presents the results. Finally, the work done is concluded in Section 3.6.

3.2   Related Work

Several works use digital image processing and machine learning algorithms to identify pests in different crops. Wang *et al.* (2012), for example, classified insects using digital images in which a manual processing approach was performed to remove the background and highlight only the insect region. Thus, feature extraction was applied to the insect images previously segmented to obtain information about the insects' body radius, body shape parameter, color complexity, head size, and thorax. Then, the acquired data was indexed to classify the insects using Support Vector Machine (SVM).

Similarly, Wen and Guyer (2012) presented an automatic method for identifying insects in digital images using local and global features. The Scale-Invariant Feature Transform (SIFT) was used to identify and record local features into a histogram. Also, a color-based clustering segmentation method was applied to obtain global information, such as the shape and contour of the insect. The K-means cluster separated the insect area from the background and the insect shape, texture, and colors corresponding to 54 global features and 100 local features for each image. These local and global features were used to categorize the images using five different classifiers (Minimum Least Square Linear, Normal Densities Base Linear, K-Nearest Neighbor Classifier, Nearest Mean, and Decision Tree).

Xie *et al.* (2015) also used the descriptors of color characteristics (color histogram), texture, shape (United Moment-Invariant), SIFT, and Histogram of Oriented Gradients (HOG) to obtain image features. The SVM classifier labeled the images using Multiple Kernel Learning (MKL). In the same way, Yang *et al.* (2015) developed a system to detect owlfly insects based on the contours of their wings. In this proposal, the image background was manually removed using graphic editing software, and the image was transformed into grayscale and binarized to separate the contours of the insect's wings. Furthermore, the C-Support Vector Classification algorithm was used to classify the images.

Thenmozhi and Reddy (2017) presented a method to detect the presence of insects in sugarcane crops. Initially, RGB images were converted to grayscale, and the images were divided into smaller regions to determine the edges or boundaries using Canny, Sobel, Gaussian HPF, and Prewitt Edge detection filters. Then, the feature extraction strategy was performed using boundary form, surface, and textures of insects, and the classification was performed to evaluate the similarity of the body of insects concerning some geometric shapes such as triangles, circles, and rectangles.

In Deng *et al.* (2018), the detection of insect pests was based on the human visual system in which the FastICA Efficient Projection Map was used to detect the region of interest (ROI). Then, the processed images were normalized, and the Otsu method was

applied to find the threshold that could better define the ROI. Next, Gabor Filters were applied to detect edges, and the SIFT and Local Binary Pattern (LBP) were used to extract gradient and texture orientation features, respectively. Finally, the images were classified by SVM with a radial basis function.

Another technique widely used to classify objects is deep learning. In Cheng *et al.* (2017), multiple layers of abstraction, called ResNet-10, were used to classify insects in digital images. Shen *et al.* (2018) used the Faster R-Convolutional Neural Networks (R-CNN) to segment insects in grain and categorize them. Likewise, Kasinathan *et al.* (2020), based on Convolutional Neural Network (CNN), proposed a method to classify and detect pests in the initial growth stage of corn, soybean, and wheat. Comparably, Nanni *et al.* (2020) prepared an ensemble of CNNs consisting of AlexNet, GoogleNet, ShuffleNet, MobileNetv2, and DenseNet201. These studies show that an advantage of deep learning networks is that they do not require explicit background removal to train and classify images. However, they do demand a significant number of samples to converge accurately.

Based on the related work, we can note that computer-aided approaches that deal with crop pest detection consider the identification and classification of insects for this task. Nevertheless, we propose a different investigation strategy in this study. According to Carvalho *et al.* (2014), the external-feeding fraction of insect damage has excellent potential for improving the understanding of ancient and extant herbivore communities. Thus, detecting sets of leaf damage types offers opportunities for assessing insect diversity or detecting changes in insect composition over climatic. Unfortunately, none of the abovementioned methods were developed to identify and isolate leaf damage, i.e., the bite signature caused by mandibular insects or insect-induced damage.

In this sense, in our proposal, leaf damage occurrences are identified and visually highlighted according to the regions in which they occur. Besides, the leaf damage lines formed from the herbivory are segmented to recognize bite patterns from their peculiarities. Therefore, we identified the presence of pests, considering their harmful effects, such as the exacerbated leaf damage that can inhibit the development of plants. From our perspective, plantation monitoring applications, especially real-time inspections, may benefit better from our present approach because it is easier to find samples of leaf damage in farming than the insects that produced them. This study demonstrates that our method is invariant to scale, rotation, and image noise changes. Also, a few leaf samples are required to construct an image model for detecting and segmenting insect bite marks, with particular attention to damage in leaf border regions. We evaluated the proposed method using a challenging image database that includes different cultivars and variations of leaf samples (apple, blueberry, cherry, corn, grape, peach, pepper, potato, raspberry, soybean, strawberry, and tomato).

3.3   Method

The proposed method is divided into five parts. The images are segmented in the first, and the image background is removed, preserving the leaf region. In the second, feature detectors are designed and used in the third step to build an image base with leaf models. In the fourth step, a similarity evaluator is formulated to select the appropriate image template for a damaged leaf image. Finally, the foliar damage regions are automatically detected and segmented in the last step. Fig. 3.1 provides an overview of the proposed method, described in the following subsections.

```
┌─────────────────────────────┐
│      Leaf Segmentation      │
└─────────────────────────────┘
               │
               ▼
┌─────────────────────────────┐
│        Leaf Features        │
└─────────────────────────────┘
               │
               ▼
┌─────────────────────────────┐
│         Leaf Models         │
└─────────────────────────────┘
               │
               ▼
┌─────────────────────────────┐
│      Template Matching      │
└─────────────────────────────┘
               │
               ▼
┌─────────────────────────────┐
│       Leaf Predation        │
└─────────────────────────────┘
```
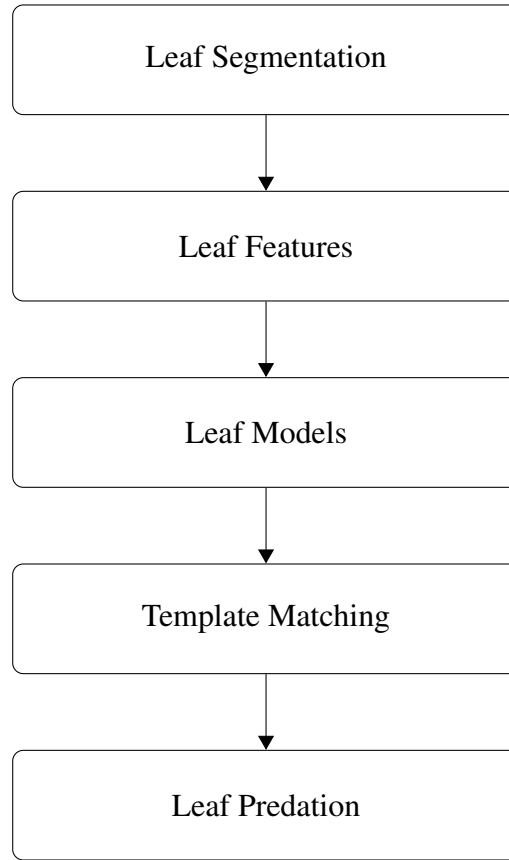
Figure 3.1: *Architecture components of the proposed method.*

3.3.1   Leaf Segmentation

The segmentation process separates the leaf region (area of interest) from the other regions of the image. In our study, each image $\mathbf{I_{RGB}}$ in the database comprises two classes that describe the leaf or background regions. We use a median filter to assist this process with a kernel κ of size 5×5. After applying this filter, we obtain new versions of the image channels, that are, $\mathbf{R}^*$, $\mathbf{G}^*$, and $\mathbf{B}^*$.

Then, we exceed the green color, $\mathbf{G}' = 2\mathbf{G}^* - \mathbf{R}^* - \mathbf{B}^*$, and the Otsu threshold method (OTSU, 1979) is applied to obtain an optimum threshold value that separates

the leaf pixels from the non-leaf pixels in $\mathbf{G}'$ and based on this step the background regions from $\mathbf{I_{RGB}}$ are removed. In this fashion, the original image is preserved without interference from the median filter applied to it and the approach of exceeding the green channel.

3.3.2   Leaf Features

The feature extraction step is performed in two ways. In the first one, the leaf geometry is used to find a line representing the length of a leaf. While the second, the edge detector, is applied to find straight line-like structural descriptors.

In the initial step, the margin of the leaf is highlighted according to a binarization process that removes interior pixels to leave only the outline of the shapes. Then, the Mahalanobis distance is used to calculate the distances $d^2 \in \mathbf{D}^2$ between the vectors v_s and $v_t \in \mathbf{V}$. The Mahalanobis distance is defined in Eq. 3-1,

$$d^2 = (v_s - v_t)C^{-1}(v_s - v_t)', \qquad (3\text{-}1)$$

where C is the covariance matrix. The vectors v_s and v_t represent the pairwise Cartesian coordinates (x, y) of the margin of the leaf, for all v_s and v_t different from each other.

Then, the index of the longest distance d^* among all vectors in the leaf border is found using Eq. 3-2:

$$d^* = \arg\max\left(\mathbf{D}^2\right) \qquad (3\text{-}2)$$

After that, the line connecting the two margin points ($A = v_s^{d^*} = (a_x, a_y)$ and $B = v_t^{d^*} = (b_x, b_y)$) represents the longest path, i.e., the length of the leaf which we refer to as the reference line.

In the second feature detection strategy, the Sobel edge detector is applied to the image $\mathbf{G}$, and the feature extraction process is performed to find straight line-like structural descriptors using the Hough transform (DUDA; HART, 1972). Due to its ability to isolate features of a particular shape, the Hough transform technique is commonly used to detect regular curves such as lines, circles, and ellipses, image analysis, computer vision, and digital image processing (GONZALEZ; WOODS, 2008).

3.3.3   Leaf Models

Those two points that define the length of the leaf points A and B, are used to adjust the leaf so that it's apex (leaf tip) or base points upwards. First, the Δ between these

two points is found using Eq. 3-3:

$$\Delta = \frac{a_y - b_y}{a_x - b_x},$$

(3-3)

Then, the inverse tangent function of Δ is calculated, and the angle of rotation θ of the leaf relative to the image plane is found (Eq. 3-4).

$$\theta = \arctan_{-90° < \theta < +90°} (\Delta)$$

(3-4)

Hence, the rotation angle θ is used to define a rotation matrix (Eq. 3-5) and to apply a planar rotation to each point $\tilde{x} \in \mathbf{I_{RGB}}$, which results in a rotated image $\mathbf{I'_{RGB}}$.

$$R = \begin{bmatrix} \cos(\theta) & -\sin(\theta) \\ \sin(\theta) & \cos(\theta) \end{bmatrix}$$

(3-5)

After the rotation transformation, the leaf area is detected and surrounded by a rectangular bounding box. This delimited area is used to crop the image to contain only the leaf parts, discarding the leafless regions. Finally, the cropped image is resized to the same size as the original image, i.e., for size, m by n, producing the $\mathbf{I''_{RGB}}$ image. The rotation angles of the lines detected by the Hough transform relative to the image plane are also used to produce other transformed images.

3.3.4 Template Matching

Template matching measures the dissimilarity between damaged leaf area distributions and the prepared image models. The earth mover's distance[1] (EMD) (RUBNER *et al.*, 2000) is used, and the dissimilarities between them quantify the proximity between the damaged leaf and the image models. To perform this evaluation and in addition to the EMD[2], we propose a cost function that evaluates the correspondence between image pairs using their dissimilarities and considering the non-overlapping areas between them.

The three terms of Eq. 3-6 represent the proposed cost function c_o.

$$c_o = \omega_1 + \omega_2 + \omega_3,$$

(3-6)

where

$$\omega_1 = EMD(\mathbf{I}_a, \mathbf{I}_b), \qquad\qquad \omega_2 = \psi + \zeta + \phi, \qquad\qquad \omega_3 = \nu + \tau$$

---

[1] It is also referred to as the Wasserstein distance and the Monge-Kantorovich problem.
[2] We use the code provided by Liu *et al.* (2018) to calculate the earth mover's distance.

and

$$F(\mathbf{I}_a, \mathbf{I}_b) = \frac{1}{nm} \sum_{i=1}^{n} \sum_{j=1}^{m} (p_{ij} \wedge q_{ij})$$

$$F_A(\mathbf{I}_a, \mathbf{I}_b) = \frac{1}{nm} \sum_{i=1}^{n} \sum_{j=1}^{m} (p_{ij} \vee q_{ij}) \wedge \neg(p_{ij} \wedge q_{ij})$$

$$\psi = F_A(\mathbf{I}_a, \mathbf{I}_b)$$

$$\zeta = F(\mathbf{I}_a, \neg\mathbf{I}_b)$$

$$\phi = F(\neg\mathbf{I}_a, \mathbf{I}_b)$$

$$\nu = F(\neg\mathbf{I}_a, \mathbf{w}_r)$$

$$\tau = F(\mathbf{I}_a, \neg\mathbf{w}_r)$$

let be $F(.,.)$ a function that averages the intersection of pixels that have true values in a binary image, for pixels $p \in \mathbf{I}_a$ and $q \in \mathbf{I}_b$. $F_A(.,.)$ is a function that calculates the area that is outside of the intersection between a damaged sample image and the input leaf; $\mathbf{I}_a$ and $\mathbf{I}_b$ are the image recovered by the method in the model and the input image of the leaf that the insect damages, respectively; ζ is the area that is in the input leaf but not in the damaged sample image; ϕ is the area that is in the damaged leaf sample but not in the input leaf; ν is the area that is in the leaf model but not in the input leaf; τ returns the area that is in the input leaf but not in the leaf model.

Then, with the cost resulting from the comparison performed, the leaf model with the minor error is the chosen one, Eq. 3-7.

$$e = \arg\min(c_o), \tag{3-7}$$

where e is the minimum error resulting from the cost function between the damaged leaf and all leaf models.

3.3.5 Leaf Predation

The margin of the damaged leaf **B** is detected to segment the insect predation areas, resulting in the logical image **B**$'$. The damaged regions **S** are detected first based on the logical conjunction operation between **B**$'$ and the retrieved image model **A** (Eq. 3-8). Hence, opening and dilating morphological operations update **S**. The opening operation is applied to remove spurious connected components with smaller pixels than β, and the dilation operation is applied to connect nearby components according to a circular

structural element of radius r. In the tests, β and r are set with 25 and 2, respectively.

$$\mathbf{S} = \mathbf{A} \wedge \mathbf{B}' \tag{3-8}$$

After applying the morphological operations, the eccentricity value of each of the remaining connected components is calculated to remove elements that have structures similar to a straight line. It is performed to prevent the damaged leaf margins from being interpreted as predation areas when the damaged leaf is smaller than the retrieved image model. The eccentricity value is calculated according to Eq. 3-9

$$E = \sqrt{1 - \left(\frac{b}{a}\right)^2}, \tag{3-9}$$

where b is the length of the minor axis, and a is the length of the major axis of an ellipse that contours a connected component in $\mathbf{S}$.

The eccentricity value E is between 0 and 1. When it is closer to 1, it is closer to being a line segment. After calculating the eccentricity, an evaluation is applied in which connected components that are more minor than a threshold t are discarded. In the tests, we define t as 0.98, a strict value so only segments similar to lines are removed. Fig. 3.2 illustrates detecting predation regions on a damaged leaf.

3.4 Materials

3.4.1 Image Database

In the experiments, we used a public database[3] prepared by Hughes and Salathé (2015). In obtaining the samples, technicians sought various lighting conditions, positioning, and foliar shapes to prepare a diverse data set of leaf images obtained in multiple lighting conditions, including healthy and disease-affected leaves. From this database, we selected healthy leaf samples from 12 plants: apple, blueberry, cherry, corn, grape, peach, bell pepper, potato, raspberry, soybean, strawberry, and tomato. The size of the images is 256×256 pixels.

3.4.2 General Setup

Each crop species in the database is divided into (1) data modeling and (2) test data. The first is used to construct the leaf models, and the second is used to validate the

---

[3]https://github.com/digitalepidemiologylab/plantvillage_deeplearning_paper_dataset
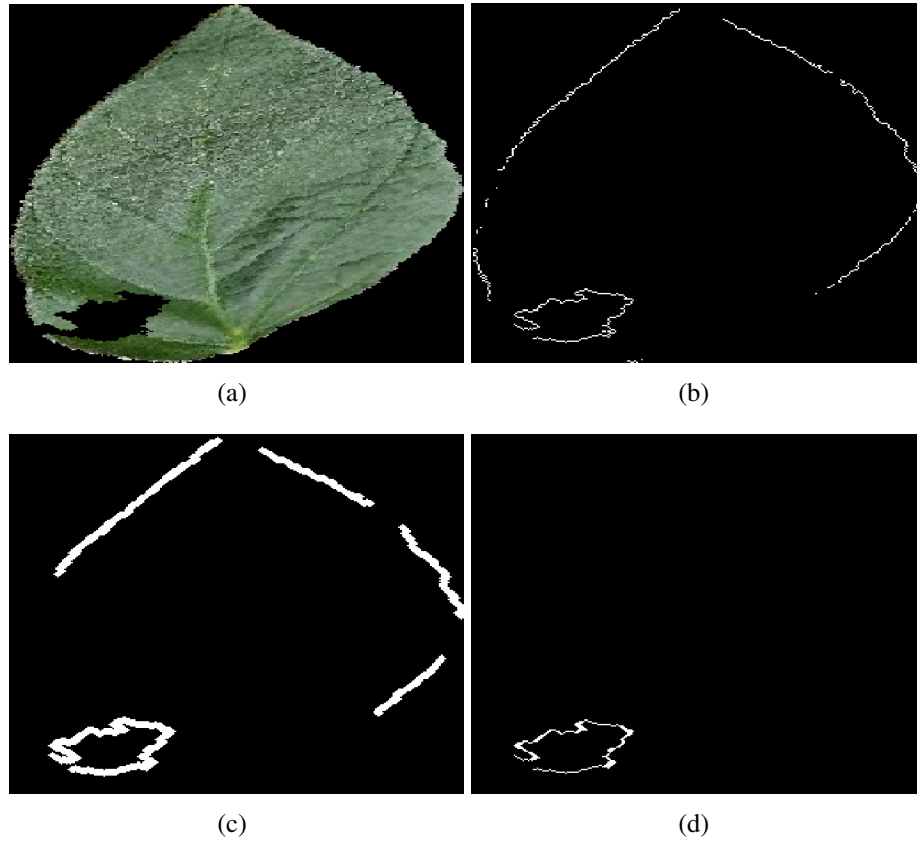
Figure 3.2: *Detection of insect predation marks: (a) damaged leaf **B**, (b) predation areas **S** after Eq. 3-8, (c) **S** after opening and dilating operations, (d) **S** after eccentricity evaluation and erosion operation.*

proposal. Tests are done individually for each leaf species, i.e., we do not mix samples from different classes. From each leaf species in the database, we select 20 leaf images to feed the data modeling group and 100 different images for the test data group. Thus, we worked with 140 images for the data modeling groups and 1.200 for the test data groups. The validation is performed using the *K-fold* cross-validation strategy, which splits the available data into K partitions, one for the data modeling group and the remaining $(K-1)$ for the test data group. In the experiments, K is set to 5, so each test is run five times.

The experiments are divided into two parts. In the first one, we evaluate the behavior of our proposal in dealing with typical computer vision challenges such as scale-variation transformations, image rotation, and noise. Furthermore, we also investigated the impact of variations in defoliation levels when using the proposed method. In this part, which includes Sections 3.5.1, 3.5.2, 3.5.3, and 3.5.4, we consider only soybean leaves to prepare the tests. In the second part of the experiment, another examination is performed to assess the capability of the proposed method in the detection and segmentation of insect predation on leaves of different crop species (apple, blueberry, cherry, corn, grape, peach, pepper, potato, raspberry, soybean, strawberry, tomato). Except for the test applied

in Section 3.5.4, the defoliation level for the composition of the test group images is randomly selected from 5% to 35%.

The accuracy of the proposed method is assessed with reference images made from healthy leaves that were automatically segmented using the image segmentation process (Section 2.3.1) and deformed to simulate leaf damage according to the synthetic defoliation strategy (Section 3.4.3). Thus, quantitative and visual inspections are obtained from different statistical measurements to compare our proposal outputs with the ground truth images.

The experiments were done in a notebook with Core i7-9750H (2.6 Gigahertz (GHz); 12 Megabytes (MB) Cache) and 16 Gigabytes (GB) Random Access Memory (RAM). As for the execution time, the entire construction process of the leaf models required 5.33 seconds for the 20 images in the data modeling group, which produced an average 48 leaf models, and 5.14 seconds to complete the process of evaluating and selecting a suitable model for each one of the features that were detected in the leaf test image. Thus, on average, each leaf in the test group has three features. The code was written using MATLAB (see Section A.1.4).

3.4.3   Synthetic Defoliation

We have prepared a synthetic defoliation strategy in which healthy leaves are subjected to a process capable of simulating insect predation. It consists of extracting bite signatures in real herbivory cases and preparing templates of foliar damage to promote different levels of leaf defoliation. The bite signature of two types of insects, *Spodoptera frugiperda* (J.E. SMITH) (LEPIDOPTERA: NOCTUIDAE) and *Chrysodeixis includens* (Walker) (Lepidoptera, Noctuidae, Plusiinae) was extracted from injured leaves, resulting in some bite samples for each of the two insects. Although the defoliation examples are based on leaf chewers insects, multiple types of damage could be equally addressed according to the type of herbivore insects, such as bud feeders, hole feeders, skeletonizers, surface abrasion feeders, and sap-sucking. Thus, it can be addressed in future studies.

We developed a computer program that receives a healthy leaf as input and returns a damaged leaf and its level of defoliation. It uses four random variables to determine (1) the number of insect bites to use, (2) select one or more samples from the bite models, (3) apply a rotation transformation to the selected bite samples, (4) and resize the bite samples to a random size. Besides that, the defoliation level is an input parameter in which the desired defoliation level can be set from 1 to 99%.
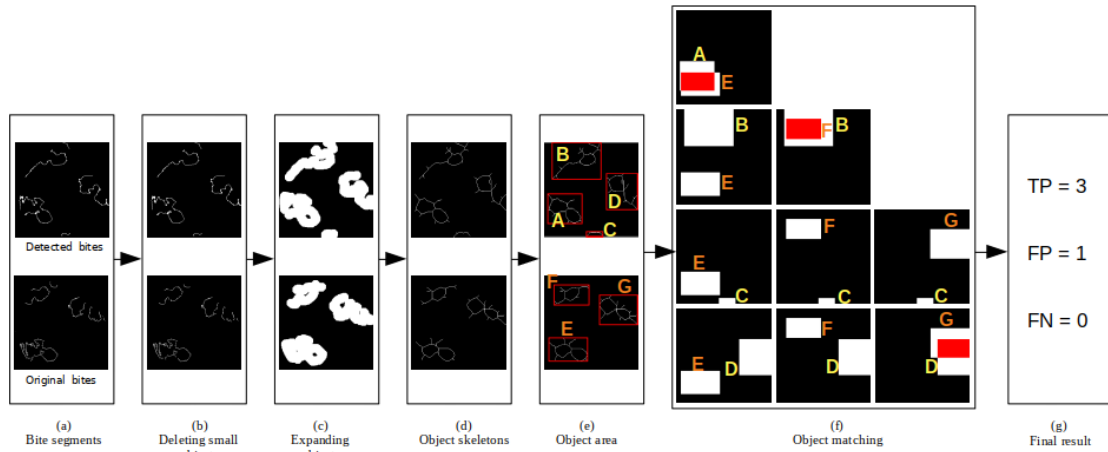
Figure 3.3: *Components of the bite segment assessment methodology.*

3.4.4   Line Segment Assessment Methodology

The evaluation of line segments (insect bite traces) considers a sequence of steps, including image transformation operations and object matching. Initially, a morphological operation is applied on both detected bite segments and ground truth image segments to remove spurious pixels, followed by a dilation operation to connect small fragments of lines. Then, the pixels at the object's boundaries are removed, and the remaining pixels constitute the image's skeleton.

The objects are surrounded by bounding boxes whose function is to mark the area occupied by these objects. Each bounding box has an identifier used to track peer-to-peer matching operations. When an intersection between a bite segment and a segment in ground truth is perceived, the intersection quality is assessed using the IoA metric (presented in Section 3.4.5). If the result is positive, it is said that a True Positive (TP) was achieved. On the other hand, if there is no match for some bite segment, it is labeled as a False Positive (FP), and if there is no match for some object in the ground truth, then it is considered a False Negative (FN). Fig. 3.3 illustrates all the steps used to evaluate bite segments.

Fig. 3.4 illustrates how this evaluation is performed. In this example, two predation regions of an injured leaf were detected. Following the ground truth, only one was correctly identified. Thus, it can be observed that for one of the segmentation results, there is a correspondence (True Positive), while for another, there is no matching (False Positive).
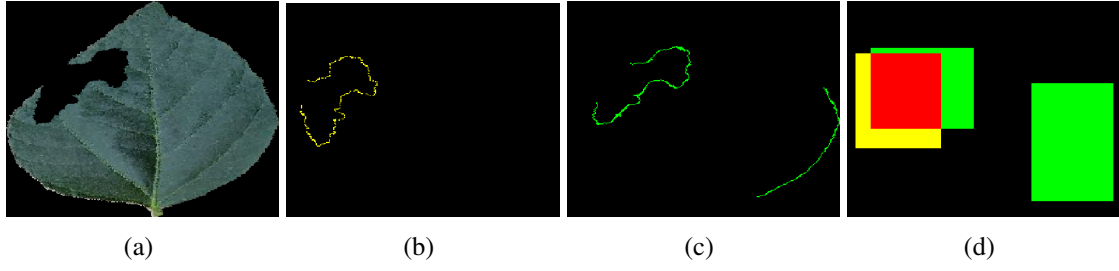
Figure 3.4: *Segmentation of insect predation marks and evaluation: (a) damaged leaf, (b) ground truth, (c) predation marks after bite detection, (d) ground truth area (yellow), predation areas (green) and the intersection between them (red).*

3.4.5 Evaluation metrics

To assess the output accuracy of our proposal, a quality factor known as Q_{seg} (SADEGHI-TEHRAN *et al.*, 2017) is used according to Eq. 3-10:

$$Q_{seg} = \frac{\sum_{i=1}^{m} \sum_{j=1}^{n} s_{i,j} \wedge r_{i,j}}{\sum_{i=1}^{m} \sum_{j=1}^{n} s_{i,j} \vee r_{i,j}}, \tag{3-10}$$

where $s_{i,j} \in \mathbf{S}$ is the retrieved leaf ($s_{i,j} = 1$) or background pixels ($s_{i,j} = 0$) and $r_{i,j} \in \mathbf{R}$ is the reference image, also in a binary format. The accuracy is based on logical operations, logical *and* ($\wedge$) and logical *or* ($\vee$), that compare the overlap between the reference image $\mathbf{R}$ and the retrieved image $\mathbf{S}$. Q_{seg} varies in a range of values between 0.00 and 1.00 in which a value 1.00 represents a perfect consistency outcome between $\mathbf{R}$ and $\mathbf{S}$ images. $\mathbf{R}$ and $\mathbf{S}$ are binary images with size *m* by *n*.

Furthermore, we compare the results between data distributions using the Kruskal-Wallis test (KRUSKAL; WALLIS, 1952), which is a non-parametric test that assesses whether the distribution functions are similar (null hypothesis H_0) or if there is any statistical difference between the functions under evaluation (alternative hypothesis H_1). A *p value* is returned, indicating which hypothesis will be rejected according to a limit of the significance level α, in our case $\alpha = 0.05$. Also, a confidence interval is calculated according to Eq. 3-11.

$$P\left(\bar{x} - Z_s.\frac{\sigma}{\sqrt{n}} \leq \mu \leq \bar{x} + Z_s.\frac{\sigma}{\sqrt{n}}\right) = \gamma, \tag{3-11}$$

where *P* refers to a probability function, $\bar{x}$, σ, and *n* are the mean value, the standard deviation, and the population sample size, respectively. Z_s is obtained from a *t-student* table regarding the confidence level γ, and μ is the unknown parameter of the average population expected to be in the confidence interval.

We also prepared a modified version of the Intersection over Union (IoU) similarity index called Intersection over Area (IoA). As conventional, in our version, the

predicted and the ground truth segments are surrounded by bounding boxes, and these areas are used to measure their overlap. However, we do not use the union of these areas. In this sense, the IoA scores either complete segments or only some parts of them so that the difference between the measured values of these two cases does not have significant differences. This property is essential for our study because the contours that represent the insect predation segments can be discontinuous and interpreted as individual segments when, in fact, they are parts of the same bite segment. Therefore, predation segments labeled by the segmentation process are evaluated individually based on the area they occupy.

The IoA similarity index is given by the intersection between the predicted predation segment and ground truth over the maximum area of predicted segments or the ground truth, Eq. 3-12.

$$IoA = \frac{\text{area}(\mathbf{Y}_i \wedge \mathbf{T}_j)}{\max(\text{area}(\mathbf{Y}_i), \text{area}(\mathbf{T}_j))} \tag{3-12}$$

where

$$\text{area}(x) = \sum_{i=1}^{m} \sum_{j=1}^{n} x_{i,j}$$

$\mathbf{Y_i}$ contains one of the i predicted predation segment area compared with all $\mathbf{T}$ areas of predation from j to the number of bites in the ground truth. Therefore, if the IoA of a bite segment is higher than 0.5, we define it as True Positive (TP). Otherwise, it is defined as False Positive (FP). Furthermore, those segments that do not match any predicted predation marks are defined as False Negative (FN).

From IoA, we used two statistical measures to evaluate the detection and segmentation of insect bite signatures. In Eq. 3-13 and Eq. 3-14, we describe the Precision and Recall measurements.

$$\text{Precision} = \frac{\text{TP}}{\text{TP+FP}} \tag{3-13}$$

$$\text{Recall} = \frac{\text{TP}}{\text{TP+FN}} \tag{3-14}$$

where TP stands for the number of segments correctly labeled as bite segments, FP represents the number of segments incorrectly labeled as a bite, and FN represents the number of bite segments not labeled as a bite. TP, FP, and FN are specified according to IoA scores.

3.5   Results and Discussion

3.5.1   Image scale variation

In this test, we simulate the variation in the positioning of cameras concerning their proximity and distance with the target objects. A factor $\lambda \in \{0.5, 0.6, 0.7, 0.8, 0.9, 1.0\}$ is used to resize the test data image group where a smaller value for λ decreases the size of the images, and a value of 1.0 means that the images are in their original size. Figures 3.5(a) to 3.5(d) presents visual examples of this process.

(a) $\lambda = 1.0$	(b) $\lambda = 0.8$	(c) $\lambda = 0.7$	(d) $\lambda = 0.5$
(e) $\theta = 0$	(f) $\theta = 90$	(g) $\theta = 180$	(h) $\theta = 270$
(i) $\eta = 0.08$	(j) $\eta = 0.16$	(k) $\eta = 0.24$	(l) $\eta = 0.40$
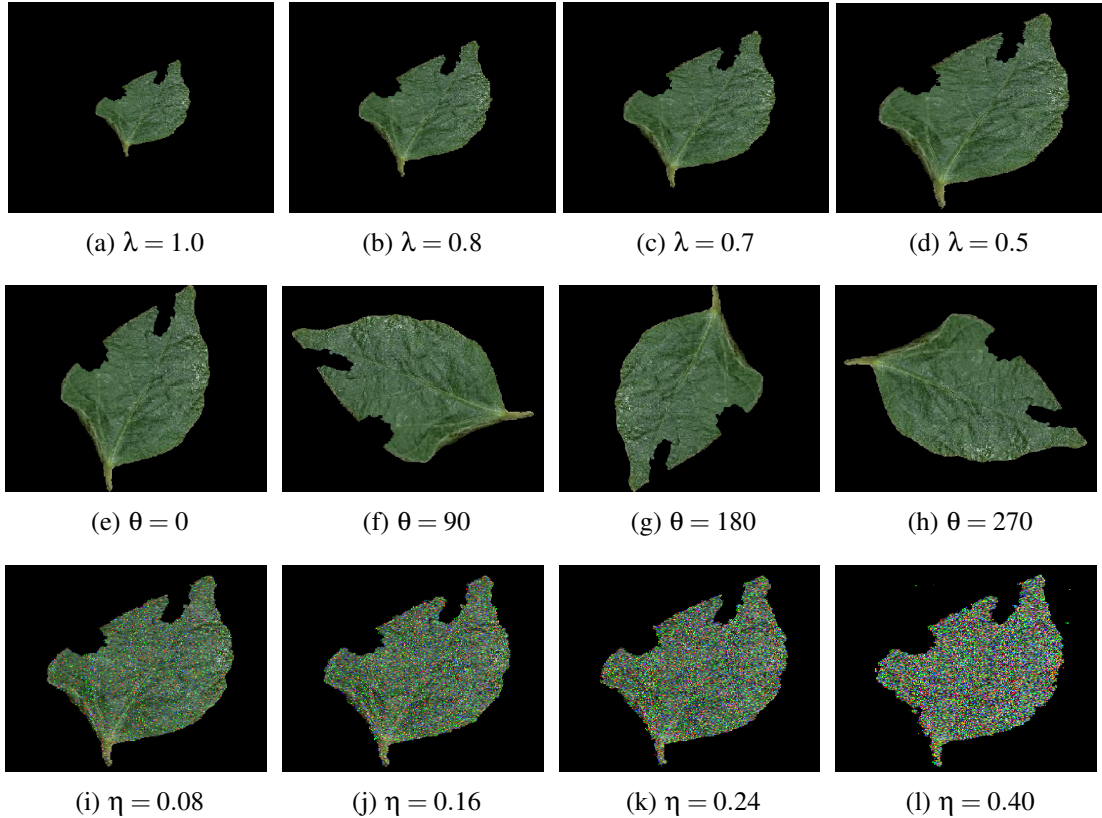
Figure 3.5: *Scale, rotation, and noise variation. These samples are presented after the segmentation process and with* 06.04% *defoliation.*

Although the scale factor applied to the images significantly affects their resolution, the proposed method reaches similar results, even with this factor variation. For example, Fig. 3.6 shows that the median of the tests has similar results, which is confirmed by a Kruskal-Wallis $p = 0.95$. Therefore, even with scale variation, the proposal obtains satisfactory responses.

3.5.2   Image rotation transformation

Continuing with the camera positioning simulation, we investigate the effect of rotational transformations either by the camera or by positioning the target objects. A
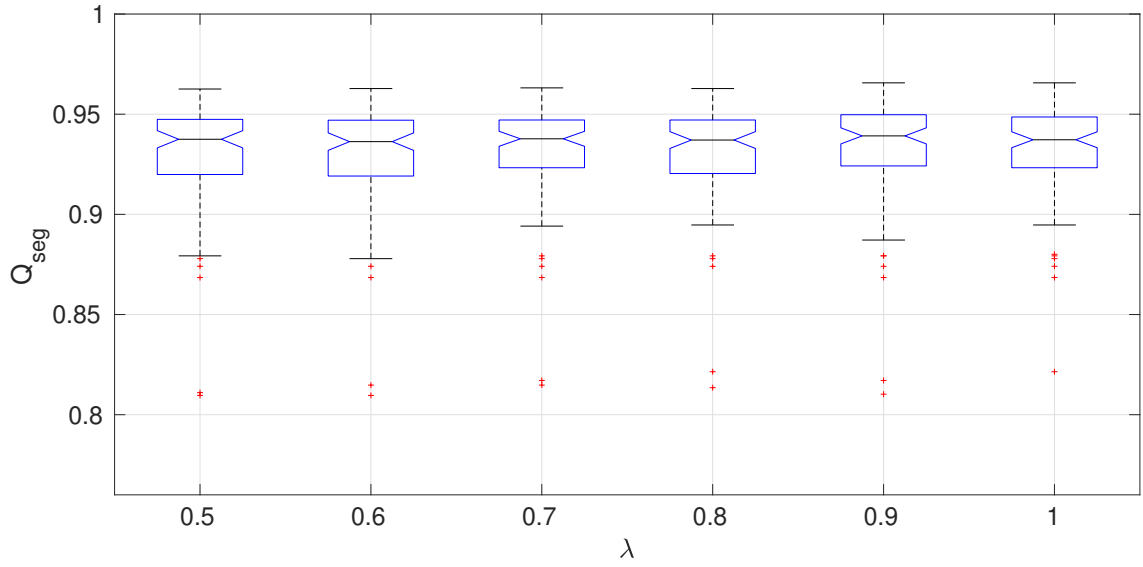
Figure 3.6: *Scale variation assessment.*

factor $\theta \in \{0, 90, 180, 270\}$ is applied to rotate the images of the test data group at different angles where $\theta = 0$ represents the images in their original positions. Figures 3.5(e) to 3.5(h) presents visual examples of this process.

In Fig. 3.7, the median values of the test cases are consistent. In this sense, a Kruskal-Wallis $p = 0.33$ value indicates that the rotation transformation did not affect the distributions to the point of refuting the null hypothesis, which means that even with the application of this type of transformation, the results are stable.
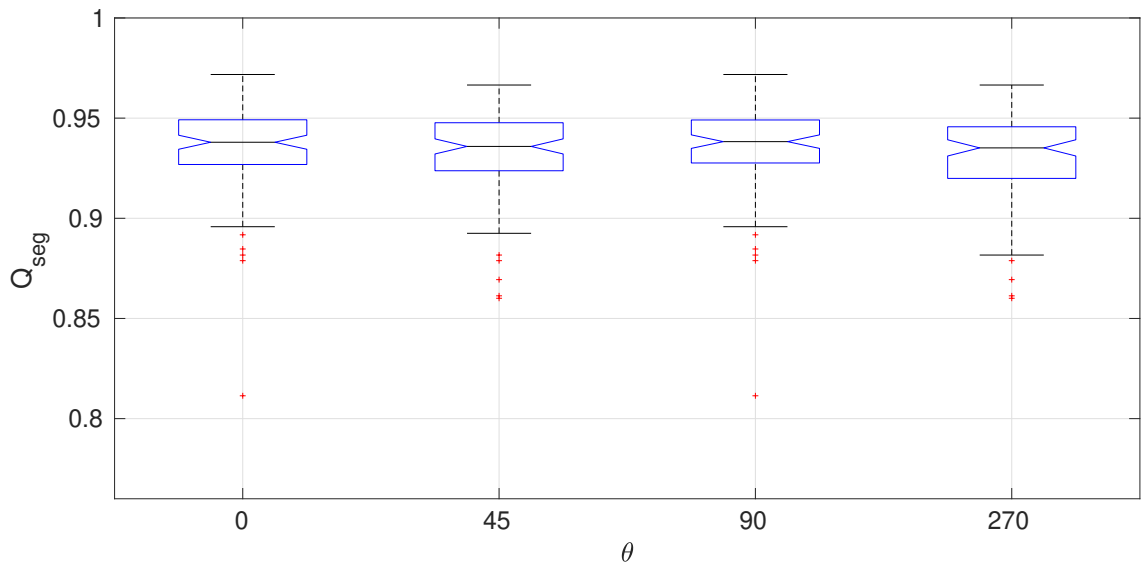
Figure 3.7: *Rotation transformation assessment.*

3.5.3   Image noise variation

We also investigated the behavior of the proposed method in dealing with noisy images. We gradually add random salt & pepper noise with an density factor η, as in Eq. 3-15,

$$\eta \in \{0, 0.08, 0.16, 0.24, 0.32, 0.40\}, \tag{3-15}$$

to the images of the test data group in which for $\eta = 0$ no noise is applied, while for $\eta = 0.40$ noisy points are inserted in 40% of the input images.

When the addition of noise is applied, there is no significant change in the results concerning the images without noise, Fig. 3.8, confirmed by Kruskal-Wallis $p = 0.97$. However, we point out that adding noise has a minor influence on the segmentation process, causing leaf area loss or labeling non-leaf parts as the target object, as shown in Figures 3.5(i) to 3.5(l).
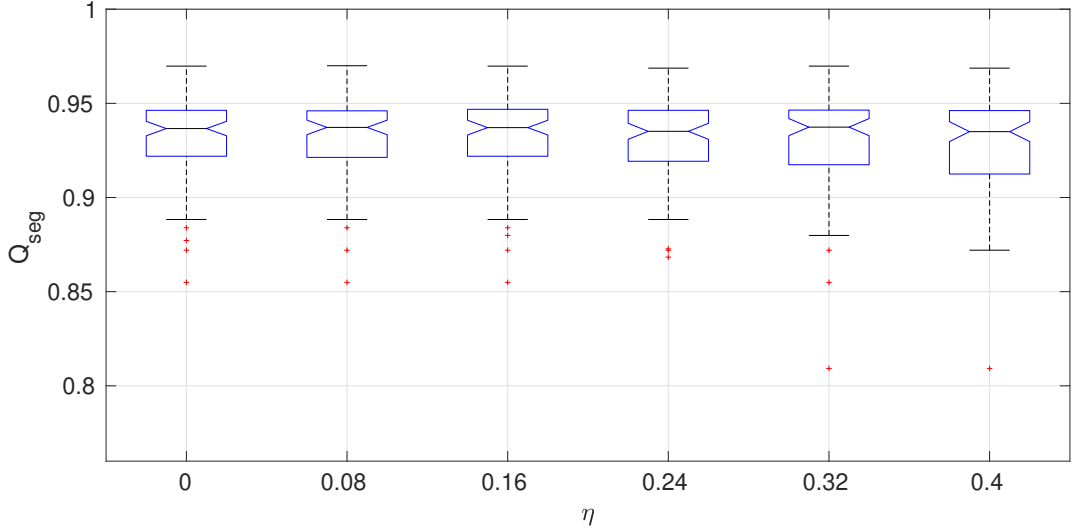
Figure 3.8: *Noise variation assessment.*

3.5.4   Defoliation level range

In this test, we analyze the proposed method when applying controlled changes in the percentage of leaf damage. Starting at 5%, we increase the defoliation level by 5% until the maximum is 99% damage. Fig. 3.9 shows the mean, median, and standard deviation of the test cases. The results are best presented when the leaf damage varies from 1% to 35%. After that, the error increases, and the Q_{seg} values decrease progressively. However, these results show that our method provides suitable outputs even with a very high defoliation level, and the average Q_{seg} is always higher than 0.79.
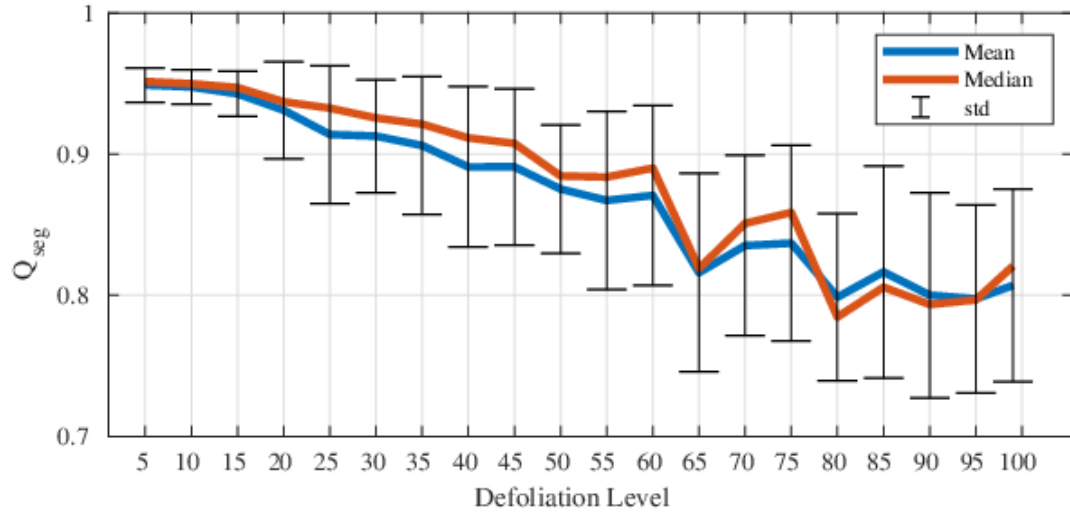
Figure 3.9: *Defoliation level assessment.*

3.5.5 Detection and segmentation of insect predation

This experiment evaluates the proposed method for detecting and segmentation insect predation marks based on precision and recall measures. Fig. 3.10 shows the average statistical results for each crop species concerning the predation areas segmentation and, as it can be noted, among the five executions (*K-fold* cross-validation), there are only minor variations between the results with standard deviation values below 0.03.

Table 3.1 shows the general results obtained from the totality of the experimentation rounds with the average ($\bar{x}$), standard deviation (s), and minimum and maximum values from the five executions. Apple, blueberry, and cherry achieved over 86% precision and more than 80% recall. The database samples' characteristics justify corn leaves' high assertiveness (99% precision). As these leaves occupy the entire image area, the template matching step can more accurately find suitable models for damaged leaves. It was expected behavior for the set of images of this class. Likewise, it was expected that the results for the peach leaf were not assertive due to the different shapes of the leaves and the shading effect on them. The results were inaccurate on the recall measure but surprising, with an average precision of 77%.

Unlike the other leaf classes, grape, strawberry, and tomato obtained greater assertiveness in the recall measure than in precision, increasing at least five percentage points. As a result, grapes and strawberries reached the second and third-best recall values, only behind corn leaves. Besides, like most leaf classes, bell pepper, potato, and raspberry achieved recall values above 80% and precision values close to or equal to 90%. However, the main highlight is the soybean leaf, which reached 98% precision in some experimental tests.

In addition, Fig. 3.11 shows histograms of the number of images by the total number of False Positive (FP) and False Negative (FN) segments across all runs. It is
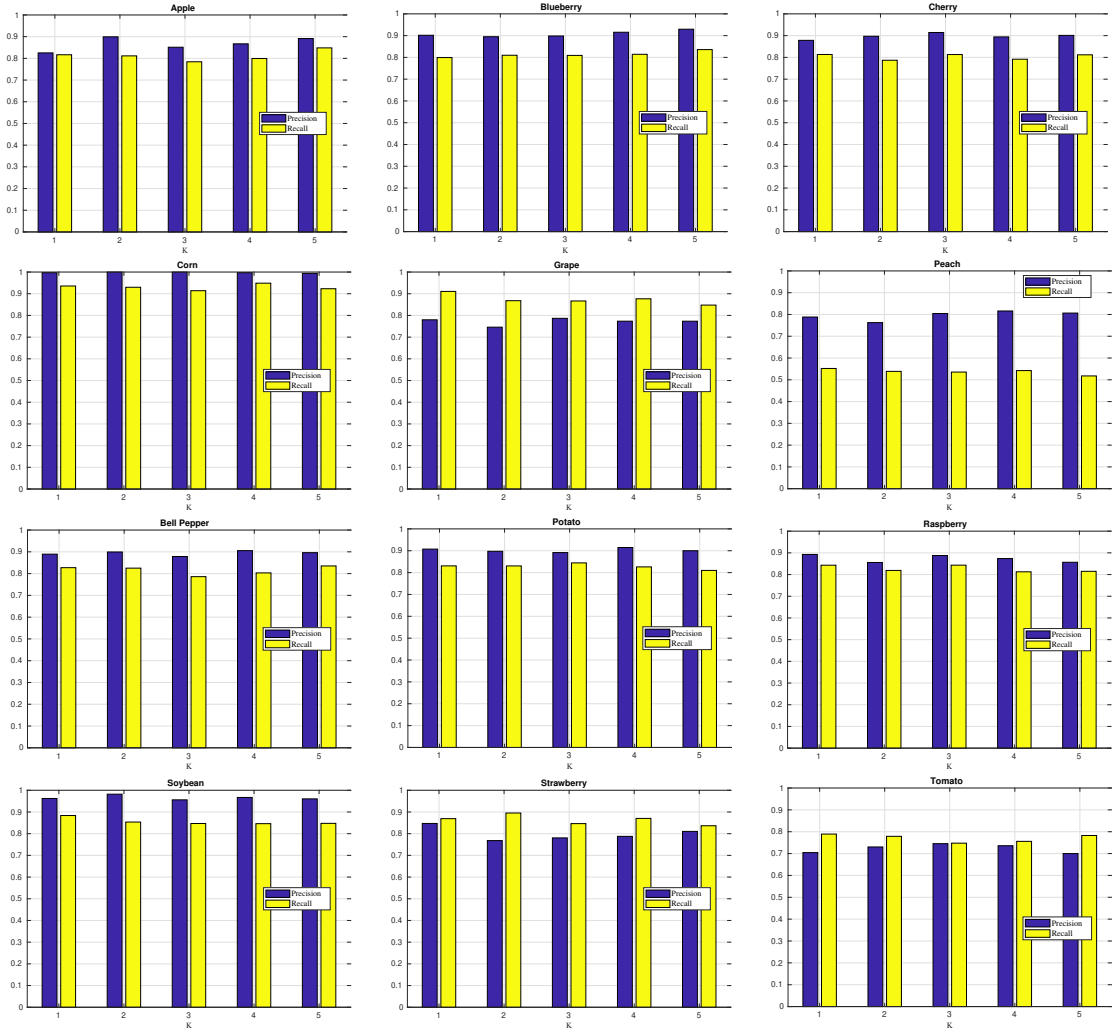
Figure 3.10: *Insect bite segmentation: average precision and recall. The x-axis represents the K-fold iteration number, while the y-axis represents the precision or recall outcomes.*

observed that most of the test images reported zero FP and FN entries; that is, 452 of the 500 test images (considering the five validation rounds) did not present FP segments, and for 318 images, there were no FN entries. Thus, there are more segments labeled as FN than FP. However, the maximum number of false-positive entries in a leaf sample was 2, while 5 false-negative entries were observed in just one image. Although these histograms were prepared with the results of the soybean leaf, this behavior pattern is quite similar for the other types of leaf.

The interpretation of False Positive (FP) and False Negative (FN) consists of the attention given to the number of segments wrongly identified or ignored. False positives occur when bite segments are detected but do not match the actual bite segments. On the other hand, when actual bite segments are not detected, the method fails to identify the segments correctly, and the number of false negatives increases. Therefore, it is essential to balance these measures to correctly recognize bite segments, preventing them from

Table 3.1: *Precision and recall with the final scores between K-folds.*

	Precision		Recall	
	$\bar{x}$ / s	Min Max	$\bar{x}$ / s	Min Max
Apple	0.86 / 0.030	0.82 0.89	0.81 / 0.02	0.78 0.84
Blueberry	0.90 / 0.010	0.89 0.92	0.81 / 0.01	0.79 0.83
Cherry	0.89 / 0.010	0.87 0.91	0.80 / 0.01	0.78 0.81
Corn	0.99 / 0.002	0.99 0.99	0.93 / 0.01	0.91 0.94
Grape	0.77 / 0.010	0.74 0.78	0.87 / 0.02	0.84 0.91
Peach	0.79 / 0.020	0.76 0.81	0.53 / 0.01	0.51 0.55
Bell Pepper	0.89 / 0.010	0.87 0.90	0.81 / 0.02	0.78 0.83
Potato	0.90 / 0.009	0.89 0.91	0.82 / 0.01	0.81 0.84
Raspberry	0.87 / 0.010	0.85 0.89	0.82 / 0.01	0.81 0.84
Soybean	0.96 / 0.010	0.95 0.98	0.85 / 0.01	0.84 0.88
Strawberry	0.79 / 0.030	0.76 0.84	0.86 / 0.02	0.83 0.89
Tomato	0.72 / 0.020	0.70 0.74	0.77 / 0.01	0.74 0.78

being lost or misidentified. As can be seen, the proposed method has good assertiveness indices to address this issue, presenting accurate results in detecting and segmenting insect bites.

3.5.6 General Analysis

Computer vision-based systems have proven essential in several areas, including agricultural in which management processes are improved, inspection activities are optimized, and decisions are made considering statistical data collected by sensors. Foliar loss caused by insect predation is an example of computer vision solutions being applied to support proactive and reactive strategies in agricultural management. On the other hand, some challenges related to the computer vision area reduce the assertiveness of automated systems. In this sense, we proposed a new method for detecting leaf damage caused by
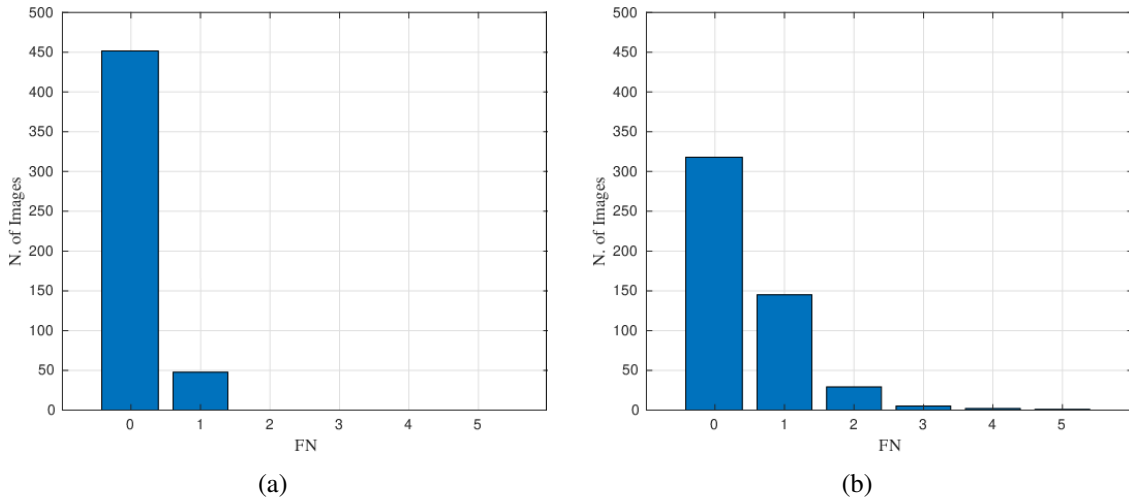
Figure 3.11: *Histogram of False Positive (FP) and False Negative (FN) obtained by the proposed method on soybean leaves. The x-axis represents the number of errors, while the y-axis represents the number of images in each range.*

insects. Also, we provided several tests using a complex database whose content includes entries of different plant species, leaf samples under different lighting conditions, leaves positioned at diverse angles, and leaf format with wide variation.

To design the experiments, we developed a defoliation method that applies synthetic damage to the edges of the leaves. We controlled the defoliation percentage and configured it so that the damage was applied randomly in the range of 5% to 35% in each leaf of the test group. The proposed method was demonstrated to be effective in the presence of noise and image transformations such as scale and rotation. Thus, the positioning of the camera, or the leaf, during the image acquisition process does not need to follow a strict control scheme (Sections 3.5.1, 3.5.2 and 3.5.3). Besides, our method showed more accurate results for leaves with up to 35% damage, which is consistent with actual assessments, as damage above that percentage would, in many cases, imply an irreparable loss (Section 3.5.4).

Furthermore, we have shown that the proposed method accurately identifies insect predation areas regardless of the plant species affected (Section 3.5.5). Statistical measures were consulted, and precision above 90% was achieved in the blueberry, corn, potato, and soybean leaves, and, except for tomato and peach, all other leaf classes, such as apple, cherry, grape, bell pepper, raspberry, and strawberry, achieved a recall higher than 80%. In this assessment, we modified the traditional metric IoU to allow a fair evaluation. We did that because the bite segments could contain discontinuities, and when compared to the ground truth, the covered area (i.e., the area that consists of the union between them) could be significantly larger than the intersection area and vice versa. Furthermore, there is no guarantee that the bite segments will align with the ground truth images, making it

difficult to perform a direct overlay comparison. These facts greatly influenced the results, increasing the false-positive or false-negative rate, even when we visually observed a significant intersection between the parts evaluated. Fig. 3.12(a) shows an example of the overlay of insect bite segments on their corresponding image model. It is noticed that the representation of the segments under the image is almost perfect, but when compared to the ground truth, there is a disarrangement between the bite segments (Fig. 3.12(b)). The assessment methodology presented in Section 3.4.4 addresses issues of this type.

(a)   (b)
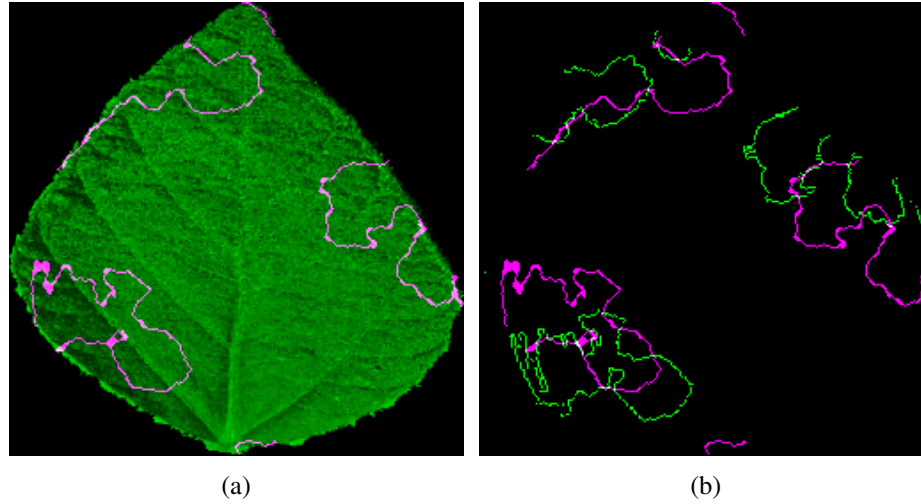
Figure 3.12: *Bite segments and ground truth: (a) Bite segments superimposed on the image model, (b) Misalignment between bite segments (magenta) and ground truth (green).*

Table 3.2 compares the proposed method with some related works. The first five studies addressed classification algorithms for different insect species. In three of these studies, the regions occupied by them were highlighted, making it possible to verify the insects' location in the scenarios investigated by the authors. However, none of them pointed to regions of insect damage. On the other hand, in the works of Machado *et al.* (2016), Silva *et al.* (2019), and Silva *et al.* (2021), methods were proposed to estimate leaf loss, and even without the detection and classification of insects, it is possible to infer their presence when considering the percentage of loss. Our proposal offers a balance between these works where the places where insects occur can be verified as well as the regions of damage they cause. In addition, the other works use machine learning to design their methods, except for our work and another one published by us ((VIEIRA *et al.*, 2021)). Also, most research uses public databases.

Regarding method limitations, we point out that the data modeling group can negatively influence the assertiveness of the proposed method if the models are significantly different from the defoliated images. For example, insect predation marks may be lost if the leaves used to build the models are smaller than those under test. On the other

Table 3.2: *Characteristis of our proposal and related work.*

Research Work	Insect Classification	Location of Insect Occurrence	Insect Damage Detection	Method	Dataset
(WANG *et al.*, 2012)	Yes	No	No	ML	PD
(DENG *et al.*, 2018)	Yes	Yes	No	ML	LD, PD
(SHEN *et al.*, 2018)	Yes	Yes	No	ML	LD
(KASINATHAN *et al.*, 2020)	Yes	Yes	No	ML	PD
(NANNI *et al.*, 2020)	Yes	No	No	ML	PD
(MACHADO *et al.*, 2016)	No	No	Yes	ML	LD
(SILVA *et al.*, 2019)	No	No	Yes	ML	LD, PD
(SILVA *et al.*, 2021)	No	No	Yes	ML	PD
(VIEIRA *et al.*, 2021)	No	No	Yes	PR	PD
Ours	No	Yes	Yes	PR	PD

LD: Local Dataset, **PD**: Public Dataset, **ML**: Machine Learning, **PR** Pattern Recognition.

hand, if the model's size is larger than the leaves under analysis, there is still a chance that insect predation segments can be preserved. Such limitations can be overcome if the image database has more homogeneous characteristics in the leaf samples. Furthermore, stems, branches, and more than one leaf per photo could interfere with the interpretation and decrease assertiveness, as can occur in images recorded directly from live plants. Despite the limitations presented, the results are promising, as shown in Fig. 3.13, where a sample of six crop species is presented with visible results of bite segmentation achieved after applying the proposed method.

3.6   Conclusions

This chapter presented an automatic method for detecting injured leaf areas caused by insect predation. We validate the proposal's performance using a complex database whose content encompasses several types of cultivation and leaf samples with different morphological structures. We show that the method effectively highlights the damaged regions and segments the bite contours of predatory insects. A precision of over 90% was achieved for blueberry, corn, potato, and soybean crops. Also, a recall of more than 86% for corn, grape, and strawberry. We conclude that this work opens up new
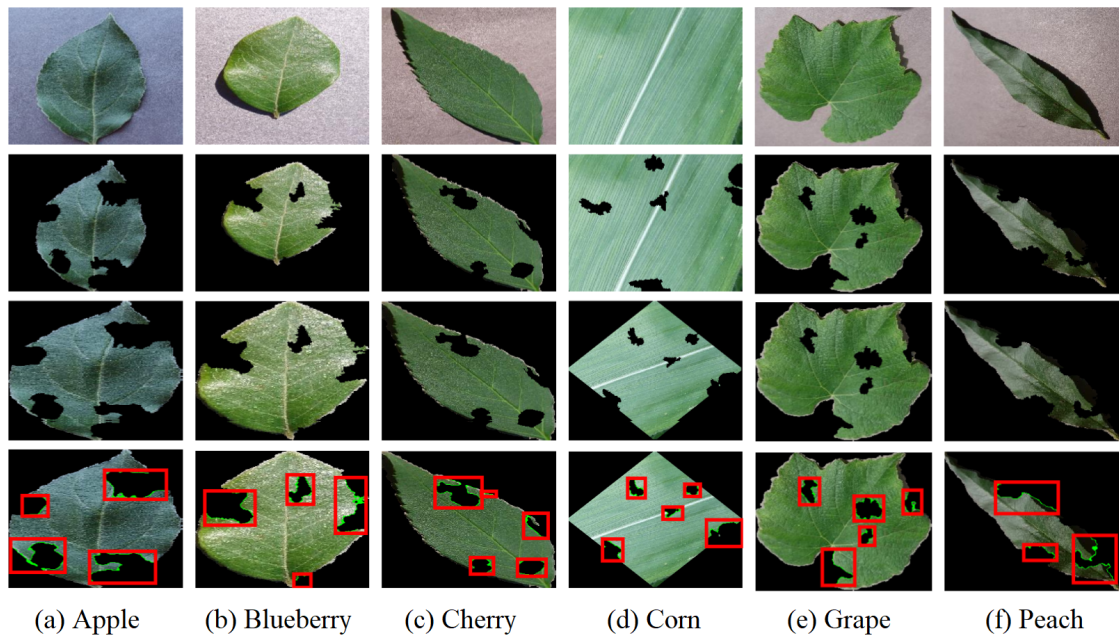
Figure 3.13: *Detection of insect predation regions and segmentation of bite marks on injured leaves. The first rows show the original images, the second rows present the images after segmentation and defoliation, the third rows show the leaves after image adjustment, and the fourth rows present the final result of the detection and segmentation of the bite segments.*

possibilities for leaf analysis, reduces human effort in visualizing the occurrence of pests, and encourages the classification of insects based on bite patterns.

Insect Predation Estimate Using Binary Leaf Models and Image-Matching Shapes

Take heart, it is I, have no fear.

Mark 6:50

Estimating foliar damage is essential in agricultural processes to provide proper crop management, such as monitoring the defoliation level to take preventive actions. Furthermore, it is helpful to avoid the reduction of plant energy production, nutrition decrement, and consequently, the reduction of the final crop production and economic losses. In this sense, numerous proposals support the defoliation estimate task, ranging from traditional methodologies to computational solutions. However, subjectivity characteristics, reproducibility limitations, and imprecise results persist. These circumstances justify the search for new solutions, especially in defoliation assessments. The main goal of this chapter is to present an automatic method to estimate the percentage of damaged leaf areas consumed by insects. As a novelty, our method provides high precision in calculating defoliation severity caused by insect predation on the leaves of various plant species that works effectively to estimate leaf loss in leaves with border damage. We describe our method and evaluate its performance concerning 12 different plant species. Our experimental results demonstrate high accuracy in the determination of leaf area loss with a correlation coefficient superior to 0.84 for apple, blueberry, cherry, corn, grape, bell pepper, potato, raspberry, soybean, and strawberry leaves, and Mean Absolute Error (MAE) less than 4% in defoliation levels up to 54% in soybean, strawberry, potato, and corn leaves. In addition, the method maintains a mean error of less than 50%, even for severe defoliation levels up to 99%. This chapter was published in the Journal of Agronomy (VIEIRA *et al.*, 2022).

4.1   Introduction

Leaf damage affects the correct quantification of the foliar area, and due to various causes, this is a non-trivial problem. For example, wind can whip the foliage, causing tears in the leaves, and hailstorms can damage them by creating holes or even causing total defoliation. Besides, leaf skeletonization and insect predation also promote the appearance of even more harmful external damage. The reasons for leaf skeletonization may result from insects or diseases and occasionally chemical damage, leading to a visual pattern of plant deformities. In contrast, the types of damage induced by maxillary insects are more diverse due to the different developmental stages of insects, such as larval, nymph, and adult stages (CARVALHO *et al.*, 2014).

Estimating leaf loss is a crucial tool for planning sustainable agricultural practices. As the leaves are inputs for monitoring, evaluation, and decision-making, when the leaves are damaged, the deformities can be used to guide the proper management of a crop. In this sense, pest control based on leaf analysis is mandatory in crop management to increase productivity. Predatory insects have caused significant economic impacts in recent decades, and an average annual loss of US$ 11.40 billion in agricultural production is estimated. From 1960 to 2020, the economic loss has progressively increased, reaching the mark of US$ 165.01 billion in 2020 (RENAULT *et al.*, 2022). The main consequence is related to the functional reduction of the total leaf surface, namely defoliation (SILVA *et al.*, 2019), which reduces the energy capacity of the plant, light interception, plant growth rate, and dry mass accumulation (FERNANDES *et al.*, 2022). Consequently, leaf injury caused by insect herbivory negatively affects crop grain yield (MACHADO *et al.*, 2016). Therefore, estimating leaf loss is a primary practice for conducting inspection methodologies and performing control services in farming.

A wide range of proposals, from traditional methodologies to computer-based solutions, address this issue, aiming to reduce subjectivity, ensure reproducibility, and increase accuracy. Some defoliation estimate methods rely on human expertise for visual evaluation and manual quantification (KVET; MARSHALL, 1971; KOGAN *et al.*, 1977), predictive models of linear leaf dimensions (SANTOS *et al.*, 2016; CARVALHO *et al.*, 2017), integrative leaf area methods (LI-COR, 2019; ADC, 2019), digital image processing for mathematical model generation (CARRASCO-BENAVIDES *et al.*, 2016; LIANG *et al.*, 2018), and deep learning algorithms (SILVA *et al.*, 2019; SILVA *et al.*, 2021). Nevertheless, many techniques and methods are applied to a specific type of plant and do not generalize across different species and issues (SILVA *et al.*, 2021).

In this context, manual, semi-automated, and fully automated methodologies address leaf area monitoring. Although their contributions are relevant to agricultural processes, they must overcome some limitations. Visual assessment may increase the error

due to its subjective characteristics. Manual quantification requires extensive work, expertise, and extended time for analysis and evaluation. Automatic meter devices are expensive, need technical support, and demand maintenance. The results of computer-based solutions that require user interaction depend heavily on prior training and proper application handling. Additionally, automated computer-aided approaches require many leaf samples to generalize the construction of statistical models or the intensive application of feature engineering in formulating mathematical models.

In addition, solutions for use in agriculture must consider devices with limited computing power, such as embedded systems, Internet of Thing (IoT) ecosystems, and intelligent agricultural machinery. As application processing requires efficient solutions, it is crucial to consider lightweight processes and energy efficiency so as not to overload systems. In this sense, we investigated image processing techniques that guarantee high performance while being simple to understand and implement and using few computational resources.

To contribute to this area, we present an automatic method to measure the percentage of insect predation on leaves. As a novelty, our method provides high precision for various targeted species such as tomato, strawberry, soybean, raspberry, potato, bell pepper, peach, grape, corn, cherry, blueberry, and apple. Furthermore, it effectively estimates leaf loss in leaves with border damage, converges quickly, and does not require human interaction. This chapter presents the processing steps of the defoliation estimate method, which is based on leaf properties, image processing techniques, and statistical measurements. We emphasize that our method uses comprehensive steps that are easy to implement and suitable for environments with limited computing power.

The remainder of the chapter is organized as follows. The work related to leaf defoliation methods is presented in Section 4.2. In Section 4.3, we present details of our method. Section 4.4 provides information about the test settings, image data set, and experimental design. Section 4.5 presents experimental tests and discusses the results. Then, in Section 4.6, we conclude the chapter and present some future work.

4.2   Related Work

Maloof *et al.* (2013) implemented a software component called LeafJ to be added to ImageJ, a popular computer program used to classify leaf shapes and compute leaf silhouettes. The LeafJ plugin is a semi-automatic tool for studies on leaf morphology that was designed to increase the features of ImageJ by providing petiole length measurement and leaf blade parameters. Although it supports leaf area measurements, it was not prepared to estimate biomass loss in damaged leaves. Therefore, its use is recommended only for healthy leaves.

Easlon and Bloom (2014) estimated leaf surface through different color thresholds and morphological operations to connect image components. Their proposal used a red calibration landmark with a known area as a visual reference point to calibrate leaf area estimation, removing the need to estimate camera distance and focal length. The authors used a leaf area meter to be compared with their method. Additionally, they used the ImageJ software in the comparative analysis. An adequate precision was shown in both leaf segmentation and leaf area estimation. However, their application is sensitive to illumination changes and perspective distortion. Additionally, it requires user interaction and intervention for the best results, and it does not measure insect predation on leaves.

Kaur *et al.* (2014) proposed an elementary computer program for calculating the plant leaf area in which a digital scanner and a threshold segmentation method are settled to separate the leaves from the image background. Likewise, Jadon *et al.* (2016) proposed a simple procedure that applies digital image processing to estimate foliar area in which a digital camera and a white background paper suppress the use of a scanner device in the image acquisition step. However, as these methods do not deal with damaged leaves, none can adequately address the problem of leaf herbivory along the borders.

To address the problem of measuring leaf area with deformation caused by insects, Machado *et al.* (2016) developed a computer application that uses image processing techniques to estimate herbivory. They compared their computer application with manual quantification of injured leaves and a leaf area electronic integrator (considered a standard method of leaf area analysis). The results showed that the defoliation estimate made by the computer program developed by the authors was close to the values measured by the other methods. However, specialized intervention is still required to draw manually the edges of the leaves that have been compromised; therefore, depending on the user's expertise, assertiveness may be better or worse achieved.

Liang *et al.* (2018) proposed some instructions to calculate soybean leaf area, border, and defoliation estimate. Their proposal requires the selection of image samples to build a representative canopy statistical model, which is used to distinguish leaves from non-leaves and backgrounds. Although they have shown adequate results, the proposed methodology may be affected by the image acquisition stage, in which unrepresentative samples may reduce the potential of their method.

In Silva *et al.* (2019), the authors compared deep learning models to estimate defoliation levels and elaborated an automatic method to compute damage in injured leaves. In addition, the authors have proposed strategies to generate images with artificial defoliation to deal with the number of data examples to feed the neural networks. Although their proposal creates new possibilities for calculating the leaf area in which deep neural networks can be used for defoliation analysis, it does require a significant amount of data samples to improve the overall learning procedure (in their experiments,

three data sets were prepared, each one with 10.000 labeled data). Likewise, Silva *et al.* (2021) investigated leaf damage estimation using deep neural networks and prepared an artificial random damage generation method to create a synthetic database. However, as in Silva *et al.* (2019), their method requires an image data set with many image samples (the authors used more than 22.000 samples during the training step.) In this sense, the processing of large databases can be restrictive for devices with limited computing power, as in smart farming ecosystems, or demand equipment with specific hardware configurations to reduce energy consumption and provide timely responses.

In the same way, Zhang *et al.* (2022b) used images taken from unmanned aerial vehicles to determine soybean defoliation in crops. This work presented a computer learning model to estimate crop defoliation. Additionally, the authors prepared computer models to characterize defoliated crops so that wrong characterizations of healthy crops could be avoided. Although promising, the author's method does not include defoliation estimation for isolated leaf samples. Manso *et al.* (2019) presented a method to detect damage in coffee leaves that uses image segmentation and an artificial neural network to identify and classify leaf damage. However, their method only works for leaves with visible leaf damage, i.e., for damage that can be determined by the difference in color between the healthy and diseased areas. Thus, this method does not include the estimate of defoliation in which the leaf area was consumed, for example, by chewing or cutting insects. Liang *et al.* (2018) presented a method to determine the soybean canopy defoliation using RGB images to provide informative data in pest management. Although these researchers show promising results for soybean leaves, they do not look at their solutions in a broader context to determine whether their solutions generalize to different plant forms and species (SILVA *et al.*, 2021).

With the advancement of machine learning algorithms, deep learning models have been widely used to support agricultural management (ALVES *et al.*, 2020; LI *et al.*, 2020; LIU; WANG, 2020). However, training stages on supervised models demand large data sets with data annotation, which can be challenging to prepare (GOMES; BORGES, 2022; TIAN *et al.*, 2014; NIU *et al.*, 2020). Moreover, they are not efficient in predicting unexpected scenarios in data sets that have not been used for training, and the learning steps of these networks are time-consuming (CHU; LIU, 2020; WEI; LIU, 2020). In this regard, computer vision has addressed pattern recognition in digital images so that the models can be less dependent on the image data sets (VIEIRA *et al.*, 2022; VIEIRA *et al.*, 2021a). Furthermore, lightweight models have been designed to consider the characteristics of agricultural environments, such as reduced computing resources, limited processing power, and embedded device systems (INTARAVANNE; SUMRIDDETCHKAJORN, 2015; PIVOTO *et al.*, 2018; LIANG *et al.*, 2018; ROCHA *et al.*, 2022; LIN *et al.*, 2022).

Our method differs from the related work in some aspects as it requires fewer image samples relative to the deep learning methods (only 60 samples) and does not demand herbivory samples to prepare the image models. Also, the method is stable against image transformation, such as rotation and scale, and is a fully automated method that uses data input to construct image models for template matching. Moreover, the method measures the percentage of the foliar damage area by counting the pixels, uses a global thresholding method to detach the leaves from the image background, and uses digital image processing techniques in its design.

In this sense, our method can automatically estimate the leaf area consumed by insects using digital images without requiring large volumes of data to build the templates. Additionally, our method indicates the severity level of defoliation regardless of whether the leaf damage occurs in inner regions or at the edge of the leaves, something that only semi-automatic methods or deep learning models could address.

4.3 Method

Our method is organized into three steps to handle background removal to highlight leaf regions, adjust images based on their geometric shape, and estimate defoliation severity. The adjusted images are used to prepare a database to retrieve leaf models similar to query images. Then, the retrieved images are used to estimate the percentage of damage in the query images. Figure 4.1 presents the flowchart of the method.
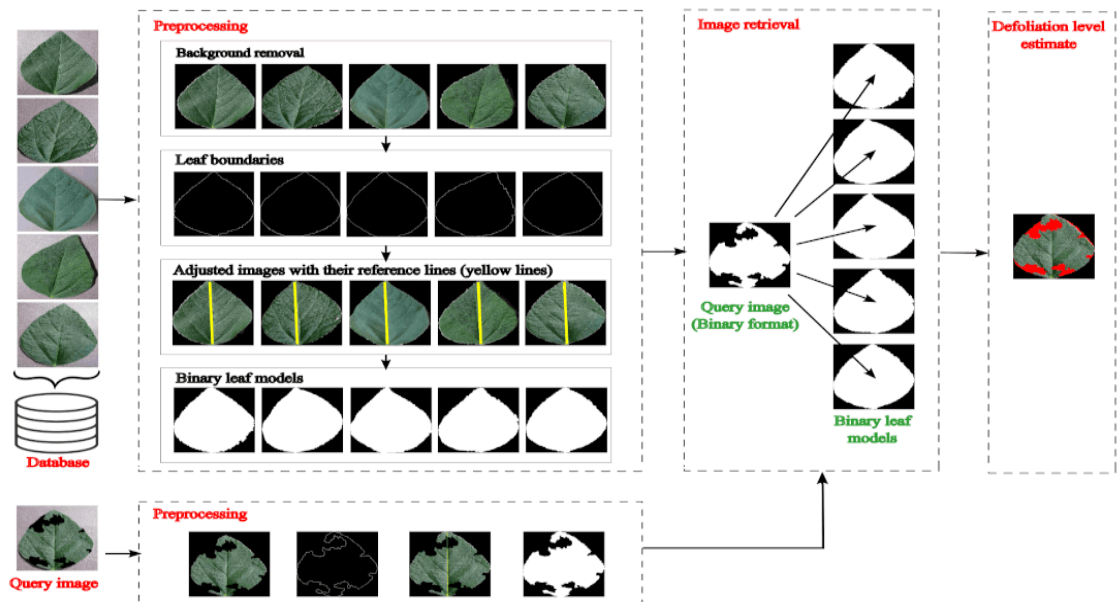
Figure 4.1: *Flowchart of the presented method.*

4.3.1 Preprocessing

The input RGB images are processed with a 5×5 median filter. From the resulting images, the channel G (Green color) is updated by multiplying its current channel values by 2 with the subtraction of the R (Red color) and B (Blue color) channel values. Then, the Otsu segmentation method (OTSU, 1979) is applied to detach the leaves from the background, and binary images are obtained where the inner pixels are removed, leaving only the boundary pixels. The distances between the remaining pixels are measured, and the two most distant points draw a line called the reference line. The reference line is used to rotate the images to the vertical position. Then, the images are surrounded by bounding boxes, their outer areas are cropped, and the images are resized to their original sizes. Thus, the resulting images are binarized, and the leaf model data set is prepared.

4.3.2 Image Retrieval

Considering a binary query image $\mathbf{Q}_{(i,j)}$ also obtained after the previous step, a comparison is made between the query image and the binary target models $\mathbf{M}_{(i,j)}$ from the model data set. The binary leaf model with the slightest difference from the query image is selected and used to determine the damaged leaf area to estimate the leaf damage area. In Equation (4-1), the damage region is obtained by the intersection of two sets.

$$D(M,Q) = \sum_{i=1}^{m} \sum_{j=1}^{n} \left(\mathbf{M}_{(i,j)} \wedge \neg \mathbf{Q}_{(i,j)} \right) \tag{4-1}$$

where m and n represent the numbers of rows and columns of the images, respectively.

Equation (4-1), which handles the correspondence between a query image and binary leaf models, is equivalent to calculating the difference between them as described in Equation (4-2).

$$D(M,Q) = \sum_{i=1}^{m} \sum_{j=1}^{n} \left| \mathbf{M}_{(i,j)} - \mathbf{Q}_{(i,j)} \right| \tag{4-2}$$

Then, after Equation (4-1) or Equation (4-2), the image model, which yields the slightest difference, is assigned to the query image according to Equation (4-3) where k is the number of binary image models.

$$d = \arg\min_{k} D_k \tag{4-3}$$

4.3.3 Defoliation Level Estimate

In Equation (4-4), the retrieved image model ($\mathbf{T}$) is compared with the damaged input leaf ($\mathbf{Q}$) through logical conjunction. After this operation, a logical image $\mathbf{L}$ is obtained, which presents the missing leaf areas.

$$\mathbf{L} = \mathbf{T} \wedge \neg \mathbf{Q} \tag{4-4}$$

After that, the percentage of pixels in $\mathbf{L}$ is calculated according to Equation (4-5),

$$p(\%) = \frac{100}{mn} \sum_{i=1}^{m} \sum_{j=1}^{n} l_{i,j} \tag{4-5}$$

where $l_{i,j} \in \mathbf{L}$ and m and n denote the number, in terms of image dimensionality (rows and columns), of the image $\mathbf{L}$.

4.4 Materials

4.4.1 Database Description

We use the database prepared by Hughes and Salathé (2015), which is available online due to (MOHANTY *et al.*, 2016). In obtaining the samples, technicians collected leaves by removing them from plants and placing them against a sheet of paper that provided a gray or black background to begin acquiring digital images. They obtained the image samples considering various lighting conditions, leaf shape, and foliar position. Based on this, we randomly selected healthy leaves from the dataset, which included samples of tomato, strawberry, soybean, raspberry, potato, bell pepper, peach, grape, corn, cherry, blueberry, and apple. The images are in RGB format and have a size equal to 256×256 pixels.

4.4.2 Experiment Design

We randomly selected 120 images for each of the 12 types of plants, totaling 1440 images for use in the experiments. We divided the data into two groups where 60 images of each plant species are used to construct the leaf model data set, and the other 60 images of each plant species are used to validate the method. The leaf images in these groups differ; therefore, a leaf sample belongs exclusively to just one.

In the data used to validate the proposal, we apply a synthetic defoliation strategy to simulate insect predation. We manually segmented insect bite traces from images with leaves consumed by the insects *Spodoptera frugiperda* (J.E. SMITH) (LEPIDOPTERA: NOCTUIDAE) and *Chrysodeixis includens* (Walker) (Lepidoptera, Noctuidae, Plusiinae).

Then, we used the bite segments to simulate real cases of herbivory in healthy leaves. Our artificial defoliation program has four random parameters. The first determines the insects used to simulate defoliation. The second specifies the number of bite segments. The third applies rotation transformations to the bite segments. Finally, the fourth parameter resizes the bite segments. In addition, the user can specify the required defoliation level from 1 to 99%. The defoliation level is computed after applying the synthetic defoliation, and the reference data (ground truth) is prepared.

This approach is necessary because the data set does not include defoliation caused by insect herbivores such as chewing or cutting insects. Additionally, data sets containing samples in this category are private and not publicly available, as in (MACHADO *et al.*, 2016; BRADSHAW *et al.*, 2007). Therefore, related works such as (SILVA *et al.*, 2019; SILVA *et al.*, 2021) used artificial defoliation strategies. Unlike other works, we used actual defoliation simulation, which is the novelty of our study.

4.4.3   Evaluation

The accuracy of our proposal is measured according to the linear correlation (SOARES *et al.*, 2011), root mean square error (RMSE), and mean absolute error (MAE) between the results and the reference data (ground-truth) following Equations (4-6), (4-7), and (4-8):

$$r = \frac{\sum_{i=1}^{n}(x_i - \bar{x})(y_i - \bar{y})}{\sqrt{\sum_{i=1}^{n}(x_i - \bar{x})^2}\sqrt{\sum_{i=1}^{n}(y_i - \bar{y})^2}}, \tag{4-6}$$

$$\text{RMSE} = \sqrt{\frac{\sum_{i=1}^{n}(x_i - y_i)^2}{n}} \tag{4-7}$$

$$\text{MAE} = \frac{\sum_{i=1}^{n}|x_i - y_i|}{n} \tag{4-8}$$

where x (the percentage of damage per leaf) contains the reference data values obtained from the synthetic defoliation strategy, and $\bar{x}$ is the average value of these defoliation levels. y contains the estimated leaf damage values, and $\bar{y}$ is the average value of the estimated defoliation levels. n represents the number of images that validate the method.

4.5   Results and Discussion

The method's accuracy is evaluated using the query images transformed with the defoliation strategy. As we compare the ground-truth images with the method's outputs, we verify the quantitative and visual results. Therefore, the performance of our method is measured according to the severity of the estimated and actual defoliation.

Figure 4.2 presents visual results of our method with a leaf sample for each of the twelve plant species under study. After the segmentation and defoliation processes, the query images are obtained from the input images, and the final result highlights the damaged leaf regions. As noted, the preprocessing steps adjust the images to a position that reduces the effects of scaling and image rotation in evaluating the correspondence between a query image and leaf models. Thus, our method can present consistent results even if the images were not acquired following a strict standard form of leaves and camera positioning. Figure 4.2 also illustrates the diversity of samples contained in the data set we used, showing that our method has the potential for generalization as it deals with different types of plant species, leaf shapes, and different levels of leaf damage.

(a) Apple	(b) Blueberry	(c) Cherry	(d) Corn	(e) Grape	(f) Peach
DE: 18.02	DE: 7.63	DE: 23.00	DE: 15.75	DE: 19.62	DE: 19.52
GT: 17.02	GT: 10.68	GT: 22.00	GT: 15.55	GT: 16.51	GT: 19.47

(g) Pepper	(h) Potato	(i) Raspberry	(j) Soybean	(k) Strawberry	(l) Tomato
DE: 18.96	DE: 20.96	DE: 16.38	DE: 14.42	DE: 11.92	DE: 16.93
GT: 17.49	GT: 19.83	GT: 15.45	GT: 12.52	GT: 10.71	GT: 12.96
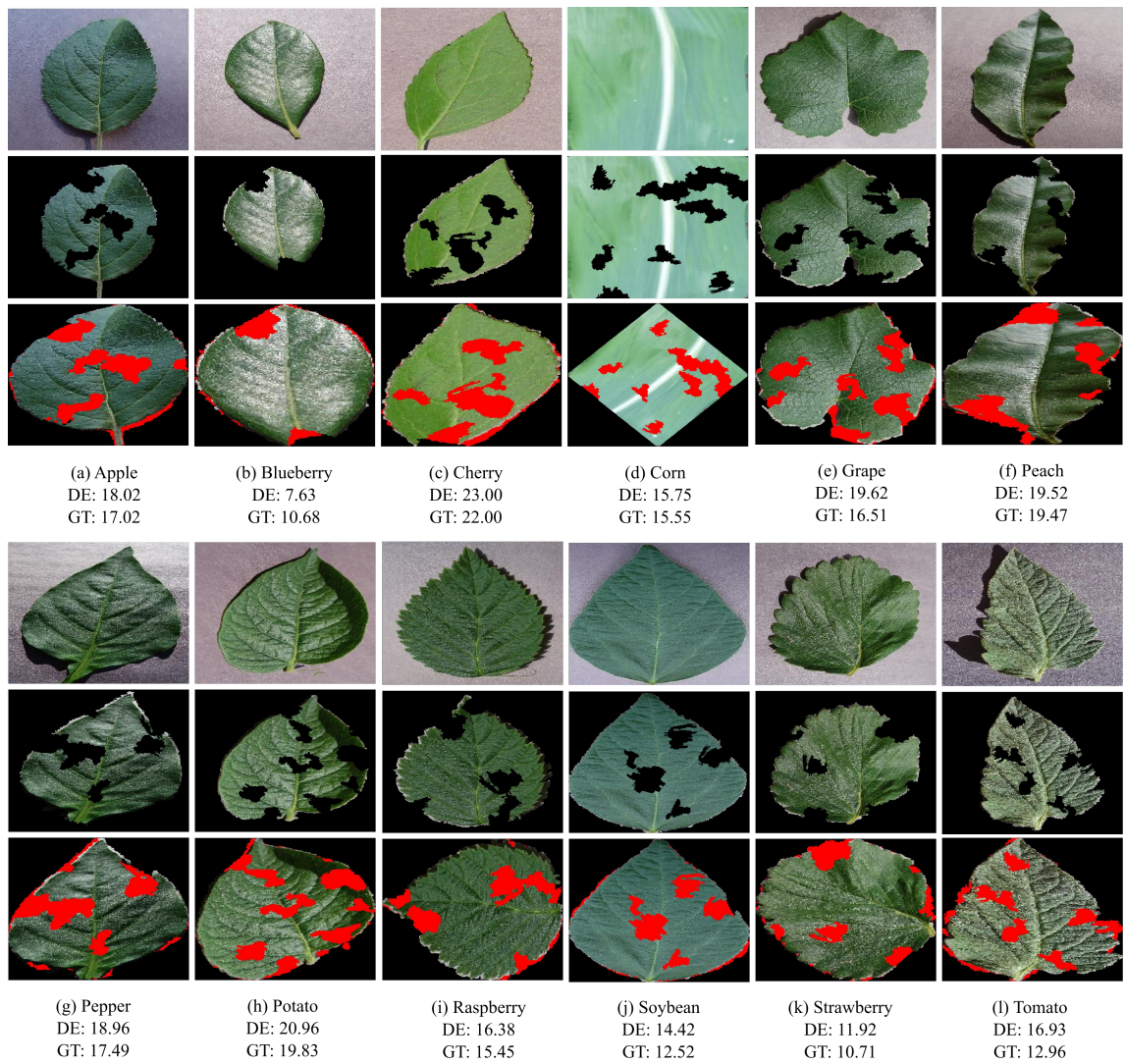
Figure 4.2: *Visual results of our method. The first row of each figure panel shows the images in the data set, the second row presents the query images after segmentation and defoliation, and the third row presents the final result with defoliation estimate (DE) and ground truth (GT).*

Additionally, we evaluate the proposal considering different defoliation levels.

We consider a gradual increase in defoliation from which we apply progressive jumps of 3% until reaching 99% leaf damage. Figure 4.3 presents the outcomes where the best results occurred when the defoliation level was between 0% and 60%. Although the error increases after 60% defoliation, the error is still less than 50% even when the leaves are destroyed, such as after 90% defoliation. It is worth mentioning that this pattern is repeated in all plant species investigated in this study. In this way, it shows the generalization potential of the method.

(a) Apple   (b) Blueberry   (c) Cherry

(d) Corn   (e) Grape   (f) Peach

(g) Pepper   (h) Potato   (i) Raspberry

(j) Soybean   (k) Strawberry   (l) Tomato
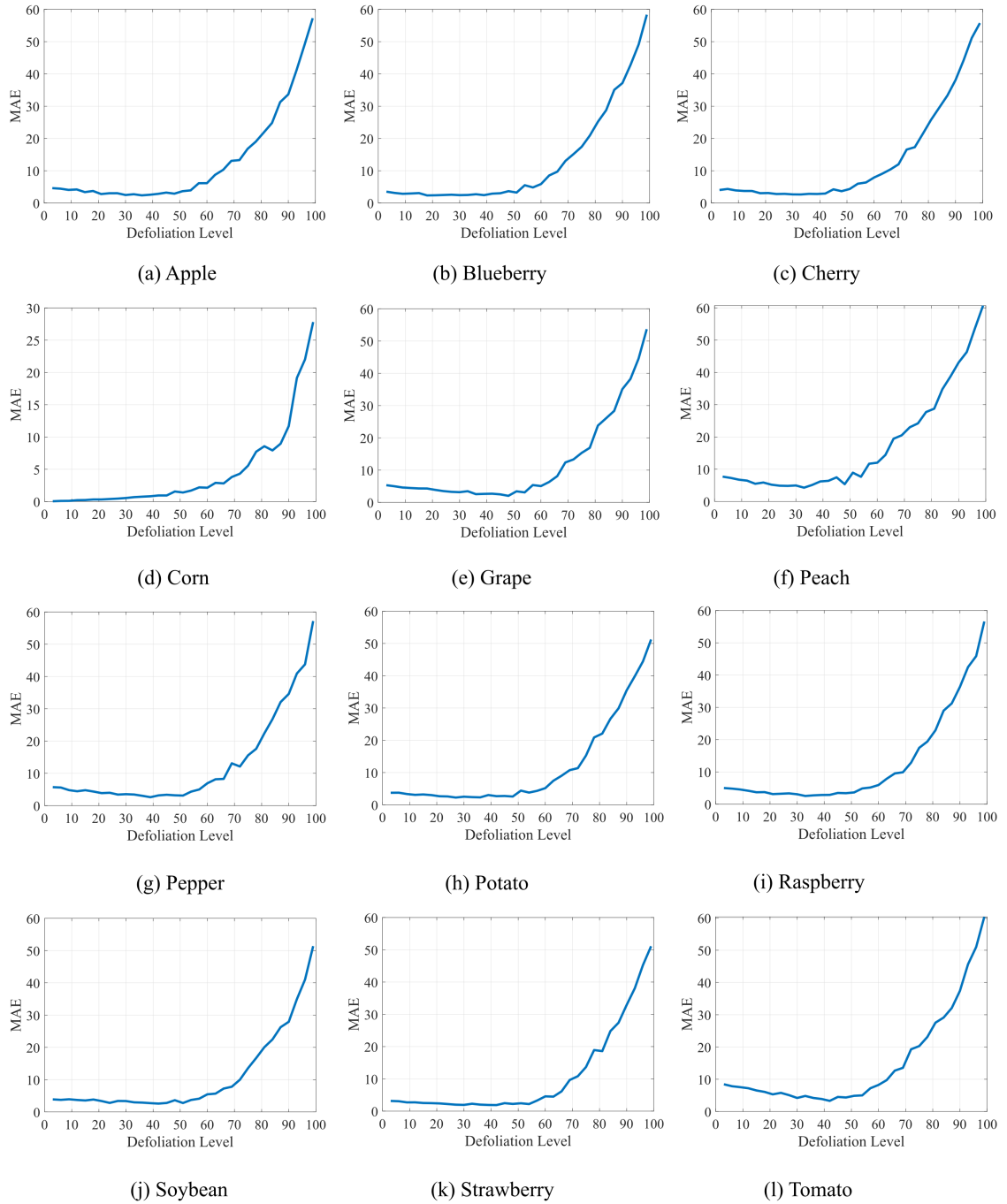
Figure 4.3: *Results of our method concerning different levels of defoliation.*

Table 4.1 shows the linear correlation and the mean error between the damaged leaves for each 12 plant species considering a maximum defoliation level of 30%. A solid linear correlation can be noted, especially for corn, strawberry, grape, potato, blueberry, and soybean, whose correlation was equal to 0.99, 0.94, 0.92, 0.92, 0.91, and 0.89, respectively. Tomato and Peach showed the lowest positive result, mainly due to the diversity of leaf shapes caused by the collection of different cultivars, different leaf growth stages, and the irregular pattern that plant species can produce. Tomatoes have samples of various tomato species with early and adult leaves, and peach leaves have minor to moderate curvature and a wide to narrow leaf canopy. Additionally, the intensity of shading on peach leaves reduced the capability of the segmentation process, justifying the weak correlation that was obtained. The effective treatment of shadows is open to being addressed in future work. Although our method presents consistent results, we point out that excessive leaf deformation can compromise the correct identification of the reference line (Section 4.3), generating an inadequate leaf positioning. Furthermore, assertiveness may decrease if the model construction images differ significantly from the query images.

Table 4.1: *Results of our method on different plant species.*

Plant Species	r	*MAE*	*RMSE*(%)	Defoliation Min	Max
Tomato	0.786	7.11	8.18	3.65	27.06
Strawberry	0.947	3.19	3.51	3.28	24.22
Soybean	0.895	3.31	3.73	3.34	20.37
Raspberry	0.909	3.64	4.09	3.36	27.66
Potato	0.923	3.41	3.94	3.28	20.60
Bell pepper	0.848	4.69	5.37	3.12	17.49
Peach	0.666	7.07	9.55	3.34	28.90
Grape	0.927	4.37	4.88	3.06	28.12
Corn	0.999	0.12	0.17	3.04	15.56
Cherry	0.848	4.20	4.71	3.20	25.61
Blueberry	0.911	3.78	4.42	3.41	29.34
Apple	0.891	3.92	4.50	3.19	24.30

Figure 4.4 presents the scatter plot between the actual and estimated defoliation levels considering the correlation results of different plant leaves for the maximum defoliation level of 30%. The correlation coefficient above 0.84 for apple, blueberry, cherry, corn, grape, bell pepper, potato, raspberry, soybean, and strawberry shows a positive linear correlation between the variables. It indicates that the estimated damage closely follows the actual damage. In addition, a large part of the data is close to the regression line, which emphasizes the strong correlation between them. The estimated data are partially overestimated since the fit line is above the reference line (Y = T).
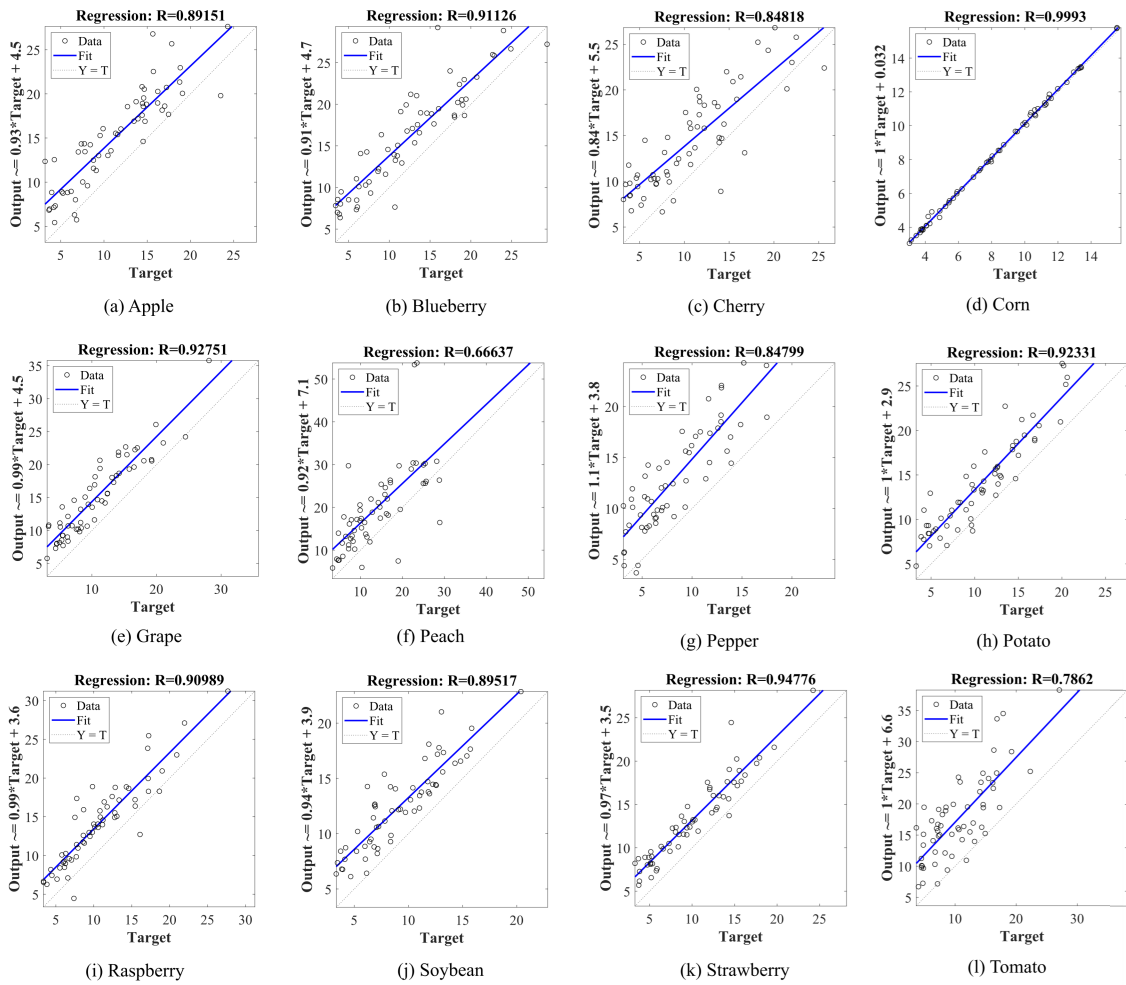
Figure 4.4: *Regression line between ground-truth defoliation levels and estimated damage by our method concerning different plant species. Target T refers to the reference data, while Y refers to the estimated value.*

Complementarily, Figure 4.5 demonstrates the method's behavior concerning the estimated defoliation level. As can be observed, the calculated values are more significant than the actual damage, i.e., the method overestimates the defoliation level, indicating percentages of leaf damage above the actual values. However, these values are not discrepant since the curves have similar shapes. In the actual scenario, this behavior is preferable to underestimated results that could induce the reduction or interruption of

management operations. Furthermore, as this behavior is repeated in other plant species, the overestimation can be measured and used in leaf analysis. For example, in soybean leaves, the mean overestimated value (mean absolute error, Table 4.1) is 3.31. Based on this knowledge, the curves that characterize the actual and estimated defoliation level (Figure 4.5) can be adjusted to present a more assertive result.
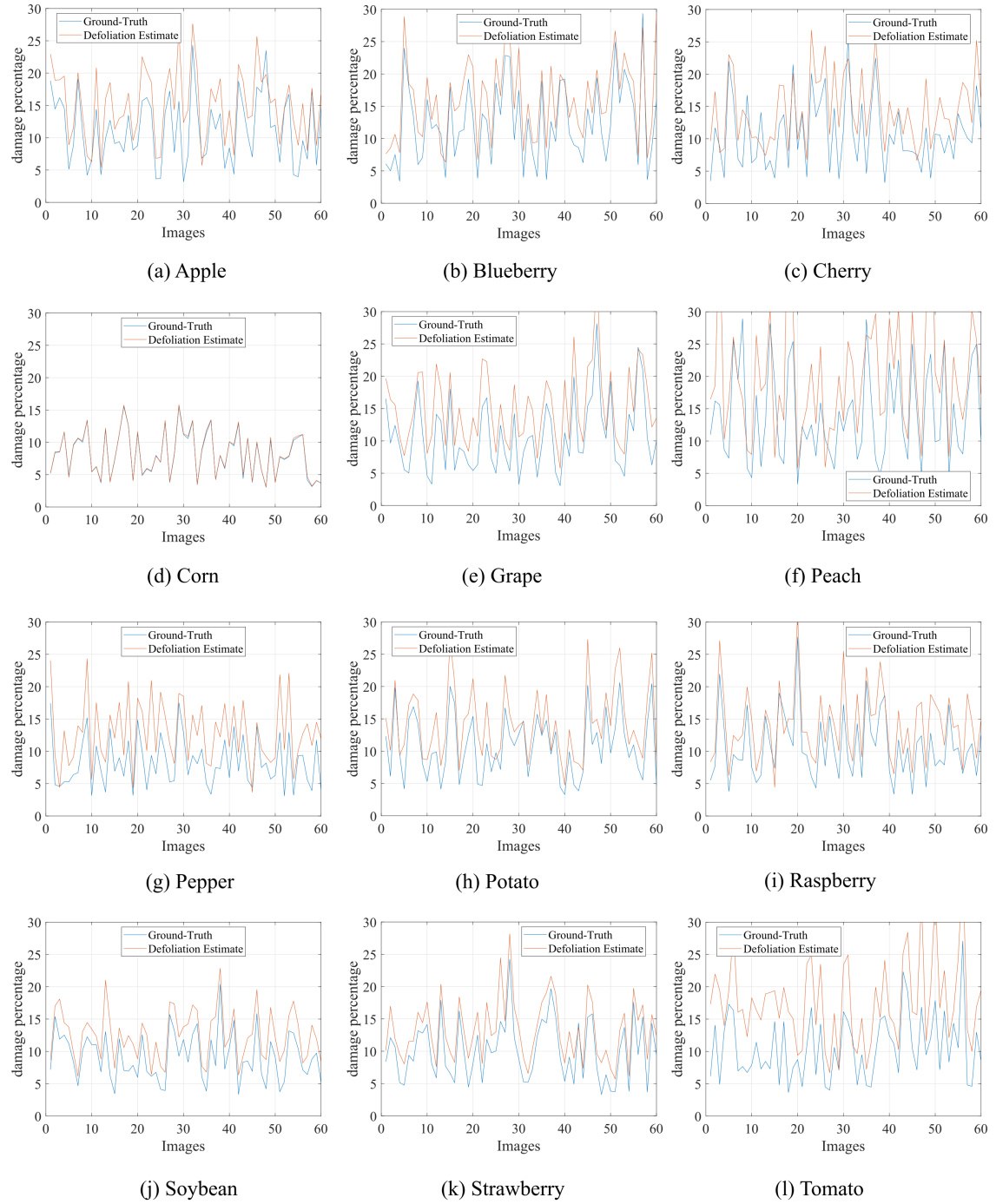
Figure 4.5: *Comparison between ground-truth defoliation levels and estimated damage by our method in different plant species.*

Table 4.2 compares our method and related work. These methods used the

automatic estimation of leaves or human intervention to delineate the leaves in the images (semi-automatic approach). Some of them were not prepared to deal with leaf losses. In opposition, other methods consider leaf damage, including the destruction in border regions with defoliation levels between 0 and 65%. Except for our method, automatic approaches were developed using deep learning models, which require many image samples. Additionally, only our method and Silva *et al.* (2014) method were evaluated exclusively with public databases. The other authors built their bases for evaluation or used local and public data sets.

Table 4.2: *Some relevant information about our method and related work.*

Paper	Method	Defoliation Level	Border Damage	Plant Species	Data set Reference	Year
(BRADSHAW *et al.*, 2007)	SA	–	Yes	1	LD	2007
(MALOOF *et al.*, 2013)	SA	–	No	1	LD	2013
(EASLON; BLOOM, 2014)	SA	–	No	5	LD	2014
(MACHADO *et al.*, 2016)	SA	$[0, 50]$	Yes	5	LD	2016
(SILVA *et al.*, 2019)	AU	$[0, 64]$	Yes	3	LD, (NOVOTNÝ; SUK, 2013)	2019
(SILVA *et al.*, 2021)	AU	$[0, 65]$	Yes	153	(WU *et al.*, 2007)	2021
Ours	AU	$[0, 60]$	Yes	12	(HUGHES; SALATHÉ, 2015)	2022

LD: Local data set, **SA**: Semi-automatic, **AU**: Automatic

Table 4.3 presents a quantitative comparison considering our method and some related works. Although each work has applied its experimental evaluations, they have some characteristics in common, such as performance measurement (*r* and RMSE) and type of plant under analysis (soybean leaf). This comparison shows that our proposal presents results close to semi-automatic methods that demand human intervention and automatic methods that use deep learning. For example, Bradshaw *et al.* (2007) and Machado *et al.* (2016) used local databases and compared their results with leaf area measurement devices (LI-COR). On the other hand, Silva *et al.* (2019) used local and public databases and synthetic defoliation methods to train computational models. In contrast, our method is evaluated with a public database that contains different plant species and variability in leaf shape. Furthermore, our method involves a few processing steps, which makes it suitable for systems with reduced computing power that generally qualify applications for smart farms.

The experimental tests were prepared using a notebook with a Core i7-9750H (2.6GHz; 12 MB Cache) and 16 GB RAM. The leaf model with 60 images executed in

Table 4.3: *Quantitative results provided by related work and our method considering soybean leaves.*

	r	RMSE
Digital scanner (BRADSHAW *et al.*, 2007)	0.938	–
BioLeaf (MACHADO *et al.*, 2016)	0.992	–
AlexNet (SILVA *et al.*, 2019)	0.987	4.57
ResNet (SILVA *et al.*, 2019)	–	14.6
Ours	0.895	3.73

09.19 s. In addition, the average time to compute the defoliation estimate was 00.21s. Our source code, written in MATLAB, is freely available for download.

4.6 Conclusions

This chapter presented a new method to calculate the percentage of damage caused by insect herbivores on plant leaves. The technique uses a few processing steps, making it suitable for intelligent farm environments with limited computing power. Based on the experimental evaluation, our method is assertive in measuring the loss of leaf area, considering different shapes, sizes, and morphology of leaves. The results were best for defoliation percentages of a maximum of 60% as the predictions deteriorated beyond 60%. For defoliation below 60%, the mean absolute error was lower or close to 10% for all plant species under study, showing the generalization potential of our method. Additionally, when verifying the correlation between leaf damage and estimated damage, we observed a positive relationship between the variables with correlation values between 0.84 and 0.89 for apple, cherry, pepper, and soybean, and above 0.90 for blueberry, corn, grape, potato, raspberry, and strawberry.

As a novelty, our method provides high precision for diverse plant species, works effectively to estimate leaf loss in leaves with border damage, converges quickly, and does not require human interaction. Furthermore, it does not require samples of herbivory to prepare the image models and does not require a massive amount of data to converge appropriately. Thus, we present a comprehensive crop monitoring and decision-making solution through quantitative and visual analysis. In this sense, our proposal is a valuable option for supporting agricultural management based on analytical information, where insect predation can be addressed before it compromises the entire plantation.

An Automatic Method for Estimating Insect Defoliation with Visual Highlights of Consumed Leaf Tissue Regions

Make requests, and they will be answered.

Luke 11:9

As an essential component of the architecture of a plant, leaves are crucial to sustaining decision-making in cultivars and effectively support agricultural processes. When the leaf area is constantly monitored, a plant's health and productive capacity can be assessed to foment proactive and reactive strategies. Because of that, one of the most critical tasks in agricultural processes is estimating foliar damage. In this sense, we present an automatic method to assess leaf stress caused by insect herbivory, including damage in border regions. As a novelty, we present a method with well-defined processing steps suitable for numerical analysis and visual inspection of defoliation severity. We describe the proposed method and evaluate its performance concerning 12 different plant species. Experimental results show high assertiveness in estimating leaf area loss with a concordance correlation coefficient of 0.98 for grape, soybean, potato, and strawberry leaves. The method's core is a classic pattern recognition approach, template matching, whose performance is compared to cutting-edge techniques. Results demonstrate that the method achieves foliar damage quantification with precision comparable to deep learning models. This chapter was published in the Journal Information Processing in Agriculture (VIEIRA *et al.*, 2024).

5.1   Introduction

Inspecting and controlling agricultural activities is essential to ensure quality and production rates according to the planting estimates (ROCHA *et al.*, 2023). However,

several variables must be observed, and the indicators must be reliable to support agricultural management and decision-making (VIEIRA *et al.*, 2019a). Monitoring insects in plantations is equally important to observe the potential damage caused by chewing and cutting insects. In a balanced ecosystem, the coexistence between plants and insects can be beneficial, as in the increase in the concentration of nutrients and water in the soil (e.g., anthills), or acceptable when production is little affected (VIEIRA *et al.*, 2022). However, it is estimated that insects consume about 14% of the total global agricultural production, and without proper control, they can bring several losses (NABITY *et al.*, 2009). Therefore, the threshold level of 30% defoliation in the leaf growth phase (vegetative stage) or 15% in the grain formation phase (reproductive stage) is still considered valid for the control of defoliating caterpillars in soybean (FERNANDES *et al.*, 2022).

Different methods have assisted in defoliation estimation. Traditional approaches use manual measurement instruments and can be assertive. However, they depend on operator experience, have cost and operational effort relative to the number of samples for analysis, and are susceptible to human subjectivity. Approaches that use leaf area measuring equipment support more significant amounts of image samples but are expensive and require maintenance and calibration. Computer-based approaches can handle more extensive image databases, reduce subjectivity, provide quick responses, and be cheaper than other approaches. Nevertheless, some solutions do not support defoliation estimation with leaf edge damage, require user interaction, or rely on many leaf images for training computer learning models.

Faced with these challenges, computing-based solutions that employ digital image processing and parametric models have been frequently used in leaf analysis. In recent years, improvements promoted by computing systems have pushed agricultural activities to a new level where automation and data analysis have become indispensable. Today, leaf loss estimation is in smartphone apps (MACHADO *et al.*, 2016; ESGARIO *et al.*, 2022), intelligent machines are analyzing weeds (SODJINOU *et al.*, 2022; LUO *et al.*, 2023a), and sensor integration is creating functional IoT ecosystems for smart farms (ANDRIANTO *et al.*, 2021). In this context, classification models (NGUGI *et al.*, 2023; SHAH *et al.*, 2022), semantic segmentation (LUO *et al.*, 2023b; KOLHAR; JAGTAP, 2023), transformer encoder (FU *et al.*, 2023), and pattern recognition (VIEIRA *et al.*, 2021a; VIEIRA *et al.*, 2022; VIEIRA *et al.*, 2022) are among the leading research trends in quantifying biotic stress and estimating defoliation caused by insect herbivory. However, image databases for leaf loss analysis and computational models using lightweight processes still need to be continuously prepared and investigated.

In our previous work, we proposed methods for insect predation detection (VIEIRA *et al.*, 2022), leaf reconstruction (VIEIRA *et al.*, 2021a), and defoliation estimation (VIEIRA *et al.*, 2022). The main limitation of previous models was related

to the use of computational memory that limited the number of template images. We also noticed that changing the similarity evaluation metric could optimize the image correspondence evaluation step. In the new version of the method, we started using binary images and overlapping areas in the matching stage (Intersection over Union - IoU). In this sense, we reduce memory usage, increase the number of image templates, reduce processing time, and increase assertiveness to levels comparable to deep neural networks.

Furthermore, the identification of plant features can be used to categorize diversity, identify vegetation types, and classify crop families through relevant patterns contained in their leaves. In this sense, anatomical and morphological studies are applied using leaf characteristics to distinguish plant species with high similarity (CHIMEZIE *et al.*, 2016), unusual biologic features (SILVA *et al.*, 2014), and their morphometric geometric properties (HEREDIA *et al.*, 2018). In addition, foliar analysis at the laboratory level (SILESHI *et al.*, 2016) or by machine learning algorithms (KS; SAHAYADHAS, 2018; GUTIERREZ *et al.*, 2019; SHAH *et al.*, 2022) can reveal diseases and guide clinical diagnoses and treatment protocols.

In this regard, agricultural systems use the information that can be obtained from leaves to assist in cultivating plants in both small and large crop production and for local or family subsistence. From monitoring to action, the information about leaves can support effective decisions based on a solid foundation for analysis and conclusions. Thus, this knowledge is an essential instrument to assess plant nutrient status (NGUY-ROBERTSON *et al.*, 2015; INTARAVANNE; SUMRIDDETCHKAJORN, 2015), guide the use of fertilizers and support pest control practices (FRIEDMAN *et al.*, 2016; LUO *et al.*, 2023a), estimate the leaf area index (BAUER *et al.*, 2019), measure foliar loss (MACHADO *et al.*, 2016; SILVA *et al.*, 2019; ESGARIO *et al.*, 2022), monitor plant diseases (EASLON; BLOOM, 2014; ZHANG *et al.*, 2019; NGUGI *et al.*, 2023), and identify insufficient nutritional resources in crop management (CROFT; CHEN, 2017).

Among the applications developed from leaf analysis, estimating foliar loss is crucial for planning sustainable agricultural practices. As leaves are inputs for monitoring, evaluation, and decision-making, the analysis process will be impacted if they are compromised, leading to inaccurate results. Therefore, estimating the leaf tissue consumed by insects is a primary practice for conducting inspection methodologies and performing control services in farming. Among the defoliation estimation approaches, there are traditional methods that use manual instruments and operator expertise and contemporary approaches that use computer-aided methods and automated models of foliar analysis. Some approaches use visual evaluation and manual quantification (KVET; MARSHALL, 1971; KOGAN *et al.*, 1977) and predictive models of leaf dimensions (SANTOS *et al.*, 2016; CARVALHO *et al.*, 2017). In contrast, others include integrative equipment for leaf analysis (LI-COR, 2023; ADC, 2023), generation of mathematical models using dig-

ital image processing techniques (CARRASCO-BENAVIDES *et al.*, 2016; LIANG *et al.*, 2018), and deep learning algorithms (SILVA *et al.*, 2019; SILVA *et al.*, 2021; ESGARIO *et al.*, 2022).

In this study, we employed the template matching technique, which has been traditionally used to solve several problems based on pattern recognition. Template matching has attracted the attention of the computer vision community in recent years (CORONA *et al.*, 2023) and has been successfully applied in biometric and facial recognition (RUSIA; SINGH, 2023) as well as in detecting objects in robotics and moving targets (FENG *et al.*, 2023). Agriculture also employs template matching to count trees (OYA *et al.*, 2023), weed detection (JUWONO *et al.*, 2023), navigation systems (BAI *et al.*, 2023), and others. To the best of our knowledge, we are the first to use template matching to construct a method for leaf loss estimation.

In designing our proposal, we considered the limitations of related works to propose a computer-based solution for defoliation estimation. In the proposal, we eliminate aspects of subjective interpretation, deal with many leaf samples in different plant species, and provide visual indications of the leaf regions where the damage occurred, including border regions. In addition, we can use conventional cameras, build the templates without involving image annotation and training, and acquire the images at different rotation angles, scale variations, and image intensities. The database used in the experimental tests supports these statements since it has different variations, as shown in Figure 5.2. Furthermore, the proposed method has lightweight processes that can be executed on time with a final response in a few seconds. In this sense, (1) we present an automated defoliation estimation method whose effectiveness and generalization capacity is evaluated considering different plant species: apple, blueberry, cherry, corn, grape, peach, pepper, potato, raspberry, soybean, strawberry, and tomato; and (2) we organized and made our program code and experimental data publicly available, including an image database that can be used for defoliation estimation purposes.

Our method was developed to assist experts and farmers in monitoring insect predation by analyzing leaf stress caused by defoliation. Severity levels are calculated, and the method's precision in estimating leaf loss can help understand crop health and support agricultural management decisions. In this program version, images can be captured by conventional cameras and processed on a workstation. In future versions, we intend to launch a smartphone application so that processing can be done directly on the device.

The main contributions of this work are:

- a new method that estimates leaf tissue lost both in internal damage and leaf edge regions.
- a comprehensive approach that enables numerical analysis and visual inspections of foliar damage.

- an architecture with well-defined processing steps.
- experimental results with supplementary material to support future comparative analysis (benchmarking).

The remainder of the chapter is structured as follows. Section 5.2 presents details of the proposed method, its mathematical formulae, and visual descriptions of the workflow. Section 5.3 provides key information about the database used and general setup settings and also describes the experimental design and evaluation metrics. Section 5.4 presents the test results and a discussion about them. Finally, the work is concluded in Section 5.5.

5.2   Method

The proposed method is divided into three main steps. In the first one, template images are prepared considering the structural shapes of healthy leaf samples. In the second one, images of damaged leaves are compared with the template images, and the results with the highest similarity are used to locate damaged areas and estimate the percentage of leaf loss (defoliation). Finally, in the third one, defoliation is estimated. We designed the proposed method to support image scale and rotation transformations and to estimate defoliation at different severity levels. The present proposal was also designed to support leaf analysis in different plant species and to delineate damage internally and in leaf edge regions. Figure 5.1 shows an overview of the proposed method.
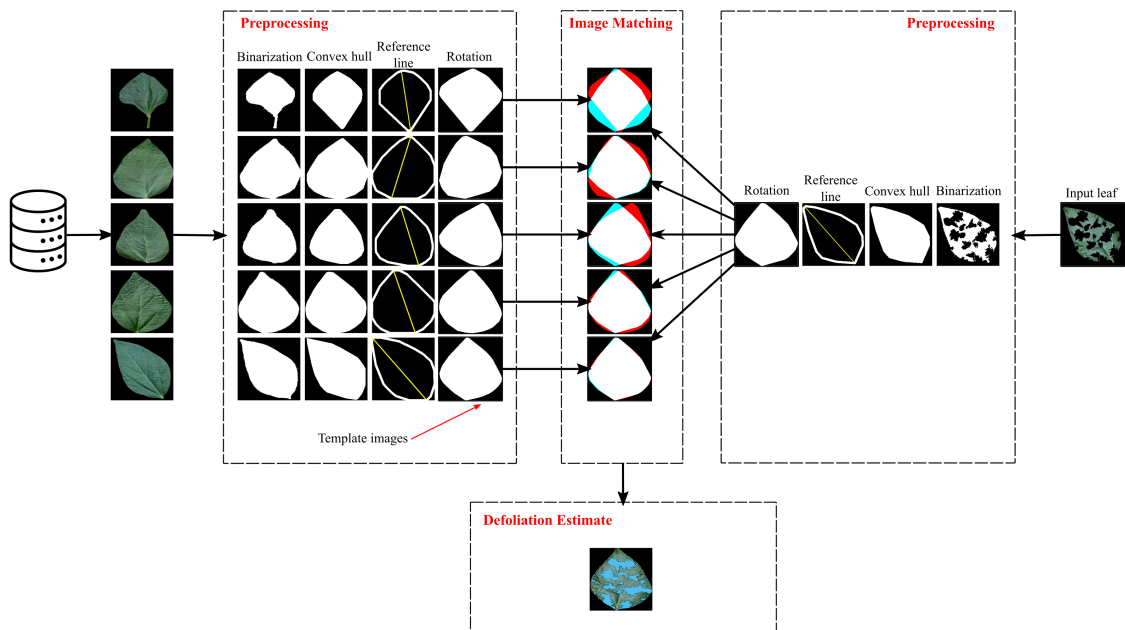
Figure 5.1: *Overview of the proposed method.*

5.2.1 Preprocessing

Initially, RGB images are binarized to differentiate leaf regions (foreground) from non-leaf regions (background). The binarization process is done automatically based on a color threshold that differentiates pixel intensities in the leaf region from other levels of color intensities. Our image database was segmented using the (MOHANTY *et al.*, 2016) method. Then, the resulting images have black pixels (background) and green color intensities (leaf). Because of that, we apply a simple strategy of labeling each image coordinate with pixels equal to 0 in the three RGB image channels as the image background. In this way, the remaining pixels are set as the target image (foreground).

After binarizing the image, the points in the image foreground are used to compute the smallest convex polygon that contains all the points of the leaf area in a computing process known as "convex hull". Following that, a morphological operation is applied to the resulting image to trace the leaf silhouette. Each point belonging to the contour of the leaf image is a coordinate in the image plane, which is used to measure the distance of a given point from the other points. By calculating the distance between all points on the leaf silhouette, we can obtain the two points with the longest distance to represent a pattern that marks a vital leaf structure feature, i.e., plants of the same species have similar leaf shapes. Because of this, their width or length can be measured from specific points that are usually in the same positions, even on different leaf samples.

We consider the Euclidean distance between its coordinate pairs to calculate the distance between the leaf silhouette points. From there, a line (reference line) is drawn to connect the two coordinate pairs farthest from each other. The slope angle of this line is computed and used to rotate the image. The rotation operation positions the reference line vertically concerning the abscissa axis by ninety degrees. The leaf area is bounded, cropped, and resized to the original image size in the resulting image. The processes performed at this stage reduce the challenges related to image scale and rotation transformations inherent to image acquisition. As the images are pre-adjusted following the geometric shapes of leaves, it is not necessary to formulate strict protocols for obtaining images nor to prepare images at different angles of inclination for image matching. All these preprocessing steps are applied to constructing template images and adjusting and positioning damaged leaf images.

5.2.2 Image matching

This step establishes a statistical measure to compare a damaged leaf sample with the template images. The objective is to find an image model that best fits the foliar area of the damaged leaf and more effectively highlights the areas of defoliation. In the comparison, we take an exemplar of the template images and compute the points in

common between the image template and the damaged leaf. We also compute the total area occupied by the two images being compared. Then, the image similarity is measured by the ratio between their common points (intersection) and their combined areas (union). This process is repeated for all images in the image models, and the comparative result of the highest similarity is used to point out the ideal image model to estimate leaf loss. The image matching process is measured according to Eq. 5-1, known as *IoU* (HU *et al.*, 2021), Jaccard index (AMIRKHANI; BASTANFARD, 2021), or Q_{seg} (SADEGHI-TEHRAN *et al.*, 2017).

$$S = \frac{\sum_{i=1}^{m} \sum_{j=1}^{n} d_{i,j} \wedge t_{i,j}}{\sum_{i=1}^{m} \sum_{j=1}^{n} d_{i,j} \vee t_{i,j}}, \qquad (5\text{-}1)$$

where $d_{i,j} \in \mathbf{D}$ is the damaged leaf ($d_{i,j} = 1$) or background pixels ($d_{i,j} = 0$) and $t_{i,j} \in \mathbf{T}$ is the template image, also in a binary format. The accuracy is based on logical operations, logical *and* ($\wedge$) and logical *or* ($\vee$), that compare the overlap between the template image $\mathbf{T}$ and the damaged leaf $\mathbf{D}$. S varies in a range of values between 0.00 and 1.00 in which a value of 1.00 represents a perfect consistency outcome between $\mathbf{D}$ and $\mathbf{T}$ images. $\mathbf{D}$ and $\mathbf{T}$ are binary images with size m by n.

5.2.3 Defoliation estimate

The defoliation estimate is calculated from the logical conjunction between the selected template image and the damaged leaf. As these images are in binary format, the leaf area of the template image that is outside the scope of the damaged leaf delineates its loss regions. It is important to note that the leaves of the same plant species have very similar characteristics, so matching between image pairs and image area overlap calculation can enable consistent results in defoliation estimation. Thus, the task consists of counting the points outside the intersection between the image pairs. In Equation 5-2, we have two binary images ($\mathbf{T}$ and $\mathbf{D}$) corresponding to the damaged leaf and retrieved template image, respectively. The logical conjunction ($\wedge$) between them results in image $\mathbf{L}$, which is the estimated missing area from image $\mathbf{D}$. The image $\mathbf{L}$ is constructed by fetching the regions of $\mathbf{T}$ that are not in $\mathbf{D}$. Thus, the symbol ($\neg$) refers to the complement of $\mathbf{D}$.

$$\mathbf{L} = \mathbf{T} \wedge \neg \mathbf{D} \qquad (5\text{-}2)$$

After that, the percentage of pixels in $\mathbf{L}$ is calculated according to Eq. 5-3,

$$p(\%) = \frac{100}{mn} \sum_{i=1}^{m} \sum_{j=1}^{n} l_{i,j} \qquad (5\text{-}3)$$

where $l_{i,j} \in \mathbf{L}$ and m and n denote the number of rows and columns in the image $\mathbf{L}$, respectively. p is the percentage of the defoliation level.

5.3 Materials

The experiments are performed in a public dataset with several specimens of plant leaves: apple, blueberry, cherry, corn, grape, peach, pepper, potato, raspberry, soybean, strawberry, and tomato. We also considered different levels of defoliation severity, with damage to border regions and inner leaf areas. This section presents general information about the conduction of the experiments, the database used, and the selected evaluation metrics.

5.3.1 Image Database Description

The database used in the experiments was prepared by Hughes and Salathé (2015) and it is available online[1] as a result of Mohanty *et al.* (2016). It consists of a collection of $54,302$ images divided into 14 crops species: Apple (*Malus pumila*), Blueberry (*Vaccinium* spp.), Cherry (*Prunus avium L.*), Corn (*Zea mays L.*), Grape (*Vitis vinifera L.*), Orange (*Citrus sinensis L.*), Peach (*Prunus persica L.*), Bell Pepper (*Capsicum annuum L.*), Potato (*Solanum tuberosum L.*), Raspberry (*Rubus idaeus L.*), Soybean (*Glycine max L.*), Squash (*Cucurbita* spp.), Strawberry (*Fragaria ananassa L.*), and Tomato (*Solanum lycopersicum L.*).

Each group has healthy and infected leaves of cultivated plants, labeled by plant pathology specialists (Table 5.1). In obtaining the samples, technicians collected leaves by removing them from plants and placing them against a sheet of paper that provided a gray or black background to begin acquiring digital images. They sought a variety of lighting conditions, positioning, and foliar shapes. For crops such as Corn and Squash, whose leaves are too large to capture in a single frame, they took images of different sections of the same leaf. The size of the images is 256×256 pixels.

The leaves in this database were infected with bacteria, mold, viruses, or mites. Although these pests present foliar deformation, they do not necessarily result in leaf area loss as occurs in situations of herbivory by insects. Because of that, our attention is focused only on images of healthy leaves. We use them to build image models of cultivated species and to prepare artificial defoliation to simulate and assess the losses caused by insect predation. Since Orange and Squash species do not have healthy images

---

[1] https://github.com/digitalepidemiologylab/plantvillage_deeplearning_paper_dataset

Table 5.1: *Number of images in the database (HUGHES; SALATHÉ, 2015)*

Crop specie	Healthy leaves	Infected leaves	Total
Apple	1,645	1,526	3,171
Blueberry	1,502	-	1,502
Cherry	854	1,052	1,906
Corn	1,162	2,690	3,852
Grape	423	3,640	4,063
Orange	-	5,507	5,507
Peach	360	2,291	2,651
Pepper	1,478	997	2,475
Potato	152	2,000	2,152
Raspberry	371	-	371
Soybean	5,090	-	5,090
Squash	-	1,835	1,835
Strawberry	456	1,109	1,565
Tomato	1,592	16,570	18,162

in this database, they are not used to evaluate the proposed method. Besides, images of infected leaves from the remaining crop species are not used.

Figure 5.2 presents some samples from the database used in this work. Images can be observed under a range of conditions, such as leaves positioned to the right or left (5.2(a) and 5.2(b)), in perspective projection (5.2(c)), with shadows (5.2(d)) and in a substantially different format from the others (5.2(e)). Also, changes in illumination can be easily seen in all of these samples, some of them with the *petiole*[2] (5.2(a), 5.2(b) and 5.2(d)), and others with an incomplete margin – curled leaves (5.2(e)).

---

[2]Petiole is a foliar structural component that attaches leaves to the plant stem.
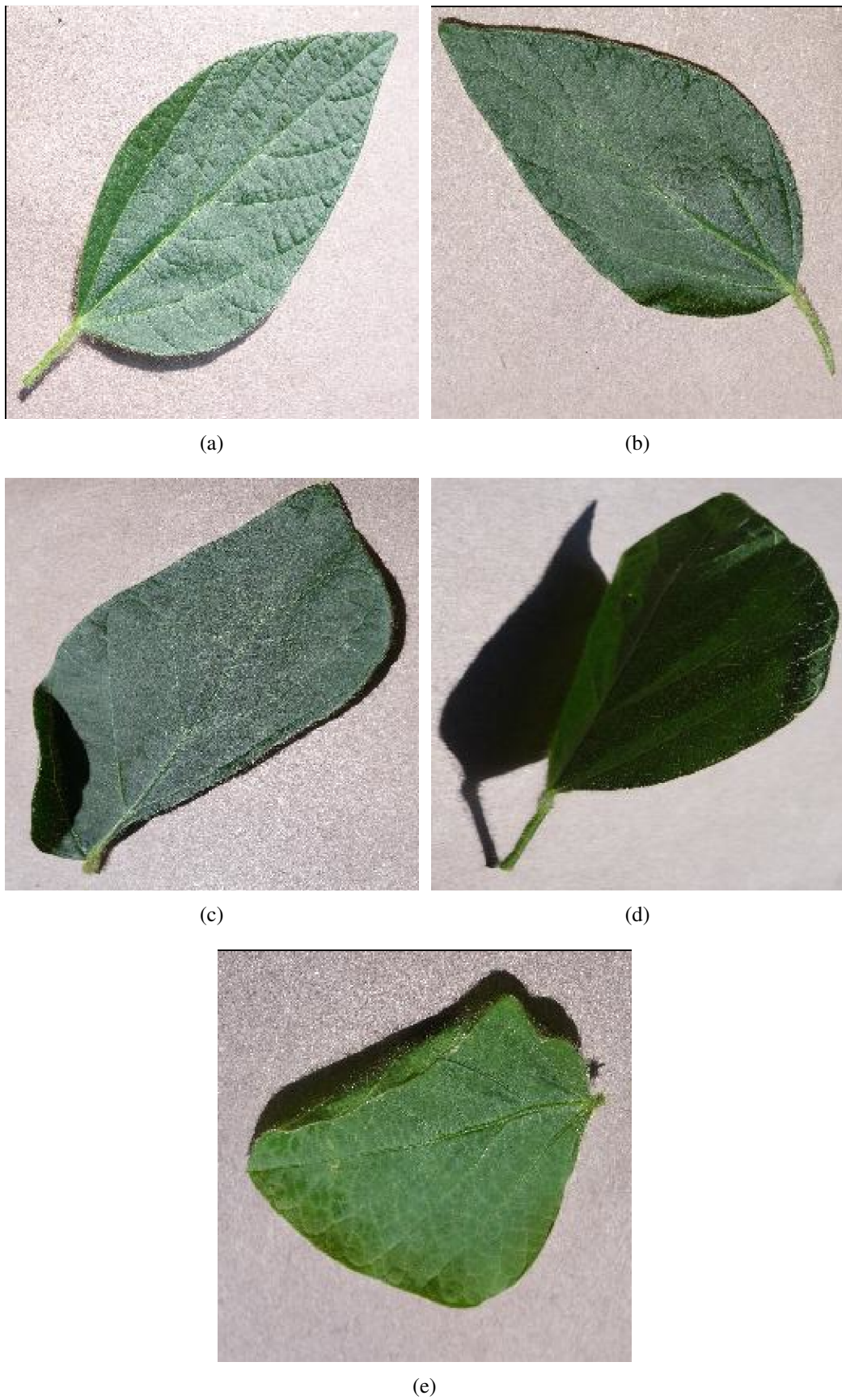
Figure 5.2: *Samples of soybean leaves in (HUGHES; SALATHÉ, 2015) database.*

5.3.2   General setup

In the proposed method, a damaged leaf is compared to template images, and the result obtained is used to estimate defoliation. First, the dataset is divided into two parts: one equivalent to 80% is used to construct template images, and another with the remaining 20% is used for evaluation purposes. Then, template images are constructed from healthy plant leaves, where a model is prepared for each plant species. The dataset is randomly split. For convenience, we use images that have been previously segmented with the (MOHANTY *et al.*, 2016) method, which is also available online with the entire dataset (Section 5.3.1). We started the process with image binarization, rotation transformation, and scale adjustment to construct template images and adjust damaged input leaves as presented in Section 5.2.1. Besides, the images selected for evaluation are preliminarily deformed to simulate defoliation as presented in Section 5.3.3. Applying synthetic damage to leaves simulates real cases of herbivory and enables the analysis of different degrees of defoliation severity. Leaf damage is applied in different amounts, which include minor damage ranging from 1 to 15%, medium damage from 16 to 30%, and severe damage from 31 to 45%. Furthermore, the damage is randomly constructed and presented both in the inner leaf area and the leaf edge regions. The image matching process (Section 5.2.2) consists of comparing an injured leaf with all the template images to obtain the most suitable model for leaf analysis. The experiments were done in a notebook with Core i7-9750H (2.6GHz; 12MB Cache) and 16 GB RAM. The code was written using MATLAB (see Section A.1.4).

5.3.3   Synthetic Defoliation Strategy

Considering that a visual diagnosis is possible by a human, computational tools can, in principle, also assist in this task. The challenge is to find sufficiently expressive samples to allow inferences from computer vision models, which is even more complicated when data labeling requires specialized manual labor, which can be time-consuming and expensive. To overcome this problem, we have prepared a synthetic defoliation strategy in which healthy leaves are subjected to a process capable of simulating leaf area loss.

Our insect predation strategy on leaves involves extracting bite signatures in real herbivory cases and preparing foliar damage templates to promote different leaf defoliation levels. The bite signature of two types of insects, *Spodoptera frugiperda* (J.E. SMITH) (LEPIDOPTERA: NOCTUIDAE) and *Chrysodeixis includens* (Walker) (Lepidoptera, Noctuidae, Plusiinae), was extracted from injured leaves, resulting in some bite samples for each of the two insects.

Considering previously collected bite samples, we built a program that uses the bite samples to generate leaf damage automatically. This program simulates insect predation considering the number of bite samples and the minimum (Min_D) and maximum (Max_D) expected defoliation level (which can range from 1 to 99%). Figure 5.3 illustrates the pipeline used in our synthetic defoliation strategy, where an input image is processed with the bite samples. The program applies image transformations (scale and rotation) to the bite samples and uses them to remove pixels from the input image. The scale factors (Min_SF and Max_SF) are dynamically adjusted, and the rotation angle is randomly set in the range 0 to 360. The program iteratively manipulates these two variables until the desired defoliation level is reached. In the program, DL is initially set to 0, which is updated with changes made to the input leaf image. When the expected defoliation level (DL) is achieved, the input image with the requested defoliation level is returned. Additionally, Figure 5.4 shows the process of applying leaf damage to an input leaf, while Figure 5.5 presents some defoliation results generated by the program. This strategy is used to obtain the reference values (ground-truth data) in the experimental tests in Section 5.4.
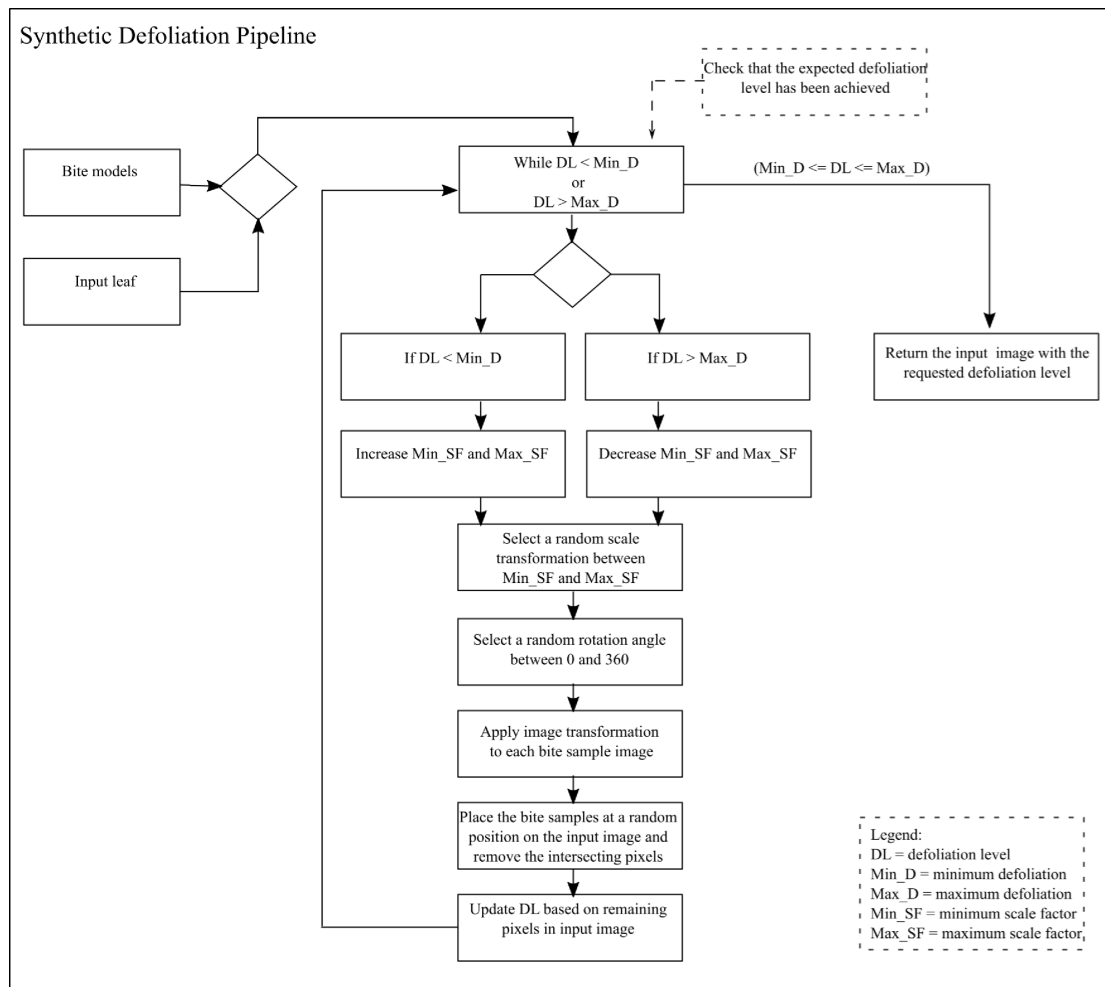
Figure 5.3: *Pipeline for applying damage to leaf images.*
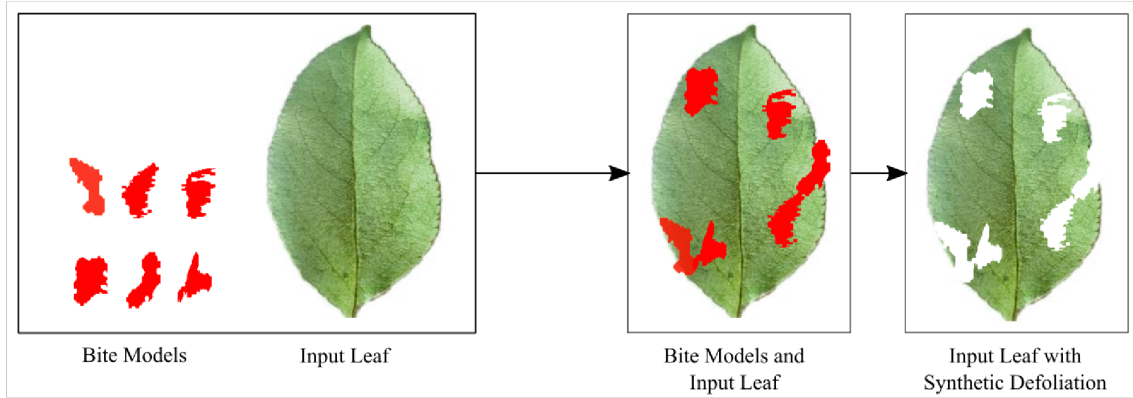
Figure 5.4: *Synthetic defoliation strategy.*

(a) *Original.*   (b) *11.67% defoliation.*   (c) *27.69% defoliation.*   (d) *53.97% defoliation.*
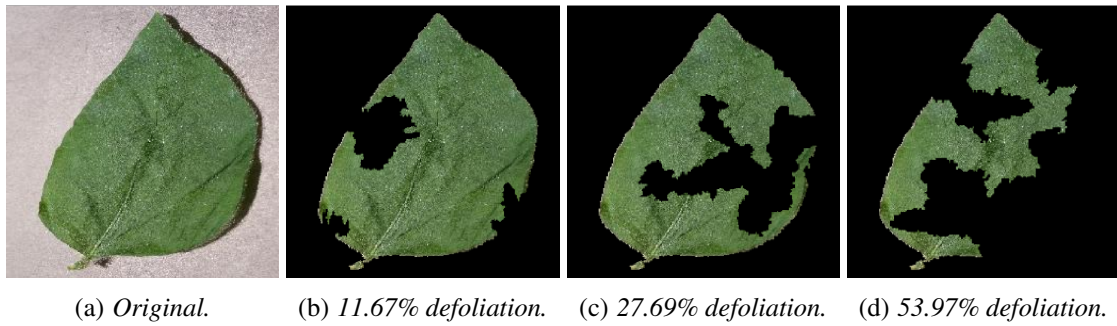
Figure 5.5: *Samples from the synthetic defoliation strategy after segmentation.*

5.3.4   Evaluation metrics

To quantify the results, we used statistical measures to analyze the reliability of the statistical relationships. The problem was modeled as a binary classification test in which the samples were labeled as damaged leaf area or non-damage leaf area. The rating assigned as correct or incorrect is measured according to the number of pixels counted and is defined as:

- True Positive (TP): damaged leaf area correctly identified as damaged regions;
- True Negative (TN): non-damaged leaf area correctly identified as such;
- False Positive (FP): regions categorized as damaged areas when they are not.
- False Negative (FN): damaged regions that have not been properly recognized.

In the analysis of the results, we used the statistical measures True Positive Rate (TPR) (Eq. 5-4) and True Negative Rate (TNR) (Eq. 5-5) to indicate the fraction of areas of leaf damage that were successfully recovered. Likewise, we consider the False Positive Rate (FPR) (Eq. 5-6) and False Negative Rate (FNR) (Eq. 5-7) to measure the percentage of incorrectly classified defoliation areas. TPR, TNR, FPR, and FNR are used

in the construction of confusion matrices to show the performance of our method in the different types of plant species investigated in this study.

$$\text{TPR} = \frac{TP}{TP + FN} \tag{5-4}$$

$$\text{TNR} = \frac{TN}{TN + FP} \tag{5-5}$$

$$\text{FPR} = \frac{FP}{FP + TN} \tag{5-6}$$

$$\text{FNR} = \frac{FN}{FN + TP} \tag{5-7}$$

Jaccard (Eq. 5-8), Dice (Eq. 5-9), and Accuracy (ACC) (Eq. 5-10) indices are also used to provide single measures related to the percentage of the identified defoliation regions. All metrics presented range from 0.00 to 1.00, in which higher results of TPR, TNR, Jaccard, Dice, and ACC point to better assertiveness. On the other hand, values of FPR and FNR close to zero indicate fewer errors in the interpretation and determination of damaged leaf areas.

$$\text{Jaccard} = \frac{TP}{TP + FP + FN} \tag{5-8}$$

$$\text{Dice} = \frac{2 \cdot TP}{2 \cdot TP + FP + FN} \tag{5-9}$$

$$\text{ACC} = \frac{TP + TN}{TP + TN + FP + FN} \tag{5-10}$$

Besides, the linear correlation between the expected and estimated defoliation level is measured with Pearson's correlation coefficient (r), which indicates the degree of relationship between two quantitative variables and expresses the degree of correlation through values between -1 and 1 (SOARES et $al.$, 2011). The correlation is calculated according to Eq. 5-11 as follows.

$$r = \frac{\sum_{i=1}^{n}(x_i - \bar{x})(y_i - \bar{y})}{\sqrt{\sum_{i=1}^{n}(x_i - \bar{x})^2}\sqrt{\sum_{i=1}^{n}(y_i - \bar{y})^2}}, \tag{5-11}$$

where x (percentage of damage per leaf) contains the reference leaf damage values obtained from the synthetic defoliation strategy, and $\bar{x}$ is the average value of these defoliation levels. y contains the estimated leaf damage values, and $\bar{y}$ is the average value of the estimated defoliation levels. n represents the number of images in the dataset for a plant species being evaluated.

Moreover, according to Eq. 5-12, Root Mean Square Error (RMSE) computes the error between the reference leaf damage (x) and the estimated leaf damage (y).

$$RMSE = \sqrt{\frac{\sum_{i=1}^{n}(x_i - y_i)^2}{n}} \qquad (5\text{-}12)$$

5.4   Results and Discussion

In this section, the results obtained with the experimental tests are presented. The effectiveness of the proposed method is verified in different plant species, and the results are discussed considering three main points: correctness in the identification of missing segments of leaf area, assertiveness in the defoliation estimation, and precision in the visual representation of the damaged leaf with its defoliation regions. We also present a qualitative comparison between our method and some related works, discuss the limitations of the proposed method and present information about the execution time. To obtain the reference data (ground truth), we used the strategy presented in Section 5.3.3.

5.4.1   Damaged area identification

Damaged areas, or areas of defoliation, are leaf regions that have been consumed and are no longer present in the image. Identifying these areas consists of predicting the regions that suffered losses and locating them. Thus, it is possible to visually show the leaf canopy, including the areas that suffered defoliation. The evaluation consists of verifying the overlap of the estimated areas with the actual losses to point out the precision in identifying the damaged areas. In this regard, the *Jaccard* and *Dice* indices were used to measure the level of overlap and confusion matrices to measure the percentage of correctly categorized pixels.

Table 5.2 presents the results for defoliation levels between 1 and 15%, 16 and 30%, and 31 and 45%. As can be seen, the indicators show very little difference between the results, and the size of the leaf damage has little influence on the final results. In most cases, the accuracy (ACC) was more significant than 90%. However, it is noted that higher levels of defoliation slightly degrade the accuracy. As damage severity increases, leaf edge regions can be compromised, altering leaf structure and leading to erroneous estimates. Therefore, the results are more accurate when slight changes in the leaf edges occur. On the other hand, the values of *Jaccard* and *Dice* increased according to the number of damage to the leaves. When the damage is minor, the injured leaf adjusts less to the template images, leaving artifacts near the leaf edges that do not overlap with the actual damage.

Table 5.2: *Statistical measures of identifying damaged leaf area in different defoliation levels.*

	Defoliation: 1-15%			Defoliation: 16-30%			Defoliation: 31-45%		
	Jaccard	Dice	ACC	Jaccard	Dice	ACC	Jaccard	Dice	ACC
Apple	34.9	49.8	94.8	57.3	72.2	93.1	63.7	77.3	90.0
Blueberry	34.6	49.7	94.6	59.1	73.9	92.2	66.1	79.3	90.9
Cherry	36.6	51.3	95.8	61.1	75.3	94.2	65.5	78.6	91.8
Corn	85.0	91.6	99.6	82.8	89.9	98.2	82.2	89.1	96.7
Grape	33.6	49.0	94.6	59.7	74.6	93.1	66.0	79.3	90.0
Peach	20.1	31.6	91.0	45.0	61.0	89.5	51.5	67.0	87.2
Pepper	33.8	48.6	95.0	58.7	73.5	93.5	65.1	78.4	91.5
Potato	37.0	52.7	95.2	60.7	75.2	93.4	67.3	80.2	91.7
Raspberry	38.5	53.8	95.7	62.1	76.2	94.3	69.9	81.5	92.6
Soybean	47.3	62.5	97.1	68.5	81.0	95.5	71.6	83.0	93.2
Strawberry	36.3	51.7	95.5	63.4	77.4	93.8	69.4	81.7	91.8
Tomato	31.5	45.7	94.0	54.3	69.8	92.5	61.7	75.8	90.5

Figure 5.6 presents confusion matrices with percentages of correct answers (TPR and TNR) and errors (FPR and FNR) for the plants under study. The data for calculating these matrices was obtained with defoliation levels from 1 to 45%. While Table 5.2 presents three defoliation intervals, the confusion matrices result from grouping these three intervals. As can be seen, Apple, Corn, Pepper, Potato, Raspberry, Soybean, Strawberry, and Tomato have hit rates above 80% (TPR) and 93% (TNR). Also, the results show low error rates (FPR $< 9.3\%$ and FNR $< 24.5\%$). Although plant species have different characteristics, assertiveness and error rates between them are very close. The FPR was generally lower because the background pixels were plain black, consequently increasing the TNR and decreasing the FPR. However, FNR is related to considering leaf pixels as background. That becomes more common in the boundary of the leaves, especially for higher defoliation levels, since those pixels have many background neighbors, which can cause some mistakes.

TPR	FNR
80.2 %	19.8 %
FPR	TNR
5.40 %	94.6 %

(a) Apple

TPR	FNR
78.4 %	21.5 %
FPR	TNR
5.10 %	94.9 %

(b) Blueberry

TPR	FNR
79.0 %	21.0 %
FPR	TNR
4.20 %	95.8 %

(c) Cherry

TPR	FNR
84.9 %	15.1 %
FPR	TNR
0.30 %	99.7 %

(d) Corn

TPR	FNR
79.8 %	20.2 %
FPR	TNR
5.30 %	94.7 %

(e) Grape

TPR	FNR
75.5 %	24.5 %
FPR	TNR
9.30 %	90.7 %

(f) Peach

TPR	FNR
81.6 %	18.4 %
FPR	TNR
5.20 %	94.8 %

(g) Pepper

TPR	FNR
82.8 %	17.2 %
FPR	TNR
5.10 %	94.9 %

(h) Potato

TPR	FNR
81.9 %	18.1 %
FPR	TNR
4.30 %	95.7 %

(i) Raspberry

TPR	FNR
81.2 %	18.8 %
FPR	TNR
2.80 %	97.2 %

(j) Soybean

TPR	FNR
81.2 %	18.8 %
FPR	TNR
4.40 %	95.6 %

(k) Strawberry

TPR	FNR
80.6 %	19.4 %
FPR	TNR
6.20 %	93.8 %

(l) Tomato

Figure 5.6: *Confusion matrices for different plant species.*

5.4.2 Defoliation estimate

The level of defoliation is measured by the linear correlation between the actual and the estimated loss. When there is a strong correlation, the error effect is considered minimal, although it is randomly distributed around the regression line. Figure 5.7 shows scatter plots for the different types of crops investigated in this study. Blueberry, Corn, Grape, Potato, Raspberry, Soybean, and Strawberry obtained a correlation coefficient greater than 0.96 where Blueberry and Raspberry reached $r = 0.97$, and Grape, Potato, Soybean, and Strawberry reached $r = 0.98$, and Corn reached $r = 0.99$. Apple, Peach, and Tomato obtained lower results than the others, with values equal to $r = 0.93$, $r = 0.77$, and $r = 0.92$, respectively. Corn obtained the most accurate result due to the leaf region

occupying the full image size. On the other hand, Peach and Tomato obtained less accurate results mainly due to the irregular pattern caused by the intensity of shading on peach leaves and the registration of different tomato species with early and adult leaves. Despite this, the results show that the method can be generalized for other plant species and is consistent at varying levels of leaf damage.
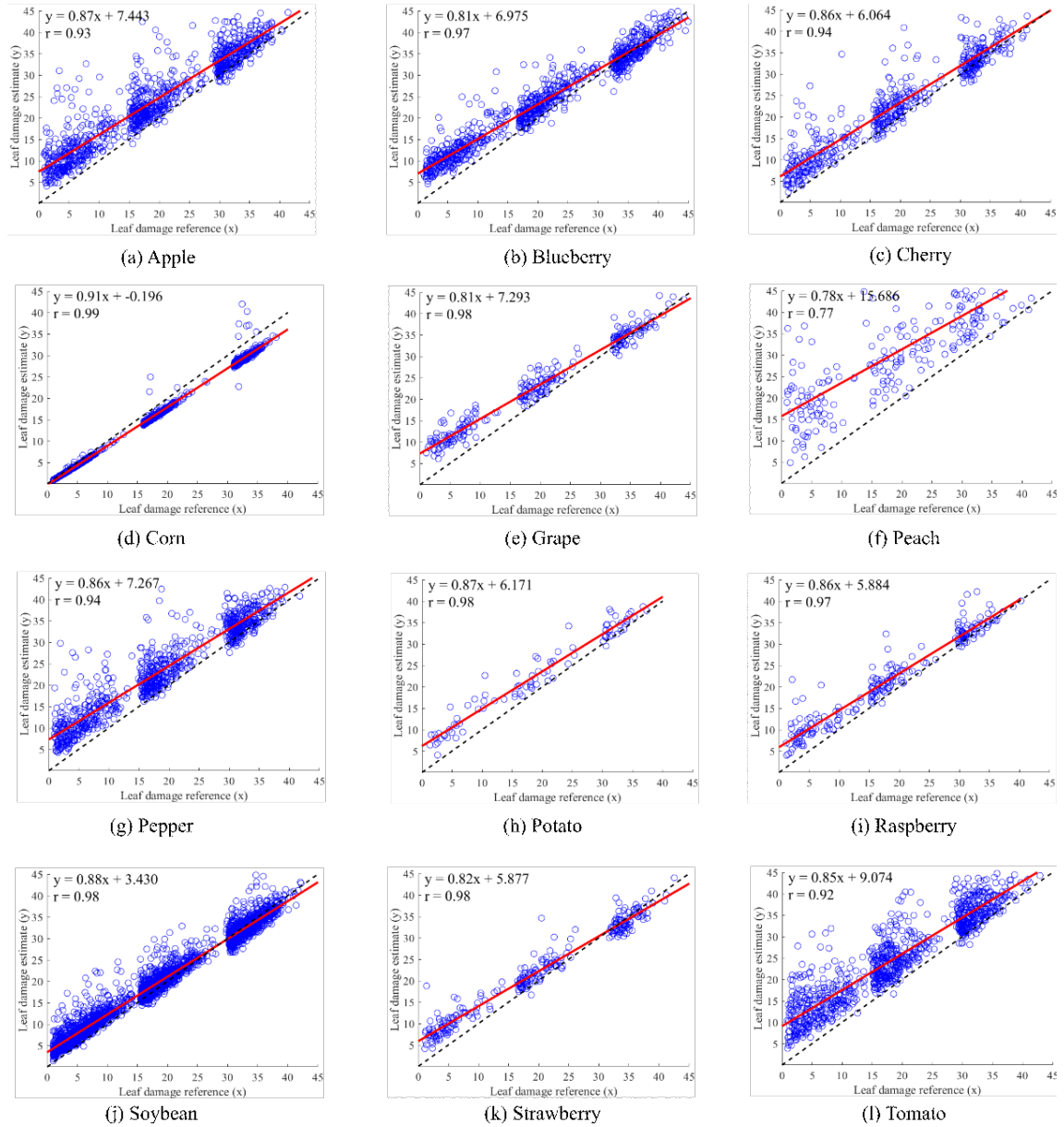
Figure 5.7: *Regression line of the proposed method in 12 different crop species.*

However, it is important to note that the estimation error differs somewhat according to the plant species. Leaf structures have their own characteristics that identify them and differ from other types of crops. For plants with more homogeneous characteristics, such as soybeans, leaf models can better represent the set. When the specimens have variations in shape caused by the stage of leaf maturity, type of cultivar, or shading in leaf regions, as in tomato, apple, and peach, the leaf models may be less assertive. In this way,

the results are linked to the conditions of the image database. Also, for this reason, the estimated error can differ from the actual error. Our method often overestimates the error estimate, indicating that the leaf models have a larger leaf area than the test set images. For leaf analysis situations, these results could better alert for preventive decision-making actions than underestimated results that could erroneously postpone safeguarding actions.

5.4.3   Visual inspection

In addition to estimating the percentage of defoliation, in our proposal, the damaged leaf regions are visually presented. It is a handy feature because it allows the analyst to check which points in the leaf region are being attacked. For example, some chewing insects initiate defoliation from the inner vein to the edges of the leaves. In contrast, cutting insects prefers to start from border regions. Therefore, visual information like the one we present can support other analyses besides the leaf loss estimate. Figure 5.8 shows some cases of defoliation and presents percentages of leaf tissue consumed and estimated for different levels of leaf loss.

GT: 7.44	GT: 21.14	GT: 39.13	GT: 5.28	GT: 17.44	GT: 30.97	GT: 2.09	GT: 16.40	GT: 32.39
DE: 10.53	DE: 23.03	DE: 39.72	DE: 6.76	DE: 19.69	DE: 31.47	DE: 2.75	DE: 15.66	DE: 29.87

(a) Apple   (b) Blueberry   (c) Cherry

GT: 3.86	GT: 17.19	GT: 36.92	GT: 7.67	GT: 17.32	GT: 33.42	GT: 5.83	GT: 26.81	GT: 41.20
DE: 3.26	DE: 15.31	DE: 34.30	DE: 9.20	DE: 18.48	DE: 33.48	DE: 8.73	DE: 28.89	DE: 40.24

(d) Corn   (e) Grape   (f) Peach

GT: 6.02	GT: 23.75	GT: 32.14	GT: 2.22	GT: 20.81	GT: 33.97	GT: 3.23	GT: 17.42	GT: 31.16
DE: 7.95	DE: 25.78	DE: 33.14	DE: 4.74	DE: 21.50	DE: 33.98	DE: 4.62	DE: 18.38	DE: 30.40

(g) Pepper   (h) Potato   (i) Raspberry

GT: 3.71	GT: 16.91	GT: 34.65	GT: 7.85	GT: 20.27	GT: 40.93	GT: 8.22	GT: 19.10	GT: 32.12
DE: 3.85	DE: 15.13	DE: 31.77	DE: 11.22	DE: 21.91	DE: 39.21	DE: 10.19	DE: 19.00	DE: 32.13

(j) Soybean   (k) Strawberry   (l) Tomato

Figure 5.8: *Estimated defoliation areas (in blue) and percentage of actual leaf damage and leaf damage estimated by the proposed method. (GT = ground truth, DE = defoliation estimate).*

Some detection errors are justified by the number of spurious pixels resulting from the image binarization process, which leads to differences between the leaf template and the test leaf. The binarization step may associate points in the leaf edge region with the area of interest when, in fact, they should be categorized as the background region. This effect can be visually observed in Figure 5.8, especially in the images of grape and strawberry leaves ((e) and (k)). Besides that, the image template may not correctly fit the shape of the test image, leading to differences between the two images. As the preprocessing stage applies image adjustments through rotation transformation, the template and test images can be in different profiles, making i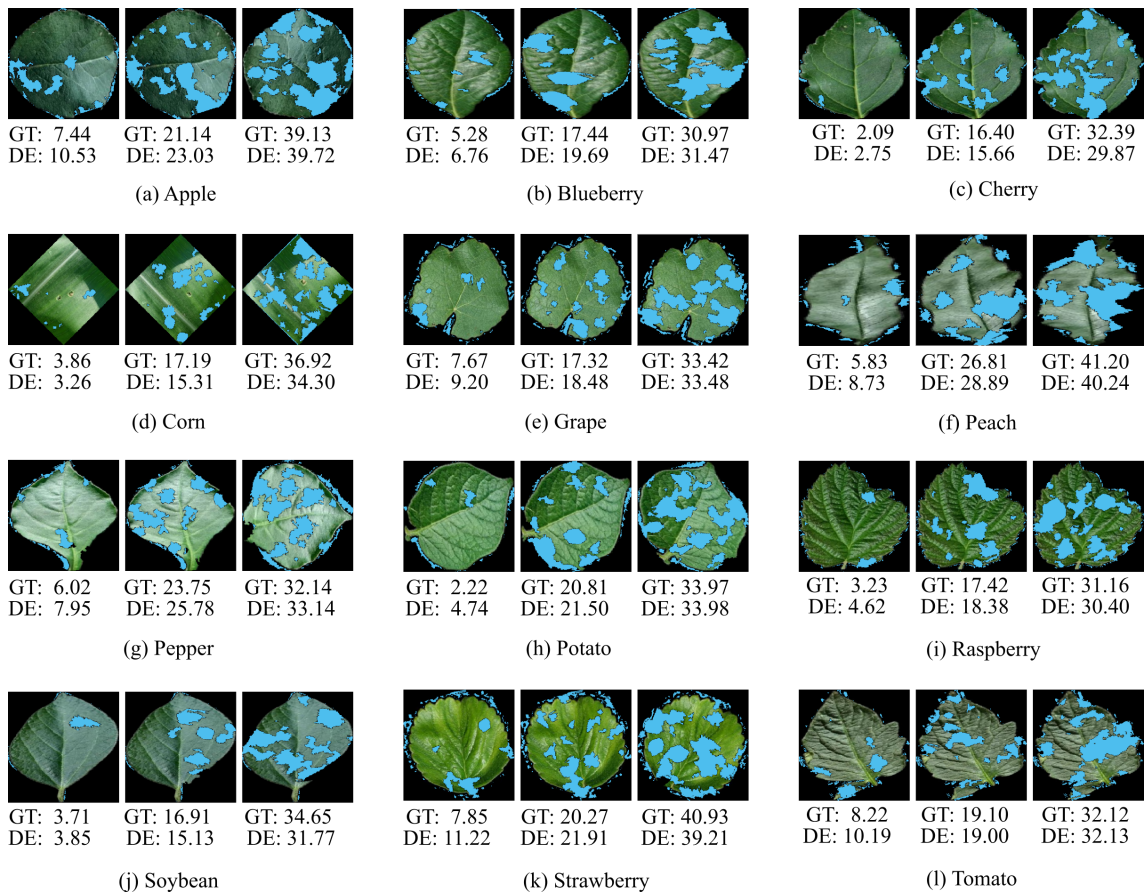t difficult to match them. In addition, the level of defoliation severity can influence the image's positioning, as seen in the corn leaf (Figure 5.8 (d)). In this case, the three images originated from the same test leaf, but due to the level of defoliation, they were rotated and placed in different positions. Also, it is worth mentioning that the actual damaged percentage is obtained with the synthetic defoliation strategy (Section 5.3.3), in which the defoliation level is computed based on the damages applied to input images.

5.4.4 Comparative analysis

A direct comparison between related works is quite challenging as no benchmarking exists. Because of this, researchers use their database, which is not accessible to the general public. Then, the data are restricted to those presented in the published works, and it is hard to verify the samples' variability, such as lighting conditions, leaf format and position, and background complexity. Also, leaf images with damage caused by real insects or artificial leaf canopy damage used in experimental tests are difficult to reproduce to compare the results. Despite this, we present a comparative analysis between our method and related works considering only soybean leaves. Figure 5.9 shows that the linear correlation (r) obtained by our method is better than using a digital scanner (BRADSHAW *et al.*, 2007) and as assertive as Bioleaf (MACHADO *et al.*, 2016), which is a semi-automatic method, and AlexNet, a convolutional neural network. Also, Figure 5.10 shows that the RMSE score of our method is smaller than those presented by the deep neural networks AlexNet, VGGNet, and ResNet (SILVA *et al.*, 2019).

Additionally, we qualitatively compare our work with related work. Unlike (MALOOF *et al.*, 2013) and (EASLON; BLOOM, 2014), the estimates performed in our proposal are fully automated so that computer-assisted processes obtain the results. Likewise, our work differs from (MACHADO *et al.*, 2016) because our method does not require user interaction and operator expertise to define leaf edge contours. It differs from (SILVA *et al.*, 2019) and (SILVA *et al.*, 2021) since our proposal does not use training steps, which are time-consuming and require many images to converge the models. It also
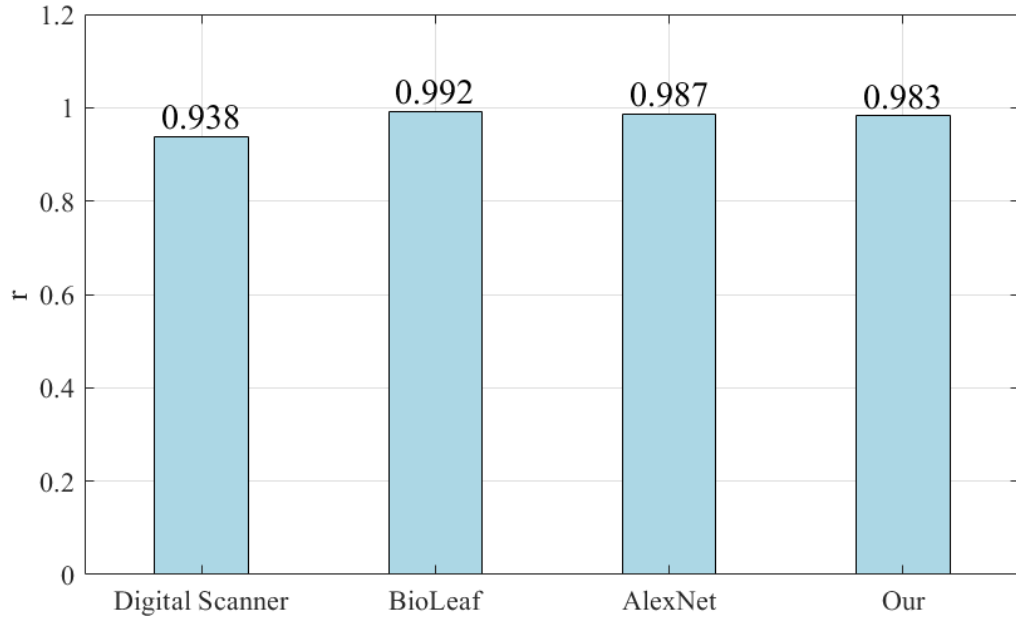
Figure 5.9: *Comparative considering linear correlation (r).*
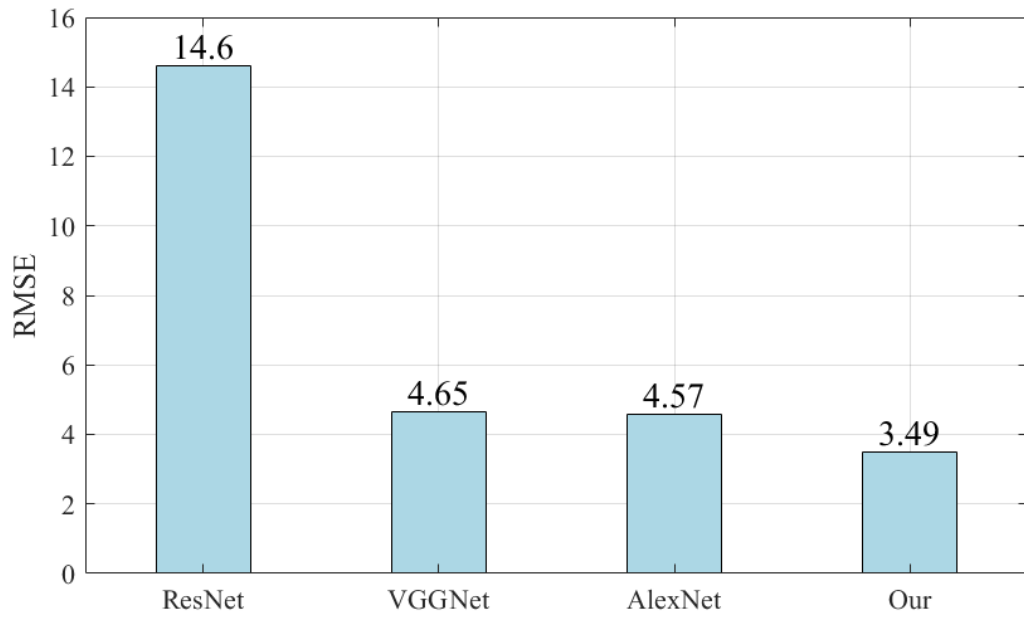
Figure 5.10: *Comparative considering RMSE.*

differs from (ESGARIO *et al.*, 2022) because our model can estimate the severity of leaf stress caused by chewing and cutting insects. Furthermore, our proposal does not require specific equipment such as those used in manual quantification or leaf area measurement equipment (KERAMATLOU *et al.*, 2015; KAUR *et al.*, 2014). Also, we demonstrate the generalization of our proposed method by considering different types of plant species. Finally, our experimentation differs substantially from the other works as we use a public database that is available online and many validation metrics, including visual inspections.

In this sense, to address the problem related to the complexity of quantitative comparisons, we organized and made our experimental data available (see Section A.1.5).

We indicate the images used in the construction of template images and those used in the tests. For the test images, we indicate their defoliation percentage in three groups: from 1 to 15%, 16 to 30%, and 31 to 45%. Figure 5.11 presents some examples used in the performance evaluation, which are available in the supplementary material. We also organized all images into subfolders for future work and comparative analysis.

(a) 1 - 15% defoliation   (b) 16 - 30% defoliation   (c) 31 - 45% defoliation
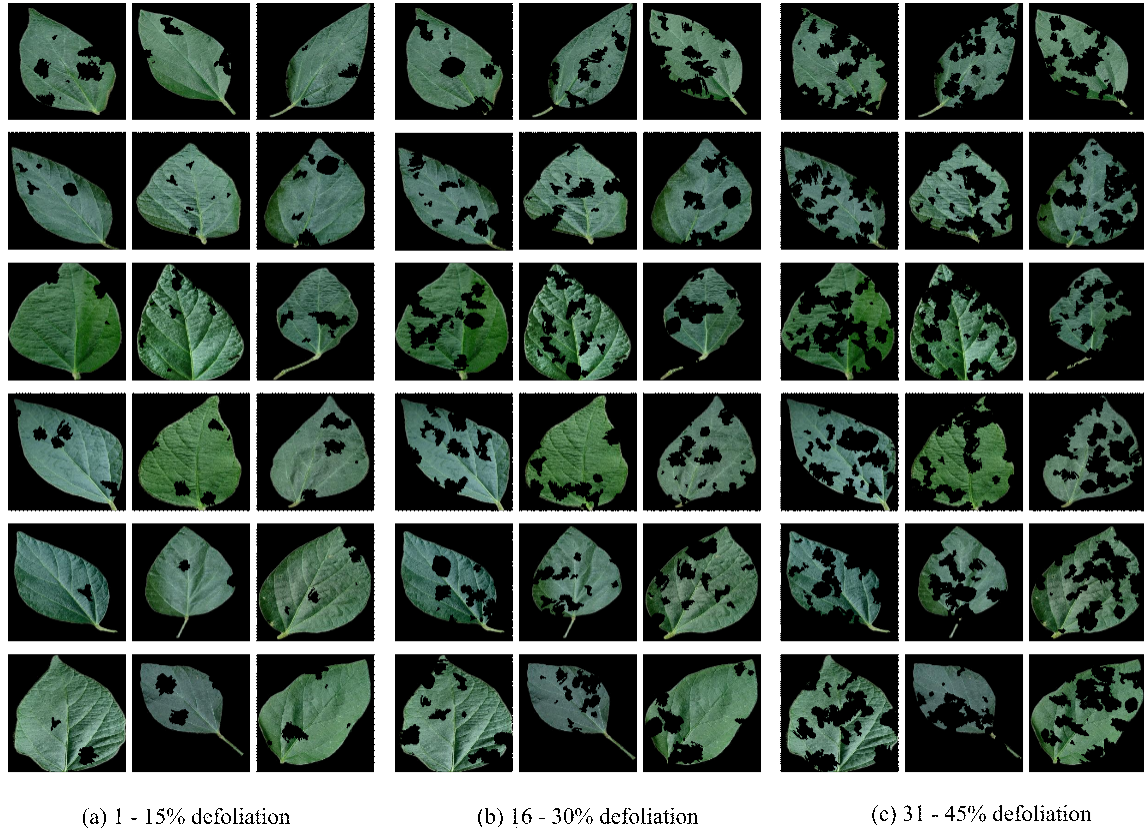
Figure 5.11: *Some samples of the soybean test images.*

5.4.5   Time performance analysis

The time to execute the leaf analysis processes depends on the number of images used to construct the template images. Therefore, processing will require more time for a more significant quantity of template images. Table 5.3 shows the average execution time and standard deviation of the three processing steps considering the number of images used in the template image construction and the number of images used as test images. The most time-consuming task is related to image preprocessing. In this task, we must binarize the image, compute its convex hull, find a reference line, and perform image rotation. The last two operations are the most time-consuming. However, each presented time in Table 5.3 represents the total time for each plant sample group. We highlight that the preprocessing time for a single image sample is about three milliseconds, which can be

considered small. In any event, we believe that is not significant since modern approaches with parallel computing can significantly reduce the preprocessing time.

Table 5.3: *Execution time (in seconds) of the proposed method steps and the number of template and test images.*

	Preprocessing	Image Matching	Defoliation Estimate	Template Images	Test Images
Apple	4.22 ± 2.42	0.18 ± 0.01	5.63e-04 $\pm$ 3.08e-04	1,316	329 x 3
Blueberry	4.46 ± 2.55	0.18 ± 0.01	4.94e-04 $\pm$ 2.52e-04	1,202	300 x 3
Cherry	2.76 ± 1.65	0.14 ± 0.01	5.31e-04 $\pm$ 3.23e-04	684	170 x 3
Corn	5.33 ± 3.04	0.15 ± 0.01	5.84e-04 $\pm$ 3.48e-04	930	232 x 3
Grape	1.31 ± 0.72	0.12 ± 0.03	6.09e-04 $\pm$ 3.63e-04	339	84 x 3
Peach	0.96 ± 0.50	0.11 ± 0.01	6.40e-04 $\pm$ 5.63e-04	288	72 x 3
Pepper	4.14 ± 2.40	0.17 ± 0.02	5.27e-04 $\pm$ 3.99e-04	1,183	295 x 3
Potato	0.60 ± 0.30	0.11 ± 0.01	5.03e-04 $\pm$ 3.26e-04	122	30 x 3
Raspberry	1.15 ± 0.62	0.11 ± 0.01	4.91e-04 $\pm$ 2.53e-04	297	74 x 3
Soybean	13.71 ± 7.92	0.37 ± 0.01	4.84e-04 $\pm$ 3.01e-04	4,072	1.018 x 3
Strawberry	1.36 ± 0.76	0.11 ± 0.01	5.05e-04 $\pm$ 2.83e-04	365	91 x 3
Tomato	4.09 ± 2.38	0.17 ± 0.01	5.42e-04 $\pm$ 2.85e-04	1,273	318 x 3

It is worth mentioning that the preparation of the template image is performed only once, so the final result can be quickly obtained. Also, the number of images used to construct the template and test images varies according to the plant species in the dataset. As we evaluate our proposal at three defoliation intervals, the number of test images is multiplied by three.

5.4.6 Limitations

Although the proposed method presents consistent results, mentioning some limitations is essential. First, results are more assertive when the leaf samples have a regular pattern in their shape. In this way, image templates can better represent groups of plant species and find better matches for damaged leaves. Furthermore, the segmentation process that separates the leaf canopy (foreground) from the rest of the image (background) can influence the results since the image templates may contain areas outside the leaf region. Therefore, complex backgrounds and multiple plant leaf samples per image can deteriorate the method's performance.

Problems related to background permeate all leaf analysis proposals. Related work deals with this problem by suggesting using a blank sheet of paper to differentiate the target object from the background or simply using databases with the target object already segmented. Background subtraction and semantic segmentation are typical computer vision problems and expand the scope of our investigation. These are topics of interest for future work, where we intend to investigate segmentation methods and apply them to scenarios with a complex background. Therefore, we plan to add new pre-processing steps in future versions of the proposed method to deal with two or more leaves in the same image and multiple overlapping leaves.

We have included a comprehensive figure to present some simulations concerning complex conditions. Figure 5.12 presents a test leaf whose background was not removed, another sample with a bigger and a smaller leaf in the same image, a shaded image, and a leaf image with the stalk (petiole) that attaches the leaf blade to the stem in a severe defoliation condition.

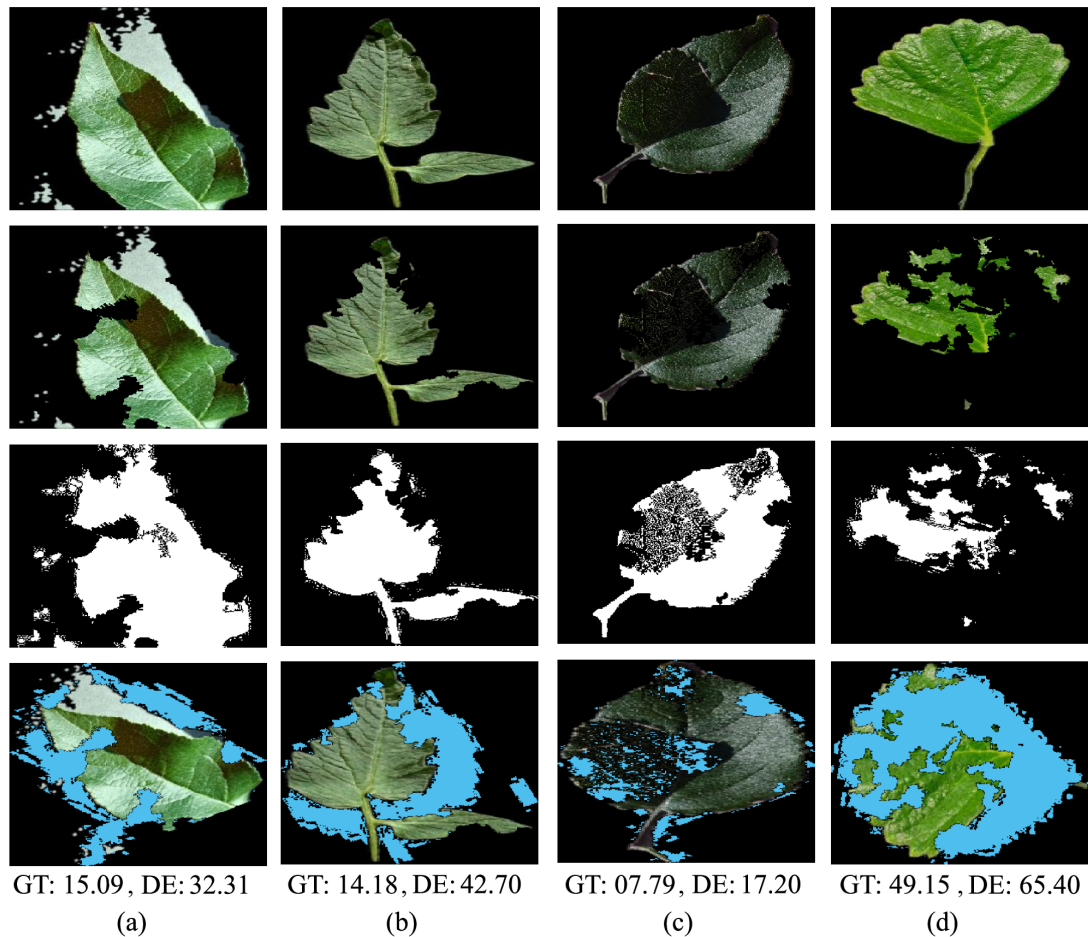| GT: 15.09 , DE: 32.31 | GT: 14.18 , DE: 42.70 | GT: 07.79 , DE: 17.20 | GT: 49.15 , DE: 65.40 |
| (a) | (b) | (c) | (d) |

Figure 5.12: *Limitation of the method. From (a) to (d): inaccurate background removal, more than one leaf per image, shaded leaf, peculiar leaf shape with severe damage. From the first row to the fourth: input leaf, damaged leaf with synthetic defoliation, binarized damaged leaf, defoliation estimated. (GT = ground truth, DE = defoliation estimate).*

Note that for all the cases in Figure 5.12, the estimated error differs from the actual error because none of the image templates fit the test leaves correctly. Thus, due to the complexity of the scene as a background region associated with the region of interest, more than one leaf per image, image shadows that limit binarization, test leaf shapes that differ from leaf templates, and excessive leaf damage, the method's accuracy may deteriorate.

However, these issues can be overcome with more homogeneous databases and image acquisition with attention to background simplification. In practice, leaf analysis is performed on homogeneous crop types, and leaf samples are separated according to their position on the plants (e.g., at the top or upper third of the plant). Besides that, image acquisition can be made using a blank sheet of paper as proposed by (MACHADO *et al.*, 2016), making it possible to collect data with leaf isolation and without removing the sample for analysis (i.e., a non-destructive approach).

Despite this, through an automatic approach to leaf analysis, the proposal deals with some challenges in estimating defoliation. In this regard, the severity of leaf damage at different levels, the impairment of the leaf surface in edge regions, the difficulty in building generalist models for different plant species, and processing steps that are performed in reasonable processing time are addressed in this work to consolidate a tool for precision agriculture. On the other hand, issues related to the collection of leaf samples are not directly discussed in this study. Our work considers a more straightforward color-based segmentation to differentiate regions of interest from background images. Thus, in cases where unfavorable conditions are involved, such as a complex background and more than one leaf per image, other segmentation strategies should be investigated.

In a scenario where our method is potentially used, an operator captures images with an RGB camera with only one leaf per record. This step could be done with some contrasting background that simplifies the target object segmentation process. An image data set is prepared to contain only healthy leaves, i.e., images with no incidence of insect predation. Likewise, injured leaves are captured and stored in another data set. Then, the method builds template images with the data set of healthy leaves and compares the damaged leaves with the templates. Finally, the method returns the estimated percentage of defoliation. In this fashion, the operator does not need to worry about the position of the leaf surface, the distance between the camera and the target image, or the outline of the leaf silhouette. The method was designed to minimize image acquisition effects such as rotation and scale transformations and work without requiring manual delineation of leaf boundary regions. In this study, we use the segmentation method proposed by (MOHANTY *et al.*, 2016), whose operation is outside the method pipeline. Other segmentation strategies can be investigated to separate the leaf from the image background.

5.5   Conclusion

In this chapter, we present a method for estimating leaf damage. As removing leaf tissue from insects reduces photosynthetic capacity, measuring the percentage of leaf area consumed is vital to verify the degree of interaction between insects and crops. In this sense, leaf analysis enhances decision-making, contributing to more efficient agricultural management actions and strategies.

The proposed method is suitable for monitoring activities with much greater sampling capacity than manual or semi-automatic leaf analysis processes. Furthermore, our method can be applied to plant species with various leaf shapes. Likewise, it can accurately estimate defoliation at multiple severity levels and visually present the area of leaf tissue consumed for further analysis and inspection. Thus, as it has a well-defined pipeline with lightweight processing steps, the proposed method is suitable for devices with limited computational power. Although we can see powerful neural networks, the computational resources to run models and memory to accommodate the size of the weights of these networks are still somewhat limiting. Current trends are easing limitations on computing power, and we will soon see new scenarios. In any case, our method will remain competitive as it can be parallelized to process even more significant amounts of data per second.

ProtectLeaf: An Insect Predation Analyzer for Agricultural Crop Monitoring

I am coming to your house today.

Luke 19:5

Agricultural production positively impacts the global economy and is crucial in delivering supplies and maintaining life. However, predatory insects are estimated to have a significant productivity impact on agricultural fields. As the excessive incidence of insects can reduce the functionality of the leaf surface, limitations can be noticed in the capability of the plants to maintain energy, which reduces the growth of grains and fruits. Therefore, leaf analysis is an essential tool in monitoring plantations, helping producers make decisions to control agricultural pests. Thus, this chapter presents ProtectLeaf, a software designed to support crop monitoring activities and decision-making in agricultural environments through defoliation estimate, detection of insect predation on plant leaves, and leaf reconstruction. This chapter was published in the Journal SoftwareX (VIEIRA *et al.*, 2023).

Nr.	Code metadata description	
C1	Current code version	*v1.0*
C2	Permanent link to code/repository used for this code version	<https://github.com/ElsevierSoftwareX/ SOFTX-D-23-00186>
C3	Permanent link to Reproducible Capsule	<https://codeocean.com/capsule/7740985/tree/v1>
C4	Legal Code License	GNU GPL-2.0 License
C5	Code versioning system used	git
C6	Software code languages, tools, and services used	MATLAB
C7	Compilation requirements, operating environments & dependencies	Linux, Microsoft Windows, MATLAB R2014a
C8	If available Link to developer documentation/manual	<https://github.com/gabrieldgf4/insect_defoliation>
C9	Support email for questions	gabriel.vieira@ifgoiano.edu.br

6.1   Introduction

Agricultural production has grown progressively and systematically in recent years to respond to the global demand for farm supplies. As an economic activity, the cultivation of plants has moved the economy positively with the increase in production each year. In 2020, domestic corn prices rose, and the price average surpassed the best sales mark in 2015 (USDA, 2020c). In this period, Brazilian soybean production has reached new records, surpassing the United States production, which was the largest soybean producer until then (USDA, 2020e). In addition, cultivating fresh deciduous fruits such as pears, grapes, and apples exceeded expectations, with production above that practiced in the years before 2022 (USDA, 2022).

Although agricultural production has achieved successive records, it is estimated that predatory insects have a significant economic impact on crop yields (RENAULT *et al.*, 2022). Insect damage leads to a considerable loss of production and increases the cost of pest management and control. The challenge is to find the balance between agriculture and the inevitable incidence of insects. When the ecosystem is balanced, i.e., the existence of insects does not harm the crop, the expected results of crop production can be achieved through previously defined interventions as planned. However, when there is an imbalance, the number of insects exceeds expectations, and agricultural production is affected, demanding contingency actions and invasive controls, such as mechanical methods with containment barriers or chemical pest control with insecticides.

In this sense, crop monitoring is crucial for making good decisions for agricultural management operations (VIEIRA *et al.*, 2019a). The plantations need to be constantly observed so that the occurrence of damages can be quantified to justify interventions or indicate that the losses are within the normal range (MOUSSAFIR *et al.*, 2022). Among the pertinent damages to crops, the attack of herbivorous insects stands out. The main consequence is the functional reduction of the leaf surface affected by the loss of leaf area, which is known as defoliation (SILVA *et al.*, 2019). Defoliation is a direct consequence of insect predation, which reduces the energy capacity of plants, the photosynthetic process, and the growth of grains and fruits (FERNANDES *et al.*, 2022).

Estimating leaf loss and detecting leaf areas affected by predation are essential tools in agricultural monitoring. Thus, the percentage of leaf damage can measure the risk of future harm to crop production by indicating whether the occurrence of insects is above acceptable tolerance limits. The estimated percentage of leaf area makes it possible to verify the balance between plantations and predatory insects. For example, measuring defoliation at 30% in the vegetative phase or 15% in the reproductive phase of soybeans are the maximum threshold levels for triggering pest control (FERNANDES *et al.*, 2022). In addition, detecting damaged leaf regions provides information so the

analyst can suggest the type of insect causing the environmental imbalance and adequate pest control. In this sense, while the estimate of leaf loss supports decision-making, the detection of injured leaves indicates the areas of cultivation in which the control of insect proliferation needs to be applied.

The estimation of leaf loss has been assisted by different proposals, including manual (KVET; MARSHALL, 1971), semi-automatic (MACHADO *et al.*, 2016), and fully automatic methods (SILVA *et al.*, 2019; SILVA *et al.*, 2021). However, they all have some limitations. Manual methods demand highly qualified professionals to evaluate only small amounts of leaf samples. Semi-automatic methods can handle more analysis requests, but they depend on the user's expertise in operating computer systems or calibrating leaf area measuring devices. Automated processes are independent of the knowledge of qualified professionals but may require large volumes of data to build viable computational models. Given the limitations of related works, we present a computer program, ProtectLeaf, that estimates leaf loss, detects leaf regions consumed by insects, and artificially reconstructs the leaf surface. Our method does not require specialized knowledge to present the results and is suitable for environments with limited computational power. It has well-defined processing steps and does not require large amounts of leaf samples to build image models.

ProtectLeaf software was developed to support leaf analysis through quantitative assessments and visual inspection regarding the detection of insect predation incidence on plant leaves. The program identifies regions with leaf damage and highlights areas where herbivory has been detected. In a complementary way, the program segments the traces of insect bites whose results can be used in classifying predatory insects. Furthermore, the software presents defoliation estimates by measuring leaf canopy consumed by insects. Many proposals do not support leaf silhouette loss or require user intervention for this task (MALOOF *et al.*, 2013; EASLON; BLOOM, 2014; MACHADO *et al.*, 2016). Unlike related works, ProtectLeaf can automatically compute insect predation in both inner leaf areas and edge regions. Another functionality of the software is the reconstruction of the affected leaf area. A visual representation is presented to artificially fill the consumed leaf areas resembling the original leaf before defoliation. The software also has an insect predation simulator that uses actual leaf damage to produce insect damage on healthy leaves. Other works simulate defoliation but only use artificial structures quite different from true damage (SILVA *et al.*, 2019; SILVA *et al.*, 2021). Figure 6.1 presents results obtained with the software.
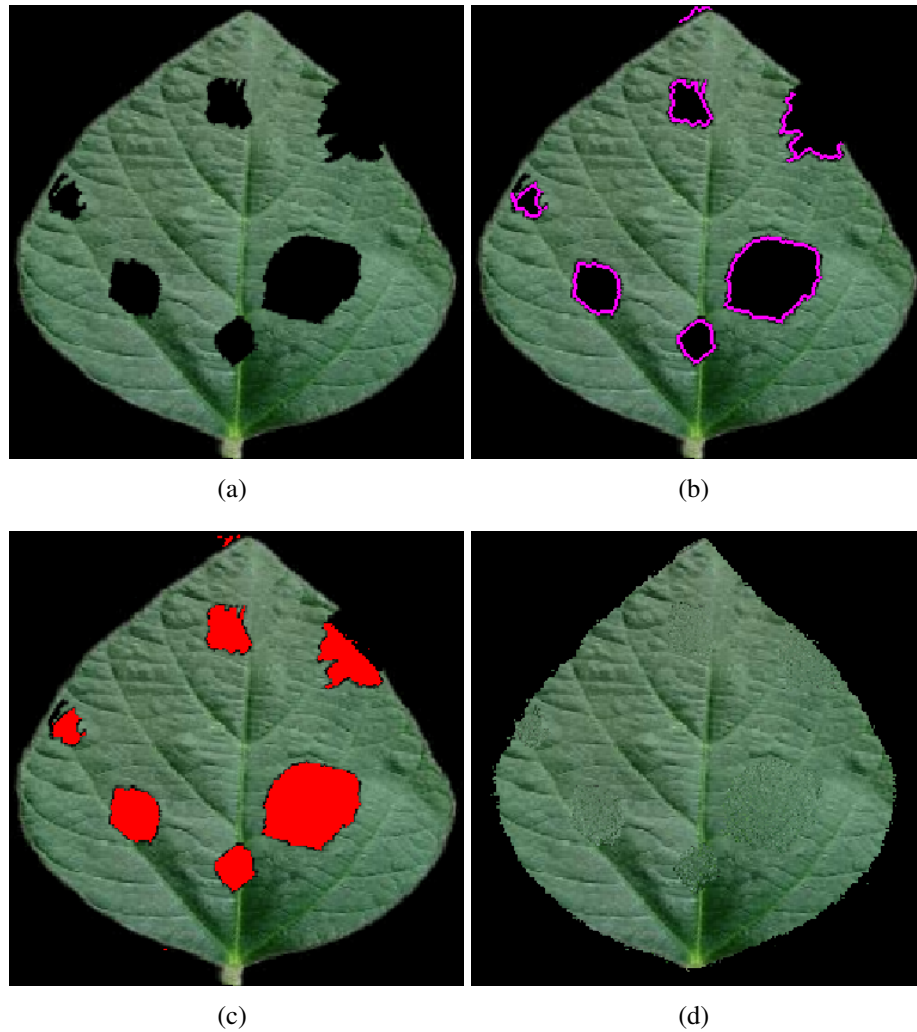
Figure 6.1: *Overview of the ProtectLeaf features. From left to right, (a) damaged leaf with artificial defoliation, (b) detection of insect predation (in magenta), (c) the estimate of injured leaf surface (in red), (d) and leaf reconstruction. (For interpretation of the references to color in this figure legend, the reader is referred to the web version of this thesis.)*

6.2   Software description

The software has three main functionalities. In the first one, the detection of damaged leaf regions is performed. As a result, the leaf surface that suffered insect predation is highlighted, and the bite traces are segmented. In the second, leaf loss is estimated, and damaged leaf areas are visually identified. In this regard, a defoliation estimate is performed in situations involving internal damage as well as leaf edge regions. The leaf silhouette is delineated in the third, and the injured leaf surface is reconstructed. The reconstruction process consists of the artificial filling of the delineated area, which is done by image blending (WANG *et al.*, 2017), or image inpainting (BORNEMANN; MÄRZ, 2007) techniques.

The software was designed with processing steps to eliminate aspects of subjective interpretation and reduce the demand for a professional specialized in leaf analysis. Likewise, the software does not require expensive equipment and strict image acquisition procedures. Also, the software was implemented with lightweight processes that considered energy efficiency and system overload aspects. In such a manner, the software is suitable for smart agriculture ecosystems that generally demand solutions for devices with limited computing power, such as embedded systems, Internet of Things (IoT) networks, and intelligent agriculture machinery (SAADANE *et al.*, 2022). Furthermore, the software uses digital image processing techniques, statistical measurements, and leaf properties, which are integrated into a comprehensive, easy-to-use computer solution. Thus, the software does not involve the intensive application of feature engineering and does not involve building statistical models based on learning algorithms.

As presented in Figure 6.2, the software architecture was designed with three main components. First, the plant leaf samples are processed and automatically adjusted based on scale, rotation, binarization, and morphological operations. After initial processing, the binarized images are grouped into an image template database to assess the correspondence between an injured leaf and template leaves. Next, the image matching step finds the image template that best fits the damaged leaf. Following that, the image template becomes a reference to compute the damage caused by insect predation, detect the leaf surface regions affected by herbivory, and reconstruct the leaf canopy. The image template database was built in previous works with 20 images (VIEIRA *et al.*, 2022), 42 images (VIEIRA *et al.*, 2021a), and 60 images (VIEIRA *et al.*, 2022). In this sense, the template images can be prepared with only a few healthy leaf samples.
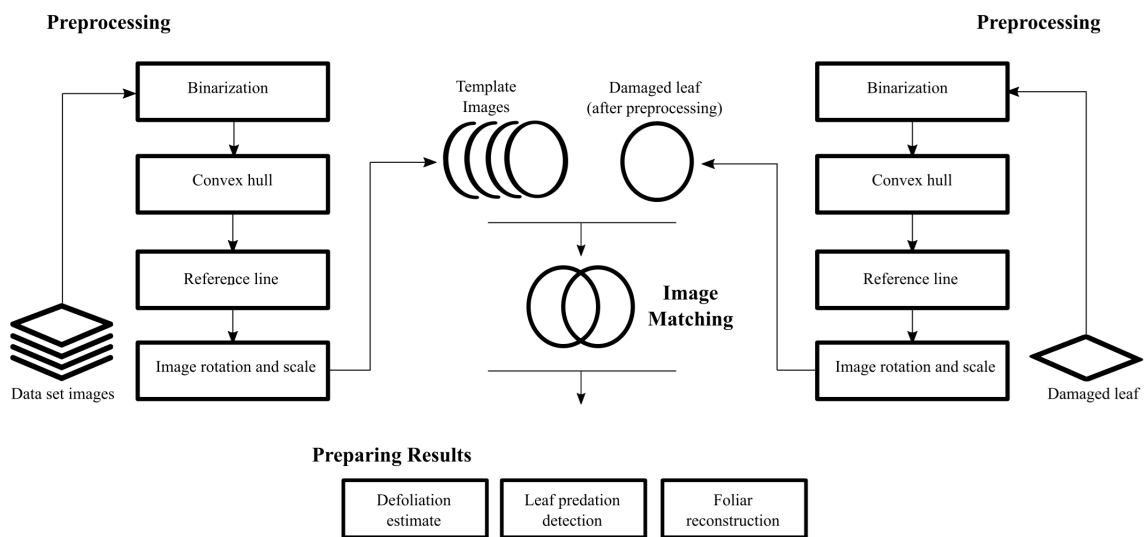

Figure 6.2: *Software architecture design.*

In `Preprocessing`, each sample of the image data set is transformed into an image template. First, an image sample is binarized where its background is labeled with 0, and its foreground (leaf surface) is labeled with 1. Then, the resulting image is processed with a convex hull operation that encloses all leaf surface points in a convex polygon. Following that, the image's border is highlighted using morphological operations, and the distances between the points that contour the leaf surface are computed. Based on the longest distance between a pair of points, a reference line is traced, which is used to rotate the image to a vertical position. In addition, the image is scaled according to the leaf surface. After concluding these steps, a set of image templates is obtained with one representation for each image in the database. Similarly, the preprocessing steps are applied to injured leaves. Figure 6.3 shows the visual results of the preprocessing steps applied to a sample of an image data set and a damaged leaf.

(a) *Original images*   (b) *Binarization*   (c) *Convex hull*   (d) *Reference line*   (e) *Rotation and scale*
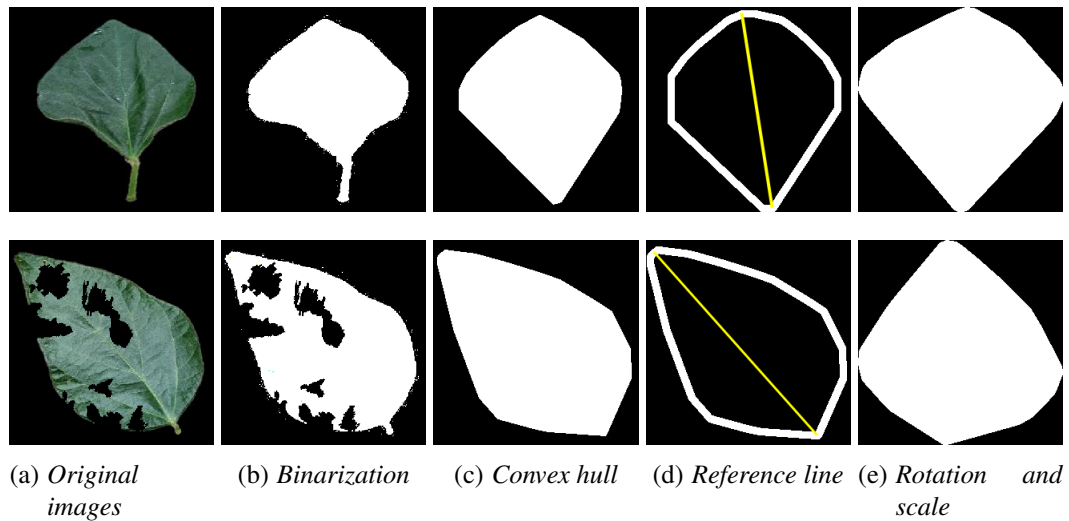
Figure 6.3: *Building an image template (first row) and adjusting a damaged leaf (second row) with preprocessing steps.*

In `Image Matching`, injured leaves are compared to the image templates, and the similarities are measured to point out correspondent images. The main goal is to find models that best fit the damaged leaf surfaces or models whose shapes are better related to the injured leaf designs. The comparison consists of computing the image profiles and checking which image pairs obtained the most significant matching. The similarity is measured by the ratio between the common points (intersection) and the combined areas (union) of damaged leaves and image templates. Therefore, the image-matching process computes the intersection over the union (IoU, (HU *et al.*, 2021)) where the results range from 0 to 1. When the results are close to 1, perfect consistency can be noted. In contrast, IoU values close to 0 points to a weak match. After comparing the damaged leaves with the entire image templates, the results with higher values indicate

better image correspondences. Figure 6.4 presents visual representations of the image-matching process.

(a) *IoU = 0.72*   (b) *IoU = 0.86*   (c) *IoU = 0.81*   (d) *IoU = 0.88*   (e) *IoU = 0.94*
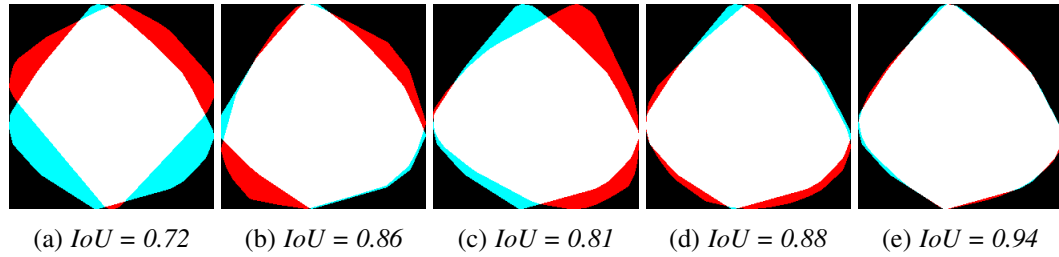
Figure 6.4: *Image matching process between template images and a pre-adjusted damaged leaf.*

In `Preparing Results`, three steps are followed: the defoliation is estimated, the leaf predation is detected, and the foliar canopy is reconstructed. The defoliation estimate is computed by the logical conjunction between damaged leaves and their corresponding image templates. The task consists of counting the points outside the intersection between the image pair and computing the percentage of pixels in the template image that are not in the damaged leaf. Likewise, the damaged regions are obtained from the logical conjunction operation between damaged leaves and the retrieved image templates in detecting leaf predation. Then, image elements outside the intersection of image pair boundaries indicate segments corresponding to insect bites. In the leaf reconstruction step, image template areas whose regions do not belong to the damaged leaves point to the compromised regions of the target image. Thus, the estimated missing areas are artificially filled with digital image processing techniques. The software implements two image reconstruction techniques: image blending (WANG *et al.*, 2017), and image inpainting (BORNEMANN; MÄRZ, 2007). Figure 6.5 presents visual results of defoliation estimate, leaf predation detection, and foliar canopy reconstruction using image inpainting.

(a) *Defoliation estimate*   (b) *Leaf predation detection*   (c) *Foliar reconstruction*

Figure 6.5: *Visual results of leaf analysis presented by the software.*

6.3   Software components

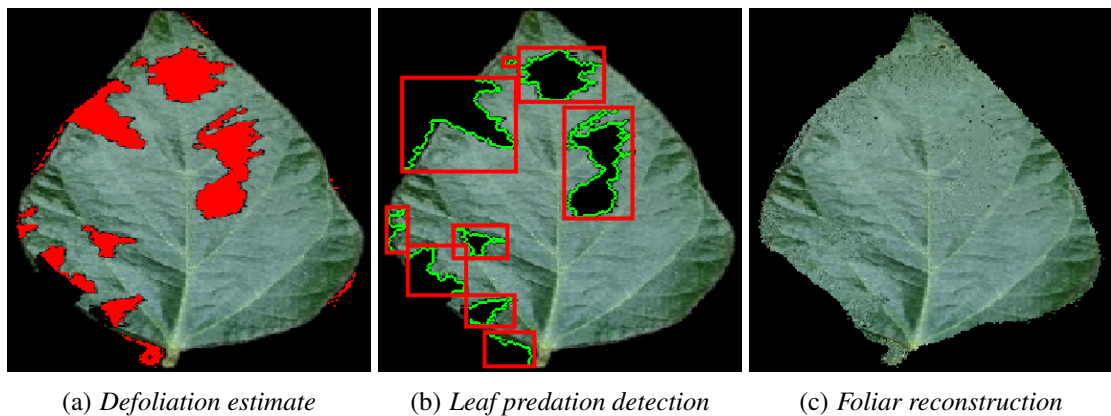This section introduces the ProtectLeaf software components and shows their intra-module connections and dependencies. Structured through thirteen components, the software contains modules for image loading, dataset organization, similarity evaluation and image matching, image reconstruction, and support modules for result analysis and artificial damage preparation. Figure 6.6 illustrates the software architecture with its provided and required interfaces and dependencies between the software components.
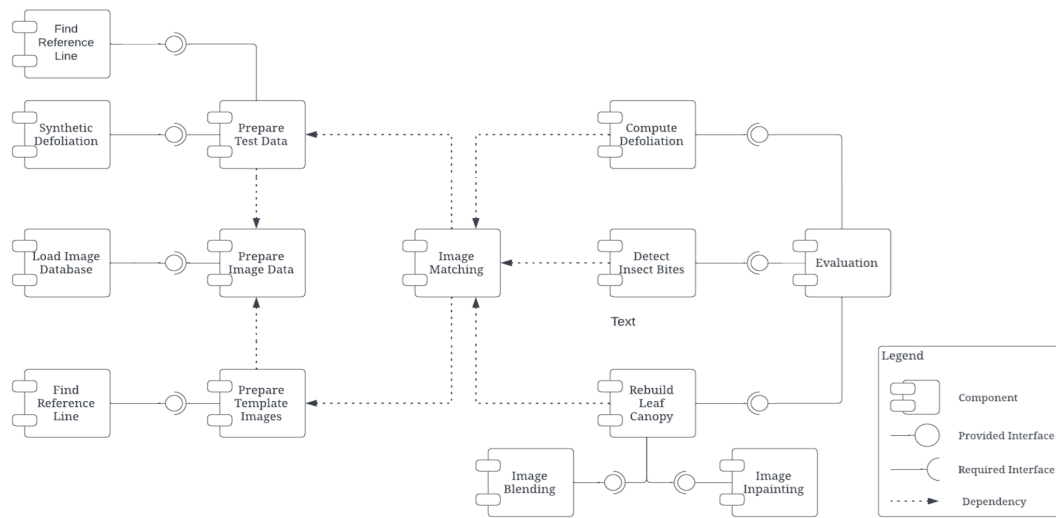
Figure 6.6: *Software architecture components.*

The `Load Image Dataset` is a utility that the software has for reading images from disk. In this module, a function that receives a folder name (or image path) reads and loads images into memory for later manipulation. The `Prepare Image Data` transforms previously loaded images to obtain two categories, area of interest and image background, in a process known as binarization.

The `Prepare Template Images` and `Prepare Test Data` components are responsible for building the template images and adjusting the test images through morphological operations (convex hull), and image rotation and scale operations. Both modules require the `Find Reference Line` component responsible for calculating leaf edge pixel distances and finding the reference line used to encapsulate the leaf shape pattern.

The `Image Matching` computes the overlap area between a damaged leaf (test image) and model leaves (template images) and returns the template that best fits the injured leaf shape. From the result obtained, the components `Compute Defoliation`, `Detect Insect Bites`, and `Rebuild Leaf Canopy`, work in the defoliation estimate, detection of insect predation, and reconstruction of the leaf surface, respectively. In this software version, leaf reconstruction can be achieved using the `Image Blending` or `Image Inpainting` components.

The software also has two other modules used mainly to analyze the results. The `Synthetic Defoliation` component applies synthetic deformations to healthy leaves by mapping the original state with the updated state. This mapping allows checking the quality of the results when labeled data is challenging to obtain. In the case of leaf analysis, building image databases has a significant operating cost as laboratory facilities are required to maintain crops and insects. In this sense, the feasibility of the ProtectLeaf software can be quickly verified for any crop using only healthy leaves. Another equally important module for this task is the `Evaluation` component, which provides evaluation metrics such as those indicated in Section 6.4.2.

6.4 Experimental design and results

In this section, the results obtained with the experimental tests are presented. The effectiveness of the ProtectLeaf software is verified in different plant species, and the results are discussed considering three main points: correctness in identifying missing segments of leaf area, assertiveness in the defoliation estimation, and precision in the visual reconstruction of the damaged leaf.

6.4.1 Image dataset

The experiments are performed in a public dataset[1] with several specimens of plant leaves: apple, blueberry, cherry, corn, grape, peach, pepper, potato, raspberry, soybean, strawberry, and tomato. The dataset was randomly split into 80% and 20%. The first set is used to construct template images, and the other is used for evaluation purposes. The template images are constructed from healthy plant leaves, where a model is prepared for each plant species, and the test images are preliminarily deformed using the synthetic defoliation component to produce injured leaves (Section 6.3). Leaf damage is applied in different amounts, which include minor damage ranging from 1 to 15%, medium damage from 16 to 30%, and severe damage from 31 to 45%. Also, the segmentation strategy proposed by (MOHANTY *et al.*, 2016) is used to detach the leaves from the image background.

6.4.2 Evaluation metrics

Linear correlation indicates the degree of relationship between the expected and estimated defoliation level and expresses the degree of correlation through values

---

[1]https://github.com/digitalepidemiologylab/plantvillage_deeplearning_paper_dataset

between -1 and 1 (SOARES *et al.*, 2011) as presented in Eq. 6-1.

$$r = \frac{\sum_{i=1}^{n}(x_i - \bar{x})(y_i - \bar{y})}{\sqrt{\sum_{i=1}^{n}(x_i - \bar{x})^2}\sqrt{\sum_{i=1}^{n}(y_i - \bar{y})^2}},$$

(6-1)

where x contains the reference leaf damage values and $\bar{x}$ is the average value of the expected defoliation levels. y contains the estimated leaf damage values, and $\bar{y}$ is the average value of the estimated defoliation levels. n represents the number of images used in the experimental test.

Intersection over Area (IoA) measures the overlap between two image segments and presents a score related to the intersection between the predicted predation segment and ground truth (VIEIRA *et al.*, 2022). Then, if the IoA of a bite segment is higher than 0.5, it is defined as True Positive (TP). Otherwise, it is defined as False Positive (FP). Those segments that do not match predicted predation marks are defined as False Negative (FN).

From IoA, Precision and Recall statistical measures are used to evaluate the detection and segmentation of insect bite signatures as presented in Eqs. 6-2 and 6-3.

$$\text{Precision} = \frac{TP}{TP+FP} \qquad (6\text{-}2) \qquad\qquad \text{Recall} = \frac{TP}{TP+FN} \qquad (6\text{-}3)$$

where TP stands for the number of segments correctly labeled as bite segments, FP represents the number of segments incorrectly labeled as a bite, and FN the segments not labeled as a bite. TP, FP, and FN are specified according to IoA scores.

Structural similarity index measure (SSIM) quantifies the image quality considering the reconstructed leaves and their corresponding ground truth images (WANG *et al.*, 2004). SSIM is standardized, ranging from -1 to 1, where a score closer to 1 means that two images are very similar, as presented in Eq. 6-4).

$$\text{SSIM}(\mathbf{T},\mathbf{Y}) = \frac{(2\mu_t\mu_y + C_1)(2\sigma_{ty} + C_2)}{(\mu_t^2 + \mu_y^2 + C_1)(\sigma_t^2 + \sigma_y^2 + C_2)},$$

(6-4)

where μ_t, μ_y, σ_t, σ_y, σ_{ty} are the local means, standard deviations, and cross-covariance for images $\mathbf{T}$ (ground truth) and $\mathbf{Y}$ (reconstructed leaf). C_1 and C_2 are regularization constants that avoid instability for image regions where the local mean or standard deviation is near zero.

Root mean square error (RMSE) computes the error between the expected defoliation level (x) and the estimated one (y) and indicates the mean error between n

images as presented in Eq. 6-5.

$$\text{RMSE} = \sqrt{\frac{\sum_{i=1}^{n}(x_i - y_i)^2}{n}} \tag{6-5}$$

6.4.3 Results

Figure 6.7 presents the linear correlation between the actual and the estimated leaf damage. Soybean, corn, potato, blueberry, grape, strawberry, and raspberry presented a correlation coefficient greater than 0.96. Corn reached $r = 0.99$, which is explained by the area occupied by the leaf. As corn leaves occupy the entire image, it is easy for the software to find a correct matching image. On the other hand, apple, tomato, and peach presented lower results, $r = 0.93$, $r = 0.92$, and $r = 0.76$, respectively, which is justified by the presence of shadows and leaf samples with different levels of maturity in the dataset.
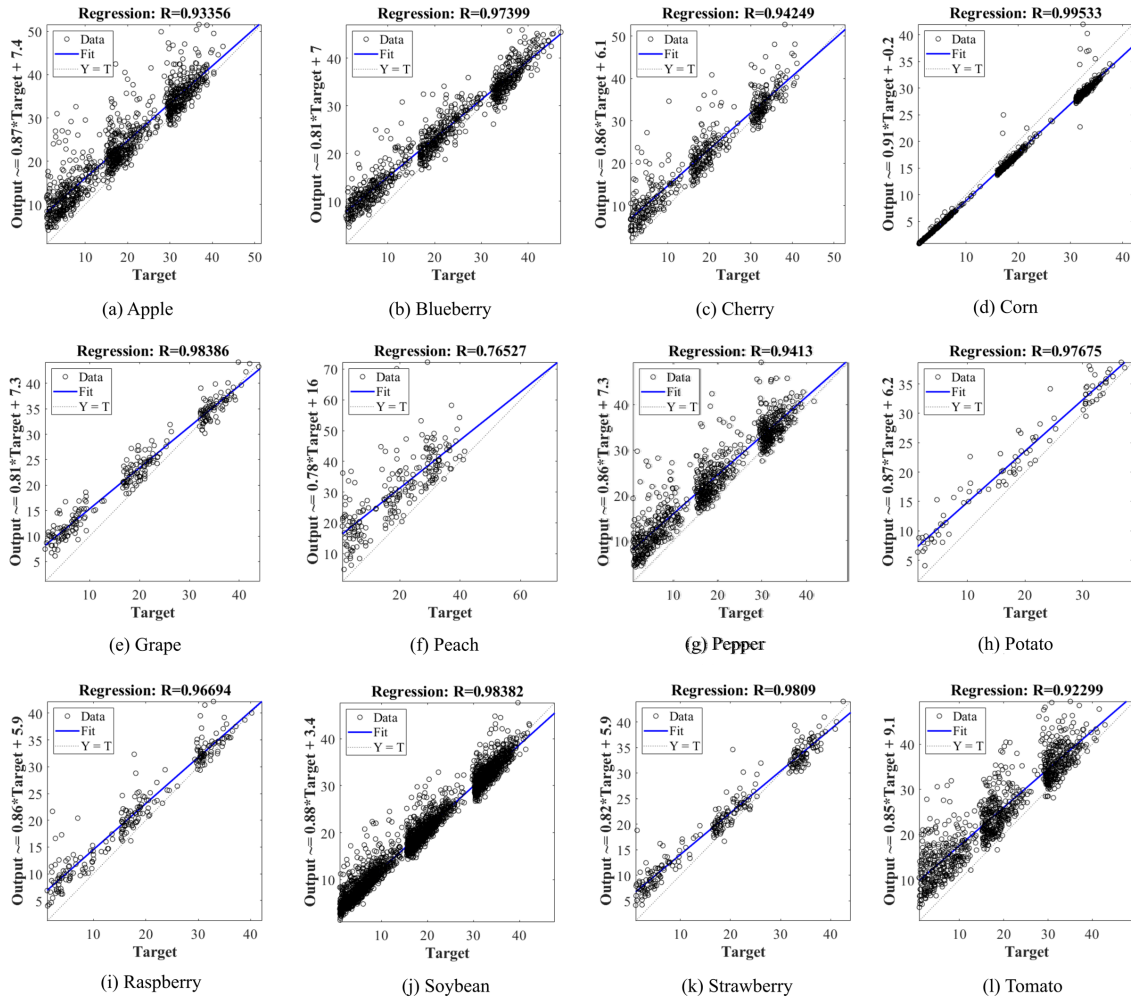
Figure 6.7: *Regression line between actual and the estimated leaf damage considering the defoliation level intervals from 1 to 45%. Y refers to the estimated value, while target T refers to the reference data.*

Figure 6.8 shows the average statistical results for detecting and segmenting insect predation marks. Blueberry, grape, and strawberry achieved similar precision and recall scores, close to 1.00, which means most of the bite segments were rightly detected. The other plant species presented a regular pattern in which the precision and recall scores increased according to the percentual damage applied to the target images.
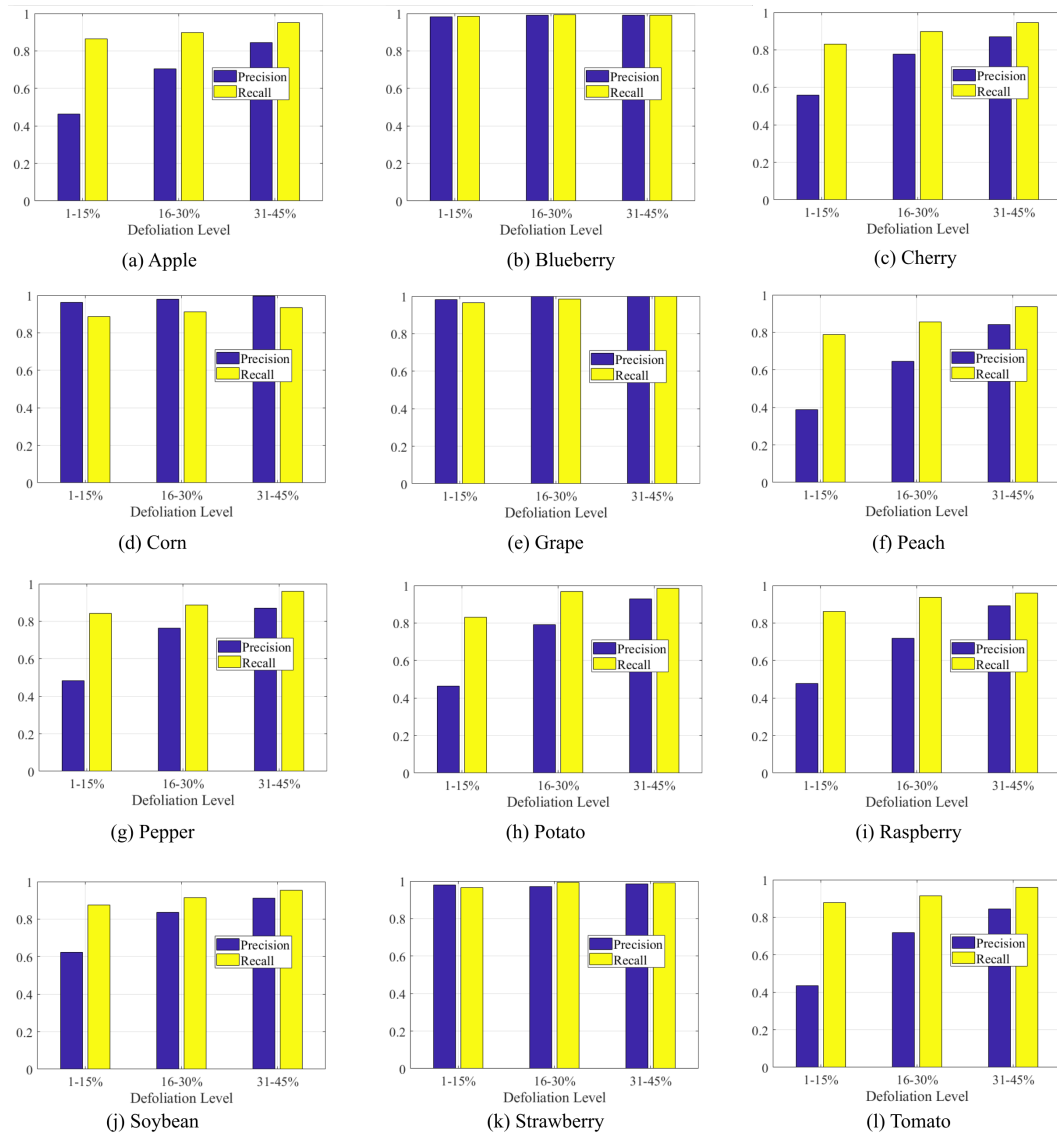
Figure 6.8: *Insect bite segmentation: average precision and recall. The x-axis represents the defoliation level intervals, while the y-axis represents the precision or recall outcomes.*

Table 6.1 shows the average ($\bar{x}$), standard deviation (s), and minimum and maximum values of precision and recall in the detection of leaf predation. Blueberry, grape, and strawberry achieved over 97% precision and more than 98% recall. Also, corn achieved over 97%, but a less assertive recall score close to 91%. Cherry, bell pepper, and potato reached over 70% precision and scores close to or higher than 90% recall. Likewise, apple and raspberry achieved precision results close to 70% and recall scores

higher than 90%. Soybean also reached good results close to 80% precision and above 91% recall. In contrast, peach and tomato obtained precision scores below 70% but recall scores similar to the other plant species, 86.03 and 91.73%, respectively. Besides that, peach, potato, raspberry, and tomato presented the highest precision standard deviation above 20%.

Table 6.1: *Precision and recall in detecting leaf predation considering defoliation level intervals from 1 to 45%.*

	Precision				Recall			
	$\bar{x}$	s	Min	Max	$\bar{x}$	s	Min	Max
Apple	67.08	19.28	46.30	84.38	90.39	04.39	86.39	95.09
Blueberry	98.73	00.56	98.08	99.11	98.90	00.44	98.42	99.30
Cherry	73.55	15.96	55.88	86.93	89.10	05.84	82.93	94.57
Corn	97.91	01.75	96.17	99.68	91.15	02.41	88.71	93.54
Grape	99.27	01.02	98.10	100.0	98.28	01.77	96.45	100.0
Peach	62.46	22.80	38.72	84.21	86.03	07.37	78.82	93.56
Bell Pepper	70.52	19.91	48.37	86.93	89.57	05.94	84.11	95.90
Potato	72.84	23.83	46.47	92.85	92.78	08.38	83.15	98.48
Raspberry	69.64	20.72	47.85	89.10	91.91	05.14	86.10	95.86
Soybean	79.03	14.97	62.29	91.13	91.40	03.89	87.53	95.31
Strawberry	97.69	00.72	96.92	98.36	98.23	01.52	96.49	99.32
Tomato	66.55	20.98	43.44	84.41	91.73	03.99	87.82	95.81

Figure 6.9 shows histograms of the number of images by the total number of False Positive (FP) bite segments considering the defoliation levels from 1% to 45%. It is observed that most of the test images reported zero FP entries. For example, from the 273 strawberry test images, less than 25 images presented one or two wrong bite segments. Blueberry, corn, and grapes also obtained similar results to strawberry leaves. Likewise, the test images in the other target species presented zero FP entries. In contrast, apple, cherry, peach, bell pepper, potato, raspberry, soybean, and tomato presented one to eight improper detected bite segments. In addition, Figure 6.10 shows the histograms of the False Negative (FN) bite segments. The interpretation of False Positive (FP) and

False Negative (FN) consists of the attention given to the number of segments wrongly identified or ignored. False positives occur when bite segments are detected but do not match the actual bite segments. On the other hand, when actual bite segments are not detected, the method fails to identify the segments correctly, and the number of false negatives increases.
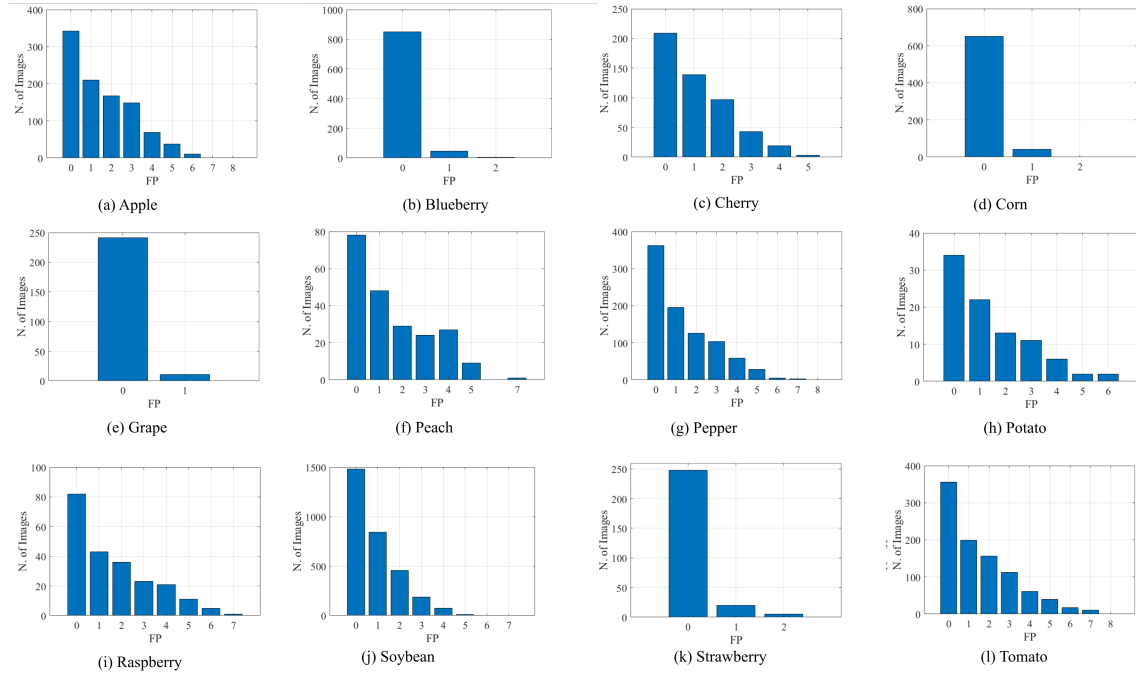

Figure 6.9: *Histogram of False Positive (FP) obtained in different types of crop leaves. The x-axis represents the number of errors, while the y-axis represents the number of images in each range.*

Figure 6.11 presents the SSIM scores obtained with ProtectLeaf in the reconstruction of leaf damages. The results indicate a slight improvement in the reconstruction process by interpolating images using inpainting. The image model, i.e., the image template that matched the damaged leaf, obtained SSIM scores from 0.48 to 0.70, while the image blending obtained SSIM scores from 0.67 to 0.87 and the image inpainting from 0.68 to 0.94.

Table 6.2 presents the average SSIM scores of each 12 target species considering the defoliation range from 1 to 45%. ProtectLeaf obtained the best results with corn, cherry, and soybean leaves, reaching an SSIM value equal to 94.58%, 85.15%, and 82.72%, respectively. Bell pepper, potato, and raspberry also showed promising results with scores equal to 79.17%, 77.45%, and 78.42%. On the other hand, peach presented the least assertive results with an SSIM score equal to 68.07%. Despite the diversity of samples and diversified lighting, the other cultivars achieved results above 73.58% using the image inpainting technique.

Table 6.3 presents a quantitative comparison between ProtectLeaf and some re-
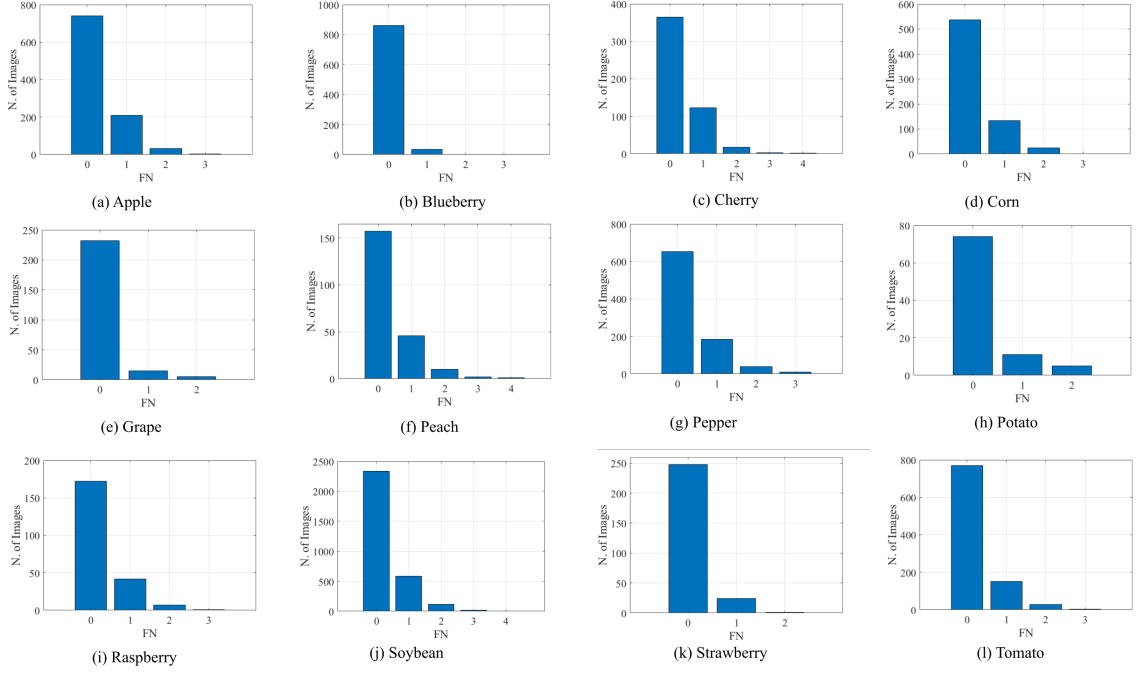
Figure 6.10: *Histogram of False Negative (FN) obtained in different types of crop leaves. The x-axis represents the number of errors, while the y-axis represents the number of images in each range.*
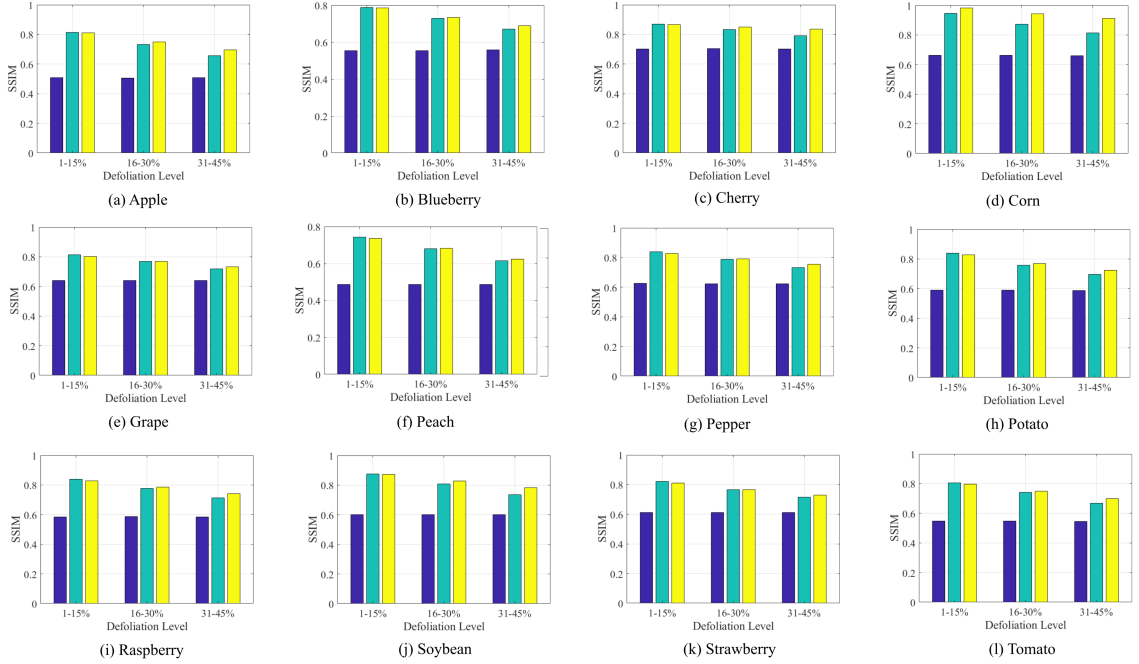
Figure 6.11: *SSIM scores of the leaf reconstruction process. The x-axis represents the defoliation level intervals, while the y-axis represents the SSIM outcomes (Legend: ■ Model; ■ Blending; ■ Inpaint).*

ported results presented by other related works. Although the performance measurements were obtained using different experimental setups, the results obtained give an intuition about the performance of ProtectLeat concerning other proposals in the defoliation esti-

Table 6.2: *Average SSIM scores and standard deviation of the image model, image blending, and image inpainting.*

	Model (%)		Blending (%)		Inpainting (%)	
	$\bar{x}$	s	$\bar{x}$	s	$\bar{x}$	s
Apple	50.75	06.50	73.45	09.36	75.12	08.05
Blueberry	55.52	05.35	72.96	07.72	73.58	07.39
Cherry	70.23	03.61	83.18	04.82	85.11	04.09
Corn	66.09	04.33	87.71	06.22	94.58	04.26
Grape	64.03	04.21	76.67	05.46	76.82	04.73
Peach	48.63	04.40	67.91	08.80	68.07	08.49
Bell Pepper	62.37	05.36	78.61	06.27	79.17	05.57
Potato	58.96	04.38	76.45	07.59	77.45	06.24
Raspberry	58.37	05.03	77.57	07.45	78.42	06.53
Soybean	60.05	05.03	80.61	07.55	82.72	06.25
Strawberry	61.20	03.70	76.78	06.19	76.90	05.59
Tomato	54.72	07.83	73.72	08.60	74.79	08.10

mation task.

6.5 Discussion and Impact Overview

Unlike related work, ProtectLeaf integrates different leaf analysis functionalities into a single solution. Therefore, the software is a valuable tool for defoliation estimate, detection of insect predation on plant leaves, and leaf reconstruction. In this sense, it can support crop monitoring activities and decision-making for agricultural management. As the software presents information for leaf analysis, it enables the diagnosis of crop plantations concerning the environmental balance between plants and the incidence of insects. Also, it promotes the rational use of agricultural resources in programmatic actions and emergencies to combat and control pests. For example, from the collection

Table 6.3: *Quantitative results provided by related work and ProtectLeaf considering soybean leaves.*

Method	r	RMSE
Digital Scanner (BRADSHAW *et al.*, 2007)	0.938	–
BioLeaf (MACHADO *et al.*, 2016)	0.992	–
AlexNet (SILVA *et al.*, 2019)	0.987	4.57
ResNet (SILVA *et al.*, 2019)	–	14.6
ProtectLeaf	0.983	3.49

of data and information presented by the software, questions related to the population growth of insects, the ability of plants to develop against predators, and the risk of loss of production can be answered. Besides, analytical information can be obtained before predatory insects compromise the entire plantation, justifying the application of insecticides and appropriate agricultural management.

Although insect classification systems using machine learning models can detect insects in crops, it is challenging to infer the fine line that differentiates insect population normality from the disruption that generates uncontrolled insect population growth (VIEIRA *et al.*, 2022). In contrast, ProtectLeaf highlights areas of agricultural damage regardless of insect classification. Our approach is more versatile as it does not rely on catching insects that can be camouflaged, move fast, hidden, or in clusters. In this sense, ProtectLeaf can help analyze environmental balance and verify the local and global health of the plantations. Figure 6.12 presents an example of detecting insect predation on leaves.

(a)   (b)   (c)
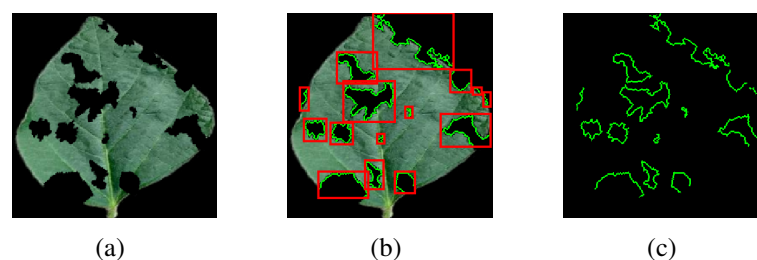
Figure 6.12: *Example of detecting insect predation on a soybean leaf. From left to right, (a) damaged leaf, (b) detection of foliar damage areas, and (c) segmentation of insect bite traces.*

Another feature that contributes to leaf analysis is the defoliation estimate. In ProtectLeaf, leaf damage is computed, and the loss percentage is presented along with the visual delineation of the injured leaf region. While in other works, only quantitative data

are presented (SILVA *et al.*, 2019; SILVA *et al.*, 2021), ProtectLeaf produces visualization for inspecting leaf tissue losses. Furthermore, ProtectLeaf can estimate defoliation both in the leaf surface's internal predation and edge regions. In other related works, the estimate of leaf damage is computed only for internal damage (MALOOF *et al.*, 2013; EASLON; BLOOM, 2014) or with human intervention in damages to leaf edges (MACHADO *et al.*, 2016). Figure 6.13 presents some examples of defoliation at different levels of leaf damage severity.
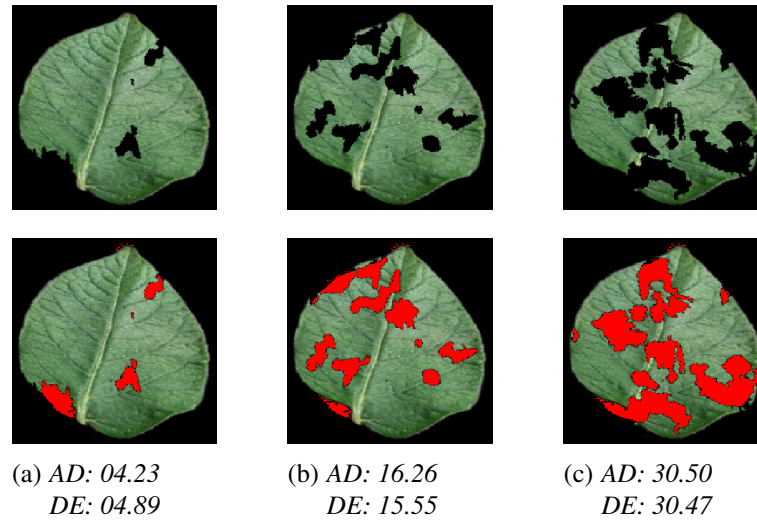

(a) *AD: 04.23*
    DE: 04.89

(b) *AD: 16.26*
    DE: 15.55

(c) *AD: 30.50*
    DE: 30.47

Figure 6.13: *Examples of defoliation estimate on potato leaves. Damaged leaves are presented in the first line, while the estimate of the injured leaf surface is shown in the second line. Actual damage percentage (AD) and defoliation estimate percentage (DE) are also presented.*

Moreover, the leaf reconstruction offered by ProtectLeaf was ideally designed to contribute to the training of machine learning models in leaf analysis. As the performance of classifiers varies depending on the variability in leaf shape, color, and texture, leaf samples with any noticeable damage are discarded (CARRANZA-ROJAS; MATA-MONTERO, 2016). The consequence of this approach is a reduction in the number of samples since only fresh and intact plant leaves are used to train computational models (BARRÉ *et al.*, 2017). On the other hand, excluding samples can generate imbalanced data and affect the performance of models (HUSSEIN *et al.*, 2020). In this sense, leaf reconstruction is crucial where injured leaves can be recovered and used in leaf analysis with machine learning (HUSSEIN *et al.*, 2021). PretectLeaf delineates damaged leaf areas, fills them with artificial filling techniques, and presents the reconstructed leaves. Figure 6.14 presents an example of leaf reconstruction using ProtectLeaf.

Furthermore, Figure 6.15 presents visual results provided by ProtectLeaf considering different types of crop species. As can be noted, ProtectLeaf can be generalized to different plant formats and species, showing that it is capable of being used in a wide range of applications.
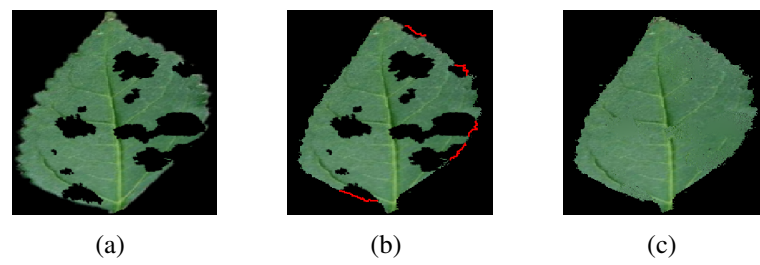
Figure 6.14: *Example of leaf surface reconstruction using ProtectLeaf on a cherry leaf. From left to right, (a) damaged leaf, (b) trace of damaged leaf edge regions, (c) leaf reconstruction using image inpainting.*

(a) Apple   (b) Blueberry   (c) Cherry   (d) Corn   (e) Grape   (f) Peach

(g) Pepper   (h) Potato   (i) Raspberry   (j) Soybean   (k) Strawberry   (l) Tomato

Figure 6.15: *Leaf analysis results. Rows 1–6 (and 7–12): images after segmentation and defoliation, leaf edge restoration, damaged areas, detection of insect predation, reconstructed leaves with image blending, and inpainting.*

6.5.1 Ongoing research projects using the software

The scientific method of leaf analysis of ProtectLeaf has been investigated in other studies, where the performance and assertiveness evaluations of the software were discussed. The potential for generalization to different species, leaf analysis at moderate to advanced levels of predation and computational efficiency with lightweight processes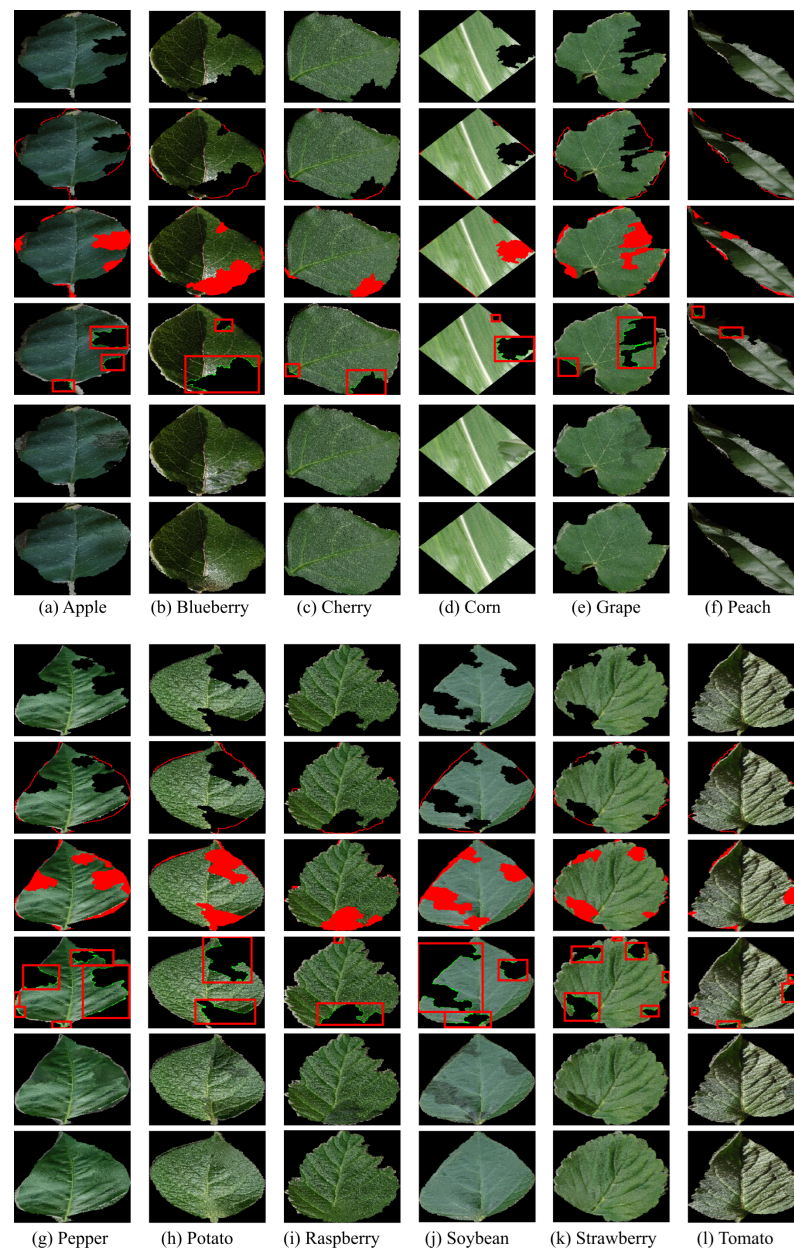 in the detection of areas affected by insects (VIEIRA *et al.*, 2022), leaf reconstruction (VIEIRA *et al.*, 2021) and defoliation estimation (VIEIRA *et al.*, 2022), (VIEIRA *et al.*, 2024) were demonstrated.

6.5.2 A list of all scholarly publications enabled by the software

1. G. S. Vieira, N. M. de Sousa, B. Rocha, A. U. Fonseca, F. Soares, A method for the detection and reconstruction of foliar damage caused by predatory insects, in: 2021 IEEE 45th Annual Computers, Software, and Applications Conference (COMPSAC),2021, pp. 1502–1507. (VIEIRA *et al.*, 2021)
2. G. S. Vieira, B. M. Rocha, A. U. Fonseca, N. M. de Sousa, J. C. Ferreira, C. D. Cabacinha, F. Soares, Automatic detection of insect predation through the segmentation of damaged leaves, Smart Agricultural Technology 2 (2022) 100056. (VIEIRA *et al.*, 2022)
3. G. S. Vieira, A. U. Fonseca, B. M. Rocha, N. M. Sousa, J. C. Ferreira, J. P. Felix, J. C. Lima, F. Soares, Insect predation estimate using binary leaf models and image-matching shapes, Agronomy 12 (11) (2022). (VIEIRA *et al.*, 2022)
4. G. S. Vieira, A. U. Fonseca, N. M. de Sousa, J. C. Ferreira, J. P. Felix, C. D. Cabacinha, and F. Soares. An automatic method for estimating insect defoliation with visual highlights of consumed leaf tissue regions. Information Processing in Agriculture (2024). (VIEIRA *et al.*, 2024)

6.6 Conclusion

This chapter presented the software developed by the authors to handle defoliation estimation, leaf damage detection, and reconstruction of the injured leaf surface. In addition to presenting quantitative results, the tool shows visual outcomes that can assist in leaf analysis and inspection. In the defoliation estimate, the soybean, corn, potato, blueberry, grape, strawberry, and raspberry presented a correlation coefficient greater than 0.96. In predation detection, the experimental tests showed precision and recall scores close to 1.00 for blueberry, grape, and strawberry. Also, SSIM scores were between 0.68 and 0.94 in leaf reconstruction. In this sense, the developed computer program can perform on different types of crops, assisting in leaf analysis with accurate results.

Soybean Pests Classification and Foliar Predation Recognition Using Bite Traces

I saw you.

John 1:48

Soybeans are a popular food source and the most essential vegetable protein worldwide. However, soybean crops are susceptible to attacks, where defoliating insects are among the most aggressive enemies. Traditionally, manual collection is used to capture and identify pests, but it is insufficient to meet production needs due to subjective aspects and low efficiency. In this sense, classification using computer models is one of the trends in agriculture. Nevertheless, unlike related works that use images for pest identification, we investigated the feasibility of classifying data based on the foliar damage. Thus, classification can be performed without capturing and collecting organisms harmful to agriculture, eliminating the need to prepare and purchase traps. We compare four deep neural network architectures (VGG16, ResNet50, Xception, and EfficientNetB0) to classify four soybean defoliators (caterpillar, green cow, gastropod, grasshopper) and prepared a novel methodology to simulate pest attack on soybean leaves. According to the experimental tests, VGG16 performed better and obtained 90.39% accuracy in the multiclass classification. On the other hand, when multi-classification was treated as a binary problem, VGG16 obtained an assertiveness of 99% for classifying caterpillars and green cows. Based on the results, we conclude that classifying pests based on the damage they cause to leaves is a viable alternative for crop monitoring.

7.1 Introduction

Numerous actions have been continuously updated to meet the agricultural demands in obtaining economically competitive products. The expansion of production to other regions, changes in cultivation systems, food production without contamination, considerations regarding environmental preservation, and adaptation of crops to local

fauna have been some of the concerns of experts and farmers. Additionally, the automation and digitalization of agricultural processes have converted hours of human work into just a few hours of activity and have enhanced application areas such as farm machinery, irrigation systems, weed and pest control, fertilizer application, greenhouse management, and storage systems (SUBEESH; MEHTA, 2021).

Actions taken by producers have demonstrated the feasibility of expanding agricultural production. Technological mastery related to crop management, the genetic potential of cultivars, and new perspectives for recovering degraded pastures have contributed to large-scale production (GAZZONI *et al.*, 2019). In addition, using a new set of agricultural technologies has helped growers in agricultural management (PIVOTO *et al.*, 2023). For example, different aspects of digital technologies such as advanced sensors, smartphone applications, image recognition (portable devices, drones, and satellites), Internet of Things (IoT), big data, computer vision, and artificial intelligence are part of agricultural ecosystems and have contributed to the positive outcomes of grain production in recent years (JÚNIOR; LOPES, 2023).

Among grain commodities, soybeans are a popular food source and are the most important vegetable protein worldwide (BUENO *et al.*, 2023; PARK *et al.*, 2023). Moreover, among world producers, Brazil is currently the world leader in soybean cultivation. In 2023, Brazilian soybean production reached 161 million metric tons (Mmt), while the second and third largest producers, the United States and Argentina, reached 112 Mmt and 48 Mmt, respectively (USDA, 2024). One factor explaining high productivity is related to correctly identifying traditional pests and those more recently adapted to soybeans. As soybean production is susceptible to attacks from germination to harvest, crops must be constantly watched. When early detection of pest population growth is not adequately monitored, production expectations can be reduced considerably.

Defoliating insects are among the most aggressive enemies of soybean plantations. These insects are most prominent in the vegetative and flowering phases and result in significant biotic stress because they consume regions of the leaf surface (SOSA-GÓMEZ *et al.*, 2023). Although there are more than six million insect species, only 20 to 30 are important pests for major crops (GARCíA-LARA; SALDIVAR, 2016). Among the herbivorous arthropods considered significant economic pests are the *Anticarsia gemmatalis* Hübner, 1818 (Insecta: Lepidoptera: Noctuidae) and the *Diabrotica speciosa* (Coleoptera: Chrysomedidae) (HORIKOSHI *et al.*, 2021; HESLER *et al.*, 2018). Other soybean pests are categorized as occasional or sporadic but can be potentially problematic, such as *Rhammatocerus schistocercoides* (Orthoptera: Acrididae: Gomphocerinae) and gastropods (slugs and snails) (SOSA-GÓMEZ *et al.*, 2023).

Leaf loss impacts agricultural productivity since defoliation reduces the photosynthetic capacity of plants (ROTH-NEBELSICK; KRAUSE, 2023; LAWSON; MIL-

LIKEN, 2023), causing damage to pod formation and grain filling (SILVA *et al.*, 2022; FERNANDES *et al.*, 2022). In addition to pests causing direct harm to cultivated plants by feeding on them, they can indirectly transmit plant viruses, which leads to significant yield losses (JEER, 2022). Herbivorous insects from the order Coleoptera and Lepidoptera, such as beetles and caterpillars (ALI *et al.*, 2024), and several other defoliators (SOSA-GÓMEZ *et al.*, 2023), compromise the structure of plants where the severity of the damage can harm the entire crop. It is estimated that defoliation rates above 30% in soybeans' vegetative stage can considerably compromise production. Defoliation at the soybean reproduction stage is even more restrictive, where defoliation control is estimated to be done before 15% to avoid significant losses (FERNANDES *et al.*, 2022; HAYASHIDA *et al.*, 2023).

Therefore, when the insect population rate is high, damage to the leaf surface becomes a concern since the productive loss indicates economic risks. In the same way, herbivorous gastropods, such as slugs and snails, can cause defoliation and even plant death. Although they mainly attack the early stages of crop development, they can also occur at the end of the soybean cycle, causing clogging of the harvesters (SOSA-GÓMEZ *et al.*, 2023). Traditionally, manual collection, such as the beating tray method, and traps, such as those based on chemical signals (pheromone traps) or adhesive substances (sticky traps), are strategies used to capture and identify pests in farming. In this case, equipment acquisition, adequate preparation of the tools, and the presence of experts are required to collect and classify the pests. Although these approaches are important, the recognition method based on manuals and instruments is insufficient to meet production needs due to its subjective characteristics and low efficiency (FU *et al.*, 2023).

On the other hand, the automation of agricultural processes has made it possible to create more efficient and low-cost work models. As computer-aided processes can deal with a massive amount of data, computational models achieve results with high precision, reduce human subjectivity, present performance comparable to experts, and assist farmers in analysis and decision-making tasks. Crop image analysis is among the most recent areas of research helping to consolidate the use of new technologies in agriculture. By registering an image, objects of interest can be observed, and their features can be used in detection, counting, and classification tasks. In this sense, pest characteristics can be encoded for subsequent processing and analysis on a computer or a smartphone device.

In the wake of the development of new cutting-edge technologies and the popularization of artificial intelligence, numerous studies have emerged proposing computational models to optimize demands arising from rural environments. Computational tools have been developed for leaf loss estimation (VIEIRA *et al.*, 2022; GOSHIKA *et al.*, 2024; VIEIRA *et al.*, 2023), tree segmentation (VIEIRA *et al.*, 2019a; VIEIRA *et al.*, 2019b; LI *et al.*, 2023), insect predation detection (VIEIRA *et al.*, 2022), foliar recon-

struction (VIEIRA *et al.*, 2021a), pest recognition (FU *et al.*, 2023), 3D insect modeling (DOAN; NGUYEN, 2023), fruit damage identification (ZHANG *et al.*, 2022a), insect monitoring (RUSTIA *et al.*, 2023), and insect classification (YANG *et al.*, 2023). These research initiatives have brought promising results for the insertion of new technologies on farms, and a contribution that stands out is the help given to rural producers in decision-making through the presentation of highly accurate information.

Other important research works are those of (ESGARIO *et al.*, 2022), which used the UNet and PSPNet architectures to segment target objects, and AlexNet, GoogLeNet, VGG16, and ResNet50 architectures to classify leaf symptoms. (YANG *et al.*, 2023) that proposed a standard garden insect classifier in complex natural environments and compared different deep neural networks such as SqueezeNet and AlexNet. (KASINATHAN *et al.*, 2021) that presented an insect pest detection algorithm consisting of foreground extraction and contour identification using an original convolutional neural network (CNN). (ZHANG *et al.*, 2024), which developed a multispecies pest counting solution based on neural network architectures such as VGG19 and FPN; and (ZHU *et al.*, 2024) that investigated the application of deep learning techniques to locate pest-infested leaves and proposed a YOLO-based network to classify pest insects.

Our recent work discussed the potential of classifying insects from leaf damage (VIEIRA *et al.*, 2022). We started a debate about the advantages of classification by foliar damage instead of classification by insect image. We pointed out that insects can be difficult to capture, requiring the preparation of appropriate traps. They can hide and camouflage among vegetation. They can live in clusters, making segmentation and isolation difficult. They can have varied habits; in some phases of development, they can be diurnal, and in other phases, they can have nocturnal habits. Furthermore, they can move fast, making insect monitoring difficult for cameras. On the other hand, the damage left by insects remains on plantations with distinct visual characteristics. The issue is to prepare models that can differentiate injured leaves and indicate the organisms that caused them.

In this line of investigation, Zhu *et al.* (2024) presented a neural network model capable of distinguishing two types of soybean-defoliating insects based on leaf damage. Like the authors, we also believe that studies of this type provide valuable support for pest monitoring and control by agricultural workers. In this sense, we conducted this study on classifying insects based on foliar defects caused by insects in soybean leaves. Using a database of healthy soybean leaves, we apply synthetic damage that simulates predation from four soybean defoliators (caterpillar, green cow, gastropod, grasshopper), and we compare four deep neural network architectures (VGG16, ResNet50, Xception, and EfficientNetB0) in classifying these disturbances. This study performs some experiments on predation recognition using only one leaf per image, where exploratory tests show the

ability of neural networks to classify bite patterns with high accuracy considering different levels of defoliation. Thus, the main research topics are related to the accuracy rates of well-known deep neural networks in classifying bite patterns on soybean leaves and what results can be obtained with variation in defoliation levels and, consequently, the impact of similar bite patterns in classifying predation on leaves.

This chapter presents four significant contributions to the field:

- An investigation into image classification using bite patterns.
- A comparison between convolutional neural networks in classifying predation on soybean leaves.
- A new methodology to simulate pest attack on the foliar canopy of soybean crops.
- A defoliation assessment considering statistical measurements and visual inspections.

The remainder of the chapter is structured as follows. Section 7.2 details the methodology used to simulate predation, the attributes of the pests considered in this study, and the preparation of a new image dataset containing defoliated soybean leaves. Section 7.3 presents the experimental results and a discussion considering models assertiveness and time performance of different convolutional neural networks. Finally, the work is concluded in Section 7.4.

7.2 Materials and Method

7.2.1 Pests that attack soybean leaves

Soybean plantations are susceptible to attacks that compromise seedlings, roots, petioles, stems, leaves, and pods. As this study proposes to investigate machine learning models for classifying leaf damage, we only considered pests that cause defoliation.

According to Sosa-Gómez *et al.* (2023), insects that attack leaves harm the energy potential of plants, causing losses in crop productivity. Among the defoliating insects, the soybean caterpillar (*Anticarsia gemmatalis* Hübner, 1818 (Insecta: Lepidoptera: Noctuidae)), gastropods (slugs and snails that are under the phylum of Mollusca (OUMA, 2023)), green cow (*Diabrotica speciosa* Germar, 1824 (Coleoptera: Chrysomelidae)), and grasshoppers (*Rhammatocerus schistocercoides* Rehn, 1906 (Orthoptera: Acrididae: Gomphocerinae)) stand out. The caterpillar is a voracious insect that can cause defoliation of up to 100% of the plantation (HOFFMANN-CAMPO *et al.*, 2000). They reproduce quickly, which requires frequent monitoring (ZHU *et al.*, 2024). Gastropods can cause defoliation and early death of plants, occurring both in the initial phase of crop development and at the end of the soybean cycle (SOSA-GÓMEZ *et al.*, 2023). The green cow

is a tiny insect that feeds on leaves, causing more or less regular and circular holes in the foliage (SANTOS, 2011). Its presence is worrying as it generally occurs in large populations (HOFFMANN-CAMPO *et al.*, 2000). Likewise, grasshoppers of migratory species tend to live in groups, causing the effect known as the "cloud of grasshoppers" (IMENES; IDE, 2002). For this reason, high populations can cause a total reduction in leaf area.

According to the mouthparts they have and, consequently, according to the way they feed, insects can be classified as suckers or chewers (IMENES; IDE, 2002). Sucking insects consume the tissue sap of green leaves, directly harming the tissue by damaging the epidermal cells or indirectly acting as viral carriers (ATA, 2024). Examples of sucking insects are aphids, whiteflies, and thrips. In contrast, chewing insects physically consume the plant tissues with their mouth parts evolved for chewing (ALI *et al.*, 2024). Chewing insects, such as caterpillars, follow a particular pattern when feeding, removing uniform pieces of leaf tissue in a highly choreographed and predictable manner (HOWE; JANDER, 2008; ALI *et al.*, 2024). On the other hand, slugs and snails damage the crops by eating plant leaves and destroying seedlings at their emergence, leading to raged holes on the plant leaves, with slime trails often close to the damaged spot (OUMA, 2023).

Caterpillars in the adult stage can cause sharp perforations in the leaves but small holes when they are in the first stages. As gastropods feed on young leaves, they can easily reduce the number of plants per unit area. The green cow causes small holes in the leaf surface, but when there are high populations of this insect, the damage can increase in size. The same happens with groups of grasshoppers whose foliar damage can be pretty severe, especially on the crop border. Considering the potential damage to agricultural yields, we investigated the capacity of deep neural network models to classify foliar damage caused by pests that are dangerous to soybean crops. Figure 7.1 shows an image of each pest investigated in this study.

7.2.2 Simulation of defoliation on soybean leaves

Preparing databases is one crucial issue for developing computational machine learning models. From the data, classifiers can learn features, the identified patterns can be used to represent categories, and new data can be evaluated according to previously encoded patterns. In the same way, when preparing deep neural networks for computer vision systems, image datasets are required so that classifiers can identify relevant features in images.

However, building image databases is not a trivial task. Although there are several accessible initiatives, such as ImageNet and Cifar-10, preparing datasets for specific problems may require a multidisciplinary team, data collection, and image annotations. Precision agriculture goes through this bottleneck where the cost of building

(a) *Anticarsia gemmatalis*
(Insecta: Lepidoptera: Noctuidae)
Caterpillar

(b) *Phylum of Mollusca* (slugs and snails)
Gastropods

(c) *Rhammatocerus schistocercoides*
(Orthoptera: Acrididae: Gomphocerinae)
Grasshopper

(d) *Diabrotica speciosa*
(Coleoptera: Chrysomelidae)
Green cow

Figure 7.1: *Dangerous pests for soybean crops.*

databases can make research proposals unfeasible or difficult to achieve. For this reason, data simulation has been an essential instrument for developing machine learning models. Simulations mimic real-world environments and can be used to test complex systems that are not always available. For example, (MUENZBERG *et al.*, 2022) used simulated data to predict decision-relevant outcomes such as agricultural management and harvest optimization. Likewise, (CECCARELLI *et al.*, 2022) proposed several simulations to predict seasonal energy needs in agricultural buildings. Also, (SILVA *et al.*, 2019), (SILVA *et al.*, 2021), and (VIEIRA *et al.*, 2024) prepared synthetic leaf image damage methods to estimate defoliation.

In this work, the data simulation process generates leaf damage at different levels of severity in healthy soybean leaves. The results obtained by the simulation resemble real damage caused by target pests whose bite characteristics are replicated. Leaf damage is inserted into the images so that the removal of pixels is visually perceived and presented as holes. Then, an artificial simulation is applied to fill the removed regions and reconstitute the images considering the background of the scenes.

The damage simulation is made from herbivory collected from natural defolia-

tion environments where the damage present on the leaves was manually segmented with fine detail of the bite traces. Each bite segment represents a sample that characterizes the predation, and the set of samples represents the diversity of pests bite shapes. For each pest, 40 samples were collected. As the pests of interest are 4, the total bite samples are 160. After segmentation, all bite samples were rescaled to size 70×70 pixels to maintain data uniformity and the resulting images were binarized with the area of interest labeled with the value 1 and the background area with the value 0. Figure 7.2 shows some of the bite segments of the target pests.
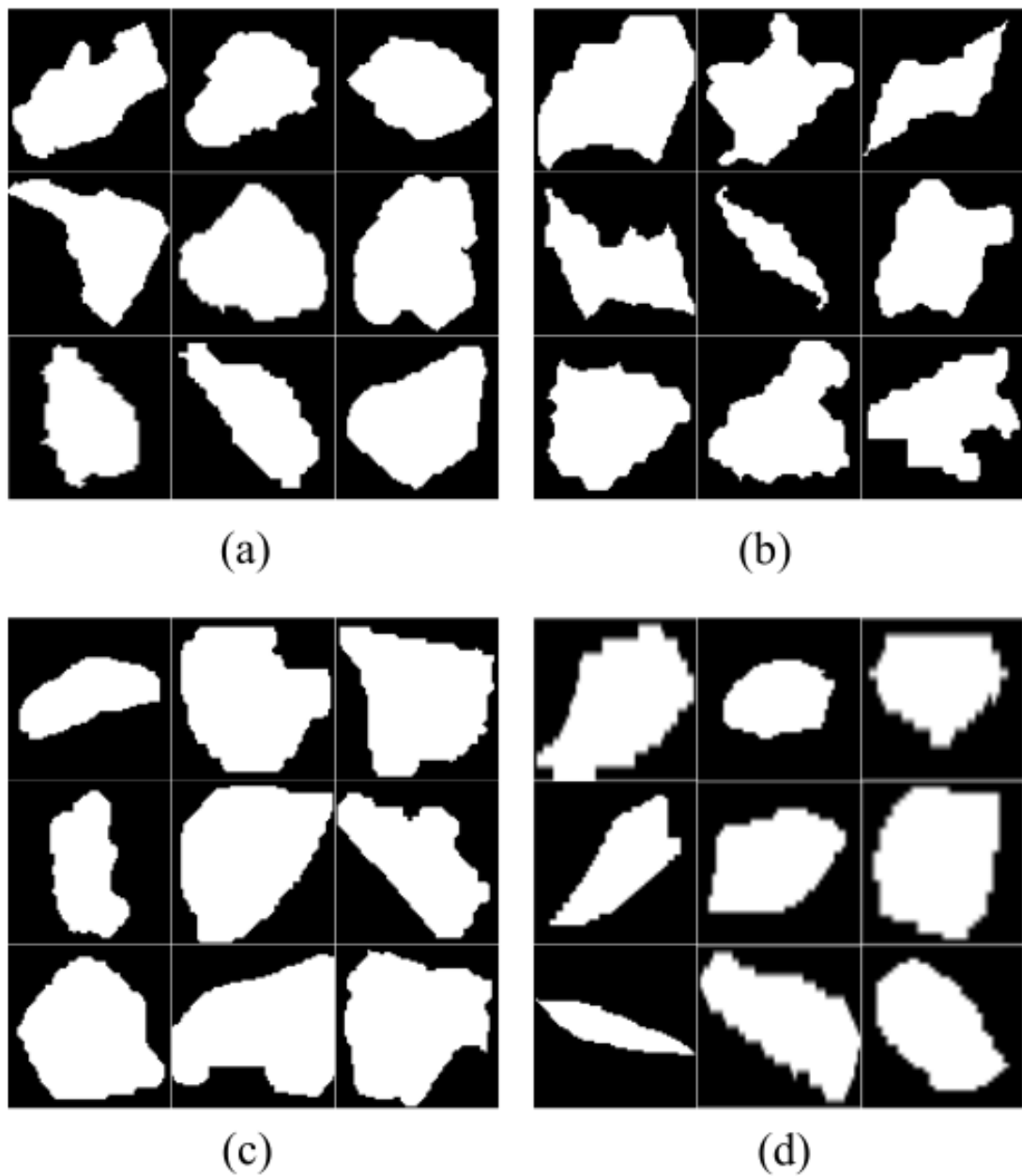

Figure 7.2: *Some bite samples from (a) caterpillars, (b) gastropods, (c) grasshoppers, and (d) green cows.*

After manually preparing the bite sample models, the following defoliation simulation steps are fully automated. The simulated leaf damage process has four steps. In the first, a bite sample is randomly selected, and the selected bite sample is randomly rotated and scaled according to adjustment limits defined by parameterization (see Section 7.2.3). In the second step, the resulting bite image is arbitrarily placed on some leaf region, and the overlapping pixels contained in the original image are removed. In the third step, the percentage of compromised leaf area is computed, and the calculated value is used to verify that the amount of damage meets the desired level of defoliation. If the percentage of defoliation is above or below the established level, the simulation process is continuously repeated until the desired level of damage is reached. Finally, in the fourth step, the damaged image regions are artificially filled by considering the background pixels of the scene. Figure 7.3 shows a complete view of the defoliation simulation workflow.
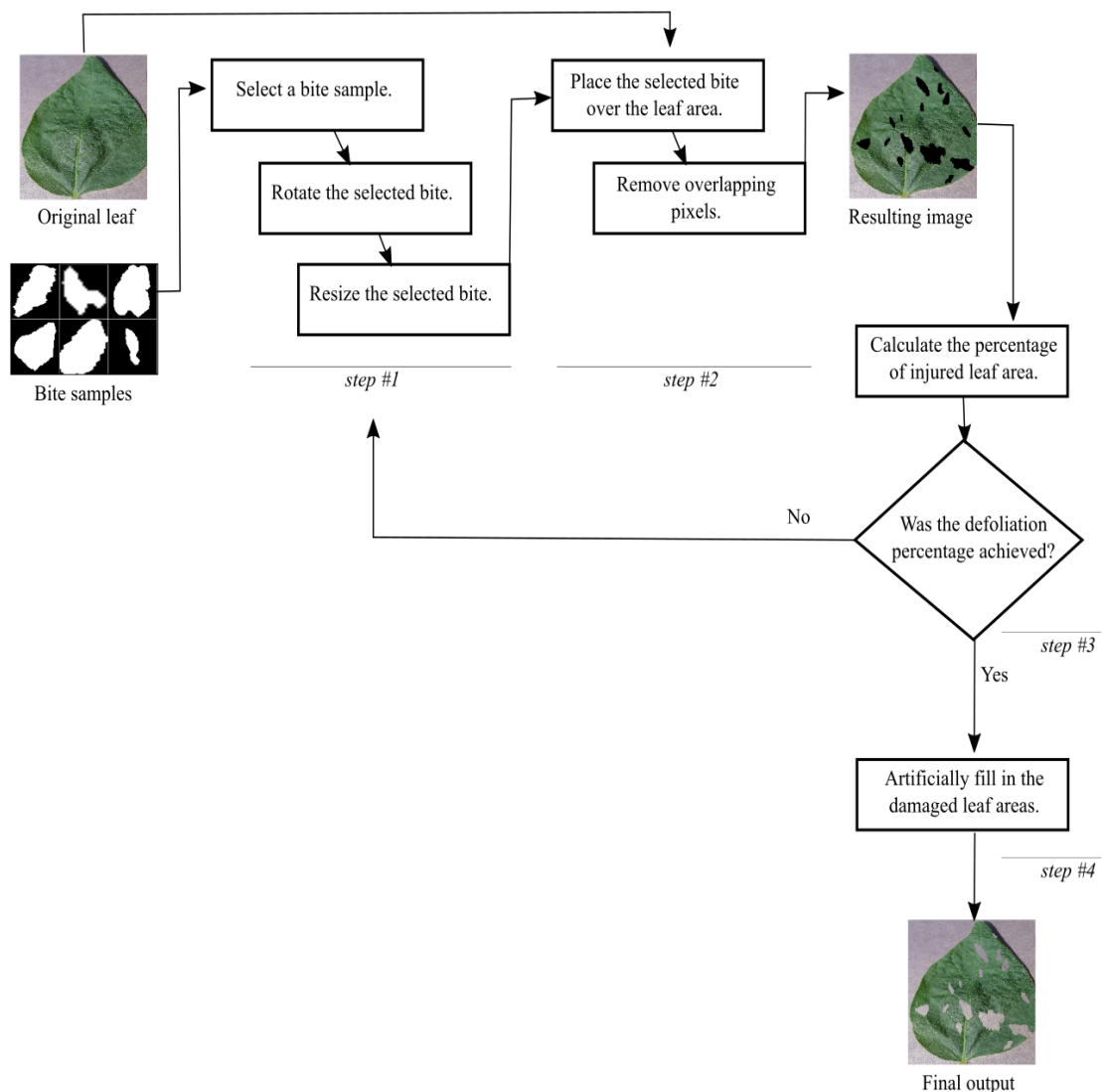

Figure 7.3: *Defoliation simulation workflow.*

Therefore, the parameters that must be defined in the simulation are the lower and upper limits for transforming bite samples (rotation and scale) and the acceptable range for the desired defoliation level. In the case of filling in injured leaf regions, the simulation uses image reconstruction through interpolation in a technique known as inpainting (BORNEMANN; MÄRZ, 2007). The program inputs are bite samples and a healthy leaf image. After selecting one of the bite samples, the selected sample is rotated and rescaled. Then, the transformed bite sample is positioned in the leaf area, and the overlapping pixels are removed from the original image. From there, the number of pixels removed is computed, serving as a parameter for the continuity or interruption of the program. If it is not within the expected defoliation limits, the program returns to the bite sample selection stage and continues. Otherwise, the loop is concluded, and the removed leaf regions are filled using inpainting.

7.2.3 Soybean leaf predation dataset

In this study, the dataset is constructed based on applying leaf damage simulation caused by different pests in healthy soybean leaf images. We partially used the dataset prepared by Hughes and Salathé (2015), which contains images from 14 plant species separated into leaf samples contaminated by different infectious diseases and leaf samples without any contamination. The healthy soybean class is our target object whose leaves category has 5,090 data points with variations in leaf canopy shape, different lighting intensities, and image acquisition with leaves in distinct positions. The size of the images is 256×256 pixels.

Before simulating defoliation, images of healthy soybean leaves are shuffled and separated into five groups of 1,008 images. In one of the groups, the images remain intact to represent the group of images with healthy leaves. The other four groups represent classes of herbivory caused by caterpillars, gastropods, grasshoppers, and green cows.

Each of the four categories representing classes of defoliating is subdivided into six subgroups of 168 images. In the first subgroup, defoliation simulation is applied at a severity level between 1 and 5%, the second subgroup contains defoliation levels between 6 and 10%, the third subgroup between 11 and 15%, the fourth subgroup between 16% and 20%, the fifth subgroup between 21 and 25%, and the sixth group between 26 and 30%. Thus, each class has images with damaged levels between 1 and 30% defoliation. In addition to the desired defoliation level, the parameters related to the transformation of the bite samples were set with rotation between 0 and 360° and resizing (width and height) between 10 and 40 pixels. These two parameters are randomly defined during the execution of the defoliation simulation program.

It is worth mentioning that the original bite sample size cannot be maintained

as a single sample could represent leaf damage above 25%. As the dataset with healthy soybean leaves is 256×256, a bite sample of size 70×70 could occupy a significant portion of the healthy leaf, making it difficult to obtain lower defoliation severity levels. This condition brings up two interesting points of observation. The first is the possibility of building more varied simulations, as more than one bite sample will be needed to reach the desired level of defoliation. On the other hand, resizing the bite sample reduces the image resolution, which can hide insect bite patterns, making leaf damage caused by different insects very similar to be distinguished by the classifiers. Figure 7.4 shows examples of valid bite samples versus the original bite sample size.
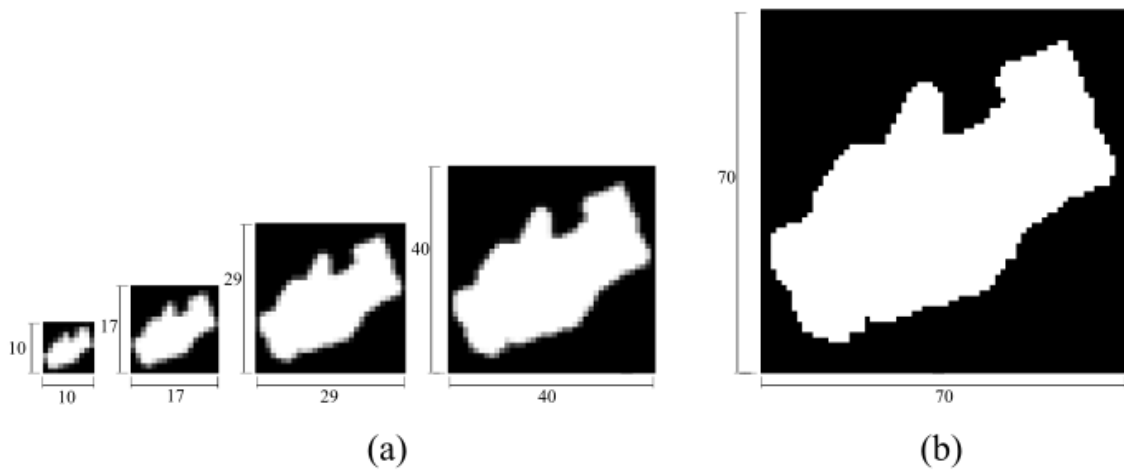

Figure 7.4: *Bite sample sizes. (a) Valid bite samples and (b) original bite size (not used).*

To study the percentage of defoliation in each picture, we calculated the level of defoliation caused in the soybean leaf images. In our dataset, the defoliation rate is equally distributed, ranging from 1.01% to 29.99%, with an average of 15.04%. As shown in Figure 7.5(a), our dataset has a diversity of damage levels that balances significant and minor damages, which is beneficial for evaluating model performance regarding generalization. Also, in actual application scenarios, the amount of damage per leaf can differ as different regions of the same leaf can be attacked. As shown in Figure 7.5(b), the amount of damage per leaf sample is also varied in our dataset, ranging from 1 to more than 50 compromised areas. Additionally, we evaluate the similarity between any two images in our dataset using the structural similarity index measure (SSIM) (WANG *et al.*, 2004). This metric provides a numerical way to understand the structural differences between two complex images. As shown in Figure 7.5(c), the dataset similarity ranges from 0.3% to 68.1%, with an average of 17.91%. Most image pairs have a similarity of less than 20%.

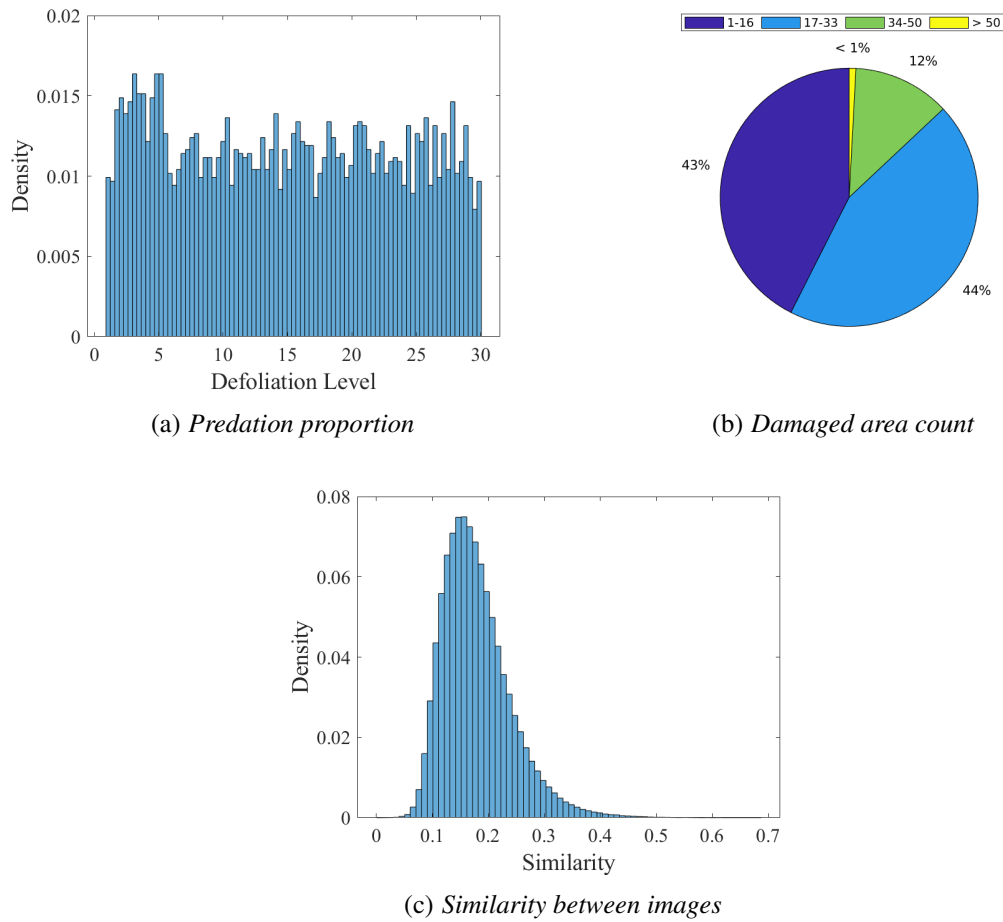After completing the defoliation simulation, the dataset was divided into three

(a) *Predation proportion*

(b) *Damaged area count*

(c) *Similarity between images*

Figure 7.5: *Statistics of the soybean leaf predation dataset.*

parts corresponding to the set of images for training, validation, and testing. The proportion used to divide the three groups was 70% for training, 20% for validation, and 10% for testing. Therefore, each of the five image classes has 702 data points for training, 204 for validation, and 102 for testing. Figure 7.6 shows some images from the leaf damage simulation process. As can be seen, the damage resembles actual insect predation, and the differentiation between image classes appears relatively complex. The dataset is publicly available (see Section A.1.5).

7.2.4 Deep classification neural networks

Deep neural networks are powerful tools for image classification tasks. Even in highly complex scenarios, these networks have achieved satisfactory results in research studies from different fields. Among neural network architectures, convolutional networks can deal with the complexity of digital images, such as lighting variations, scale and rotation problems, scene shading, occlusion, and object discontinuity, in such a way that the prepared computational models obtain very assertive results.
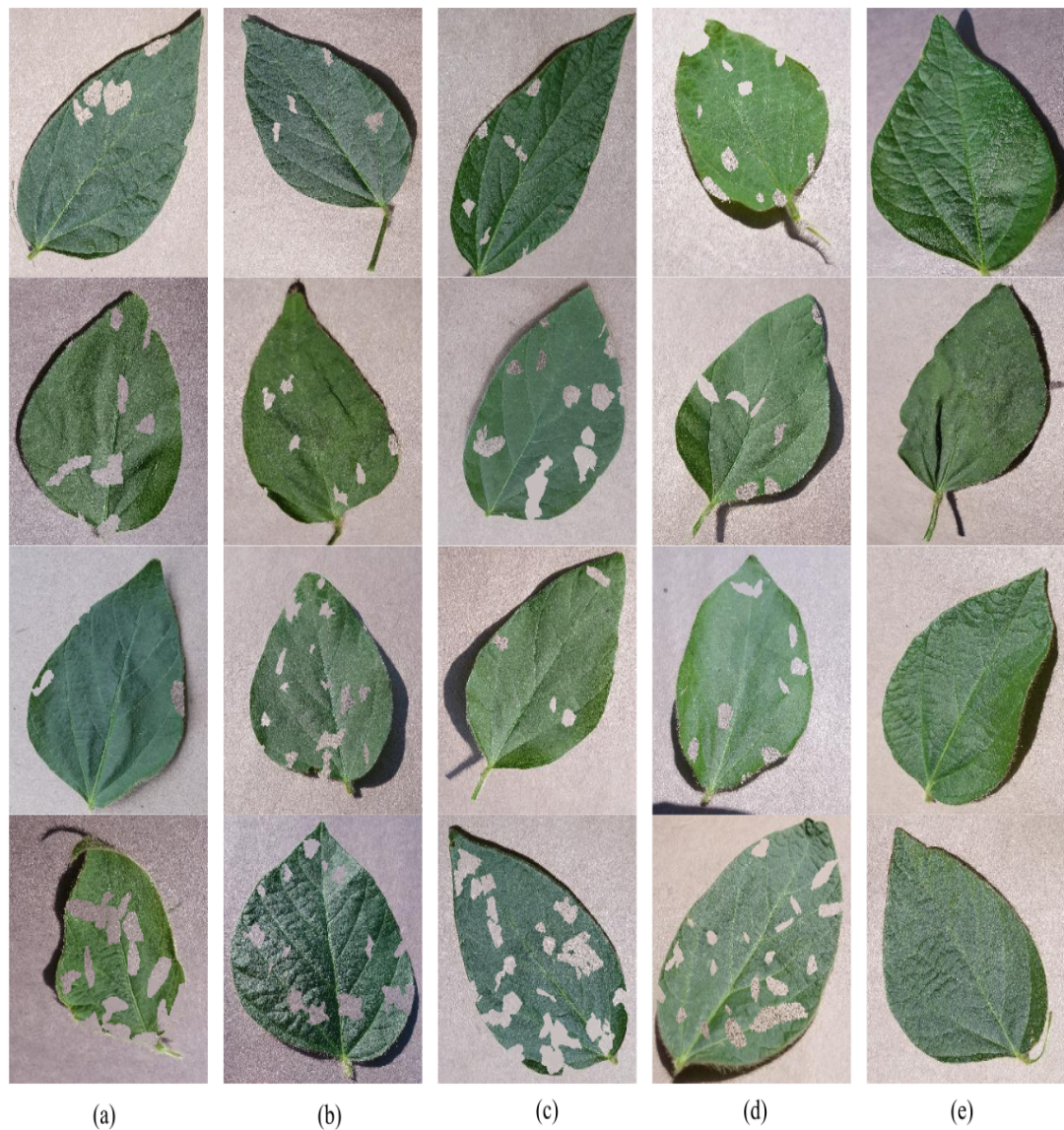
Figure 7.6: *Image samples from the soybean leaf predation dataset. Simulation of leaf damage caused by (a) caterpillars, (b) gastropods, (c) grasshoppers, and (d) green cows. Healthy leaves are presented in (e).*

In convolutional networks, an ordered series of matrix operators transforms data into multidimensional images to highlight features and identify patterns. The input images (input layer) are processed by convolutional layers that produce a series of resulting images, which are successively processed by other blocks (hidden layers) in a pipeline. The first convolutional layers identify low-level patterns such as edges and corners, and the deeper layers identify high-level patterns as unambiguous features that differentiate target objects. Although each architecture has different building blocks and several layers, convolutional networks always end with a fully connected layer that connects all the outputs before presenting the classifier's responses.

We selected four well-known convolutional networks and compared them in classifying insect predation on soybean leaves. VGG16 (SIMONYAN; ZISSERMAN, 2014), ResNet50 (HE *et al.*, 2016), Xception (CHOLLET, 2017), and EfficientNetB0 (TAN; LE, 2019) are networks frequently investigated in agriculture and were selected for study in this work. (ISHENGOMA *et al.*, 2022) analyzed VGG16, ResNet50, and Xception in detecting infested maize plants with fall armyworms. (NIGAM *et al.*, 2023) investigated EfficientNet's performance in disease identification in wheat crops. (SUTAJI; YıLDıZ, 2022) applied Xception to improve plant disease prediction. Furthermore, (LIN *et al.*, 2024) and (HU *et al.*, 2022) combined RestNet50 with other networks for forest-type identification and diseased pine detection and classification, respectively.

From deep learning architectures, it is possible to build new models from pre-trained data. In this sense, we consider applying a machine learning technique, named transfer learning, to fine-tune a model trained on one task to a different task. For this, the last layer of the convolutional network, i.e., the fully connected layer, must be replaced by a new layer suitable for the number of classes of the new task. Thus, we replaced the last layer of the pre-trained networks VGG16, ResNet50, Xception, and EfficientNetB0 with a global average pooling layer, a fully connected layer, a dropout, and a softmax layer. The softmax layer classifies the input leaf images into five classes: caterpillar, gastropod, grasshopper, green cow, and healthy.

Transfer learning is best suited for scenarios with somewhat similar databases. Thus, the convolutional layers are frozen to keep the network weights unchanged. As the databases used in pre-training differ from those for the new tasks, the layers must be unfrozen to obtain better results. In our study case, the models were pre-trained on the ImageNet dataset, which differs considerably from our database. For this reason, we unfreeze all layers of the networks and apply small changes to the previously trained weights using the backpropagation algorithm until the models fit the data.

Data augmentation techniques were applied to produce and propagate new images in each new batch, and the images were standardized with height and width equal to 256 and 3 color channels. In total, 3,510 images were used to train the models, 1,020 images to validate them, and 510 for the testing stage. During network training, the models with the best accuracy results in the validation set were saved, and their performance was verified with the test images using known evaluation metrics. The experiments were programmed using Python, Keras, and Tensorflow and conducted on a notebook with a Core i7-9750H (2.6GHz; 12MB Cache), 16 GB RAM, and an NVIDIA RTX 2060 Graphics Processing Unit (GPU) with CUDA 11.8. Table 7.1 presents the hyperparameters used in all experiments.

Table 7.1: *Training hyperparameters of the deep neural networks.*

Parameter	Value
Optimizer	Stochastic Gradient Descent
Loss function	Cross entropy
Epochs	200
Learning rate	0.0001
Momentum	0.9
Batch size	16

7.2.5   Evaluation metrics

For the classification task, the following metrics were considered: Precision, Recall, F1-score, Accuracy, and False Positive Rate (FPR). Precision shows how much the models get right when the prediction labels the data into a true class. If there are few false positives, the percentage of success increases and shows the assertiveness of the models in correctly classifying the data (Eq. 7-1). On the other hand, data belonging to one class but labeled for a different class are considered false negatives and can be measured with Recall. The Recall score indicates the models' ability to correctly label the data considering data mistakenly labeled for other classes (Eq. 7-2). As Precision and Recall operate in different data analysis perspectives, the F1-score harmonizes these two metrics by considering the number of false positive and false negative results in a single evaluation measure (Eq. 7-3). Likewise, Accuracy promotes a conciliatory view of the data regarding classification success and errors (Eq. 7-4).

These metrics are computed by observing a classifier's correct prediction of a target class and its penalty when the wrong prediction occurs. In this case, the number of true positive (TP), true negative (TN), false positive (FP), and false negative (FN) is calculated. TP represents the number of correctly predicted data points for a target class, TN indicates the number of data points belonging to other classes that were not predicted for a target class, FP is the number of data points belonging to other classes but wrongly predicted for a target class, and FN denotes the number of data points belonging to a target class but not labeled for it.

$$\text{Precision} = \frac{TP}{TP+FP} \tag{7-1}$$

$$\text{Recall} = \frac{TP}{TP+FN} \tag{7-2}$$

$$\text{F1-score} = \frac{2*TP}{2*TP+FP+FN} \tag{7-3}$$

$$\text{Accuracy} = \frac{TP+TN}{TP+TN+FP+FN} \tag{7-4}$$

$$\text{FPR} = \frac{FP}{FP+TN} \tag{7-5}$$

In evaluating the architectures of deep neural networks, we also present confusion matrices, Receiver Operating Characteristic (ROC) curves, and visual results with Gradient-weighted Class Activation Mapping (Grad-CAM). Confusion matrices show the number of correctly classified target points and indicate incorrect predictions by pointing out which classes the data points were mistakenly labeled for. ROC curves show the behavior of the models in the face of variation in the rates of true and false positives, i.e., the variation between True Positive Rate (or Recall - Eq. 7-2) and False Positive Rate (FPR, Eq . 7-5). From the ROC curves, a statistical concept known as the Area Under the Curve (AUC) is computed so that the performance of the models can be compared. Additionally, the outputs of the convolutional layers can be observed by building localization maps that highlight important regions of images for classification in a technique known as Grad-CAM (SELVARAJU *et al.*, 2017).

7.3   Results and Discussion

In supervised learning, models are trained from labeled data that categorizes each data point. During training, machine learning algorithms identify relevant patterns using training data, and the effectiveness of the learning is evaluated with validation data used to tune the models progressively. After training is complete, the models are tested with data not seen in the training stage, and the overall performance of the models is established. In this sense, while validation checks the training behavior, evaluation verifies the generalization capacity of the tested models.

In this session, we present results from the evaluation of the models and comparative analyses that discuss the assertiveness of deep neural architectures in the face of unseen data. Table 7.2 shows the performance of the VGG16, ResNet50, Xception, and EfficientNetB0 architectures in classifying insects based on leaf damage. The Xception network obtained the best precision values for classifying gastropods and the second-best average recall, precision, and F1 score. The ResNet50, Xception, and EfficientNetB0 net-

works correctly classify the healthy leaf images without getting confused with the other categories, and Resnet50 presented the best recall score for the classification of gastropod bites. On the other hand, the VGG16 network obtained the best results in average precision, recall, and F1-score, with an average score above 90%.

Table 7.2: *Comparison of deep learning architectures in classifying insect predation on leaves. The bold values indicate the best results.*

Category	Performance	VGG16	ResNet50	Xception	EfficientNetB0
Caterpillar	Precision	**88.39**	70.00	85.21	86.60
	Recall	**97.05**	96.07	96.07	95.09
	F1-score	**92.52**	80.99	90.32	90.65
Gastropod	Precision	88.54	77.67	**89.85**	86.04
	Recall	83.33	**85.29**	60.78	36.27
	F1-score	**85.85**	81.30	72.51	51.03
Grasshopper	Precision	**81.90**	81.69	67.76	54.77
	Recall	**84.31**	56.86	80.39	**84.31**
	F1-score	**83.09**	67.05	73.54	66.40
Green cow	Precision	**94.73**	90.36	86.13	90.42
	Recall	**88.23**	73.52	85.29	83.33
	F1-score	**91.37**	81.08	85.71	86.73
Healthy	Precision	**99.01**	98.07	98.07	98.07
	Recall	99.01	**100.0**	**100.0**	**100.0**
	F1-score	99.01	**99.02**	**99.02**	**99.02**
Average	Precision	**90.51**	83.56	85.41	83.18
	Recall	**90.39**	82.35	84.50	79.80
	F1-score	**90.37**	81.89	84.22	78.77

The confusion matrices presented in Figure 7.7 complement the analysis by showing which direction the classifiers were mistaken. As can be seen, the models presented errors mainly when classifying gastropods and grasshoppers. ResNet50 correctly classifies only 56.9% of grasshoppers and EfficientNetB0 only 36.3% of gastropods. VGG16 and Xception achieved better results but had incorrect predictions with gastropods and grasshoppers. Despite this, EfficientNetB0, ResNet50, Xception, and VGG16 achieved accuracy of 79.8%, 82.3%, 84.5%, and 90.3%, respectively.

(a) *VGG16*

(b) *ResNet50*

(c) *Xception*
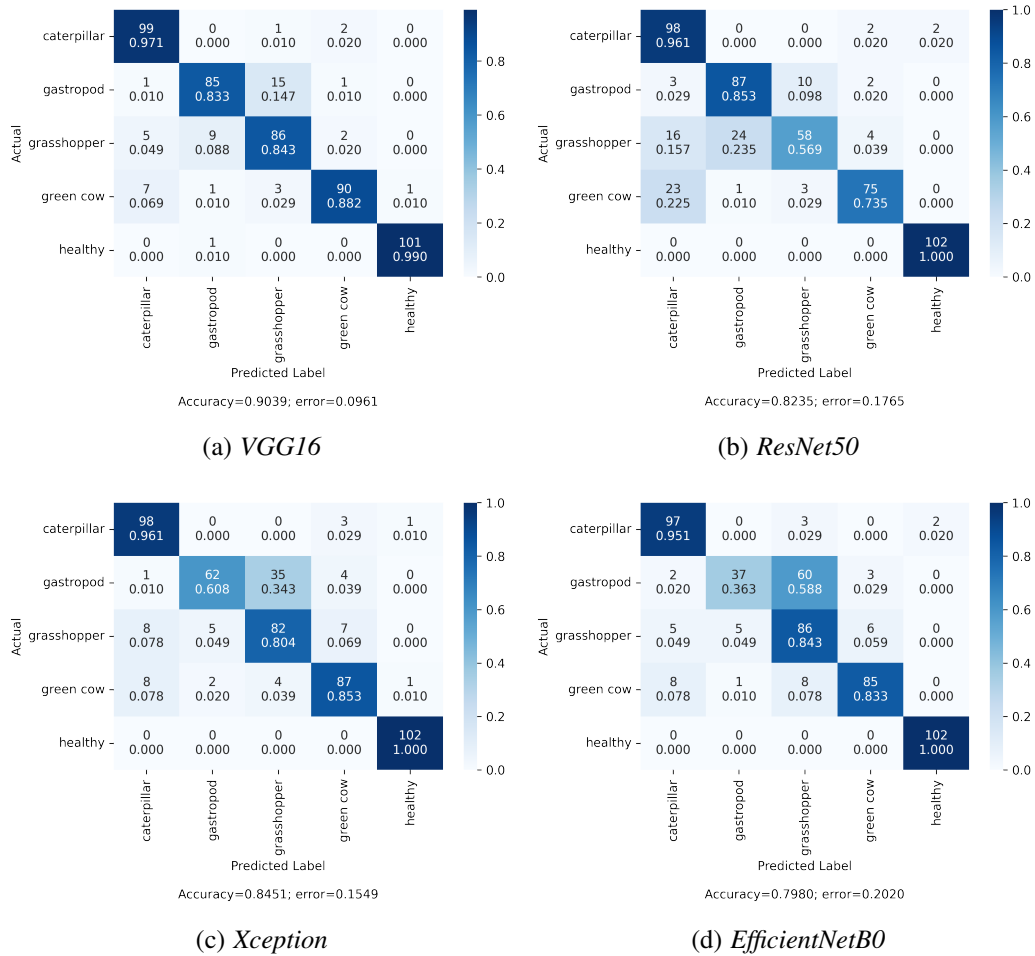
(d) *EfficientNetB0*

Figure 7.7: *Confusion matrix with the prediction results using VGG16, ResNet50, Xception, and EfficientNetB0 architectures.*

Figure 7.8 shows the prediction results when the multi-classification problem is treated as a binary problem. For example, when Caterpillar is the target class, the others are put together in a unique class, and the classifier's task is to predict whether leaf damage was caused by caterpillars or not. This is a valuable way of interpreting the data because, in many cases, the farmer does not need to classify each insect but checks whether a typical inset is present in his/her crop. Some insects are more prominent in some continental regions than others, and some cultivars may be less prepared to deal with a specific insect. In these cases, checking whether a particular insect is present can be

sufficient. As demonstrated by the ROC and AUC curves, all neural network architectures achieved high accuracy in binary classification. VGG16 correctly classified 99% of images with caterpillar and green cow damage. ResNet50, Xception, and EfficientNetB0 presented results above 97% for these two insects. Even in the classification of gastropods and grasshoppers, the classifiers achieved scores above 92%.
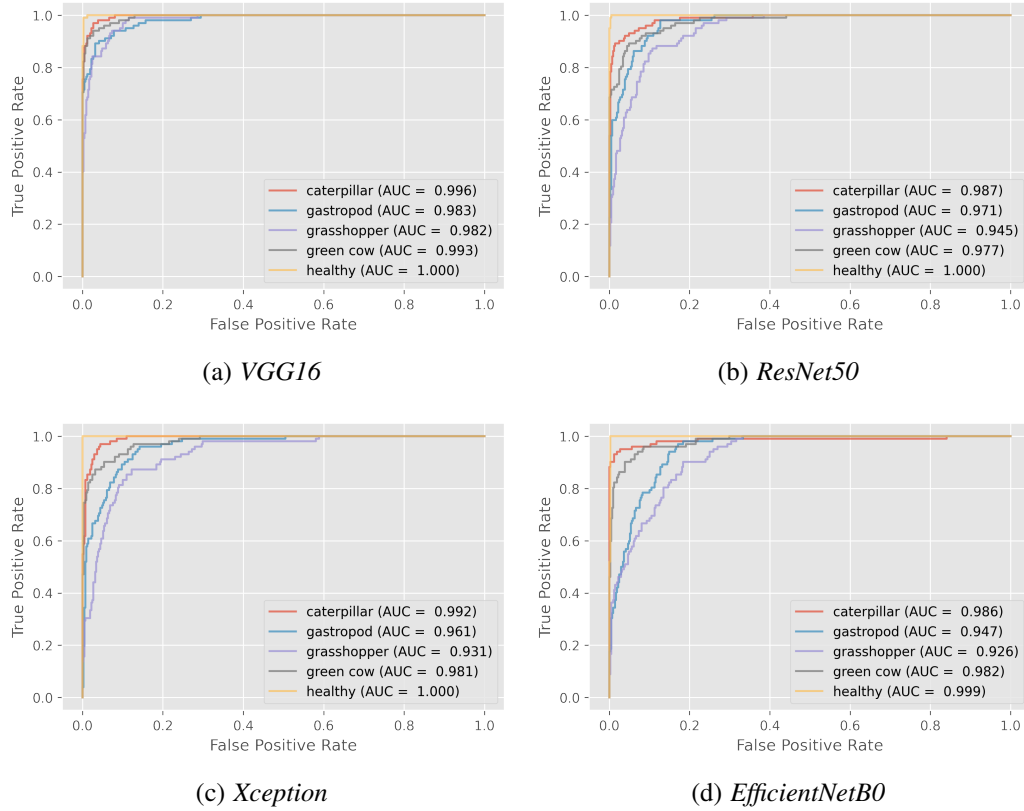

(a) *VGG16*

(b) *ResNet50*

(c) *Xception*

(d) *EfficientNetB0*

Figure 7.8: *ROC curves using VGG16, ResNet50, Xception, and EfficientNetB0 architectures.*

Figure 7.9 presents the activation maps (Grad-CAM) of each of the thirteen convolutional layers of the VGG16 architecture considering an injured leaf. As can be seen, the edge regions, such as leaf canopy and insect bite contours, are highlighted in the initial convolutional layers (Figures 7.9a–7.9d). Then, the leaf loss regions begin to attract the attention of the classifier, which are visually presented in Figures 7.9k–7.9m. This visual inspection shows that the classifier emphasizes some image regions before presenting the prediction.

According to the activation maps obtained with Grad-CAM, image regions that deserve attention are highlighted, and the presentation of visual results can help us understand the models' limitations. In Figure 7.10a, VGG16 and ResNet50 performed an excellent assignment detecting leaf damage regions. However, the models presented erroneous predictions due to the similarities between the bite patterns of caterpillars and grasshoppers. In contrast, Figure 7.10b shows that Xception and EfficientNetB0 did not
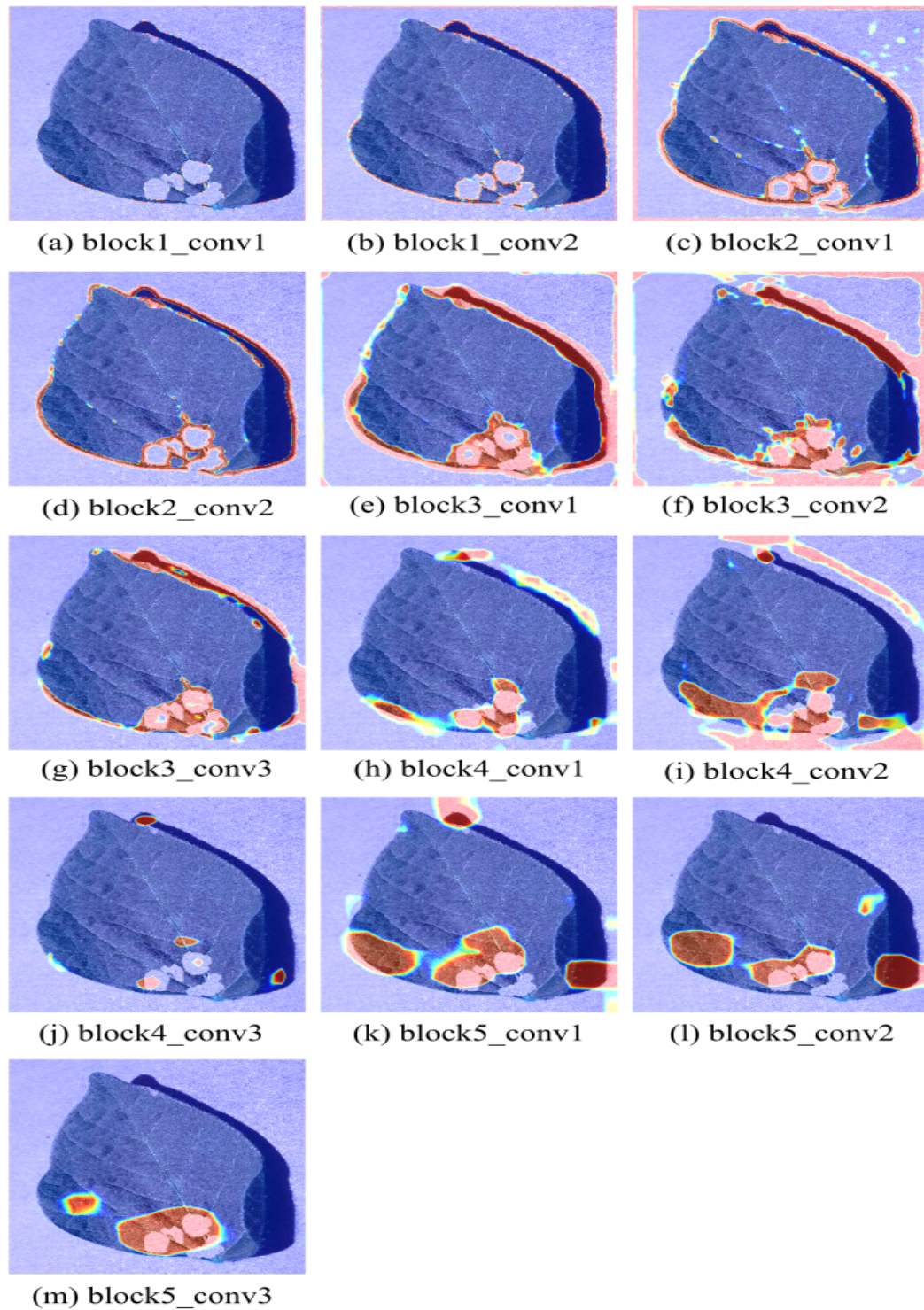
(a) block1_conv1
(b) block1_conv2
(c) block2_conv1

(d) block2_conv2
(e) block3_conv1
(f) block3_conv2

(g) block3_conv3
(h) block4_conv1
(i) block4_conv2

(j) block4_conv3
(k) block5_conv1
(l) block5_conv2

(m) block5_conv3

Figure 7.9: *Activation maps of the VGG16 convolutional layers using Grad-CAM.*

correctly highlight areas of leaf damage, leading the classifiers to predict erroneous insect categories.

In this sense, this case study observes two limitations. The first refers to the similarity between leaf damage marks that can lead classifiers to make incorrect predictions. The second occurs when models are unable to focus their attention on leaf damage and, for this reason, present wrong predictions. To overcome these limitations, databases with more leaf samples injured by insects can help classifiers better distinguish bite patterns. Likewise, other machine learning architectures, fine-tuning strategies, and hyperparameter configurations can be investigated in insect leaf predation classification to improve prediction results.

Actual: Caterpillar   Predicted: Grasshopper Model: VGG16

Actual: Grasshopper   Predicted: Caterpillar Model: ResNet50

Actual: Gastropod   Predicted: Grasshopper Model: Xception

Actual: Green Cow   Predicted: Caterpillar Model: EfficientNetB0

(a)   (b)
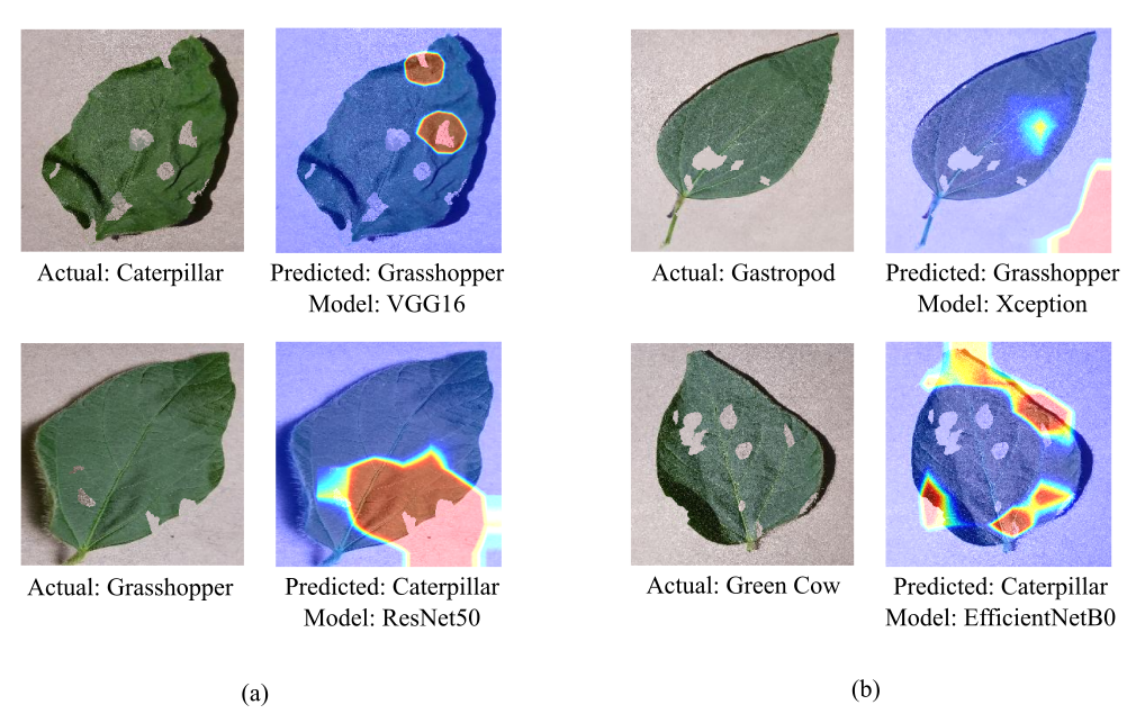
Figure 7.10: *Model limitations observed with Grad-CAM. (a) Models accurately detect leaf damage but perform inaccurate predictions. (b) Models emphasize erroneous leaf regions and, consequently, make wrong predictions.*

Finally, Table 7.3 presents the average training time per epoch in seconds and the average inference time in milliseconds of the selected architectures. The training time of Xception is longer than the others, and its number of parameters is relatively high. The inference time was similar among the architectures, but the EfficientNetB0 obtained the shortest time, requiring fewer parameters. Although VGG16 obtained the most assertive results, it presented the third-best inference time, and it was the second architecture with the smallest number of parameters.

Table 7.3: *Model size, average training and inference time.*

Model	Parameters (M)	Training (s/epoch)	Inference (ms)
VGG16	14.9	63.3	7.03
ResNet50	24.6	61.6	5.81
Xception	87.9	81.6	7.32
EfficientNetB0	4.06	63.3	4.28

7.4 Conclusion

This work investigated the feasibility of classifying pests from injured leaves. We prepared a dataset to simulate damage to soybean leaves caused by caterpillars, gastropods, grasshoppers, and green cows. The dataset was prepared with different amounts of compromised leaf areas and defoliation levels ranging from 1 to 30%. Also, we fine-tuned the VGG16, ResNet50, Xception, and EfficientNetB0 convolutional neural networks to differentiate bite patterns and classify predation.

The evaluated deep neural network architectures presented promising classification results for predicting predation on soybean leaves, where VGG16 achieved the best results in our dataset with an accuracy of 90.39%. When multi-classification was treated as a binary problem, VGG16 obtained an assertiveness of 99% for classifying caterpillars and green cows. Besides, VGG16's training and inference time was similar to those obtained by other architectures, and it was modeled with the second smallest number of parameters. Hence, in this case study, VGG16 performed better.

We conclude that identifying the pest causing leaf damage directly on the compromised leaf can be a profitable tool in pest control. The classification can help farmers monitor their crops and manage agricultural pesticides or biological control suitable for combating the identified insects. With this new approach, classification can be performed without capturing and collecting insects and mollusks, eliminating the need to prepare and purchase traps. Therefore, classifying pests based on the damage they cause to leaves is a viable alternative for crop monitoring and a complementary approach for decision-making processes that involve increasing production and yields.

Although this case study focused on soybean leaves, the methodology presented can be extended to other crops by preparing other datasets and configuring convolutional networks according to the number of classes. In future work, we intend to investigate predation on different plants and harmful species by exploring the construction of simulated leaf damage and preparing databases with true defoliation by considering the complexity of natural environments.

Final Considerations

> I am ever with you, even to the end of the world.
>
> *Matthew 28:20*

In this thesis, we present original computer-based methods for leaf analysis and describe improvements made to proposed computational models for leaf loss estimation, predation detection, leaf surface reconstruction, and pest classification. To perform leaf analysis, we identify compromised leaf areas and use them to estimate the percentage of leaf damage, highlight leaf predation, and perform leaf reconstruction. Recognizing injured regions makes it possible to indicate areas of attention that experts can use to direct strategic planning actions through precision information.

As the defoliation location is crucial for leaf analysis tasks, we built models based on template matching to indicate compromised leaf areas. This computational technique allowed the tracing of compromised leaf silhouettes and the preparation of efficient and low-cost algorithms. With template matching, our models only require a few samples of healthy leaves to detect defoliation points. In other research, variations of leaf damage in numerous samples were necessary to train learning models. The experimental results showed a linear correlation for defoliation estimate above 0.98 for soybean, grape, strawberry, and potato leaves. In detecting and segmenting bite marks, precision close to 1.00 was achieved for blueberry, grape, and strawberry, and reconstruction scores between 68% and 94% by using image inpainting.

Another novelty of this thesis is image classification based on the signature of bite traces. While related work has prepared insect shape, color, and texture descriptors, we investigate leaf damage tracks to encode and classify biting features. In comparing convolutional neural networks, VGG16 performed better and obtained 90% accuracy in the multi-class classification. Also, VGG16 obtained an impressive result above 98% when the classification was treated as a binary problem, and the classification purpose could correctly determine classes such as caterpillars, green cows, and grasshoppers.

Thus, deep learning models could determine which pest caused the leaf damage by considering only bite traces.

In conducting this study, we needed databases to investigate our research problems, but datasets with defoliation samples are not available to the general public. To overcome this limitation, we proposed defoliation simulation strategies in which algorithms were developed to apply damage in various formats and different levels of severity using samples of actual pest damage. Hence, we showed that defoliation can be simulated by developing computer programs capable of deforming healthy leaves. As a result, we were able to build image databases with samples of injured leaves that closely resemble leaves with actual damage.

Based on the results, we underline that agricultural producers can use the solutions presented to optimize leaf analysis through automated processes. It is well known that automation reduces subjectivity, human effort in tedious and repetitive tasks, and the operational complexity of hiring expert analysts. Furthermore, automation increases data processing capacity, investigative possibilities, and accuracy in presenting results. In this sense, our method for estimating leaf damage can assist producers in agricultural management by supporting decision-making on applying insecticides or biological pest control. Likewise, our predation detection method can assist in applying selective spraying in farming areas with a strong presence of pests, and our leaf reconstruction proposal can assist analysts in recognizing the main damaged regions of the leaf surface. Additionally, our classification strategy based on bite signatures eliminates the use of traps and the laborious collection of insects and mollusks that may be camouflaged, hidden, or living in clusters, as well as venomous, nocturnal, or fast-moving insects. Experimental tests demonstrate that our results are highly assertive, converge quickly, and can be generalized to different plant species.

In future work, we intend to work with leaf image samples that illustrate the complexity of crop plantations, such as complex backgrounds, more than one leaf per image, occlusions, and variations in natural lighting. This research study used a database of leaf images acquired in environments with some background and lighting controls. Although it was sufficient to evaluate the proposals, our models must be continually updated to meet new application scenarios and reduce limitations such as dealing with leaf samples at different growth stages, shading on leaf surfaces, and discrepant leaf shapes. In this way, we intend to build new image databases, explore image classification models for detecting leaf damage, investigate semantic segmentation methods to highlight bite traces and classify different pest species using their mandibular signatures.

Bibliography

ADC. *AM350 Portable leaf area meter*. 2019. Accessed: 10-10-2019. Available at: <https://www.adc.co.uk>.

ADC. *AM350 Portable leaf area meter*. 2023. Accessed: 11-10-2023. Available at: <https://www.adc.co.uk>.

ALI, J.; TONĞA, A.; ISLAM, T.; MIR, S.; MUKARRAM, M.; KONÔPKOVÁ, A. S.; CHEN, R. Defense strategies and associated phytohormonal regulation in brassica plants in response to chewing and sap-sucking insects. *Frontiers in Plant Science*, Frontiers Media SA, v. 15, p. 1376917, 2024.

ALVES, A. N.; SOUZA, W. S.; BORGES, D. L. Cotton pests classification in field-based images using deep residual networks. *Computers and Electronics in Agriculture*, Elsevier, v. 174, p. 105488, 2020.

AMIRKHANI, D.; BASTANFARD, A. An objective method to evaluate exemplar-based inpainted images quality using jaccard index. *Multimedia Tools and Applications*, Springer, v. 80, n. 17, p. 26199–26212, 2021.

ANDRIANTO, H.; FAIZAL, A.; KURNIAWAN, N. B.; AJI, D. P. P. *et al.* Performance evaluation of iot-based service system for monitoring nutritional deficiencies in plants. *Information Processing in Agriculture*, Elsevier, 2021.

ATA, T. E. Influence of different vegetable plants on the population density of some piercing-sucking insect pests. *Journal of Plant Protection and Pathology*, Mansoura University, Faculty of Agriculture, v. 15, n. 7, p. 183–190, 2024.

BAI, Y.; ZHANG, B.; XU, N.; ZHOU, J.; SHI, J.; DIAO, Z. Vision-based navigation and guidance for agricultural autonomous vehicles and robots: A review. *Computers and Electronics in Agriculture*, Elsevier, v. 205, p. 107584, 2023.

BARRÉ, P.; STÖVER, B. C.; MÜLLER, K. F.; STEINHAGE, V. Leafnet: A computer vision system for automatic plant species identification. *Ecological Informatics*, Elsevier, v. 40, p. 50–56, 2017.

BAUER, J.; JARMER, T.; SCHITTENHELM, S.; SIEGMANN, B.; ASCHENBRUCK, N. Processing and filtering of leaf area index time series assessed by in-situ wireless sensor networks. *Computers and Electronics in Agriculture*, v. 165, p. 104867, 2019. ISSN 0168-1699.

BERECIARTUA-PÉREZ, A.; GÓMEZ, L.; PICÓN, A.; NAVARRA-MESTRE, R.; KLUKAS, C.; EGGERS, T. Multiclass insect counting through deep learning-based density maps estimation. *Smart Agricultural Technology*, Elsevier, v. 3, p. 100125, 2023.

BORNEMANN, F.; MÄRZ, T. Fast image inpainting based on coherence transport. *Journal of Mathematical Imaging and Vision*, Springer, v. 28, n. 3, p. 259–278, 2007.

BRADSHAW, J. D.; RICE, M. E.; HILL, J. H. Digital analysis of leaf surface area: effects of shape, resolution, and size. *Journal of the Kansas Entomological Society*, BioOne, v. 80, n. 4, p. 339–347, 2007.

BRASIL. *Agropecuária brasileira em números - dezembro de 2020*. 2020. Accessed: 2020-12-31. Available at: <https://www.gov.br/agricultura>.

BUENO, A. d. F.; SUTIL, W. P.; JAHNKE, S. M.; CARVALHO, G. A.; CINGOLANI, M. F.; COLMENAREZ, Y. C.; CORNIANI, N. Biological control as part of the soybean integrated pest management (ipm): Potential and challenges. *Agronomy*, MDPI, v. 13, n. 10, p. 2532, 2023.

CARRANZA-ROJAS, J.; MATA-MONTERO, E. Combining leaf shape and texture for costa rican plant species identification. *CLEI Electronic journal*, Centro Latinoamericano de Estudios en Informática, v. 19, n. 1, p. 7–7, 2016.

CARRASCO-BENAVIDES, M.; MORA, M.; MALDONADO, G.; OLGUíN-CáCERES, J.; BENNEWITZ, E. von; ORTEGA-FARIAS, S.; GAJARDO, J.; FUENTES, S. Assessment of an automated digital method to estimate leaf area index (lai) in cherry trees. *New Zealand Journal of Crop and Horticultural Science*, 06 2016.

CARVALHO, J. O. D.; TOEBE, M.; TARTAGLIA, F. L.; BANDEIRA, C. T.; TAMBARA, A. a. L. Leaf area estimation from linear measurements in different ages of Crotalaria juncea plants. *Anais da Academia Brasileira de Ciencias*, scielo, v. 89, p. 1851 − 1868, 09 2017. ISSN 0001-3765.

CARVALHO, M. R.; WILF, P.; BARRIOS, H.; WINDSOR, D. M.; CURRANO, E. D.; LABAN-DEIRA, C. C.; JARAMILLO, C. A. Insect leaf-chewing damage tracks herbivore richness in modern and ancient forests. *PloS one*, Public Library of Science, v. 9, n. 5, p. e94950, 2014.

CECCARELLI, M.; BARBARESI, A.; MENICHETTI, G.; SANTOLINI, E.; BOVO, M.; TASSI-NARI, P.; BARRECA, F.; TORREGGIANI, D. Simulations in agricultural buildings: a machine learning approach to forecast seasonal energy need. In: IEEE. *2022 IEEE Workshop on Metrology for Agriculture and Forestry (MetroAgriFor)*. [S.l.], 2022. p. 116–120.

CHENG, X.; ZHANG, Y.; CHEN, Y.; WU, Y.; YUE, Y. Pest identification via deep residual learning in complex background. *Computers and Electronics in Agriculture*, v. 141, p. 351–356, Sep. 2017. ISSN 01681699.

CHICKERUR, S.; M, A. K. *et al.* Image restoration: Past, present and future. *Recent Patents on Computer Science*, Bentham Science Publishers, v. 3, n. 2, p. 108–126, 2010.

CHIMEZIE, E.; OGAZIE, C.; STEPHEN, M. Importance of leaf, stem and flower stalk anatomical characters in the identification of emilia cass. *International Journal of Plant and Soil Science*, v. 12, p. 1–12, 09 2016.

CHOLLET, F. Xception: Deep learning with depthwise separable convolutions. In: *Proceedings of the IEEE conference on computer vision and pattern recognition*. [S.l.: s.n.], 2017. p. 1251–1258.

CHU, K.; LIU, G.-H. Image retrieval based on a multi-integration features model. *Mathematical Problems in Engineering*, Hindawi, v. 2020, 2020.

CORONA, G.; MACIEL-CASTILLO, O.; MORALES-CASTAÑEDA, J.; GONZALEZ, A.; CUEVAS, E. A new method to solve rotated template matching using metaheuristic algorithms and the structural similarity index. *Mathematics and Computers in Simulation*, Elsevier, v. 206, p. 130–146, 2023.

CROFT, H.; CHEN, J. Leaf pigment content. *Reference Module in Earth Systems and Environmental Sciences*, 12 2017.

DENG, L.; WANG, Y.; HAN, Z.; YU, R. Research on insect pest image detection and recognition based on bio-inspired methods. *Biosystems Engineering*, v. 169, p. 139–148, May 2018. ISSN 15375110.

DOAN, T.-N.; NGUYEN, C. V. A low-cost digital 3d insect scanner. *Information Processing in Agriculture*, 2023. ISSN 2214-3173. Available at: <https://www.sciencedirect.com/science/article/pii/S2214317323000471>.

DODGE, Y. *The concise encyclopedia of statistics*. New York, NY: Springer New York, 2008. 325–326 p. ISBN 978-0-387-32833-1.

DUDA, R. O.; HART, P. E. Use of the hough transformation to detect lines and curves in pictures. *Communications of the ACM*, ACM New York, NY, USA, v. 15, n. 1, p. 11–15, 1972.

EASLON, H. M.; BLOOM, A. J. Easy leaf area: Automated digital image analysis for rapid and accurate measurement of leaf area. *Applications in plant sciences*, Wiley Online Library, v. 2, n. 7, 2014.

ERGASHEVA, N.; MAKHMUDOVA, S. Types of soybean pests and measures against them. In: EDP SCIENCES. *E3S Web of Conferences*. [S.l.], 2023. v. 371, p. 01031.

ESGARIO, J. G.; de Castro, P. B.; TASSIS, L. M.; KROHLING, R. A. An app to assist farmers in the identification of diseases and pests of coffee leaves using deep learning. *Information Processing in Agriculture*, v. 9, n. 1, p. 38–47, 2022. ISSN 2214-3173. Available at: <https://www.sciencedirect.com/science/article/pii/S2214317321000044>.

FELIX, J. P.; NASCIMENTO, H. A. D. D.; GUIMARÃES, N. N.; PIRES, E. D. O.; FONSECA, A. U. D.; VIEIRA, G. D. S. Automatic classification of amyotrophic lateral sclerosis through gait dynamics. In: IEEE. *2021 IEEE 45th Annual Computers, Software, and Applications Conference (COMPSAC)*. [S.l.], 2021. p. 1942–1947.

FELIX, J. P.; NASCIMENTO, H. A. D. do; GUIMARÃES, N. N.; PIRES, E. D. O.; VIEIRA, G. da S.; ALENCAR, W. de S. An effective and automatic method to aid the diagnosis of amyotrophic lateral sclerosis using one minute of gait signal. In: IEEE. *2020 IEEE International Conference on Bioinformatics and Biomedicine (BIBM)*. [S.l.], 2020. p. 2745–2751.

FELIX, J. P.; VIEIRA, F. H. T.; VIEIRA, G. da S.; FRANCO, R. A. P.; COSTA, R. M. da; SALVINI, R. L. An automatic method for identifying huntington's disease using gait dynamics. In: IEEE. *2019 IEEE 31st International Conference on Tools with Artificial Intelligence (ICTAI)*. [S.l.], 2019. p. 1659–1663.

FENG, C.; CAO, Z.; XIAO, Y.; FANG, Z.; ZHOU, J. T. Multi-spectral template matching based object detection in a few-shot learning manner. *Information Sciences*, Elsevier, v. 624, p. 20–36, 2023.

FERNANDES, E. T.; ÁVILA, C. J.; SILVA, I. F. da. Effects of different levels of artificial defoliation on the vegetative and reproductive stages of soybean. *EntomoBrasilis*, v. 15, p. e991–e991, 2022.

FONSECA, A.; FELIX, J.; VIEIRA, G.; ROCHA, B.; NOGUEIRA, E.; FERNANDES, D.; SOARES, F. Detecção eficiente de tuberculose em raio-x de tórax via seleção de atributos lbp por algoritmo de otimização da borboleta monarca. In: *XIX Congresso Brasileiro de Informática em Saúde - CBIS*. [S.l.: s.n.], 2022.

FONSECA, A.; FELIX, J.; VIEIRA, G.; MOURãO, Y.; MONTEIRO, J.; SOARES, F. Uma rede neural artificial para suporte ao diagnóstico de carcinoma espinocelular oral. In: *IX Congresso Latino Americano de Engenharia Biomédica e XXVIII Congresso Brasileiro de Engenharia Biomédica*. [S.l.: s.n.], 2022.

FONSECA, A.; VIEIRA, G. S.; FELIX, J.; SOBRINHO, P. F.; SILVA, Á. V. P.; SOARES, F. Automatic orientation identification of pediatric chest x-rays. In: IEEE. *2020 IEEE 44th Annual Computers, Software, and Applications Conference (COMPSAC)*. [S.l.], 2020. p. 1449–1454.

FONSECA, A. U.; FÉLIX, J. de P.; VIEIRA, G. da S.; FERNANDES, D.; SOARES, F. Automated lung region segmentation in pediatric chest radiography. *Revista de Informática Teórica e Aplicada*, v. 30, n. 2, p. 114–123, 2023.

FONSECA, A. U.; FELIX, J. P.; PINHEIRO, H.; VIEIRA, G. S.; MOURÃO, Ý. C.; MONTEIRO, J. C.; SOARES, F. An intelligent system to improve diagnostic support for oral squamous cell carcinoma. In: MDPI. *Healthcare*. [S.l.], 2023. v. 11, n. 19, p. 2675.

FONSECA, A. U.; FELIX, J. P.; VIEIRA, G. S.; FERNANDES, D. S.; SOARES, F. Detecção de covid-19 e avaliação de nível de severidade: Uma abordagem com bppc e redes neurais artificiais rasas. In: *Congresso Brasileiro de Automática-CBA*. [S.l.: s.n.], 2022. v. 3, n. 1.

FONSECA, A. U.; FELIX, J. P.; VIEIRA, G. S.; ROCHA, B. M.; NOGUEIRA, E. A.; ARAÚJO, C. E. E.; FERNANDES, D.; SOARES, F. Diagnosticando tuberculose com redes neurais artificiais e recursos bppc. *Journal of Health Informatics*, v. 15, n. Especial, 2023.

FONSECA, A. U.; ROCHA, B. M.; NOGUEIRA, E. A.; VIEIRA, G. S.; FERNANDES, D. S.; LIMA, J. C.; FERREIRA, J. C.; SOARES, F. Tuberculosis detection in chest radiography: A combined approach of local binary pattern features and monarch butterfly optimization algorithm. In: IEEE. *2022 IEEE 46th annual computers, software, and applications conference (COMPSAC)*. [S.l.], 2022. p. 1408–1413.

FONSECA, A. U.; VIEIRA, G. S.; SOARES, F. Screening of viral pneumonia and covid-19 in chest x-ray using classical machine learning. In: IEEE. *2021 IEEE 45th annual computers, software, and applications conference (COMPSAC)*. [S.l.], 2021. p. 1936–1941.

FONSECA, A. U. D.; FELIX, J. P.; VIEIRA, G. D. S.; FERNANDES, D.; SOARES, F. Automatic tuberculosis detection using binary pattern of phase congruency. In: IEEE. *2022 international conference on computational science and computational intelligence (CSCI)*. [S.l.], 2022. p. 1646–1651.

FONSECA, A. U. da; PARREIRA, P. L.; VIEIRA, G. da S.; FELIX, J. P.; CONTE, M. B.; RABAHI, M. F.; SOARES, F. A novel tuberculosis diagnosis approach using feed-forward neural networks and binary pattern of phase congruency. *Intelligent Systems with Applications*, Elsevier, v. 21, p. 200317, 2024.

FRIEDMAN, J. M.; HUNT, E. R.; MUTTERS, R. G. Assessment of leaf color chart observations for estimating maize chlorophyll content by analysis of digital photographs. *Agronomy Journal*, The American Society of Agronomy, Inc., v. 108, n. 2, p. 822–829, 2016.

FU, X.; MA, Q.; YANG, F.; ZHANG, C.; ZHAO, X.; CHANG, F.; HAN, L. Crop pest image recognition based on the improved vit method. *Information Processing in Agriculture*, 2023. ISSN 2214-3173. Available at: <https://www.sciencedirect.com/science/article/pii/S2214317323000173>.

GARCíA-LARA, S.; SALDIVAR, S. S. Insect pests. In: CABALLERO, B.; FINGLAS, P. M.; TOLDRá, F. (Ed.). *Encyclopedia of Food and Health*. Oxford: Academic Press, 2016. p. 432–436. ISBN 978-0-12-384953-3. Available at: <https://www.sciencedirect.com/science/article/pii/B9780123849472003962>.

GAZZONI, D.; CATTELAN, A.; NOGUEIRA, M. *O aumento da produção brasileira de soja representa uma ameaça para a floresta amazônica?* [S.l.]: Londrina: Embrapa Soja, 2019., 2019. ISSN 2176-2937.

GOMES, J. C.; BORGES, D. L. Insect pest image recognition: A few-shot machine learning approach including maturity stages classification. *Agronomy*, Multidisciplinary Digital Publishing Institute, v. 12, n. 8, p. 1733, 2022.

GOMES, P.; CASTRO, M.; FERNANDES, D.; SOARES, F.; VIEIRA, G.; FELIX, J.; NASCIMENTO, T. H. Drumsvr: Simulating drum percussion in a virtual environment using gesture recognition on smartwatches. In: *Proceedings of the 28th International ACM Conference on 3D Web Technology*. [S.l.: s.n.], 2023. p. 1–5.

GONZALEZ, R. C.; WOODS, R. E. *Digital image processing*. Upper Saddle River, N.J.: Prentice Hall, 2008. ISBN 9780131687288 013168728X 9780135052679 013505267X.

GOSHIKA, S.; MEKSEM, K.; AHMED, K. R.; LAKHSSASSI, N. Deep learning model for classifying and evaluating soybean leaf disease damage. *International Journal of Molecular Sciences*, v. 25, n. 1, 2024. ISSN 1422-0067. Available at: <https://www.mdpi.com/1422-0067/25/1/106>.

GUTIERREZ, A.; ANSUATEGI, A.; SUSPERREGI, L.; TUBÍO, C.; RANKIĆ, I.; LENŽA, L. A benchmarking of learning strategies for pest detection and identification on tomato plants for autonomous scouting robots using internal databases. *Journal of Sensors*, Hindawi, v. 2019, 2019.

HAYASHIDA, R.; HOBACK, W. W.; BUENO, A. de F. A test of economic thresholds for soybeans exposed to stink bugs and defoliation. *Crop Protection*, Elsevier, v. 164, p. 106128, 2023.

HE, K.; ZHANG, X.; REN, S.; SUN, J. Deep residual learning for image recognition. In: *Proceedings of the IEEE conference on computer vision and pattern recognition*. [S.l.: s.n.], 2016. p. 770–778.

HEREDIA, U. L. D.; DURO-GARCIA, M.; SOTO, A. Leaf morphology of progenies in Q. suber, Q. ilex, and their hybrids using multivariate and geometric morphometric analysis. *iForest - Biogeosciences and Forestry*, n. 1, p. 90–98, 2018. Available at: <https://iforest. sisef.org/contents/?id=ifor2577-010>.

HESLER, L. S.; ALLEN, K. C.; LUTTRELL, R. G.; SAPPINGTON, T. W.; PAPIERNIK, S. K. Early-season pests of soybean in the united states and factors that affect their risk of infestation. *Journal of Integrated Pest Management*, Oxford University Press US, v. 9, n. 1, p. 19, 2018.

HOFFMANN-CAMPO, C. B.; MOSCARDI, F.; CORRÊA-FERREIRA, B. S.; OLIVEIRA, L. J.; SOSA-GÓMEZ, D. R.; PANIZZI, A. R.; CORSO, I. C.; GAZZONI, D. L.; OLIVEIRA, E. d. *Pragas da soja no Brasil e seu manejo integrado*. [S.l.]: Embrapa soja Londrina, 2000.

HORIKOSHI, R. J.; DOURADO, P. M.; BERGER, G. U.; FERNANDES, D. de S.; OMOTO, C.; WILLSE, A.; MARTINELLI, S.; HEAD, G. P.; CORRÊA, A. S. Large-scale assessment of lepidopteran soybean pests and efficacy of cry1ac soybean in brazil. *Scientific Reports*, Nature Publishing Group UK London, v. 11, n. 1, p. 15956, 2021.

HOWE, G. A.; JANDER, G. Plant immunity to insect herbivores. *Annu. Rev. Plant Biol.*, Annual Reviews, v. 59, n. 1, p. 41–66, 2008.

HU, G.; WEI, K.; ZHANG, Y.; BAO, W.; LIANG, D. Estimation of tea leaf blight severity in natural scene images. *Precision Agriculture*, Springer, v. 22, n. 4, p. 1239–1262, 2021.

HU, G.; YAO, P.; WAN, M.; BAO, W.; ZENG, W. Detection and classification of diseased pine trees with different levels of severity from uav remote sensing images. *Ecological Informatics*, v. 72, p. 101844, 2022. ISSN 1574-9541. Available at: <https://www.sciencedirect. com/science/article/pii/S1574954122002941>.

HUGHES, D. P.; SALATHÉ, M. An open access repository of images on plant health to enable the development of mobile disease diagnostics through machine learning and crowdsourcing. *ArXiv*, abs/1511.08060, 2015.

HUSSEIN, B. R.; MALIK, O. A.; ONG, W.-H.; SLIK, J. W. F. Automated classification of tropical plant species data based on machine learning techniques and leaf trait measurements. In: *Computational Science and Technology*. [S.l.]: Springer, 2020. p. 85–94.

HUSSEIN, B. R.; MALIK, O. A.; ONG, W.-H.; SLIK, J. W. F. Reconstruction of damaged herbarium leaves using deep learning techniques for improving classification accuracy. *Ecological Informatics*, v. 61, p. 101243, 2021. ISSN 1574-9541. Available at: <https://www.sciencedirect.com/science/article/pii/S1574954121000340>.

IMENES, S. D. L.; IDE, S. Principais grupos de insetos pragas em plantas de interesse econômico. *O Biológico, São Paulo*, v. 64, n. 2, p. 235–238, 2002.

INDEX MUNDI. *Commodity prices*. 2020. Accessed: 2020-12-31. Available at: <https://www.indexmundi.com/commodities/?commodity=soybeans>.

INTARAVANNE, Y.; SUMRIDDETCHKAJORN, S. Android-based rice leaf color analyzer for estimating the needed amount of nitrogen fertilizer. *Computers and Electronics in Agriculture*, v. 116, p. 228 – 233, 2015. ISSN 0168-1699.

ISHENGOMA, F. S.; RAI, I. A.; NGOGA, S. R. Hybrid convolution neural network model for a quicker detection of infested maize plants with fall armyworms using uav-based images. *Ecological Informatics*, v. 67, p. 101502, 2022. ISSN 1574-9541. Available at: <https://www.sciencedirect.com/science/article/pii/S1574954121002934>.

JADON, M.; AGARWAL, R.; SINGH, R. An easy method for leaf area estimation based on digital images. In: IEEE. *2016 International Conference on Computational Techniques in Information and Communication Technologies (ICCTICT)*. [S.l.], 2016. p. 307–310.

JAVAID, M.; HALEEM, A.; SINGH, R. P.; SUMAN, R. Enhancing smart farming through the applications of agriculture 4.0 technologies. *International Journal of Intelligent Networks*, Elsevier, v. 3, p. 150–164, 2022.

JEER, M. Chapter 17 - recent developments in silica-nanoparticles mediated insect pest management in agricultural crops. In: ETESAMI, H.; Al Saeedi, A. H.; EL-RAMADY, H.; FUJITA, M.; PESSARAKLI, M.; Anwar Hossain, M. (Ed.). *Silicon and Nano-silicon in Environmental Stress Management and Crop Quality Improvement*. Academic Press, 2022. p. 229–240. ISBN 978-0-323-91225-9. Available at: <https://www.sciencedirect.com/science/article/pii/B9780323912259000169>.

JÚNIOR, G. B. M.; LOPES, M. A. Charting new sustainable agricultural innovation pathways in brazil. *Scientia Agricola*, SciELO Brasil, v. 80, p. e20230067, 2023.

JUWONO, F. H.; WONG, W.; VERMA, S.; SHEKHAWAT, N.; LEASE, B. A.; APRIONO, C. Machine learning for weed–plant discrimination in agriculture 5.0: An in-depth review. *Artificial Intelligence in Agriculture*, Elsevier, 2023.

KAI, P. M.; OLIVEIRA, B. M. de; VIEIRA, G. S.; SOARES, F.; COSTA, R. M. Effects of resampling image methods in sugarcane classification and the potential use of vegetation indices related to chlorophyll. In: IEEE. *2021 IEEE 45th Annual Computers, Software, and Applications Conference (COMPSAC)*. [S.l.], 2021. p. 1526–1531.

KANOPOULOS, N.; VASANTHAVADA, N.; BAKER, R. L. Design of an image edge detection filter using the sobel operator. *IEEE Journal of solid-state circuits*, IEEE, v. 23, n. 2, p. 358–367, 1988.

KARUNATHILAKE, E.; LE, A. T.; HEO, S.; CHUNG, Y. S.; MANSOOR, S. The path to smart farming: Innovations and opportunities in precision agriculture. *Agriculture*, MDPI, v. 13, n. 8, p. 1593, 2023.

KASINATHAN, T.; SINGARAJU, D.; UYYALA, S. R. Insect classification and detection in field crops using modern machine learning techniques. *Information Processing in Agriculture*, 2020. ISSN 2214-3173.

KASINATHAN, T.; SINGARAJU, D.; UYYALA, S. R. Insect classification and detection in field crops using modern machine learning techniques. *Information Processing in Agriculture*, v. 8, n. 3, p. 446–457, 2021. ISSN 2214-3173. Available at: <https://www.sciencedirect.com/science/article/pii/S2214317320302067>.

KAUR, G.; DIN, S.; BRAR, A. S.; SINGH, D. Scanner image analysis to estimate leaf area. *International Journal of Computer Applications*, Citeseer, v. 107, n. 3, 2014.

KERAMATLOU, I.; SHARIFANI, M.; SABOURI, H.; ALIZADEH, M.; KAMKAR, B. A simple linear model for leaf area estimation in persian walnut (juglans regia l.). *Scientia Horticulturae*, Elsevier, v. 184, p. 36–39, 2015.

KHAN, M. M. R.; SAKIB, S.; ARIF, R. B.; SIDDIQUE, M. A. B. Digital image restoration in matlab: A case study on inverse and wiener filtering. In: IEEE. *2018 International Conference on Innovation in Engineering and Technology (ICIET)*. [S.l.], 2018. p. 1–6.

KOGAN, M.; TURNIPSEED, S.; SHEPARD, M.; OLIVEIRA, E. D.; BORGO, A. Pilot insect pest management program for soybean in southern brazil. *Journal of Economic Entomology*, Oxford University Press Oxford, UK, v. 70, n. 5, p. 659–663, 1977.

KOLHAR, S.; JAGTAP, J. Plant trait estimation and classification studies in plant phenotyping using machine vision – a review. *Information Processing in Agriculture*, v. 10, n. 1, p. 114–135, 2023. ISSN 2214-3173. Available at: <https://www.sciencedirect.com/science/article/pii/S2214317321000238>.

KRUSKAL, W. H.; WALLIS, W. A. Use of ranks in one-criterion variance analysis. *Journal of the American statistical Association*, Taylor & Francis Group, v. 47, n. 260, p. 583–621, 1952.

KS, A.; SAHAYADHAS, A. Automatic rice leaf disease segmentation using image processing techniques. *International Journal of Engineering and Technology(UAE)*, v. 7, p. 182–185, 01 2018.

KVET, J.; MARSHALL, J. Assessment of leaf area and other assimilating plant surfaces. *Sestak, Z. Plant photosynthetic production*, 1971.

LAWSON, T.; MILLIKEN, A. L. Photosynthesis–beyond the leaf. *New Phytologist*, Wiley Online Library, v. 238, n. 1, p. 55–61, 2023.

LI-COR. *LI-3000C Area Meter*. 2019. Accessed: 10-10-2019. Available at: <https://www.licor.com/>.

LI-COR. *LI-3000C Area Meter*. 2023. Accessed: 11-10-2023. Available at: <https://www.licor.com/>.

LI, R.; SUN, G.; WANG, S.; TAN, T.; XU, F. Tree trunk detection in urban scenes using a multiscale attention-based deep learning method. *Ecological Informatics*, Elsevier, v. 77, p. 102215, 2023.

LI, Y.; WANG, H.; DANG, L. M.; SADEGHI-NIARAKI, A.; MOON, H. Crop pest recognition in natural scenes using convolutional neural networks. *Computers and Electronics in Agriculture*, Elsevier, v. 169, p. 105174, 2020.

LIANG, W.; KIRK, K. R.; GREENE, J. K. Estimation of soybean leaf area, edge, and defoliation using color image analysis. *Computers and Electronics in Agriculture*, v. 150, p. 41 − 51, 2018. ISSN 0168-1699.

LIN, F.-C.; SHIU, Y.-S.; WANG, P.-J.; WANG, U.-H.; LAI, J.-S.; CHUANG, Y.-C. A model for forest type identification and forest regeneration monitoring based on deep learning and hyperspectral imagery. *Ecological Informatics*, v. 80, p. 102507, 2024. ISSN 1574-9541. Available at: <https://www.sciencedirect.com/science/article/pii/S1574954124000499>.

LIN, J.; CHEN, X.; PAN, R.; CAO, T.; CAI, J.; CHEN, Y.; PENG, X.; CERNAVA, T.; ZHANG, X. Grapenet: A lightweight convolutional neural network model for identification of grape leaf diseases. *Agriculture*, Multidisciplinary Digital Publishing Institute, v. 12, n. 6, p. 887, 2022.

LIU, D. H.; RAFTERY, A. E. Bayesian projections of total fertility rate conditional on the united nations sustainable development goals. *The Annals of Applied Statistics*, Institute of Mathematical Statistics, v. 18, n. 1, p. 375–403, 2024.

LIU, J.; WANG, X. Tomato diseases and pests detection based on improved yolo v3 convolutional neural network. *Frontiers in plant science*, Frontiers Media SA, v. 11, p. 898, 2020.

LIU, J.; YIN, W.; LI, W.; CHOW, Y. T. Multilevel optimal transport: a fast approximation of wasserstein-1 distances. *arXiv preprint arXiv:1810.00118*, 2018.

LU, C.-Y.; Arcega Rustia, D. J.; LIN, T.-T. Generative adversarial network based image augmentation for insect pest classification enhancement. *IFAC-PapersOnLine*, v. 52, n. 30, p. 1 − 5, 2019. ISSN 2405-8963. 6th IFAC Conference on Sensing, Control and Automation Technologies for Agriculture AGRICONTROL 2019.

LUO, T.; ZHAO, J.; GU, Y.; ZHANG, S.; QIAO, X.; TIAN, W.; HAN, Y. Classification of weed seeds based on visual images and deep learning. *Information Processing in Agriculture*, v. 10, n. 1, p. 40–51, 2023. ISSN 2214-3173. Available at: <https://www.sciencedirect.com/science/article/pii/S2214317321000809>.

LUO, Z.; YANG, W.; YUAN, Y.; GOU, R.; LI, X. Semantic segmentation of agricultural images: A survey. *Information Processing in Agriculture*, 2023. ISSN 2214-3173. Available at: <https://www.sciencedirect.com/science/article/pii/S2214317323000112>.

MACHADO, B. B.; ORUE, J. P.; ARRUDA, M. S.; SANTOS, C. V.; SARATH, D. S.; GONCALVES, W. N.; SILVA, G. G.; PISTORI, H.; ROEL, A. R.; RODRIGUES-JR, J. F. Bioleaf: A professional mobile application to measure foliar damage caused by insect herbivory. *Computers and electronics in agriculture*, Elsevier, v. 129, p. 44–55, 2016.

MALOOF, J. N.; NOZUE, K.; MUMBACH, M. R.; PALMER, C. M. Leafj: an imagej plugin for semi-automated leaf shape measurement. *JoVE (Journal of Visualized Experiments)*, n. 71, p. e50028, 2013.

MANSO, G. L.; KNIDEL, H.; KROHLING, R. A.; VENTURA, J. A. A smartphone application to detection and classification of coffee leaf miner and coffee leaf rust. *arXiv preprint arXiv:1904.00742*, 2019.

MOHANTY, S. P.; HUGHES, D. P.; SALATHÉ, M. Using deep learning for image-based plant disease detection. *Frontiers in plant science*, Frontiers, v. 7, p. 1419, 2016. ISSN 1664-462X.

MOUSSAFIR, M.; CHAIBI, H.; SAADANE, R.; CHEHRI, A.; RHARRAS, A. E.; JEON, G. Design of efficient techniques for tomato leaf disease detection using genetic algorithm-based and deep neural networks. *Plant and Soil*, Springer, v. 479, n. 1-2, p. 251–266, 2022.

MUENZBERG, A.; TROOST, C.; MARTINI, D.; MENDOZA, F.; SRIVASTAVA, R. K.; BERGER, T.; SEURING, L.; REINOSCH, N.; STRECK, T.; BERNARDI, A. Machine learning on simulated and real farm data based on an ontology-controlled data infrastructure. In: *AAAI Spring Symposium: MAKE*. [S.l.: s.n.], 2022.

NABITY, P. D.; ZAVALA, J. A.; DELUCIA, E. H. Indirect suppression of photosynthesis on individual leaves by arthropod herbivory. *Annals of botany*, Oxford University Press, v. 103, n. 4, p. 655–663, 2009.

NANNI, L.; MAGUOLO, G.; PANCINO, F. Insect pest image detection and recognition based on bio-inspired methods. *Ecological Informatics*, v. 57, p. 101089, May 2020. ISSN 15749541.

NASCIMENTO, T. H.; FERNANDES, D.; SIQUEIRA, D.; VIEIRA, G.; MOREIRA, G.; SILVA, L.; SOARES, F. Land vehicle control using continuous gesture recognition on smartwatches. In: SPRINGER. *International Conference on Human-Computer Interaction*. [S.l.], 2024. p. 207–224.

NASCIMENTO, T. H.; FERNANDES, D.; VIEIRA, G.; FELIX, J.; CASTRO, M.; SOARES, F. Mazevr: Immersion and interaction using google cardboard and continuous gesture recognition on smartwatches. In: *Proceedings of the 28th International ACM Conference on 3D Web Technology*. [S.l.: s.n.], 2023. p. 1–5.

NGUGI, L. C.; ABDELWAHAB, M.; ABO-ZAHHAD, M. A new approach to learning and recognizing leaf diseases from individual lesions using convolutional neural networks. *Information Processing in Agriculture*, v. 10, n. 1, p. 11–27, 2023. ISSN 2214-3173. Available at: <https://www.sciencedirect.com/science/article/pii/S2214317321000822>.

NGUY-ROBERTSON, A.; PENG, Y.; ARKEBAUER, T.; SCOBY, D.; SCHEPERS, J.; GITELSON, A. Using a simple leaf color chart to estimate leaf and canopy chlorophyll a content in maize (zea mays). *Communications in Soil Science and Plant Analysis*, Taylor and Francis, v. 46, n. 21, p. 2734–2745, 2015.

NIGAM, S.; JAIN, R.; MARWAHA, S.; ARORA, A.; HAQUE, M. A.; DHEERAJ, A.; SINGH, V. K. Deep transfer learning model for disease identification in wheat crop. *Ecological Informatics*, v. 75, p. 102068, 2023. ISSN 1574-9541. Available at: <https://www.sciencedirect.com/science/article/pii/S1574954123000973>.

NIU, D.; ZHAO, X.; LIN, X.; ZHANG, C. A novel image retrieval method based on multi-features fusion. *Signal Processing: Image Communication*, v. 87, p. 115911, 2020. ISSN 0923-5965.

NOGUEIRA, E. A.; FELIX, J. P.; FONSECA, A. U.; VIEIRA, G.; FERREIRA, J. C.; FERNANDES, D. S.; OLIVEIRA, B. M.; SOARES, F. Deep learning for super resolution of sugarcane crop line imagery from unmanned aerial vehicles. In: SPRINGER. *International Symposium on Visual Computing*. [S.l.], 2023. p. 597–609.

NOGUEIRA, E. A.; FELIX, J. P.; FONSECA, A. U.; VIEIRA, G.; FERREIRA, J. C.; FERNANDES, D. S.; OLIVEIRA, B. M.; SOARES, F. Upsampling of unmanned aerial vehicle images of sugarcane crop lines with a real-esrgan. In: IEEE. *2023 IEEE Canadian Conference on Electrical and Computer Engineering (CCECE)*. [S.l.], 2023. p. 285–290.

NOGUEIRA, E. A.; ROCHA, B. M.; VIEIRA, G. S.; FONSECA, A. U.; FELIX, J. P.; OLIVEIRA, A.; SOARES, F. Enhancing corn image resolution captured by unmanned aerial vehicles with the aid of deep learning. *IEEE Access*, IEEE, 2024.

NOVOTNÝ, P.; SUK, T. Leaf recognition of woody species in central europe. *Biosystems Engineering*, Elsevier, v. 115, n. 4, p. 444–452, 2013.

NUKALA, R.; PANDURU, K.; SHIELDS, A.; RIORDAN, D.; DOODY, P.; WALSH, J. Internet of things: A review from 'farm to fork'. In: IEEE. *2016 27th Irish signals and systems conference (ISSC)*. [S.l.], 2016. p. 1–6.

OTSU, N. A threshold selection method from gray-level histograms. *IEEE transactions on systems, man, and cybernetics*, IEEE, v. 9, n. 1, p. 62–66, 1979.

OUMA, J. *Management of Whiteflies and Slugs on Greenhouse Poinsettia in Kenya*. PhD Thesis (PhD Thesis) — University of Nairobi, 2023.

OYA, N.; RUSDI, M.; FAZLINA, Y.; SUGIANTO, S. Template matching method to determine oil palm trees. In: IOP PUBLISHING. *IOP Conference Series: Earth and Environmental Science*. [S.l.], 2023. v. 1183, n. 1, p. 012077.

PANDEY, P.; RAMEGOWDA, V.; SENTHIL-KUMAR, M. Shared and unique responses of plants to multiple individual stresses and stress combinations: physiological and molecular mechanisms. *Frontiers in plant science*, Frontiers Media SA, v. 6, p. 723, 2015.

PARK, Y.-H.; CHOI, S. H.; KWON, Y.-J.; KWON, S.-W.; KANG, Y. J.; JUN, T.-H. Detection of soybean insect pest and a forecasting platform using deep learning with unmanned ground vehicles. *Agronomy*, MDPI, v. 13, n. 2, p. 477, 2023.

PIVOTO, D.; LAIMER, C. G.; MORES, G. D. V.; WAQUIL, P. D.; TALAMINI, E.; CORTE, V. D.; MATOS, E. D. Smart farming in brazil: an overview of technology, adoption and farmer perception. *Revista Brasileira de Gestão e Desenvolvimento Regional*, v. 19, n. 1, 2023.

PIVOTO, D.; WAQUIL, P. D.; TALAMINI, E.; FINOCCHIO, C. P. S.; CORTE, V. F. D.; MORES, G. de V. Scientific development of smart farming technologies and their application in brazil. *Information Processing in Agriculture*, v. 5, n. 1, p. 21 – 32, 2018. ISSN 2214-3173.

PRAKASH, C.; SINGH, L. P.; GUPTA, A.; LOHAN, S. K. Advancements in smart farming: A comprehensive review of iot, wireless communication, sensors, and hardware for agricultural automation. *Sensors and Actuators A: Physical*, Elsevier, p. 114605, 2023.

PRESTI, D. L.; TOCCO, J. D.; MASSARONI, C.; CIMINI, S.; GARA, L. D.; SINGH, S.; RAUCCI, A.; MANGANIELLO, G.; WOO, S. L.; SCHENA, E. *et al.* Current understanding, challenges and perspective on portable systems applied to plant monitoring and precision agriculture. *Biosensors and Bioelectronics*, Elsevier, v. 222, p. 115005, 2023.

QIN, K.; ZHANG, J.; HU, Y. Identification of insect pests on soybean leaves based on sp-yolo. *Agronomy*, v. 14, n. 7, 2024.

RAFFA, K. F.; BROCKERHOFF, E. G.; GRÉGOIRE, J.-C.; HAMELIN, R. C.; LIEBHOLD, A. M.; SANTINI, A.; VENETTE, R. C.; WINGFIELD, M. J. Approaches to forecasting damage by invasive forest insects and pathogens: a cross-assessment. *Bioscience*, Oxford University Press, v. 73, n. 2, p. 85–111, 2023.

RENAULT, D.; ANGULO, E.; CUTHBERT, R. N.; HAUBROCK, P. J.; CAPINHA, C.; BANG, A.; KRAMER, A. M.; COURCHAMP, F. The magnitude, diversity, and distribution of the economic costs of invasive terrestrial invertebrates worldwide. *Science of the Total Environment*, Elsevier, v. 835, p. 155391, 2022.

ROCHA, B.; VIEIRA, G.; PEDRINI, H.; FONSECA, A.; FERNANDES, D.; LIMA, J. C. de; FERREIRA, J. C.; SOARES, F. Skew angle detection and correction in text images using rgb gradient. In: SPRINGER. *International Conference on Image Analysis and Processing*. [S.l.], 2022. p. 249–262.

ROCHA, B. M.; FONSECA, A. U. da; PEDRINI, H.; SOARES, F. Automatic detection and evaluation of sugarcane planting rows in aerial images. *Information Processing in Agriculture*, v. 10, n. 3, p. 400–415, 2023. ISSN 2214-3173. Available at: <https://www.sciencedirect.com/science/article/pii/S2214317322000439>.

ROCHA, B. M.; VIEIRA, G. da S.; FONSECA, A. U.; PEDRINI, H.; SOUSA, N. M. de; SOARES, F. Evaluation and detection of gaps in curved sugarcane planting lines in aerial images. In: IEEE. *2020 IEEE Canadian conference on electrical and computer engineering (CCECE)*. [S.l.], 2020. p. 1–4.

ROCHA, B. M.; VIEIRA, G. S.; FONSECA, A. U.; SOUSA, N. M.; PEDRINI, H.; SOARES, F. Detection of curved rows and gaps in aerial images of sugarcane field using image processing techniques détection de rangées courbes et de lacunes dans des images aériennes de champs de canne à sucre à l'aide de techniques de traitement d'images. *IEEE Canadian Journal of Electrical and Computer Engineering*, IEEE, 2022.

RODRIGUES, W. G.; CABACINHA, C. D.; SALVINI, R.; VIEIRA, G.; FERNANDES, D. S.; SOARES, F. Eucalyptus volume estimation for eucalyptus clones trees using artificial

neural networks. In: IEEE. *2020 IEEE Canadian Conference on Electrical and Computer Engineering (CCECE)*. [S.l.], 2020. p. 1–5.

RODRIGUES, W. G.; VIEIRA, G. S.; CABACINHA, C. D.; BULCÃO-NETO, R. F.; SOARES, F. Applications of artificial intelligence and lidar in forest inventories: A systematic literature review. *Computers and Electrical Engineering*, Elsevier, v. 120, p. 109793, 2024.

ROMÁN, J. C. M.; NOGUERA, J. L. V.; LEGAL-AYALA, H.; PINTO-ROA, D. P.; GOMEZ-GUERRERO, S.; TORRES, M. G. Entropy and contrast enhancement of infrared thermal images using the multiscale top-hat transform. *Entropy*, Multidisciplinary Digital Publishing Institute, v. 21, n. 3, p. 244, 2019.

ROTH-NEBELSICK, A.; KRAUSE, M. The plant leaf: A biomimetic resource for multifunctional and economic design. *Biomimetics*, MDPI, v. 8, n. 2, p. 145, 2023.

RUBNER, Y.; TOMASI, C.; GUIBAS, L. J. The earth mover's distance as a metric for image retrieval. *International journal of computer vision*, Springer, v. 40, n. 2, p. 99–121, 2000.

RUSIA, M. K.; SINGH, D. K. A comprehensive survey on techniques to handle face identity threats: challenges and opportunities. *Multimedia Tools and Applications*, Springer, v. 82, n. 2, p. 1669–1748, 2023.

RUSTIA, D. J. A.; LEE, W.-C.; LU, C.-Y.; WU, Y.-F.; SHIH, P.-Y.; CHEN, S.-K.; CHUNG, J.-Y.; LIN, T.-T. Edge-based wireless imaging system for continuous monitoring of insect pests in a remote outdoor mango orchard. *Computers and Electronics in Agriculture*, v. 211, p. 108019, 2023. ISSN 0168-1699. Available at: <https://www.sciencedirect.com/science/article/pii/S0168169923004076>.

SAADANE, R.; CHEHRI, A.; JEON, S. *et al.* Ai-based modeling and data-driven evaluation for smart farming-oriented big data architecture using iot with energy harvesting capabilities. *Sustainable Energy Technologies and Assessments*, Elsevier, v. 52, p. 102093, 2022.

SADEGHI-TEHRAN, P.; VIRLET, N.; SABERMANESH, K.; HAWKESFORD, M. J. Multi-feature machine learning model for automatic segmentation of green fractional vegetation cover for high-throughput field phenotyping. *Plant methods*, BioMed Central, v. 13, n. 1, p. 103, 2017.

SANTOS, B. A origem e a importância dos insetos como praga das plantas cultivadas. *Universidade Federal do Paraná–SCB*, 2011.

SANTOS, J.; COSTA, R.; SILVA, D.; SOUZA, A.; MOURA, F.; JUNIOR, J.; SILVA, J. Use of allometric models to estimate leaf area in hymenaea courbaril l. *Theoretical and Experimental Plant Physiology*, v. 28, 07 2016.

SANTOS, S.; VIEIRA, G.; LIMA, J.; SANTOS, A. Tecnologia assistiva para reconhecimento de cartas de baralho utilizando aprendizado profundo. In: INSTITUTO FEDERAL GOIANO. *SIBGRAPI-Conference on Graphics, Patterns and Images*. [S.l.], 2019.

SARANYA, T.; DEISY, C.; SRIDEVI, S.; ANBANANTHEN, K. S. M. A comparative study of deep learning and internet of things for precision agriculture. *Engineering Applications of Artificial Intelligence*, Elsevier, v. 122, p. 106034, 2023.

SELVARAJU, R. R.; COGSWELL, M.; DAS, A.; VEDANTAM, R.; PARIKH, D.; BATRA, D. Grad-cam: Visual explanations from deep networks via gradient-based localization. In: *Proceedings of the IEEE international conference on computer vision*. [S.l.: s.n.], 2017. p. 618–626.

SHAH, D.; TRIVEDI, V.; SHETH, V.; SHAH, A.; CHAUHAN, U. Rests: Residual deep interpretable architecture for plant disease detection. *Information Processing in Agriculture*, v. 9, n. 2, p. 212–223, 2022. ISSN 2214-3173. Available at: <https://www.sciencedirect.com/science/article/pii/S2214317321000482>.

SHEN, Y.; ZHOU, H.; LI, J.; JIAN, F.; JAYAS, D. S. Detection of stored-grain insects using deep learning. *Computers and Electronics in Agriculture*, v. 145, p. 319–325, Feb. 2018. ISSN 01681699.

SILESHI, F.; GALANO, T.; BIRI, B. *Plant Disease Diagnosis Practical Laboratory Manual*. [S.l.: s.n.], 2016.

SILVA, A. d. L.; ALVES, M. V. d. S.; COAN, A. I. Importance of anatomical leaf features for characterization of three species of mapania (mapanioideae, cyperaceae) from the amazon forest, brazil. *Acta Amazonica*, SciELO Brasil, v. 44, n. 4, p. 447–456, 2014.

SILVA, J. L. S.; VIEIRA, G. S.; FONSECA, A. U.; SOARES, F. Reconhecimento e tradução de sinais de libras para língua portuguesa escrita usando redes neurais profundas. In: *Congresso Brasileiro de Automática-CBA*. [S.l.: s.n.], 2022. v. 3, n. 1.

SILVA, L. A. da; BRESSAN, P. O.; GONçALVES, D. N.; FREITAS, D. M.; MACHADO, B. B.; GONçALVES, W. N. Estimating soybean leaf defoliation using convolutional neural networks and synthetic images. *Computers and Electronics in Agriculture*, v. 156, p. 360 – 368, 2019. ISSN 0168-1699.

SILVA, M.; RIBEIRO, S.; BIANCHI, A.; OLIVEIRA, R. An improved deep learning application for leaf shape reconstruction and damage estimation. In: INSTICC. *Proceedings of the 23rd International Conference on Enterprise Information Systems - Volume 1: ICEIS*,. [S.l.]: SciTePress, 2021. p. 484–495. ISBN 978-989-758-509-8.

SILVA, R. A.; SANTOS, G. H.; REGERT, M. P.; SILVA, G. N.; OLIVEIRA, A. A.; MOTA, L. H. C. Temporal variation and spatial distribution of euschistus heros (hemiptera: Pentatomidae) during the soybean grain formation period. *Research, Society and Development*, v. 11, n. 9, p. e6411931102–e6411931102, 2022.

SIMONYAN, K.; ZISSERMAN, A. Very deep convolutional networks for large-scale image recognition. *arXiv preprint arXiv:1409.1556*, 2014.

SOARES, F. A. A.; FLÔRES, E. L.; CABACINHA, C. D.; CARRIJO, G. A.; VEIGA, A. C. P. Recursive diameter prediction and volume calculation of eucalyptus trees using multilayer perceptron networks. *Computers and electronics in agriculture*, Elsevier, v. 78, n. 1, p. 19–27, 2011.

SODJINOU, S. G.; MOHAMMADI, V.; Sanda Mahama, A. T.; GOUTON, P. A deep semantic segmentation-based algorithm to segment crops and weeds in agronomic color images. *Information Processing in Agriculture*, v. 9, n. 3, p. 355–364, 2022. ISSN 2214-3173. Available at: <https://www.sciencedirect.com/science/article/pii/S2214317321000731>.

SOSA-GÓMEZ, D. R.; CORRÊA-FERREIRA, B. S.; HOFFMANN-CAMPO, C. B.; CORSO, I. C.; OLIVEIRA, L. J.; MOSCARDI, F.; PANIZZI, A. R.; BUENO, A. d. F.; HIROSE, E.; ROGGIA, S. *Manual de identificação de insetos e outros invertebrados da cultura da soja*. [S.l.]: Londrina: Embrapa Soja, 2023., 2023.

SOUSA, N. M. de; FELIX, J. P.; VIEIRA, G. da S.; ROCHA, B. M.; SOARES, F. A study of saliency methods for tree detection in aerial images of rural areas. In: IEEE. *2021 IEEE Canadian Conference on Electrical and Computer Engineering (CCECE)*. [S.l.], 2021. p. 1–4.

SOUSA, N. M. de; VIEIRA, G. da S.; FELIX, J. P.; LIMA, J. C. de; SOARES, F. Image saliency analysis in agricultural environments: A survey. In: IEEE. *2020 IEEE Canadian Conference on Electrical and Computer Engineering (CCECE)*. [S.l.], 2020. p. 1–4.

SUBEESH, A.; MEHTA, C. Automation and digitization of agriculture using artificial intelligence and internet of things. *Artificial Intelligence in Agriculture*, v. 5, p. 278–291, 2021. ISSN 2589-7217. Available at: <https://www.sciencedirect.com/science/article/pii/S2589721721000350>.

SUTAJI, D.; YıLDıZ, O. Lemoxinet: Lite ensemble mobilenetv2 and xception models to predict plant disease. *Ecological Informatics*, v. 70, p. 101698, 2022. ISSN 1574-9541. Available at: <https://www.sciencedirect.com/science/article/pii/S1574954122001480>.

TAN, M.; LE, Q. Efficientnet: Rethinking model scaling for convolutional neural networks. In: PMLR. *International conference on machine learning*. [S.l.], 2019. p. 6105–6114.

TANG, W.; JIA, F.; WANG, X. Image large rotation and scale estimation using the gabor filter. *Electronics*, MDPI, v. 11, n. 21, p. 3471, 2022.

THENMOZHI, K.; REDDY, U. S. Image processing techniques for insect shape detection in field crops. In: *2017 International Conference on Inventive Computing and Informatics (ICICI)*. Coimbatore: IEEE, 2017. p. 699–704. ISBN 978-1-5386-4031-9.

THENMOZHI, K.; Srinivasulu Reddy, U. Crop pest classification based on deep convolutional neural network and transfer learning. *Computers and Electronics in Agriculture*, v. 164, p. 104906, 2019. ISSN 0168-1699.

TIAN, X.; JIAO, L.; LIU, X.; ZHANG, X. Feature integration of eodh and color-sift: Application to image retrieval based on codebook. *Signal Processing: Image Communication*, Elsevier, v. 29, n. 4, p. 530–545, 2014.

UN-DESA. *World Population Prospects 2024 Summary of Results*. 2022. Accessed: 24-08-2024. Available at: <https://www.un.org/development/desa/pd/>.

UN-DESA. *World Population Prospects 2024 Summary of Results*. 2024. Accessed: 24-08-2024. Available at: <https://population.un.org/wpp/Publications/Files/WPP2024_Key-Messages.pdf>.

USDA. *Fresh apples, grapes, and pears: world markets and trade*. 2020. Accessed: 2020-12-30. Available at: <https://apps.fas.usda.gov/PSDOnline/Circulars/2020/10/Fruit.pdf>.

USDA. *Fresh peaches and cherries: world markets and trade*. 2020. Accessed: 2020-12-30. Available at: <https://apps.fas.usda.gov/PSDOnline/Circulars/2020/11/StoneFruit.pdf>.

USDA. *Grain: world markets and trade*. 2020. Accessed: 2020-12-30. Available at: <https://apps.fas.usda.gov/PSDOnline/Circulars/2020/11/Grain.pdf>.

USDA. *Sugar: world markets and trade*. 2020. Accessed: 2020-12-30. Available at: <https://apps.fas.usda.gov/PSDOnline/Circulars/2020/10/Sugar.pdf>.

USDA. *World Agricultural Production*. 2020. Accessed: 2020-12-30. Available at: <https://downloads.usda.library.cornell.edu/usda-esmis/files/5q47rn72z/ft849d88n/q811m8874/production.pdf>.

USDA. *Fresh apples, grapes, and pears: world markets and trade*. 2022. Accessed: 2022-11-02. Available at: <https://downloads.usda.library.cornell.edu/usda-esmis/files/1z40ks800/44559m20c/02872238m/fruit.pdf>.

USDA. *World Agricultural Production.* 2024. Accessed: 02-01-2024. Available at: <https://apps.fas.usda.gov/psdonline/circulars/production.pdf>.

VERMA, R. C.; WASEEM, M. A.; SHARMA, N.; BHARATHI, K.; SINGH, S.; RASHWIN, A. A.; PANDEY, S. K.; SINGH, B. V. The role of insects in ecosystems, an in-depth review of entomological research. *International Journal of Environment and Climate Change*, v. 13, n. 10, p. 4340–4348, 2023.

VIEIRA, G.; SOUSA, N.; ROCHA, B.; FONSECA, A. U.; SOARES, F. A method for the detection and reconstruction of foliar damage caused by predatory insects. In: *2021 IEEE 45th Annual Computers, Software, and Applications Conference (COMPSAC)*. [S.l.: s.n.], 2021. p. 1502–1507.

VIEIRA, G. D. S.; SOARES, F. A. A.; LIMA, J. C. D.; NASCIMENTO, H. A. D.; LAUREANO, G. T.; COSTA, R. M. D.; FERREIRA, J. C.; RODRIGUES, W. G. A disparity computation framework. In: IEEE. *2019 IEEE 43rd Annual Computer Software and Applications Conference (COMPSAC)*. [S.l.], 2019. v. 2, p. 634–639.

VIEIRA, G. D. S.; SOUSA, N. M. de; ROCHA, B.; FONSECA, A. U.; SOARES, F. A method for the detection and reconstruction of foliar damage caused by predatory insects. In: IEEE. *2021 IEEE 45th Annual Computers, Software, and Applications Conference (COMPSAC)*. Los Alamitos, CA, USA: IEEE Computer Society, 2021. p. 1502–1507. ISSN 0730-3157. Available at: <https://doi.ieeecomputersociety.org/10.1109/COMPSAC51774.2021.00223>.

VIEIRA, G. da S.; LIMA, J. C. de; SOUSA, N. M. de; SOARES, F. A three-layer architecture to support disparity map construction in stereo vision systems. *Intelligent Systems with Applications*, Elsevier, v. 12, p. 200054, 2021.

VIEIRA, G. da S.; ROCHA, B. M.; FONSECA, A. U.; SOUSA, N. M. de; FERREIRA, J. C.; CABACINHA, C. D.; SOARES, F. Automatic detection of insect predation through the segmentation of damaged leaves. *Smart Agricultural Technology*, Elsevier, v. 2, p. 100056, 2022. ISSN 2772-3755. Available at: <https://www.sciencedirect.com/science/article/pii/S2772375522000211>.

VIEIRA, G. da S.; ROCHA, B. M.; PEDRINI, H.; SOUSA, N. M.; LIMA, J. C. de; COSTA, R.; SOARES, F. Visual detection of productive crop and pasture fields from aerial image analysis. In: IEEE. *2020 IEEE Canadian Conference on Electrical and Computer Engineering (CCECE)*. [S.l.], 2020. p. 1–4.

VIEIRA, G. da S.; ROCHA, B. M.; SOARES, F.; LIMA, J. C.; PEDRINI, H.; COSTA, R.; FERREIRA, J. Extending the aerial image analysis from the detection of tree crowns. In: IEEE. *2019 IEEE 31st International Conference on Tools with Artificial Intelligence (ICTAI)*. [S.l.], 2019. p. 1681–1685.

VIEIRA, G. da S.; SOARES, F. A.; LIMA, J. C. de; LAUREANO, G. T.; SANTOS, S. A.; COSTA, R. M.; SALVINI, R. Trunk detection and tree disparity calculation in uncontrolled environments. In: IEEE. *2019 IEEE Symposium on Computers and Communications (ISCC)*. [S.l.], 2019. p. 1–6.

VIEIRA, G. da S.; SOARES, F. A.; SANTOS, S. A.; LAUREANO, G. T.; LIMA, J. C. de; COSTA, R. M.; FÉLIX, J. P.; NASCIMENTO, T. H. Ground segmentation from outdoor environments in rural areas. In: IEEE. *2019 IEEE Canadian Conference of Electrical and Computer Engineering (CCECE)*. [S.l.], 2019. p. 1–4.

VIEIRA, G. da S.; SOARES, F. A.; SANTOS, S. A.; LAUREANO, G. T.; LIMA, J. C. de; COSTA, R. M.; FÉLIX, J. P.; NASCIMENTO, T. H. Towards integrated image contrast models in segmentation of trees. In: IEEE. *2019 IEEE Canadian Conference of Electrical and Computer Engineering (CCECE)*. [S.l.], 2019. p. 1–4.

VIEIRA, G. da S.; SOUSA, N. M. de; FÉLIX, J. P.; LIMA, J. C. de; SOARES, F. Application of saliency methods for extracting tree features in outdoor scenes. In: IEEE. *2020 IEEE Canadian Conference on Electrical and Computer Engineering (CCECE)*. [S.l.], 2020. p. 1–4.

VIEIRA, G. S.; FONSECA, A. U.; de Sousa, N. M.; FERREIRA, J. C.; FELIX, J. P.; CABACINHA, C. D.; SOARES, F. An automatic method for estimating insect defoliation with visual highlights of consumed leaf tissue regions. *Information Processing in Agriculture*, 2024. ISSN 2214-3173. Available at: <https://www.sciencedirect.com/science/article/pii/S2214317324000192>.

VIEIRA, G. S.; FONSECA, A. U.; FERREIRA, J. C.; SOARES, F. Protectleaf: An insect predation analyzer for agricultural crop monitoring. *SoftwareX*, v. 24, p. 101537, 2023. ISSN 2352-7110. Available at: <https://www.sciencedirect.com/science/article/pii/S2352711023002339>.

VIEIRA, G. S.; FONSECA, A. U.; ROCHA, B. M.; SOUSA, N. M.; FERREIRA, J. C.; FELIX, J. P.; LIMA, J. C.; SOARES, F. Insect predation estimate using binary leaf models and image-matching shapes. *Agronomy*, MDPI, v. 12, n. 11, p. 2769, 2022. ISSN 2073-4395. Available at: <https://www.mdpi.com/2073-4395/12/11/2769>.

VIEIRA, G. S.; FONSECA, A. U.; SOARES, F. Cbir-anr: A content-based image retrieval with accuracy noise reduction. *Software Impacts*, Elsevier, v. 15, p. 100486, 2023.

VIEIRA, G. S.; FONSECA, A. U.; SOUSA, N. M.; FELIX, J. P.; SOARES, F. A novel content-based image retrieval system with feature descriptor integration and accuracy noise reduction. *Expert Systems with Applications*, Elsevier, v. 232, p. 120774, 2023.

VIEIRA, G. S.; LIMA, J. C.; SOUSA, N. M.; SOARES, F. Dcf: Disparity computing framework for stereo vision systems. *Software Impacts*, Elsevier, v. 14, p. 100442, 2022.

WÄLDCHEN, J.; MÄDER, P. Plant species identification using computer vision techniques: A systematic literature review. *Archives of Computational Methods in Engineering*, Springer, v. 25, n. 2, p. 507–543, 2018.

WANG, J.; LIN, C.; JI, L.; LIANG, A. A new automatic identification system of insect images at the order level. *Knowledge-Based Systems*, v. 33, p. 102–110, Sep. 2012. ISSN 09507051.

WANG, M.; ZHU, Z.; ZHANG, S.; MARTIN, R.; HU, S.-M. Avoiding bleeding in image blending. In: IEEE. *2017 IEEE International Conference on Image Processing (ICIP)*. [S.l.], 2017. p. 2139–2143.

WANG, Z.; BOVIK, A. C.; SHEIKH, H. R.; SIMONCELLI, E. P. *et al.* Image quality assessment: from error visibility to structural similarity. *IEEE transactions on image processing*, v. 13, n. 4, p. 600–612, 2004.

WEI, Z.; LIU, G.-H. Image retrieval using the intensity variation descriptor. *Mathematical Problems in Engineering*, Hindawi, v. 2020, 2020.

WEN, C.; GUYER, D. Image-based orchard insect automated identification and classification method. *Computers and Electronics in Agriculture*, v. 89, p. 110–115, Nov. 2012. ISSN 01681699.

WIETZKE, A.; WESTPHAL, C.; GRAS, P.; KRAFT, M.; PFOHL, K.; KARLOVSKY, P.; PAWELZIK, E.; TSCHARNTKE, T.; SMIT, I. Insect pollination as a key factor for strawberry physiology and marketable fruit quality. *Agriculture, ecosystems & environment*, Elsevier, v. 258, p. 197–204, 2018.

WU, S. G.; BAO, F. S.; XU, E. Y.; WANG, Y.-X.; CHANG, Y.-F.; XIANG, Q.-L. A leaf recognition algorithm for plant classification using probabilistic neural network. In: IEEE. *2007 IEEE international symposium on signal processing and information technology*. [S.l.], 2007. p. 11–16.

XIE, C.; ZHANG, J.; LI, R.; LI, J.; HONG, P.; XIA, J.; CHEN, P. Automatic classification for field crop insects via multiple-task sparse representation and multiple-kernel learning. *Computers and Electronics in Agriculture*, v. 119, p. 123–132, Nov. 2015. ISSN 01681699.

YANG, H.-P.; MA, C.-S.; WEN, H.; ZHAN, Q.-B.; WANG, X.-L. A tool for developing an automatic insect identification system based on wing outlines. *Scientific Reports*, v. 5, n. 1, p. 12786, Oct. 2015. ISSN 2045-2322.

YANG, Z.; YANG, X.; LI, M.; LI, W. Automated garden-insect recognition using improved lightweight convolution network. *Information Processing in Agriculture*, v. 10, n. 2, p. 256–266, 2023. ISSN 2214-3173. Available at: <https://www.sciencedirect.com/science/article/pii/S2214317321000986>.

ZHANG, J.; HUANG, Y.; PU, R.; GONZALEZ-MORENO, P.; YUAN, L.; WU, K.; HUANG, W. Monitoring plant diseases and pests through remote sensing technology: A review. *Computers and Electronics in Agriculture*, v. 165, p. 104943, 2019. ISSN 0168-1699.

ZHANG, M.; LIANG, H.; WANG, Z.; WANG, L.; HUANG, C.; LUO, X. Damaged apple detection with a hybrid yolov3 algorithm. *Information Processing in Agriculture*, 2022. ISSN 2214-3173. Available at: <https://www.sciencedirect.com/science/article/pii/S2214317322000889>.

ZHANG, Z.; KHANAL, S.; RAUDENBUSH, A.; TILMON, K.; STEWART, C. Assessing the efficacy of machine learning techniques to characterize soybean defoliation from unmanned aerial vehicles. *Computers and Electronics in Agriculture*, v. 193, p. 106682, 2022. ISSN 0168-1699. Available at: <https://www.sciencedirect.com/science/article/pii/S0168169921006992>.

ZHANG, Z.; RONG, J.; QI, Z.; YANG, Y.; ZHENG, X.; GAO, J.; LI, W.; YUAN, T. A multi-species pest recognition and counting method based on a density map in the greenhouse. *Computers and Electronics in Agriculture*, Elsevier, v. 217, p. 108554, 2024.

ZHAO, Y.; HE, Y.; XU, X. A novel algorithm for damage recognition on pest-infested oilseed rape leaves. *Computers and Electronics in Agriculture*, v. 89, p. 41 – 50, 2012. ISSN 0168-1699. Available at: <http://www.sciencedirect.com/science/article/pii/S0168169912002001>.

ZHU, L.; LI, X.; SUN, H.; HAN, Y. Research on cbf-yolo detection model for common soybean pests in complex environment. *Computers and Electronics in Agriculture*, Elsevier, v. 216, p. 108515, 2024.

Contributions

A.1   Original Papers, Software, and Datasets

Scientific manuscripts, original software, and datasets published in journals, international conferences, and online repositories during this research are presented below.

A.1.1   Publications directly related to this thesis

1. Vieira, Gabriel S., Afonso U. Fonseca, Naiane Maria de Sousa, Julio C. Ferreira, Juliana Paula Felix, Christian Dias Cabacinha, and Fabrizzio Soares. "An automatic method for estimating insect defoliation with visual highlights of consumed leaf tissue regions." Information Processing in Agriculture (2024). (VIEIRA *et al.*, 2024) **(Qualis A1)**

2. Vieira, Gabriel S., Afonso U. Fonseca, Julio C. Ferreira, and Fabrizzio Soares. "ProtectLeaf: An insect predation analyzer for agricultural crop monitoring." SoftwareX 24 (2023): 101537. (VIEIRA *et al.*, 2023) **(Qualis A3)**

3. da Silva Vieira, Gabriel, Bruno Moraes Rocha, Afonso Ueslei Fonseca, Naiane Maria de Sousa, Julio Cesar Ferreira, Christian Dias Cabacinha, and Fabrizzio Soares. "Automatic detection of insect predation through the segmentation of damaged leaves." Smart Agricultural Technology 2 (2022): 100056. (VIEIRA *et al.*, 2022) **(Qualis A3)**

4. Vieira, Gabriel S., Afonso U. Fonseca, Bruno M. Rocha, Naiane M. Sousa, Julio C. Ferreira, Juliana P. Felix, Junio C. Lima, and Fabrizzio Soares. "Insect predation estimate using binary leaf models and image-matching shapes." Agronomy 12, no. 11 (2022): 2769. (VIEIRA *et al.*, 2022) **(Qualis A2)**

5. Vieira, Gabriel Da Silva, Naiane Maria de Sousa, Bruno Rocha, Afonso U. Fonseca, and Fabrizzio Soares. "A method for the detection and reconstruction of foliar damage caused by predatory insects." In 2021 IEEE 45th Annual Computers,

Software, and Applications Conference (COMPSAC), pp. 1502-1507. IEEE, 2021. (VIEIRA *et al.*, 2021) **(Qualis A2)**

6. Vieira, Gabriel S., et al. Soybean Pests Classification and Foliar Predation Recognition Using Bite Traces. The manuscript is being prepared for submission to a journal.

A.1.2 Other publications as first author

1. Vieira, Gabriel S., Afonso U. Fonseca, Naiane M. Sousa, Juliana P. Felix, and Fabrizzio Soares. "A novel content-based image retrieval system with feature descriptor integration and accuracy noise reduction." Expert Systems with Applications 232 (2023): 120774. (VIEIRA *et al.*, 2023b) **(Qualis A1)**

2. Vieira, Gabriel S., Afonso U. Fonseca, and Fabrizzio Soares. "CBIR-ANR: A content-based image retrieval with accuracy noise reduction." Software Impacts 15 (2023): 100486. (VIEIRA *et al.*, 2023a) **(Qualis B4)**

3. Vieira, Gabriel S., Junio C. Lima, Naiane M. Sousa, and Fabrizzio Soares. "DCF: Disparity computing framework for stereo vision systems." Software Impacts 14 (2022): 100442. (VIEIRA *et al.*, 2022) **(Qualis B4)**

4. da Silva Vieira, Gabriel, Junio Cesar de Lima, Naiane Maria de Sousa, and Fabrizzio Soares. "A three-Layer architecture to support disparity map construction in stereo vision systems." Intelligent Systems with Applications 12 (2021): 200054. (VIEIRA *et al.*, 2021b) **(Qualis A3)**

5. da Silva Vieira, Gabriel, Bruno M. Rocha, Helio Pedrini, Naiane M. Sousa, Junio Cesar de Lima, Ronaldo Costa, and Fabrizzio Soares. "Visual Detection of Productive Crop and Pasture Fields from Aerial Image Analysis." In 2020 IEEE Canadian Conference on Electrical and Computer Engineering (CCECE), pp. 1-4. IEEE, 2020. (VIEIRA *et al.*, 2020)**(Qualis A3)**

6. da Silva Vieira, Gabriel, Naiane Maria de Sousa, Juliana Paula Félix, Junio Cesar de Lima, and Fabrizzio Soares. "Application of Saliency Methods for Extracting Tree Features in Outdoor Scenes." In 2020 IEEE Canadian Conference on Electrical and Computer Engineering (CCECE), pp. 1-4. IEEE, 2020. (VIEIRA *et al.*, 2020) **(Qualis A3)**

7. Vieira, Gabriel Da Silva, Fabrizzio Alphonsus AMN Soares, Junio Cesar De Lima, Hugo AD Do Nascimento, Gustavo T. Laureano, Ronaldo Martins Da Costa, Júlio C. Ferreira, and Wellington Galvão Rodrigues. "A disparity computation framework." In 2019 IEEE 43rd Annual Computer Software and Applications

Conference (COMPSAC), vol. 2, pp. 634-639. IEEE, 2019. (VIEIRA *et al.*, 2019) **(Qualis A2)**

8. da Silva Vieira, Gabriel, Fabrizzio AAMN Soares, Samuel A. Santos, Gustavo T. Laureano, Junio Cesar de Lima, Ronaldo M. Costa, Juliana Paula Félix, and Thamer H. Nascimento. "Ground segmentation from outdoor environments in rural areas." In 2019 IEEE Canadian Conference of Electrical and Computer Engineering (CCECE), pp. 1-4. IEEE, 2019. (VIEIRA *et al.*, 2019c) **(Qualis A3)**

9. da Silva Vieira, Gabriel, Fabrizzio AAMN Soares, Samuel A. Santos, Gustavo T. Laureano, Junio Cesar de Lima, Ronaldo M. Costa, Juliana Paula Félix, and Thamer H. Nascimento. "Towards Integrated Image Contrast Models in Segmentation of Trees." In 2019 IEEE Canadian Conference of Electrical and Computer Engineering (CCECE), pp. 1-4. IEEE, 2019. (VIEIRA *et al.*, 2019d) **(Qualis A3)**

10. da Silva Vieira, Gabriel, Bruno M. Rocha, Fabrizzio Soares, Júnio César Lima, Helio Pedrini, Ronaldo Costa, and Júlio Ferreira. "Extending the aerial image analysis from the detection of tree crowns." In 2019 IEEE 31st International Conference on Tools with Artificial Intelligence (ICTAI), pp. 1681-1685. IEEE, 2019. (VIEIRA *et al.*, 2019a)**(Qualis A3)**

11. da Silva Vieira, Gabriel, Fabrizzio AAMN Soares, Junio Cesar de Lima, Gustavo T. Laureano, Samuel A. Santos, Ronaldo M. Costa, and Rogerio Salvini. "Trunk detection and tree disparity calculation in uncontrolled environments." In 2019 IEEE Symposium on Computers and Communications (ISCC), pp. 1-6. IEEE, 2019. (VIEIRA *et al.*, 2019b) **(Qualis A2)**

12. Vieira, Gabriel S., et al. Accelerated stereo matching using parallel programming approaches in CUDA. The manuscript is being prepared for submission to a journal.

A.1.3   Other publications as coauthor

1. Rodrigues, Welington G., Gabriel S. Vieira, Christian D. Cabacinha, Renato F. Bulcão-Neto, and Fabrizzio Soares. "Applications of artificial intelligence and LiDAR in forest inventories: A Systematic Literature Review." Computers and Electrical Engineering 120 (2024): 109793. (RODRIGUES *et al.*, 2024) **(Qualis A2)**

2. Nogueira, Emília Alves, Bruno Moraes Rocha, Gabriel S. Vieira, Afonso U. Fonseca, Juliana Paula Felix, Antonio Oliveira, and Fabrizzio Soares. "Enhancing Corn Image Resolution Captured by Unmanned Aerial Vehicles with the Aid of Deep Learning." IEEE Access (2024). (NOGUEIRA *et al.*, 2024) **(Qualis A3)**

3. da Fonseca, Afonso Ueslei, Poliana Lopes Parreira, Gabriel da Silva Vieira, Juliana Paula Felix, Marcus Barreto Conte, Marcelo Fouad Rabahi, and Fabrizzio Soares. "A novel tuberculosis diagnosis approach using feed-forward neural networks and binary pattern of phase congruency." Intelligent Systems with Applications 21 (2024): 200317. (FONSECA *et al.*, 2024) **(Qualis A3)**

4. Nascimento, Thamer Horbylon, Deborah Fernandes, Diego Siqueira, Gabriel Vieira, Gustavo Moreira, Leonardo Silva, and Fabrizzio Soares. "Land Vehicle Control Using Continuous Gesture Recognition on Smartwatches." In International Conference on Human-Computer Interaction, pp. 207-224. Cham: Springer Nature Switzerland, 2024. (NASCIMENTO *et al.*, 2024) **(Qualis A3)**

5. Fonseca, Afonso U., Juliana P. Felix, Hedenir Pinheiro, Gabriel S. Vieira, Ýleris C. Mourão, Juliana CG Monteiro, and Fabrizzio Soares. "An Intelligent System to Improve Diagnostic Support for Oral Squamous Cell Carcinoma." In Healthcare, vol. 11, no. 19, p. 2675. MDPI, 2023. (FONSECA *et al.*, 2023b) **(Qualis A3)**

6. Fonseca, Afonso Ueslei, Juliana Paula Felix, Gabriel Silva Vieira, Bruno Moraes Rocha, Emília Alves Nogueira, Carlos Eduardo Egito Araújo, Deborah Fernandes, and Fabrizzio Soares. "Diagnosticando Tuberculose com Redes Neurais Artificiais e Recursos BPPC." Journal of Health Informatics 15, no. Especial (2023). (FONSECA *et al.*, 2023) **(Qualis A4)**

7. Fonseca, Afonso Ueslei, Juliana de Paula Félix, Gabriel da Silva Vieira, Deborah Fernandes, and Fabrizzio Soares. "Automated Lung Region Segmentation in Pediatric Chest Radiography." Revista de Informática Teórica e Aplicada 30, no. 2 (2023): 114-123. (FONSECA *et al.*, 2023a) **(Qualis B3)**

8. Nogueira, Emília A., Juliana Paula Felix, Afonso Ueslei Fonseca, Gabriel Vieira, Julio Cesar Ferreira, Deborah SA Fernandes, Bruna M. Oliveira, and Fabrizzio Soares. "Upsampling of unmanned aerial vehicle images of sugarcane crop lines with a Real-ESRGAN." In 2023 IEEE Canadian Conference on Electrical and Computer Engineering (CCECE), pp. 285-290. IEEE, 2023. (NOGUEIRA *et al.*, 2023b) **(Qualis A3)**

9. Gomes, Pedro, Murillo Castro, Deborah Fernandes, Fabrizzio Soares, Gabriel Vieira, Juliana Felix, and Thamer Horbylon Nascimento. "DrumsVR: Simulating Drum Percussion in a Virtual Environment Using Gesture Recognition on Smartwatches." In Proceedings of the 28th International ACM Conference on 3D Web Technology, pp. 1-5. 2023. (GOMES *et al.*, 2023) **(Qualis A4)**

10. Nascimento, Thamer Horbylon, Deborah Fernandes, Gabriel Vieira, Juliana Felix, Murillo Castro, and Fabrizzio Soares. "MazeVR: Immersion and Interaction Using Google Cardboard and Continuous Gesture Recognition on Smartwatches." In Proceedings of the 28th International ACM Conference on 3D Web Technology,

pp. 1-5. 2023. (NASCIMENTO *et al.*, 2023) **(Qualis A4)**

11. Nogueira, Emília A., Juliana Paula Felix, Afonso Ueslei Fonseca, Gabriel Vieira, Julio Cesar Ferreira, Deborah SA Fernandes, Bruna M. Oliveira, and Fabrizzio Soares. "Deep Learning for Super Resolution of Sugarcane Crop Line Imagery from Unmanned Aerial Vehicles." In International Symposium on Visual Computing, pp. 597-609. Cham: Springer Nature Switzerland, 2023. (NOGUEIRA *et al.*, 2023a) **(Qualis A4)**

12. Rocha, Bruno Moraes, Gabriel S. Vieira, Afonso U. Fonseca, Naiane M. Sousa, Helio Pedrini, and Fabrizzio Soares. "Detection of Curved Rows and Gaps in Aerial Images of Sugarcane Field Using Image Processing Techniques." IEEE Canadian Journal of Electrical and Computer Engineering 45, no. 3 (2022): 303-310. (ROCHA *et al.*, 2022) **(Qualis A3)**

13. Fonseca, Afonso U., Bruno M. Rocha, Emília A. Nogueira, Gabriel S. Vieira, Deborah SA Fernandes, Júnio C. Lima, Júlio C. Ferreira, and Fabrizzio Soares. "Tuberculosis Detection in Chest Radiography: A Combined Approach of Local Binary Pattern Features and Monarch Butterfly Optimization Algorithm." In 2022 IEEE 46th annual Computers, Software, and Applications Conference (COMPSAC), pp. 1408-1413. IEEE, 2022. (FONSECA *et al.*, 2022) **(Qualis A2)**

14. Rocha, Bruno, Gabriel Vieira, Helio Pedrini, Afonso Fonseca, Deborah Fernandes, Júnio César de Lima, Júlio César Ferreira, and Fabrizzio Soares. "Skew angle detection and correction in text images using RGB gradient." In International Conference on Image Analysis and Processing, pp. 249-262. Cham: Springer International Publishing, 2022. (ROCHA *et al.*, 2022) **(Qualis A3)**

15. Da Fonseca, Afonso Ueslei, Juliana Paula Felix, Gabriel Da Silva Vieira, Deborah Fernandes, and Fabrizzio Soares. "Automatic tuberculosis detection using binary pattern of phase congruency." In 2022 international conference on computational science and computational intelligence (CSCI), pp. 1646-1651. IEEE, 2022. (FONSECA *et al.*, 2022) **(Qualis A4)**

16. Fonseca, Afonso U., Juliana P. Felix, Gabriel S. Vieira, Deborah SA Fernandes, and Fabrizzio Soares. "Detecção de COVID-19 e Avaliação de Nível de Severidade: Uma abordagem com BPPC e Redes Neurais Artificiais Rasas." In Congresso Brasileiro de Automática-CBA, vol. 3, no. 1. 2022. (FONSECA *et al.*, 2022) **(Qualis B4)**

17. Fonseca, Afonso U., Juliana P. Felix, Gabriel S. Vieira, Rocha, Bruno, Nogueira, Emília, Fernandes, Deborah, Soares, Fabrizzio. (2022). Detecção Eficiente de Tuberculose em Raio-X de Tórax via Seleção de Atributos LBP por Algoritmo de Otimização da Borboleta Monarca. In XIX Congresso Brasileiro de Informática em Saúde - CBIS. (FONSECA *et al.*, 2022a) **(Qualis B4)**

18. Fonseca, Afonso, Felix, Juliana, Vieira, Gabriel, Mourão, Yleris, Monteiro, Juliana, Soares, Fabrizzio. (2022). Uma Rede Neural Artificial para Suporte ao Diagnóstico de Carcinoma Espinocelular Oral. In IX Congresso Latino Americano de Engenharia Biomédica e XXVIII Congresso Brasileiro de Engenharia Biomédica. (FONSECA *et al.*, 2022b) **(Qualis B4)**

19. Silva, Jhon Lucas S., Gabriel S. Vieira, Afonso U. Fonseca, and Fabrizzio Soares. "Reconhecimento e Tradução de Sinais de Libras para Língua Portuguesa Escrita usando Redes Neurais Profundas." In Congresso Brasileiro de Automática-CBA, vol. 3, no. 1. 2022. (SILVA *et al.*, 2022) **(Qualis B4)**

20. Felix, Juliana Paula, Hugo Alexandre Dantas Do Nascimento, Nilza Nascimento Guimarães, Eduardo Di Oliveira Pires, Afonso Ueslei Da Fonseca, and Gabriel Da Silva Vieira. "Automatic Classification of Amyotrophic Lateral Sclerosis through Gait Dynamics." In 2021 IEEE 45th Annual Computers, Software, and Applications Conference (COMPSAC), pp. 1942-1947. IEEE, 2021. (FELIX *et al.*, 2021) **(Qualis A2)**

21. Fonseca, Afonso U., Gabriel S. Vieira, and Fabrizzio Soares. "Screening of viral pneumonia and covid-19 in chest x-ray using classical machine learning." In 2021 IEEE 45th annual Computers, Software, and Applications conference (COMPSAC), pp. 1936-1941. IEEE, 2021. (FONSECA *et al.*, 2021) **(Qualis A2)**

22. Kai, Priscila M., Bruna M. de Oliveira, Gabriel S. Vieira, Fabrizzio Soares, and Ronaldo M. Costa. "Effects of resampling image methods in sugarcane classification and the potential use of vegetation indices related to chlorophyll." In 2021 IEEE 45th Annual Computers, Software, and Applications Conference (COMPSAC), pp. 1526-1531. IEEE, 2021. (KAI *et al.*, 2021) **(Qualis A2)**

23. de Sousa, Naiane Maria, Juliana Paula Felix, Gabriel da Silva Vieira, Bruno Morais Rocha, and Fabrizzio Soares. "A Study of Saliency Methods for Tree Detection in Aerial Images of Rural Areas." In 2021 IEEE Canadian Conference on Electrical and Computer Engineering (CCECE), pp. 1-4. IEEE, 2021. (SOUSA *et al.*, 2021) **(Qualis A3)**

24. Fonseca, Afonso, Gabriel Silva Vieira, Juliana Felix, Paulo Freire Sobrinho, Áurea Valéria Pereira Silva, and Fabrizzio Soares. "Automatic orientation identification of pediatric chest x-rays." In 2020 IEEE 44th Annual Computers, Software, and Applications Conference (COMPSAC), pp. 1449-1454. IEEE, 2020. (FONSECA *et al.*, 2020) **(Qualis A2)**

25. Felix, Juliana Paula, Hugo Alexandre Dantas do Nascimento, Nilza Nascimento Guimarães, Eduardo Di Oliveira Pires, Gabriel da Silva Vieira, and Wanderley de Souza Alencar. "An Effective and Automatic Method to Aid the Diagnosis of Amyotrophic Lateral Sclerosis Using One Minute of Gait Signal." In 2020 IEEE

International Conference on Bioinformatics and Biomedicine (BIBM), pp. 2745-2751. IEEE, 2020. (FELIX *et al.*, 2020) **(Qualis A2)**

26. Rocha, Bruno Moraes, Gabriel da Silva Vieira, Afonso U. Fonseca, Helio Pedrini, Naiane Maria de Sousa, and Fabrizzio Soares. "Evaluation and detection of gaps in curved sugarcane planting lines in aerial images." In 2020 IEEE Canadian conference on electrical and computer engineering (CCECE), pp. 1-4. IEEE, 2020. (ROCHA *et al.*, 2020) **(Qualis A3)**

27. Rodrigues, Welington Galvão, Christian D. Cabacinha, Rogerio Salvini, Gabriel Vieira, Deborah SA Fernandes, and Fabrizzio Soares. "Eucalyptus Volume Estimation for Eucalyptus Clones Trees Using Artificial Neural Networks." In 2020 IEEE Canadian Conference on Electrical and Computer Engineering (CCECE), pp. 1-5. IEEE, 2020.(RODRIGUES *et al.*, 2020) **(Qualis A3)**

28. de Sousa, Naiane Maria, Gabriel da Silva Vieira, Juliana Paula Felix, Junio Cesar de Lima, and Fabrizzio Soares. "Image Saliency Analysis in Agricultural Environments: A Survey." In 2020 IEEE Canadian Conference on Electrical and Computer Engineering (CCECE), pp. 1-4. IEEE, 2020. (SOUSA *et al.*, 2020) **(Qualis A3)**

29. Santos, Samuel, Gabriel Vieira, Junio Lima, and Allan Santos. "Tecnologia assistiva para reconhecimento de cartas de baralho utilizando aprendizado profundo." In SIBGRAPI-Conference on Graphics, Patterns and Images. Instituto Federal Goiano, 2019. (SANTOS *et al.*, 2019) **(Qualis A3)**

30. Felix, Juliana Paula, Flávio Henrique Teles Vieira, Gabriel da Silva Vieira, Ricardo Augusto Pereira Franco, Ronaldo Martins da Costa, and Rogerio Lopes Salvini. "An Automatic Method for Identifying Huntington's Disease using Gait Dynamics." In 2019 IEEE 31st International Conference on Tools with Artificial Intelligence (ICTAI), pp. 1659-1663. IEEE, 2019. (FELIX *et al.*, 2019) **(Qualis A3)**

A.1.4   Original Software

1. *ProtectLeaf*

   Description:

   ProtectLeaf is a software designed to support crop monitoring activities and decision-making in agricultural environments through defoliation estimate, detection of insect predation on plant leaves, and leaf reconstruction.

   Elsevier Repository:

   <https://github.com/ElsevierSoftwareX/SOFTX-D-23-00186>

   CodeOcean Capsule:

<https://codeocean.com/capsule/7740985/tree/v1>

2. *CBIR-ANR*

Description:

CBIR-ANR is an acronym for content-based image retrieval (CBIR) with accuracy noise reduction (ANR), which was developed to increase assertiveness in image retrieval from large-scale data sets.

Elsevier Repository:

<https://github.com/SoftwareImpacts/SIMPAC-2022-294>

CodeOcean Capsule:

<https://codeocean.com/capsule/3022749/tree/v1>

3. *DCF*

Description:

The Disparity Computing Framework (DCF) is a software implemented with the main components of a stereo vision system to facilitate disparity map construction.

Elsevier Repository:

<https://github.com/SoftwareImpacts/SIMPAC-2022-236>

CodeOcean Capsule:

<https://codeocean.com/capsule/4854862/tree/v1>

4. *ATD*

Description:

The Aerial Tree Detection (ATD) is a software developed for detecting and segmenting treetops, delineating shaded areas, and indicating the source of the light source.

Github Repository:

<https://github.com/gabrieldgf4/aerial-tree-detection>

5. *SCC*

Description:

The Segment Consistency Check (SCC) is a program designed for the refinement of depth information obtained from a pair of images (disparity maps).

Github Repository:

<https://github.com/gabrieldgf4/disparity-refinement-SCC>

A.1.5   New Datasets

1. *Insect Defoliation Dataset*

    Description:

    Defoliation estimation methods are difficult to compare because there is no benchmarking for this purpose. Researchers use their datasets, which are not accessible to the general public. In this sense, we prepared a public image database with model data and test data by considering 12 plant species: apple, blueberry, cherry, corn, grape, peach, pepper, potato, raspberry, soybean, strawberry, and tomato.

    Github Repository:

    <https://github.com/gabrieldgf4/insect-defoliation-dataset>

2. *Insect Leaf Predation Dataset*

    Description:

    The Insect Leaf Predation Dataset results from applying leaf damage simulation caused by different insects in healthy soybean leaf images. The dataset contains five classes. One class represents intact leaf samples, and the other four classes include images damaged by caterpillars, gastropods, grasshoppers, and green cows. The defoliation rate is equally distributed, ranging from 1.01% to 29.99%, with an average of 15.04%. The damage per leaf sample ranged from 1 to more than 50 compromised areas.

    Github Repository:

    <https://github.com/gabrieldgf4/insect-leaf-predation-dataset>

3. *Tree Stereo Dataset*

    Description:

    The Tree Stereo Dataset contains stereo image pairs and ground truth disparity maps. Also, it contains tree and ground image masks and segmented trees prepared by hand. The dataset was prepared with images from rural and semi-rural environments registered with a monocular RGB camera. For each scene, two shots shifted by a horizontal movement of the camera were taken, which provided a stereo image pair.

    Github Repository:

    <https://github.com/gabrieldgf4/tree-stereo-dataset>

    Github Repository:

    <https://github.com/gabrieldgf4/insect-leaf-predation-dataset>

4. *Tree Segmentation Dataset*

    Description: The Tree Segmentation Dataset contains images manually segmented from outdoor environments in areas with trees. The dataset also contains

tree and ground image masks. Image segmentation is key in providing data to be analyzed, influencing overall success in understanding the image. When it comes to external scenes, the extraction of fundamental features can be quite complex due to exposure to various adverse conditions, such as frequent changes in illumination that create artifacts like shading, photometric distortion, and noise. Thus, this dataset can be used to validate segmentation methods.

Github Repository:

<https://github.com/gabrieldgf4/tree-segmentation-dataset>

Authorization for Reuse of Published Papers

All papers originating from the thesis research were duly cited, and the publishers granted the authors the right to use them in theses and/or dissertations, as follows.

IEEE - COMPSAC

Clearance Center.pdf

CCC
RightsLink

Sign in/Register

A Method for the Detection and Reconstruction of Foliar Damage caused by Predatory Insects

Conference Proceedings:
2021 IEEE 45th Annual Computers, Software, and Applications Conference (COMPSAC)

Author: Gabriel Da Silva Vieira

Publisher: IEEE

Date: July 2021

Copyright © 2021, IEEE

Thesis / Dissertation Reuse

The IEEE does not require individuals working on a thesis to obtain a formal reuse license, however, you may print out this statement to be used as a permission grant:

Requirements to be followed when using any portion (e.g., figure, graph, table, or textual material) of an IEEE copyrighted paper in a thesis:

1) In the case of textual material (e.g., using short quotes or referring to the work within these papers) users must give full credit to the original source (author, paper, publication) followed by the IEEE copyright line © 2011 IEEE.
2) In the case of illustrations or tabular material, we require that the copyright line © [Year of original publication] IEEE appear prominently with each reprinted figure and/or table.
3) If a substantial portion of the original paper is to be used, and if you are not the senior author, also obtain the senior author's approval.

Requirements to be followed when using an entire IEEE copyrighted paper in a thesis:

1) The following IEEE copyright/ credit notice should be placed prominently in the references: © [year of original publication] IEEE. Reprinted, with permission, from [author names, paper title, IEEE publication title, and month/year of publication]
2) Only the accepted version of an IEEE copyrighted paper can be used when posting the paper or your thesis on-line.
3) In placing the thesis on the author's university website, please display the following message in a prominent place on the website: In reference to IEEE copyrighted material which is used with permission in this thesis, the IEEE does not endorse any of [university/educational entity's name goes here]'s products or services. Internal or personal use of this material is permitted. If interested in reprinting/republishing IEEE copyrighted material for advertising or promotional purposes or for creating new collective works for resale or redistribution, please go to http://www.ieee.org/publications_standards/publications/rights/rights_link.html to learn how to obtain a License from RightsLink.

If applicable, University Microfilms and/or ProQuest Library, or the Archives of Canada may supply single copies of the dissertation.

BACK   CLOSE WINDOW

ELSEVIER - Smart Agricultural Technology

MDPI - Agronomy

Important Note: some articles (especially *Reviews*) may contain figures, tables or text taken from other publications, for which MDPI does not hold the copyright or the right to re-license the published material. Please note that you should inquire with the original copyright holder (usually the original publisher or authors), whether or not this material can be re-used.

Advantages of Open Access for Authors

The High Availability and Visibility of our open access articles is guaranteed through the free and unlimited accessibility of the publication over the Internet. Everyone can freely access and download the full text of all articles published with MDPI: readers of open access journals, *i.e.*, mostly other researchers, do not need to pay any subscription or pay-per-view charges to read articles published by MDPI. Open access publications are also more likely to be included in search engines and indexing databases.

The Higher Citation Impact of open access articles results from their high publicity and availability. Open access publications are demonstrably more frequently cited [1,2].

Lower Publishing Costs: Open access publishers cover their costs for editorial handling and editing of a paper by charging authors' institutes or research funding agencies. The cost of handling and producing an article is covered through the one-time payment of an **article processing charge (APC)** for each accepted article. The APCs of open access publishers are only a fraction of the average income per paper earned by traditional, subscription-based publishers. MDPI's **article processing charge (APC)** is the same, irrespective of article length, because we wish to encourage publication of long papers with complete results and full experimental or computational details [3].

Faster Publication in MDPI's open access journals is achieved by online-only availability. Accepted articles are typically published online more rapidly in MDPI journals than those of traditional, subscription-based and printed journals are [4].

Links and Notes

1. Open access citation impact advantage:
   http://en.wikipedia.org/wiki/Open_access#Authors_and_researchers . For example, a standard research paper "Shutalev, A.D.; Kishko, E.A.; Sivova, N.V.; Kuznetsov, A.Y. *Molecules* **1998**, *3*, 100-106" has been cited 51 times, the highest number among all the papers published so far by the same author.

2. Lin, S.-K. *Editorial:* Non-Open Access and Its Adverse Impact on Molecules. *Molecules* **2007**, *12*, 1436-1437 (PDF format 16 K, HTML format).

3. A research paper of 30 pages has been published: *Molecules* **2008**, *13*(5), 1081-1110.

4. Some well written papers have been peer reviewed and published in less than two weeks from manuscript submission, see e.g.: *Molecules* **2006**, *11*(4), 212-218.

Back to Top

ELSEVIER - Information Processing in Agriculture

ScienceDirect®

Information Processing in Agriculture
Open access

	21.1 CiteScore	7.7 Impact Factor

Submit your article	Guide for authors

Menu 🔍 Search in this journal

Open access information

Introduction

Open Access Licences

- User rights
- Creative Commons Attribution (CC BY)
- Creative Commons Attribution-NonCommercial-NoDerivs (CC BY-NC-ND)

Article Publishing Charge (APC)

Policies

- Research4Life
- Best price promise
- Open access agreements
- Funding arrangements
- Responsible sharing

Author Resources and Support

- Learn more about
- Contact details

Introduction

Information Processing in Agriculture is a peer reviewed, open access journal.

Open Access Licences

User rights

All articles published gold open access will be immediately and permanently free for everyone to read and download, copy and distribute. We offer authors a choice of user licenses, which define the permitted reuse of articles. We currently offer the following license(s) for this journal:

Creative Commons Attribution (CC BY)

Allows users to: distribute and copy the article; create extracts, abstracts, and other revised versions, adaptations or derivative works of or from an article (such as a translation); include in a collective work (such as an anthology); and text or data mine the article. These uses are permitted even for commercial purposes, provided the user: gives appropriate credit to the author(s) (with a link to the formal publication through the relevant DOI); includes a link to the license; indicates if changes were made; and does not represent the author(s) as endorsing the adaptation of the article or modify the article in such a way as to

damage the authors' honor or reputation.

Creative Commons Attribution-NonCommercial-NoDerivs (CC BY-NC-ND)

Allows users to: distribute and copy the article; and include in a collective work (such as an anthology). These uses are permitted only for non-commercial purposes, and provided the user: gives appropriate credit to the author(s) (with a link to the formal publication through the relevant DOI); provides a link to the license; and does not alter or modify the article.

If you need to comply with your funding body policy you can apply for a CC BY license after your manuscript is accepted for publication.

Article Publishing Charge (APC)

As an open access journal with no subscription charges, a fee (Article Publishing Charge, APC) is payable by the authors, or their institution or funders, to cover the costs associated with publication. This ensures your article will be immediately and permanently free to access by everyone.

The Article Publishing Charge for this journal is:

Article type	Article Publishing Charge (excl. taxes)
All articles	USD 2000

Policies

Research4Life

We automatically apply Article Publishing Charge waivers or discounts to those articles in gold open access journals for which all authors are based in a country eligible for the Research4Life program. Find out more about the APC waiver and discount eligibility.

Best price promise

Our Online Author Communication System (OACS) ensures you are offered the lowest possible Article Publishing Charge to publish an article in your chosen journal. During submission you will be presented with a personalized OA Article Publishing Charge based on your individual context (your country, institutional affiliation, and any society membership for example) as well as considering the journal involved.

Learn more about Elsevier's pricing policy.

Open access agreements

Elsevier has reached open access agreements with an increasing number of institutions and university consortia around the world. Find out what this means for authors on our open access agreements page.

Funding arrangements

Elsevier partners with funding bodies to provide guidance for authors on how to comply with funding body open access policies. Find out more on our funding arrangements page.

Responsible sharing

Find out how you can share your research published in Elsevier journals.

Author Resources and Support

Open access information - Information Processing in A...   https://www.sciencedirect.com/journal/information-pr...

Learn more about

- Benefits of publishing open access with Elsevier

- Open access agreements

- Funding arrangements

- Open access license policy

- Open access pricing policy

Contact details

Frequently asked questions and answers are available in the Journal Article Publishing Support Center.

Please contact support@elsevier.com for any further questions.

ELSEVIER - Software X